Summer 2018

Identification of potential conservation practices and hydrologic modeling of the upper Iowa watershed

Trevor Julian Rundhaug
University of Iowa

Identification of Potential Conservation Practices and Hydrologic Modeling of the Upper Iowa Watershed

By

Trevor Rundhaug

A thesis submitted in partial fulfillment
of the requirements for the Master of Science
degree in Civil and Environmental Engineering in the
Graduate College of
The University of Iowa

August 2018

Thesis Supervisors: Professor Larry Weber
Adjunct Assistant Professor Antonio Arenas Amado

Graduate College

The University of Iowa

Iowa City, Iowa

CERTIFICATE OF APPROVAL

_____

MASTER'S THESIS

_____

This is to certify that the Master's thesis of

Trevor Julian Rundhaug

has been approved by the Examining Committee
for the thesis requirement for the Master of Science
degree in Civil and Environmental Engineering at the August 2018 graduation.

Thesis Committee: _____
Larry Weber, Thesis Supervisor

_____
Antonio Arena Amado, Thesis Supervisor

_____
A. Allen Bradley

Acknowledgements

First, I would like to thank my advisors for both of their advice throughout this project. Thanks to Larry Weber for your guidance both for this project and professionally and for giving me the opportunity to work on your land which was a nice break from the office. Thanks to Antonio Arenas Amado for your continued help, advice, and guidance throughout this project especially in the final stretch. I have learned a lot about modeling and watershed processes through your help. Thanks to my committee member Allen Bradley for your patient teaching and suggestions put forward to improve the outcome of this project.

To the IWA team as a whole, thank you for giving me the opportunity to work on an applied project. Thanks to Marcela Politano for her work developing and explaining GHOST. Thanks to Calvin Wolter for his work and guidance with GIS and the IBMP project. Thanks to Chad Drake, Maral Razmand, and Greg Geimer, for all of your support, help, and friendship throughout this project.

To the people of IIHR – Hydroscience & Engineering and the friends I have made during my time here, thanks for making this a place I look forward to coming to every day. This truly is a unique place where one can both learn and enjoy the day.

Lastly, to my friends and family for your continued love, support, and encouragement throughout my life. Without their support I would not be where I am today.

Abstract

In 2016 the Iowa Watershed Approach (IWA) was created to increase community resiliency against flooding, to develop hydrologic assessments that would identify strategies to reduce flooding, and to implement those strategies within nine identified watersheds that experienced flooding between 2011 and 2013. One of the nine watersheds was the Upper Iowa watershed located in northeast Iowa. This thesis focuses on the work that has been done to create a hydrologic assessment of the Upper Iowa watershed. The hydrologic assessment identifies potential conservation practices, creates a hydrologic model to assess the hydrologic cycle over the past ten years, and identifies strategies to reduce flooding within the watershed.

Many potential agricultural conservation practices within the Upper Iowa watershed were identified and trends relating to the soil, land use, and topography were determined. In addition, a methodology to compare potential conservation practices with existing conservation practices actually in place was developed including a tool to estimate the size of grassed waterways to NRCS design guidelines. The comparison validated the methodologies used to identify potential practice placements, identified locations where potential practices could be implemented, and showed how stakeholder preferences influence conservation implementation.

Additionally, a hydrologic model of the Upper Iowa watershed was developed, using the new Generic Hydrologic Overland-Subsurface Toolset model and calibrated to simulate the time period of 2007 through 2016. The model was evaluated against water balance ratios and performance statistics calculated from measured data. The model achieved Nash Sutcliffe Efficiency scores for streamflow above 0.7 and percent bias scores between ±12% for the three wettest years of 2008, 2013, and 2016. With the calibrated model, the benefits of continuous cover crop implementation were investigated under current conditions and under increased extreme

precipitation intensity expected from climate change over the next half century. The results of this investigation determined that continuous cover crops increased evapotranspiration within the early half of the year creating more storage within the soil. Thus the flood risk from convective storms during the summer was lowered. In addition, the benefits from cover crops in terms of peak flow and volume reductions were cumulative increasing each consecutive year and were proportional to the percentage of cover cropped area. Lastly, a scenario using cover crops in a future extreme precipitation environment resulted in a reduction of peak discharge to current conditions. The results of this thesis will guide both future work within the Upper Iowa watershed and contribute to the knowledge of hydrologic planning and modeling within agricultural watersheds.

Public Abstract

In 2016 the Iowa Watershed Approach (IWA) was created to help communities improve the landscape of Iowa by implementing conservation that would reduce flooding and retain nutrients on farm fields. One of the watersheds chosen as part of the IWA was the Upper Iowa watershed located in northeast Iowa. To inform stakeholders within the watershed on potential flood reduction strategies, potential conservation practices were identified to show the range of practices that could be used. In addition, a model assessing the hydrologic cycle of the watershed was created. With a working model of the watershed, the benefits of cover crops were investigated. Cover crops are plants that are planted after the harvest of corn and soybeans that grow when the fields would normally be fallow. The simulated results indicated that cover crops can reduce peak flows and volumes of future flood events.

Table of Contents

List of Tables

List of Figures

Chapter 1. Introduction

Due to agricultural development, Iowa and the Midwestern United States represent one of the most altered landscapes in the world. Historically, Iowan prairies represented the majority of the state occupying approximately 80% of the land area (Gallant et al. 2011). However by 2016, the majority of Iowa, 65%, was planted into corn and soybeans (Miller et al. 2017). The conversion of prairie into agricultural land has resulted in hydrologic changes (Zhang and Schilling 2006; Raymond et al. 2008) and a decline in water quality with the formation of the Gulf of Mexico hypoxia problem (Goolsby et al. 1999; Hatfield et al. 2009) and deterioration in ecosystem services (Kremen et al. 2007; Lawler et al. 2014). Compounding the problems caused by the altering of the Midwestern landscape are changes in the climate. Villarini et al. (2013) documented an increasing trend in extreme precipitation events in areas of Missouri, Illinois, Iowa, Minnesota and Wisconsin, where the largest increasing trend in temperature was occurring. Mallakpour and Villarini (2015) documented increasing flood frequency across central United States. To mitigate these issues, states and federal governments are creating action plans. For instance, in response to the Gulf Coast hypoxia the 2008 Gulf Hypoxia Action Plan was created, calling for the 12 states in the Mississippi River Basin to develop plans to reduce nutrient loadings, nitrogen and phosphorous, by 45%. The state of Iowa's plan, the Iowa Nutrient Reduction Strategy, assesses and develops strategy to address point and non-point source pollution resulting in a reduction of total nitrogen and total phosphorus by 45% (Iowa Nutrient Reduction Strategy Science Team 2017).

In Iowa, the coupled alterations in landscape and climate have contributed to widespread flooding in the summer of 1993 (Parrett et al. 1993), May and June 2008 (Buchmiller and Eash 2010), and most recently in August and September of 2016 (Quad Cities 2016). In response, Iowa took action with the formation of the Iowa Flood Center in 2009 and the passage of legislation in

2010 authorizing the creation of Watershed Management Authorities (WMAs). WMAs serve the purpose of helping governmental organizations and local stakeholders cooperate in creating watershed plans and management efforts to address flooding and water-quality concerns (Weber et al. 2017). At the same time, Iowa received $8.8 million from the U.S. Department of Housing and Urban Development Disaster Recovery Enhancement Fund (DREF) grants for the Iowa Watersheds Project (IWP) with the main objective of reducing and preventing future flood impacts (Weber et al. 2017). Then in January 2016 Iowa received a $97 million grant from the U.S. Department of Housing and Urban Development (HUD) for the Iowa Watershed Approach for Urban and Rural Resilience (IWA).

1.1 Iowa Watershed Approach

The IWA is a five year project that brings together government agencies, universities, non-profits, and municipalities to address factors contributing to floods and nutrient loads. The IWA is composed of two primary components flood resiliency and flood mitigation. Flood resiliency is the ability of a watershed community to collectively plan and take action to mitigate, prepare, respond and recover from a flood using the available resources (Weber et al. 2017). The flood mitigation component is broken into two phases the first is the development of a hydrologic assessment. Hydrologic assessments are used by water resources professionals to understand the systems within a watershed, identify vulnerabilities in terms of flood and water quality risks, and to identify solutions to reduce those vulnerabilities. With solutions selected, the second phase of the project will be the construction of the chosen conservation practices within the watershed. In total approximately 88% of the IWA grant will go towards practice construction within the urban and agricultural areas of Iowa. Watersheds included in this project were selected based on flooding in the years 2011 through 2013 and include; Bee Branch Creek watershed, Clear Creek watershed, English River watershed, North Raccoon River watershed, East Nishnabotna River watershed,

West Nishnabotna River watershed, Middle Cedar River watershed, Upper Wapsipinicon River watershed, and Upper Iowa River watershed, the focus of this thesis (Figure 1.1).

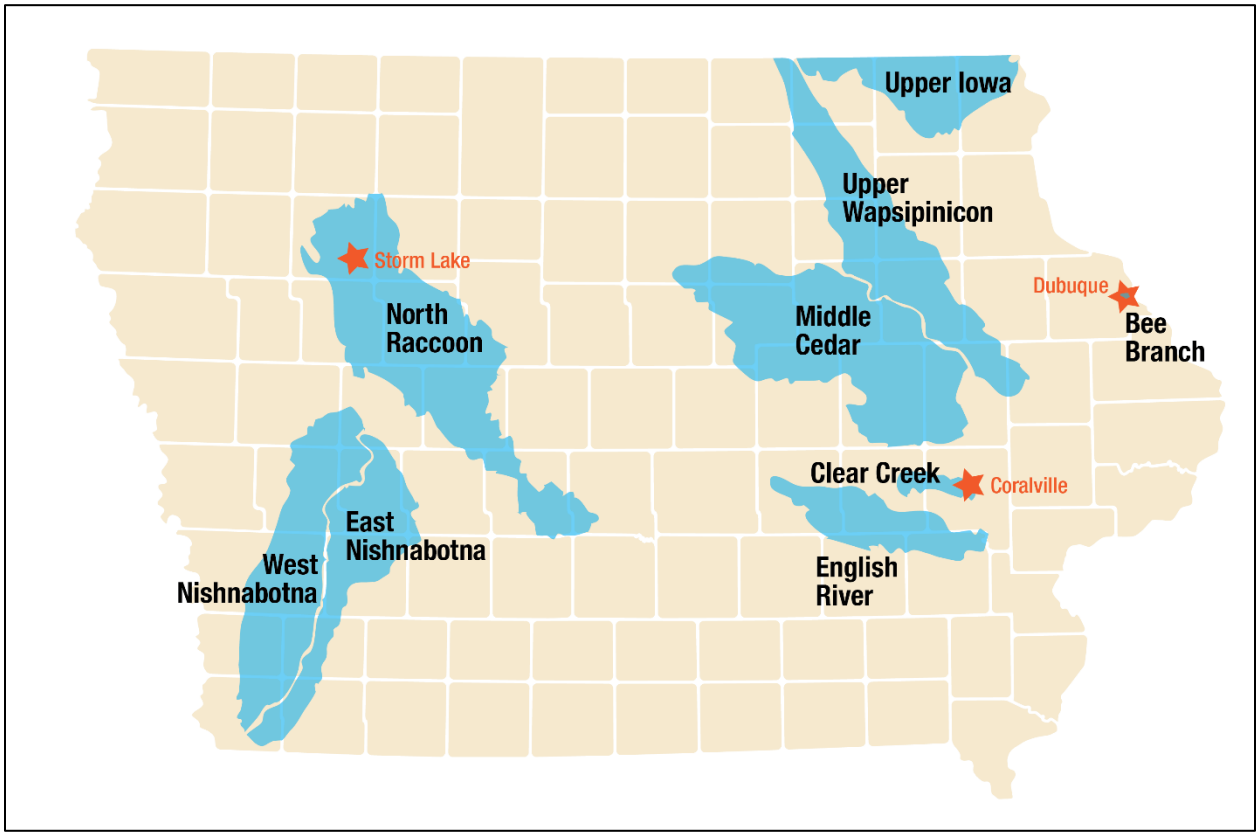

Figure 1.1. Urban and Rural Iowa Watershed Approach project watersheds (IIIHR 2015).

1.2 Goals and Objectives

As part of the IWA this thesis will be focused on the hydrologic assessment of the Upper Iowa River watershed. The first objective will be to identify potential conservation practices that could be implemented within the watershed. Some examples are wetlands, farm ponds, bioreactors, buffer strips, and saturated buffers. The potential conservation practices will then be compared to existing conservation projects with the purpose of validating the methods used, identifying areas of improvement, and improving the watershed planning process as a whole. With potential conservation practices identified, the next objective will be to develop a hydrologic model that will be capable of modelling the benefits of conservation in terms of flood reductions. The hydrologic model will be calibrated to simulate the measured discharges throughout the basin

with an emphasis on replicating wet year. With the calibrated model, the last objective will be the creation of scenarios that will model the impacts of future climate change and the benefits that could be imposed by the use of conservation in the landscape. The benefits will be quantified in terms of peak discharge reductions. This thesis is unique in that it will; one create a methodology and compare existing conservation practices with potential conservation practices, two be one of the first HUC 8 scale watershed to be modeled with the Generic Hydrologic Overland Subsurface tool set (GHOST), and three the benefits of continuous cover crops with and without climate change will be examined.

1.3 Summary

Agricultural development has altered the Midwestern U.S. landscape contributing to hydrologic alterations, increases in nutrient loading in the streams, and deterioration in ecosystem services. The issues relating to the changed landscape is coupled with the changing climate increasing the probability of higher precipitation events and flood events in the Upper Midwest. The federal and state governments are beginning to take action. In Iowa after historic flooding in 2008, the state created the IFC and legislation allowing the formation of WMA. Continuing this effort is the IWA, a $97 million HUD grant that will develop plans and implement projects to reduce flooding in 9 Iowa watersheds. The focus of this thesis is on one of the 9 Iowa watersheds, the Upper Iowa watershed. This thesis will identify potential conservation practices within the watershed, compare those practices to existing conservation practices and model the hydrologic processes of the watershed, and the potential benefit of conservation in terms of flood reduction.

Chapter 2. Literature Review

To accomplish the goals of the thesis it is important to first identify similar studies within the literature to gain insight into what has been done previously and the current methodologies that are being used to accomplish similar projects. For this thesis, it was important to first investigate the potential benefits, history, and current siting of the conservation practices to provide context for the project. In addition to current conservation practices information, basic knowledge of the history and current types of hydrologic models is important to know what is reasonable in analyzing the results of hydrologic models. Lastly, similar studies modeling the benefits of conservation with hydrological models are important to gain ideas of how to incorporate practices within the model so that the results are comparable to similar studies. In this chapter, the information gained from the literature review will be discussed.

2.1 Benefits of Conservation Practices

Approximately, 25% of assessed lakes and 16% of assessed streams are reported as impaired due to nutrient-related causes according to the 305(b) Water Quality Assessment Report (EPA 2011) and approximately 60% of coastal rivers and bays in the U.S. are moderately to severely degraded due to nutrient pollution (Howarth et al. 2002). Conservation practices are commonly used techniques and structures used to reduce the impacts of runoff from agricultural farm fields in terms of nutrient and soil loss reduction, peak flow reduction, and increases in ecosystem services. On a field scale, conservation practices are shown to be very effective. For instance, water and sediment control basins trap sediment at an efficiency of 97% (Mielke 1985), constructed wetlands reduce total nitrogen concentrations by 40-50% and phosphate concentrations by 50-60% (Vymazal 2007), grassed waterways reduce runoff by 90% and 10% and reduce sediment delivery by 97% and 77%, depending on the shape of the grassed waterway (Fiener and Auerswald 2003). At the watershed-scale the impacts of conservation continues

downstream. Schilling and Spooner (2006) documented a 25% conversion from row crop to prairie restoration resulted in a decrease in nitrate concentration of 1.2 mg/L over 10 years. Ayalew et al. (2017) modeled the reduction in peak flow from 144 small distributed dams in the 660 km^2 Soap Creek Basin to be between 20 and 70% with the reduction diminished as the drainage area increased. Over a 14 year monitoring period of the Beasley Lake (625 ha drainage area) Lizotte et al. (2017) were able to correlate a decrease in total phosphorus lake concentrations to increases in vegetative buffers and rainfall, a decrease in ammonium lake concentrations to increases in conservation tillage and CRP land, and a decrease in nitrate lake concentrations to increases in vegetative buffers. On a national scale the Conservation Effects Assessment Project (CEAP), assessing 14 watersheds across the U.S., is providing in site into the benefits of conservation practices and different watershed management strategies (M. D. Tomer et al. 2014).

2.2 History of Conservation in Iowa

In Iowa watersheds many conservation practices have been implemented however, nationwide the documentation of the practices are fragmented. Nationally, conservation practices began to gain attention during the Dust Bowl in the 1930s with the creation of the Soil Conservation Service (SCS) in 1935 (Cain and Lovejoy 2004). Starting with demonstration projects such as the Soil Conservation Experiment Station, Missouri Valley Loess Region in Clarinda, Iowa in 1932 (Musgrave and Norton 1937) and the Coon Creek Basin in Wisconsin in 1933 (Trimble and Lund 1982) conservation implementation began to grow over the next several decades. One example of conservation implementation during this time is within the Walnut Creek watershed in south central Iowa. Aerial photographs of the watershed show significant change between 1940, when most fields were rectangular, and 1971, when many of the fields followed the contour along with terraces and grassed waterways being implemented (Schilling 2000). In addition, the first National Resources Inventory in 1982 reported that 30% of Iowa land had at

least one conservation practice (Burkart et al. 1994). By the 1980s, the Natural Resources Conservation Service (NRCS, formerly the SCS) began to shift their focus from supply control and rural development to reducing agriculture's impact on the environment (Cain and Lovejoy 2004). Programs introduced during the next couple of decades included Conservation Compliance, Conservation Reserve Program (CRP), Environmental Quality Incentive Program (EQIP), and several more. As evidence of these conservation programs taking effect, an estimated 90% of farm fields in the South Fork River Basin in Iowa with greater than 33% highly erodible land had erosion control practices implemented by 2008 (M. D. Tomer et al. 2008). Currently, the entire state of Iowa is being inventoried by the Iowa Best Management Mapping Project (IBMP). The IBMP will provide a benchmark on conservation efforts leading up to the 2007-2010 time frame (Iowa BMP Mapping Project 2018).

2.3 Conservation Siting Tools

The siting of new conservation practices by federal, state and local agricultural programs relies heavily on a volunteer approach to conservation implementation. The volunteer approach has been termed as a "shot gun" approach to conservation or "random acts of conservation" (Knight 2005) as cited in (Arbuckle 2013) with the idea that if enough conservation is implemented randomly that the goals of conservation will be met. To help inform the voluntary approach to conservation, a more targeted approach to watershed planning has been proposed typically called precision conservation. Precision conservation uses spatial technologies to obtain relationships between mapped data that can be used to plan conservation efforts (Delgado and Berry 2008). Some examples of recent conservation siting tools include; using topographic wetness index to identify potential wetland locations (Babbar-Sebens et al. 2013), the AgBufferBuilder, a geographic information system (GIS) tool used to identify and size potential filter strip location (Dosskey et al. 2015), a web-based GIS decision support system to help prioritize CRP (Rao et al.

2007), and the Agricultural Conservation Planning Framework (ACPF) a GIS tool that uses high resolution Light Detection and Ranging (LiDAR) elevation, soils, land use, and farm field information to identify potential conservation practices within a watershed (Mark D. Tomer et al. 2013).

2.4 History of Hydrologic Modeling

Another way of improving the current volunteer approach to conservation is quantifying the impacts of conservation practices in terms of flood reduction and improvement to water quality with hydrologic models, as this will simulate different implementation scenarios without spending the money to construct the practices. In general, the purpose of hydrologic modeling is to quantify the hydrologic cycle as water moves from precipitation through the land surface as overland and subsurface flow resulting as outflows of streamflow or evapotranspiration. The first hydrologic models focused on components of the hydrologic cycle. For instance, in 1850 Mulvaney developed the rational method, relating runoff peak flow to rainfall intensity and in 1933 Horton developed a theory for infiltration, creating a rainfall separation technique (Singh and Woolhiser 2002). These component models continued developing towards more realistic models. The first attempt at a complete watershed model, however, was during the 1960s with the development of the Stanford Watershed Model-SWM that is now called HSPF (Singh and Woolhiser 2002). Many other watershed models have followed especially with the increase in computational power since the digital revolution. Currently, models are increasing in complexity in one, two, and three dimensional simulations and other systems are being coupled with the hydrologic process (Maxwell et al. 2014). Some examples of these models include CATHY, HydroGeosphere, and ParFlow (Maxwell et al. 2014).

2.5 Comparison of Modeling Approaches

Hydrologic models are generally classified based on three different criteria: the model formulation, the spatial configuration, and the output results. The model formulation can be divided into three different groups; empirical models, conceptual models, physically-based models. Empirical models are the most narrowly focused and are derived mathematical relationships between measured input and output for a given study area (Devia et al. 2015). Conceptual models are more universal and involve semi empirical equations that quantify all of the components of the hydrologic process but, some of the parameters may not have physical meaning (Devia et al. 2015). Physically-based models are the most complex, requiring large amounts of data. The equations are derived from conservation equations of mass, momentum, and energy (Islam 2011). Based on spatial configuration hydrologic models can be grouped as either lumped or distributed. Lumped models group watersheds into uniform areas removing spatial variability while distributed models discretize the watershed into smaller subunits usually triangles or squares to capture the variability on the land surface and sub surface (Islam 2011). The last classification is based on the amount of outputs from a given set of initial conditions and parameters. A hydrologic model can either be deterministic where for a given input there is a defined output or stochastic where for a given input the results are provided as a probability distribution (Devia et al. 2015).

2.6 Hydrologic Modeling of Conservation Practices

One common application of hydrologic models both lumped and distributed models are in modeling the impacts of agricultural conservation practices within a watershed in terms of water quality and quantity. With water quality a commonly used model is the Soil and Water Assessment Tool (SWAT), a lumped conceptual continuous model (Arnold et al. 1998). SWAT has been used by Kalcic et al. (2015) to optimize six conservation practices within two west-central Indiana

watersheds to obtain a modeled reduction of 60% in total pollutant loads. With water quantity several models have been used. HEC-HMS, a lumper parameter surface water model was used by Drake (2014) to assess the impact of increased infiltration due to soil improvements and land use change, and increased storage from flood control ponds for the 4364 km^2 Upper Cedar watershed in northeast Iowa. TOPMODEL, a distributed physically-based model was used by Gao et al. (2017) to simulate the impact to flood peaks of grazing, vegetation burning, and bare ground restoration for the 84.0 km^2 Coverdale catchment of the United Kingdom. HydroGeoSphere, a coupled surface-subsurface distributed model was used by Thomas (2015) to simulate the hydrologic impacts of distributed flood mitigation wetlands, terraces, and drainage tile in the 44 km^2 Bear Creek basin in northeast Iowa.

2.7 Summary

Conservation practices reduce the impact of agriculture by reducing peak discharges and runoff, capturing and reducing nutrients and sediments from farm fields and improve previously deteriorated ecosystem services. The improvement is greatest on a local scale but, continues to the watershed level. The use of conservation practices originated in the U.S. since the 1930s with the Dust Bowl. Today, conservation practices continue to be implemented voluntarily and by local, state and federal agencies. In addition, new developments such as, GIS and remote sensing are making it possible to develop tools to help prioritize conservation siting and design.

In addition, new developments in hydrologic modeling are making it possible to investigate the cumulative effects of conservation practices within a watershed. These hydrologic models originated in 1850. Component models, estimating portions of the hydrologic cycle were the common method of estimating hydrologic processes until the 1960s when the first complete watershed model. Today's hydrologic models have added complexity and improved upon previous versions. The models can be classified based on three criteria the model formulation, the spatial

configuration, and the form of results. Models such as, SWAT, HEC-HMS, TOPMODEL, and HydroGeosphere are estimating the benefits of conservation in terms of water quality improvements and beneficial hydrologic alterations to the landscape.

Chapter 3. Description of the Watershed

The first step in developing a hydrologic model is to gather information about the project area including physical and hydrologic information. The physical information for instance, location, location of population centers, available sensor network within the watershed, land cover, elevations, slope, soils, and geology, provide information that will be useful when developing the model and will usually be required as inputs for the model. Hydrologic information provides a benchmark to compare the

3.1 Watershed Physical Description

The Upper Iowa watershed is located in northeast corner of Iowa and the south east corner of Minnesota (Figure 3.1). The Upper Iowa River drains 2587 km^2 and is defined as a hydrologic unit code 8 watershed 07060002. The largest city within the watershed is Decorah located close to the center of the watershed in Winneshiek County (Figure 3.1).

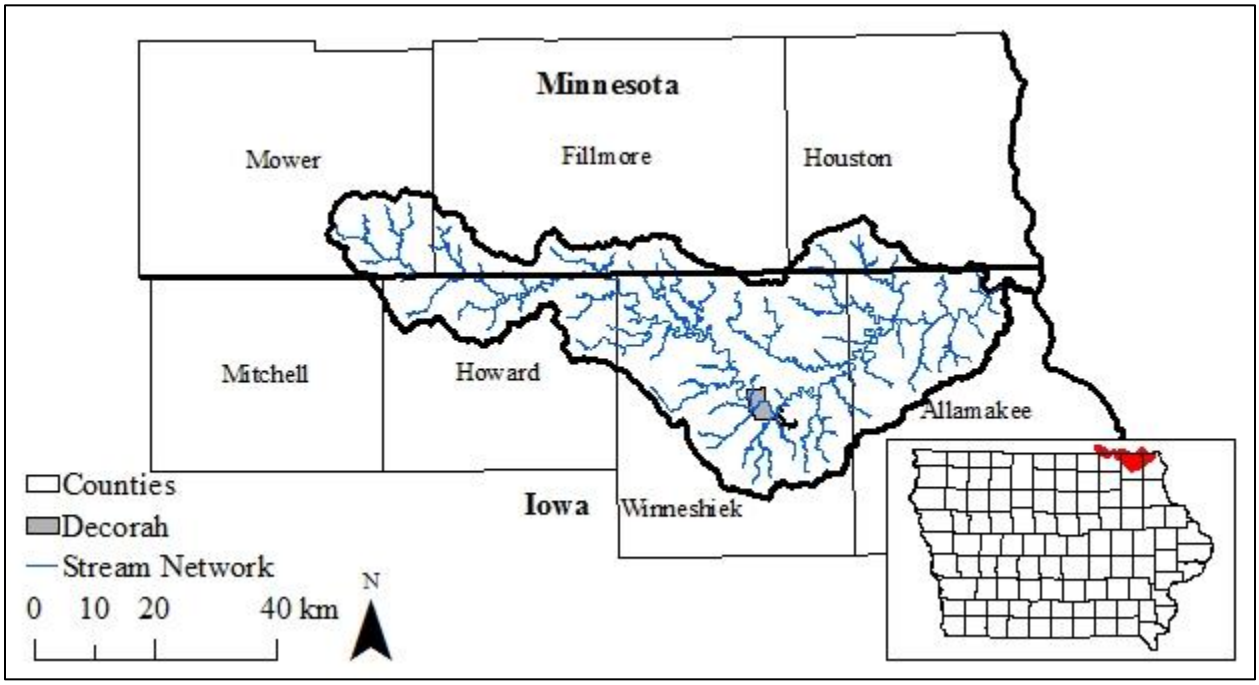

Figure 3.1. Location of the Upper Iowa watershed in northeast with Decorah, the major population center, located in the central portion of the watershed.

3.1.1 Land Use

The watershed is dominated by agriculture with 45% planted into cultivated crops and 21% used as pasture and hay leaving 17% for forest and 11% for grassland. A relatively small percentage 5% is developed urban areas (Figure 3.2). The distribution of this land use changes as one moves from the west where the land use is almost entirely cultivated crops to the east, where the land use changes to a mixture of forest, pasture/hay, and cultivated crops (Figure 3.2).

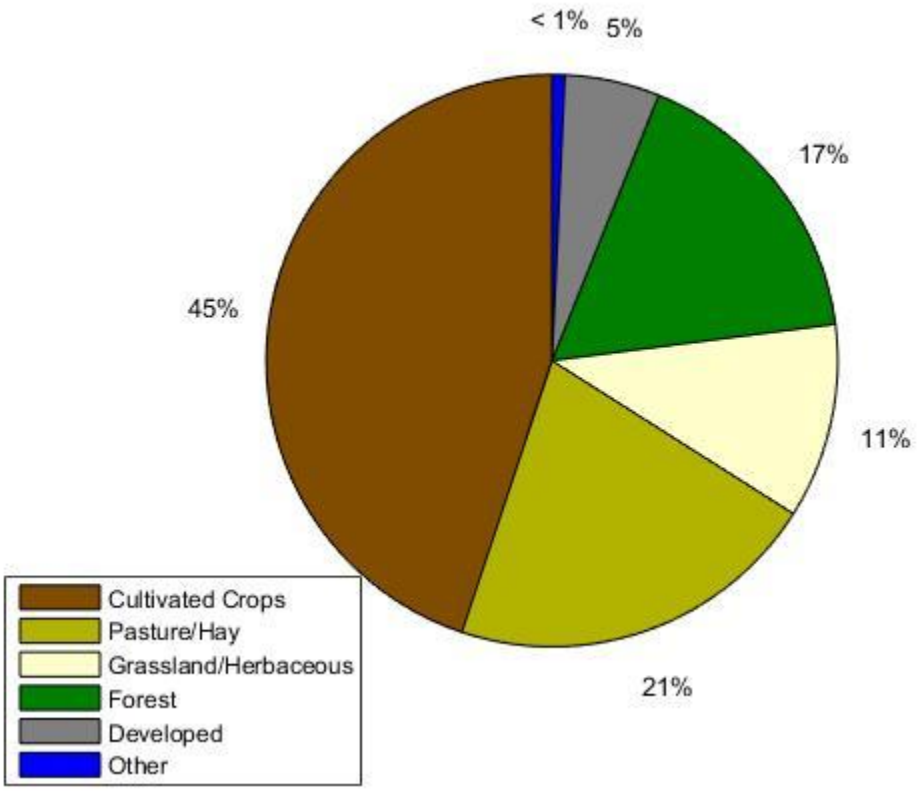

Figure 3.2. Upper Iowa land use described by the National Land Cover Database in 2011 (USGS 2011).

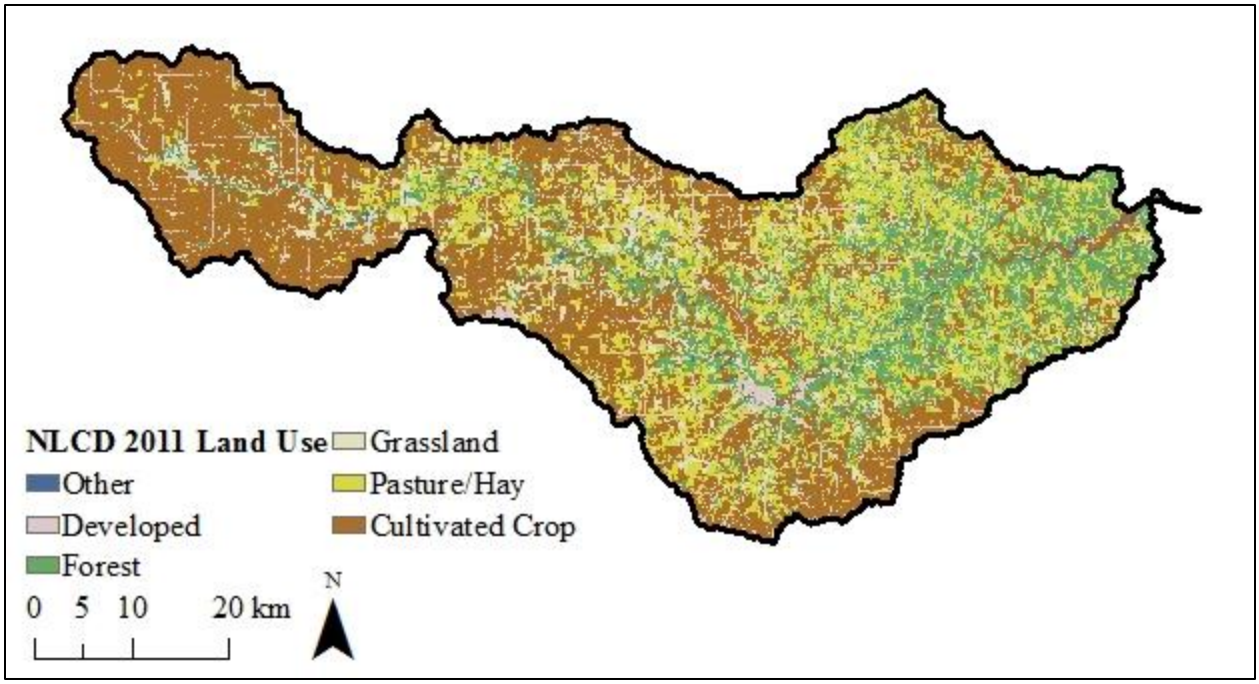

Figure 3.3. Distribution of the land use described by the National Land Cover Database in 2011.

3.1.2 Topography

The elevations and slopes of the watershed also follow a west to east trend. The elevation of the watershed is at its maximum at 440 m in the western headwaters of the watershed and decreases to 110 m at the outlet into the Mississippi River (Figure 3.4). Adversely, the slopes at the headwaters of the watershed are at a minimum with general ranges between 0% and 6%, and at a maximum in the eastern portion of the watershed with slopes ranging between 11% to 20% and even 100% to 1800% as the maximum slope indicating steep cliffs (Figure 3.5).

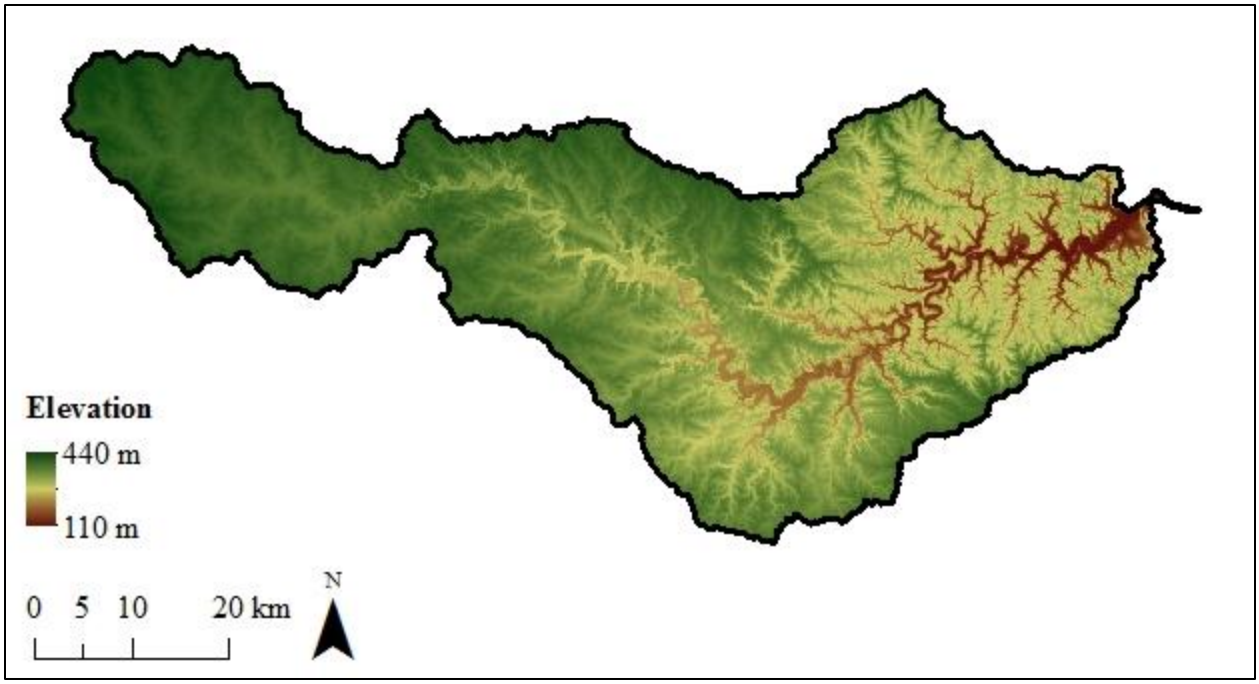

Figure 3.4. Elevations of the Upper Iowa watershed from three m LiDAR.

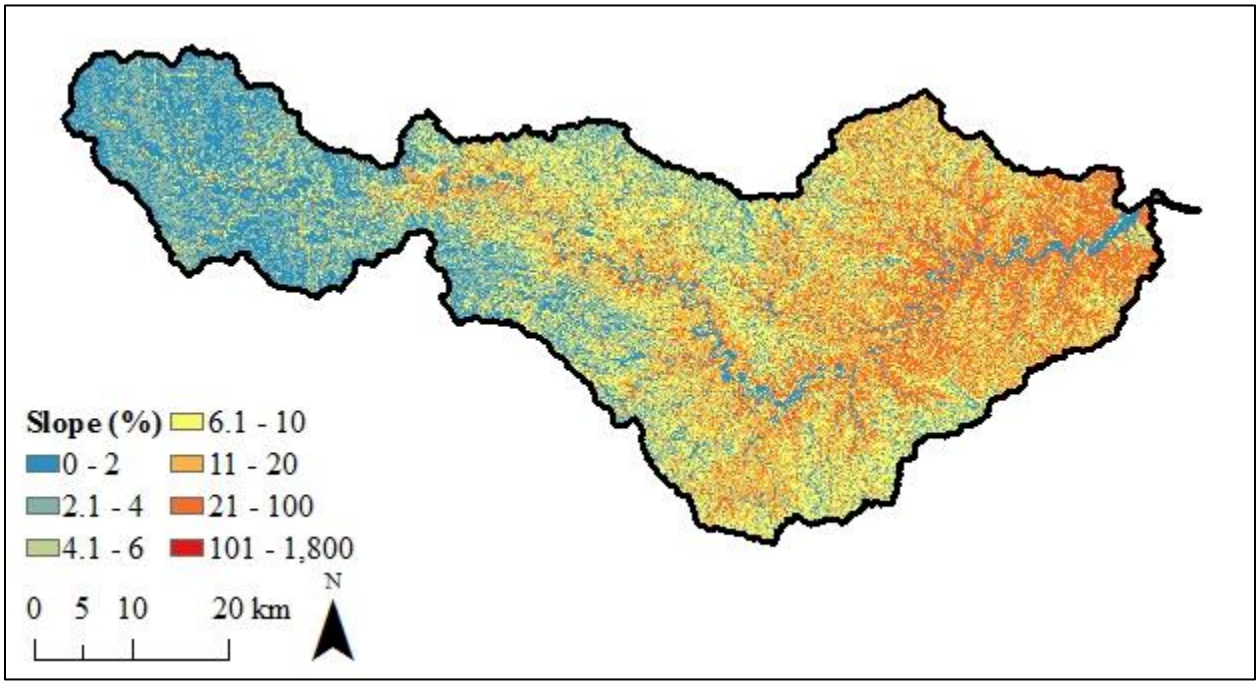

Figure 3.5. Slopes for the Upper Iowa watershed derived from three m LiDAR.

3.1.3 Geology

Contributing to the west-east trend in land use and topography, especially, the difference in slopes across the watershed is the geology of the watershed. The Upper Iowa watershed lies within the Iowan Surface (27%) in the west, the Paleozoic Plateau (73%) in the east, and the

Mississippi Alluvial Plain (<1%) at the outlet (Figure 3.6). The Iowan Surface extends across north central Iowa and is characterized by level to gently rolling hills with long slopes. This region of "stepped topography" was last glaciated during the Pre-Illinoisan (Prior 1976). Unlike the Iowan Surface, the Paleozoic Plateau was not glaciated during the Pleistocene glaciers and is located in the northeast corner of Iowa. Because of the lack of glaciation, the Paleozoic Plateau is characterized by well-developed river valleys, bedrock close to the surface and high bluffs (Prior 1976). In addition much of limestone bedrock is exposed to weathering creating karst features such as, caves and sinkholes. These features are identified in Figure 3.6. Lastly, the Mississippi River Alluvial Plain contains the region along the Mississippi River that floods frequently. It is characterized by low-lying, flat surfaces that are poorly drained (Prior 1976).

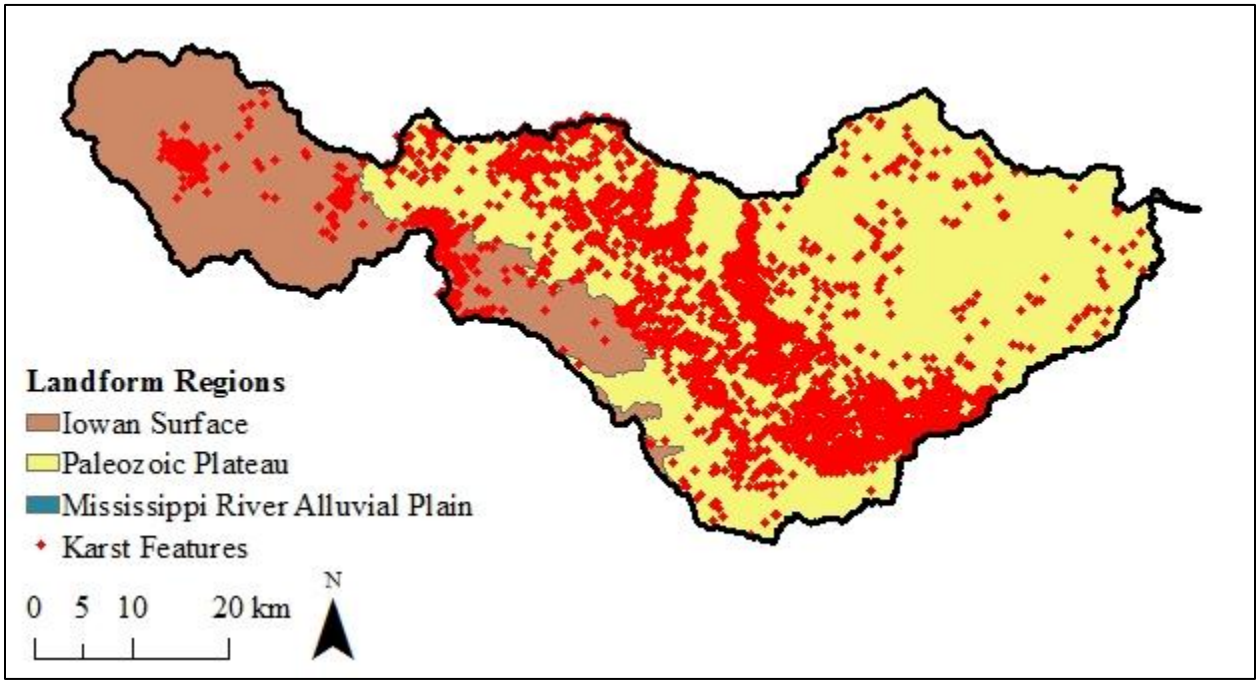

Figure 3.6. Landform regions located within the Upper Iowa watershed.

3.1.4 Soils

The Upper Iowa watershed contains nine texture classes defined by the NRCS (NRCS 2016). The majority of the watershed is comprised of silt loam (68%), loam (16%), and silty clay loam (13%). The remaining 3% of the watershed is mostly comprised of different mixtures of loam

and sand (Figure 3.7). The majority of the watershed is well drained except for the poorly drained portion located in the western headwaters of the watershed (Figure 3.9).

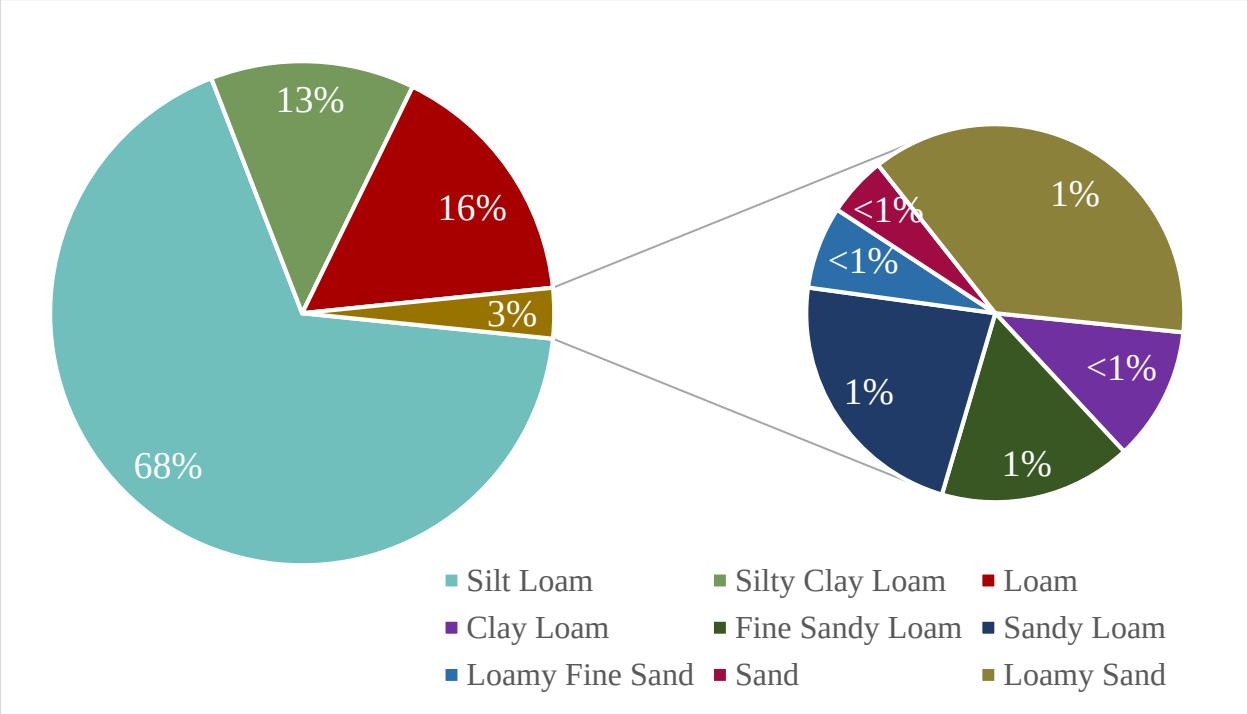

Figure 3.7. Upper Iowa soil texture class described by the NRCS gridded soil data (NRCS 2016).

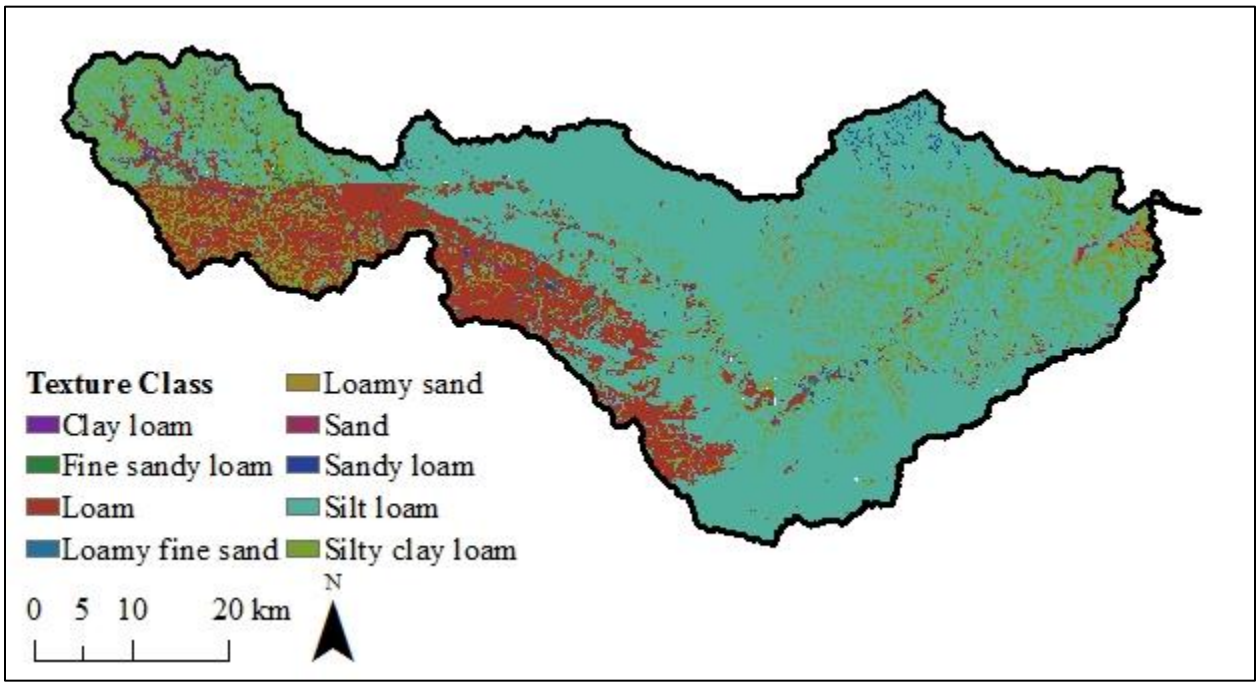

Figure 3.8. Distribution of the soil texture class described by the NRCS gridded soil data (NRCS 2016) for the Upper Iowa watershed.

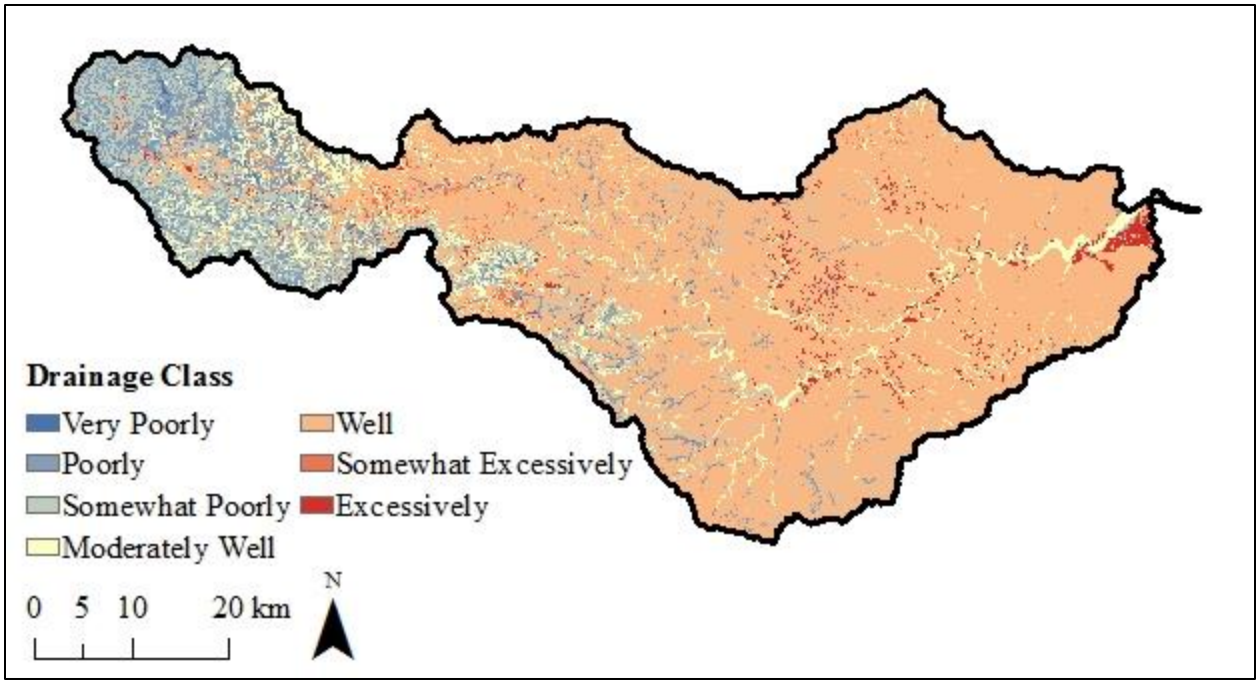

Figure 3.9. Drainage class based on the NRCS gridded soil data (NRCS 2016) for the Upper Iowa watershed.

3.1.5 Monitoring Network

The monitoring network within the Upper Iowa watershed includes monitoring of precipitation, streamflow, and nutrients. The data collected by the instrumentation is important in determining historical trends relating to the water balance of the watershed. Within the watershed there are five daily NOAA rain gages, one Iowa Flood Center (IFC) steam stage sensor, seven USGS stream gages, where four measure stage, two measure stage and discharge, and one measures stage, discharge, and nutrients. The instrumentation is distributed throughout the watershed (Figure 3.10) and the time period of operation is shown in Table 3.1. For this study, the most important instruments are the USGS stream gages at Bluffton, IA, Decorah IA, and near Dorchester, IA because there records start in 2002 at the earliest and are recording the discharge of the Upper Iowa. In addition, the USGS stream gage near Dorchester is part of the Iowa Department of Natural Resources (IDNR) Ambient Stream Monitoring network where monthly measurements of nitrate and phosphorous are being recorded since 1999. Further efforts to

estimate the nutrients within the watershed are being conducted by the Upper Iowa River Alliance (UIRA) and the Northeast Iowa Resources Conservation and Development organization (NEIARCD). The first continuous water quality sensor will be deployed within the basin as part of the IWA project.

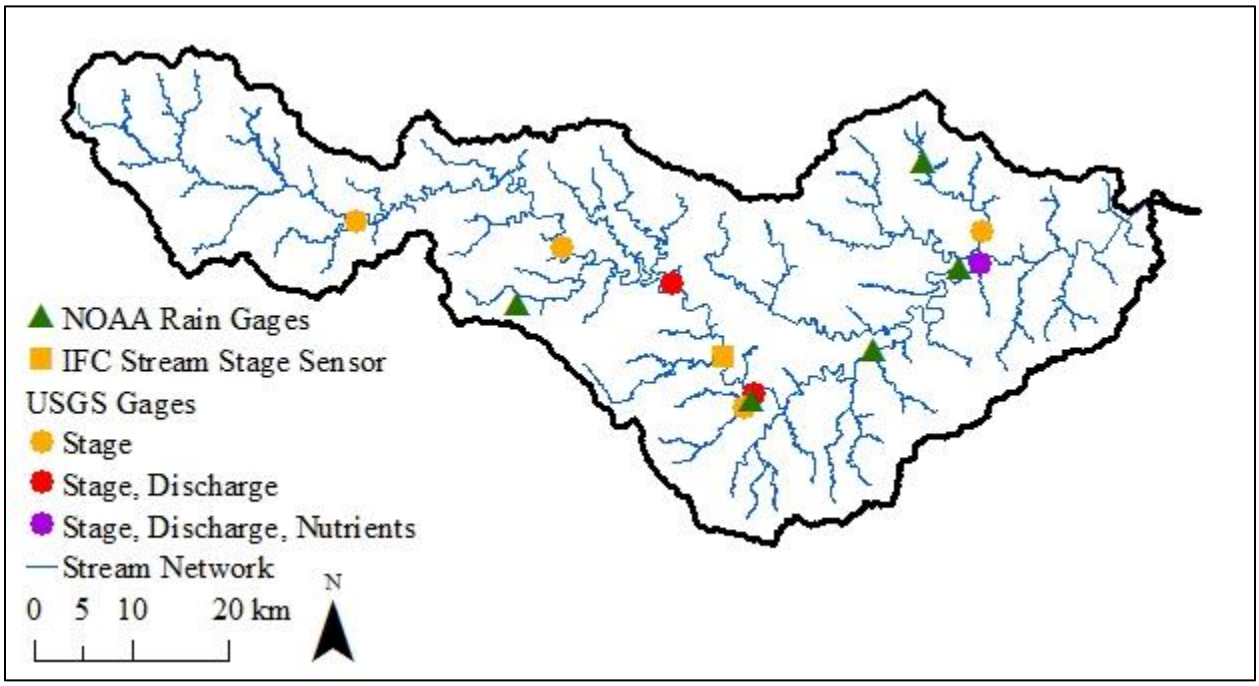

Figure 3.10. Hydrologic instrumentation within the Upper Iowa watershed including NOAA rain gages, IFC stage sensors, and USGS stream gages.

Table 3.1. Upper Iowa River Watershed Instrumentation Period of Record

Gage Type	Location	Period of Record
NOAA Daily Precipitation	Cresco 1 NE, IA	1893-present
NOAA Daily Precipitation	Decorah 7.9 ENE, IA	2007-present
NOAA Daily Precipitation	Decorah, IA	1893-1940, 1948-present
NOAA Daily Precipitation	Dorchester, IA	1947-2013
NOAA Daily Precipitation	Spring Grove, MN	1935-2001
NOAA Daily Precipitation	Spring Grove 4.4 SE, MN	2011-2015
IFC Stream Sensor (Stage)	Upper Iowa River, Decorah, IA, Bluffton Rd., County W20, Winneshiek County	2010-present
USGS Stage	Dry Run Creek near Decorah, IA, 05387490	2016-present
USGS Stage	Upper Iowa River at Kendallville, IA, 05387405	2016-present
USGS Stage	Upper Iowa River at Lime Springs, IA, 05387320	2016-present
USGS Stage	Waterloo Creek near Dorchester, IA, 05388310	2016-present
USGS Stage, Discharge	Upper Iowa River at Bluffton, IA, 05387440	2002-present
USGS Stage, Discharge	Upper Iowa River at Decorah, IA, 05387500	1951-1983, 2002-present
USGS Stage, Discharge, Nutrients*	Upper Iowa River near Dorchester, IA, 05388250	1938-1939, 1975-present

*Nutrients are measured monthly as part of the Iowa Ambient Stream Monitoring Network from 1999-Present.

3.2 Hydrology

With the use of the measured data collected by monitoring networks in a watershed, characteristics of how water flows through the watershed are described. Using a water balance approach, where the change in storage within a year is assumed to be negligible, it is generally assumed precipitation, the main driver of the hydrologic cycle, is equivalent to the two major

outflows of the watershed, evapotranspiration and discharge at the outlet of the watershed. In this way, water balance ratios for each year on record for discharge to precipitation (Q/P) and evapotranspiration to precipitation (ET/P) are calculated. The discharge component can be further simplified with the use of baseflow separation techniques into the two modes of transport to the river surface runoff and subsurface flow. Thus, the baseflow to discharge ratio (Q_B/Q) is calculated. With the water balance information long term trends are determined for the watershed on how water generally flows through the watershed. To determine the variability of streamflow within a year a smaller time scale of a month is used. The monthly analysis determines potential reasoning for higher flows and determine when flood risk is highest in the watershed. In this section, the annual and monthly hydrologic information will be discussed.

3.2.1 Annual Water Cycle

Annually, the Upper Iowa watershed, using precipitation data from PRISM Climate Group (2016), receives 85 cm of precipitation with an overall increasing trend since 1950 (Figure 3.11). Using the USGS stream gage near Dorchester on average 33% of the precipitation results as streamflow, leaving 67% as evapotranspiration. Since 1950, the fraction of streamflow is increasing with the three USGS stream gage stations trending slightly higher; however, the USGS stream gage at Bluffton has a short period of record and therefore the very high increasing trend is not realistic (Figure 3.12). Using the cursive digital filter for perennial streams with porous aquifers within the Web GIS Based Hydrograph Analysis Tool (WHAT) from Purdue University, the base flow was separated from the daily average flow measured from the three USGS stream gages in the Upper Iowa watershed (Jae Lim et al. 2005). The estimated average discharge from baseflow is equal to 73% with an increasing trend at Decorah and near Dorchester (Figure 3.13). The USGS stream gage at Bluffton indicates a decreasing trend; however, once again the trend is questionable to the short time period of the measured data (Figure 3.13).

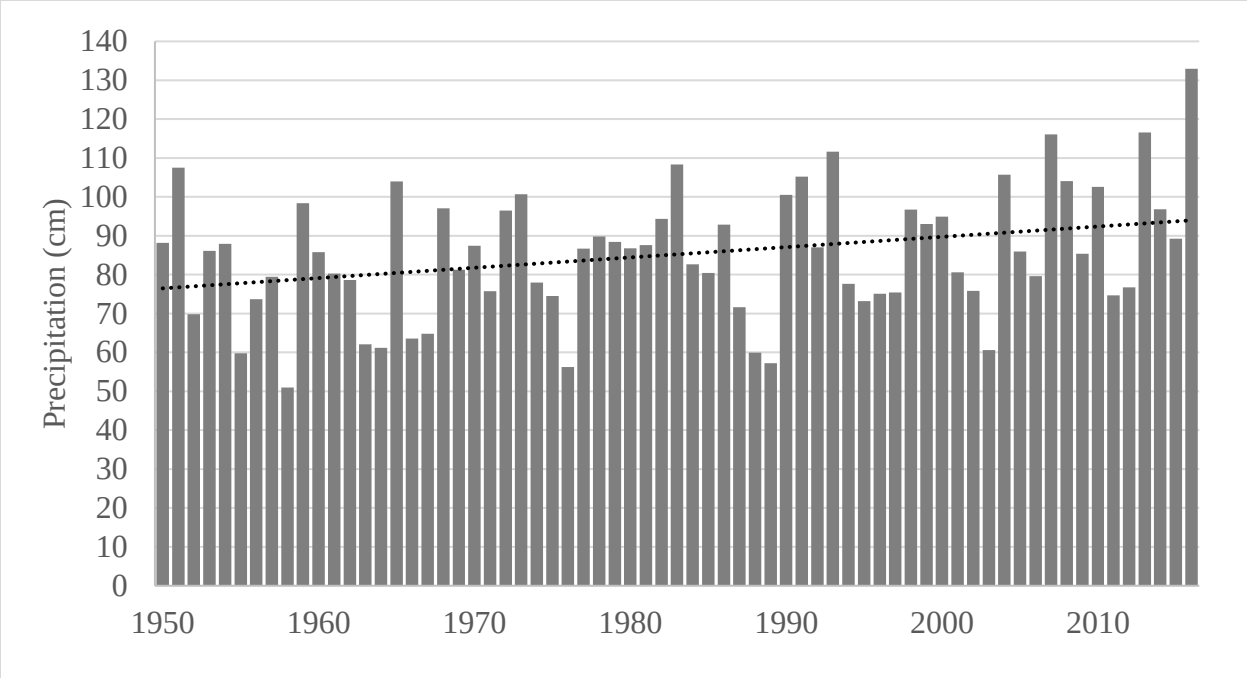

Figure 3.11. PRISM annual precipitation in cm for the Upper Iowa watershed (PRISM Climate Group 2017).

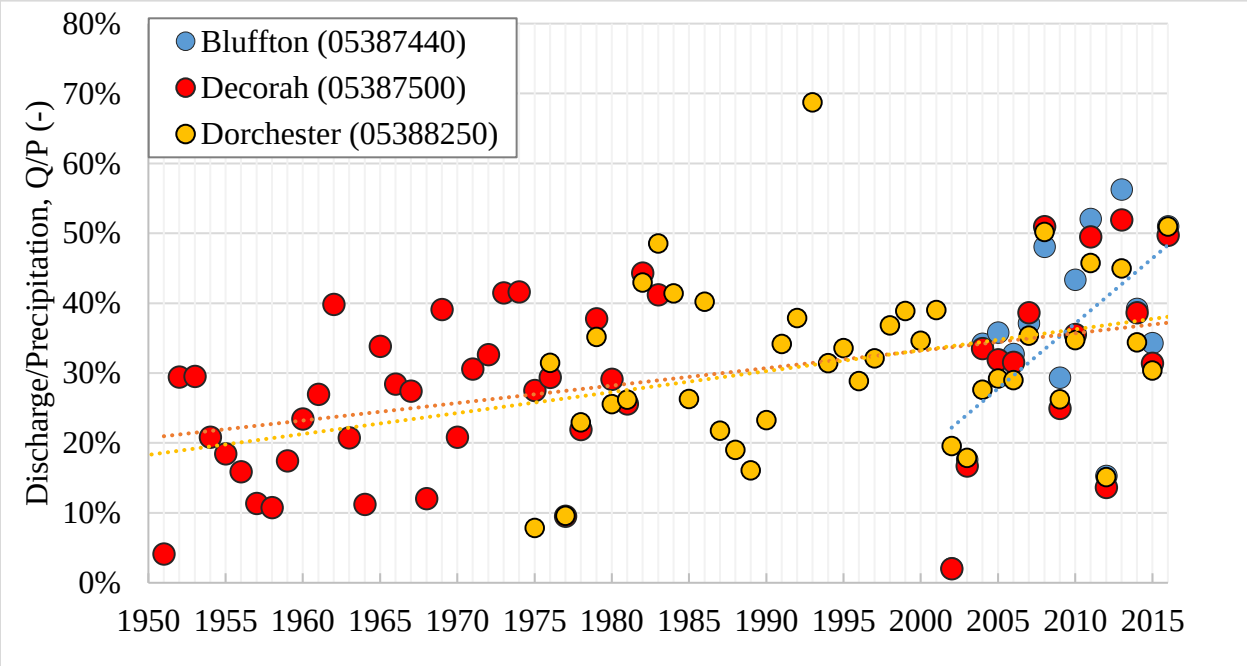

Figure 3.12. USGS Discharge to PRISM Precipitation ratio for the three USGS stream gages in the Upper Iowa watershed, Bluffton, Decorah, and Dorchester.

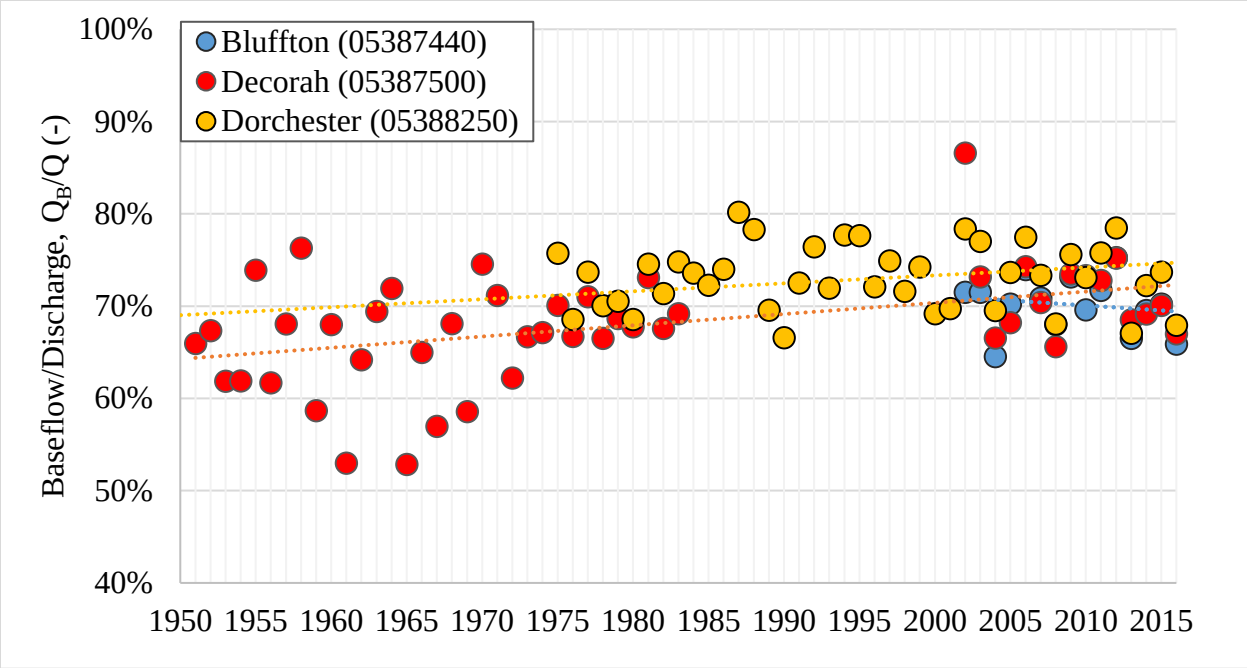

Figure 3.13. WHAT separated base flow to USGS Discharge ratio for the three USGS stream gages in the Upper Iowa watershed, Bluffton, Decorah, and Dorchester.

3.2.2 Monthly Water Cycle

Discretizing the annual balance into the monthly time spans the average distribution of rainfall and streamflow are shown in Figure 3.14 and Figure 3.15. The highest precipitation occurs during the summer, June to August, where June has the highest precipitation at 12.5 cm. The lowest precipitation occurs during the winter, December to February, with precipitation of 2.5 cm (Figure 3.14). The Upper Iowa River highest monthly average streamflow varies by stream gage with the highest flow occurring in Bluffton in June at 22.8 cms and April for Decorah and Dorchester at 20.4 and 32 cms respectively (Figure 3.15). The four highest average monthly stream flow months are shifted from the highest precipitation months and occurs from March to June (Figure 3.15). The reason for the difference is due to snow melt and evapotranspiration. Snow melt increases the discharge in March and leaves the soil close to saturation throughout the spring due to the small potential evapotranspiration during the cool spring months. Then the discharge decreases during late summer because the potential evapotranspiration is highest due to the long warm days of July

and August. The lowest discharge months follow a similar trend with precipitation with December to February having the lowest monthly discharge because of the below freezing temperatures limiting surface flow to the stream (Figure 3.15).

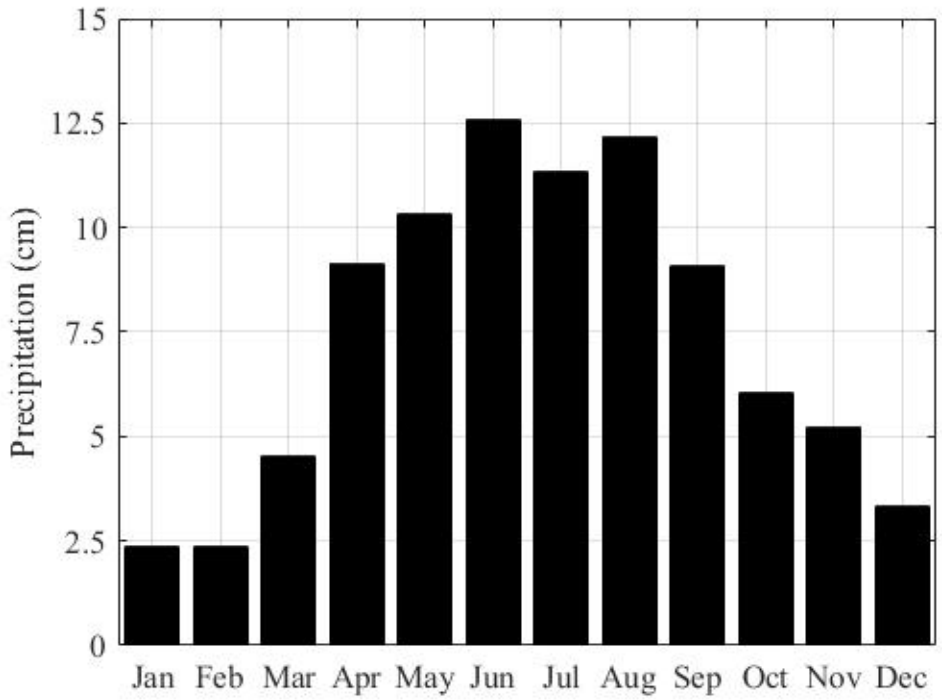

Figure 3.14. PRISM 1981-2010 average monthly precipitation (cm) for the Upper Iowa watershed.

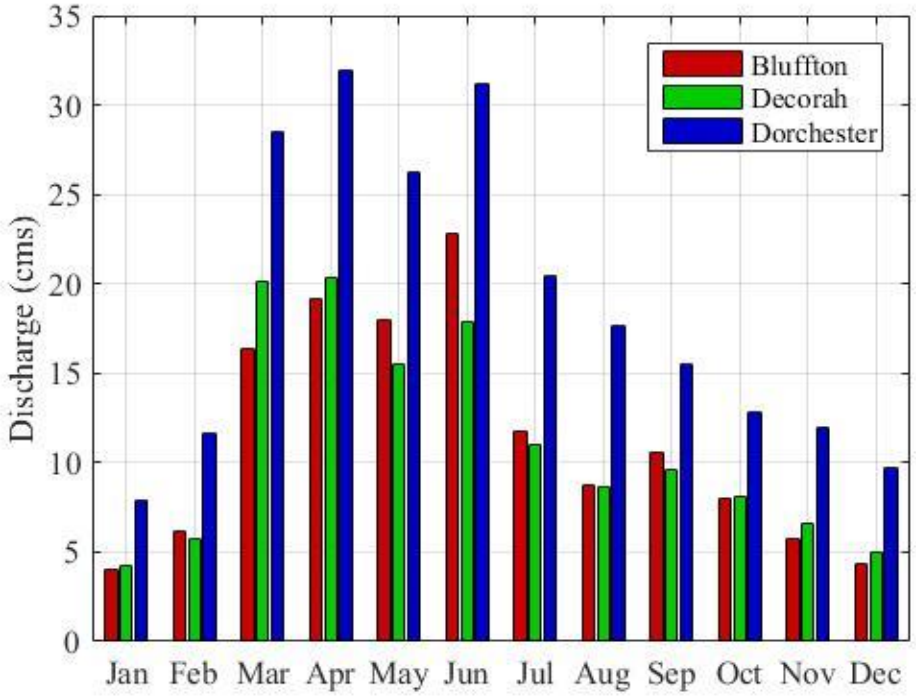

Figure 3.15. Average monthly discharge (cms) for the three USGS Stations at Bluffton (2002-present), at Decorah (1951-1983, 2002-present), and near Dorchester (1938-1939, 1975-present).

3.2.3 Flood Climatology

To understand extreme hydrologic events, it is first important to identify the time of the year when they occur. Figure 3.16 depicts day of the year the annual maximum discharge for the three USGS stations on the Upper Iowa River occurred for each recorded year. The annual maximum discharges typically occur from the end of February to the end of June with some sporadic events occuring until early September. The early spring events are typically caused by snow melt while the June events are caused large rainfall events occuring within a couple of hours to days. An estimation of whether the annual maximum discharge will cause flooding is to use the average maximum discharge as a benchmark. For the Upper Iowa River the average annual maximum discharge increases from 144 cms at Bluffton, the upstream end, to 196 cms, near Dorchester, the downstream end (Figure 3.16).

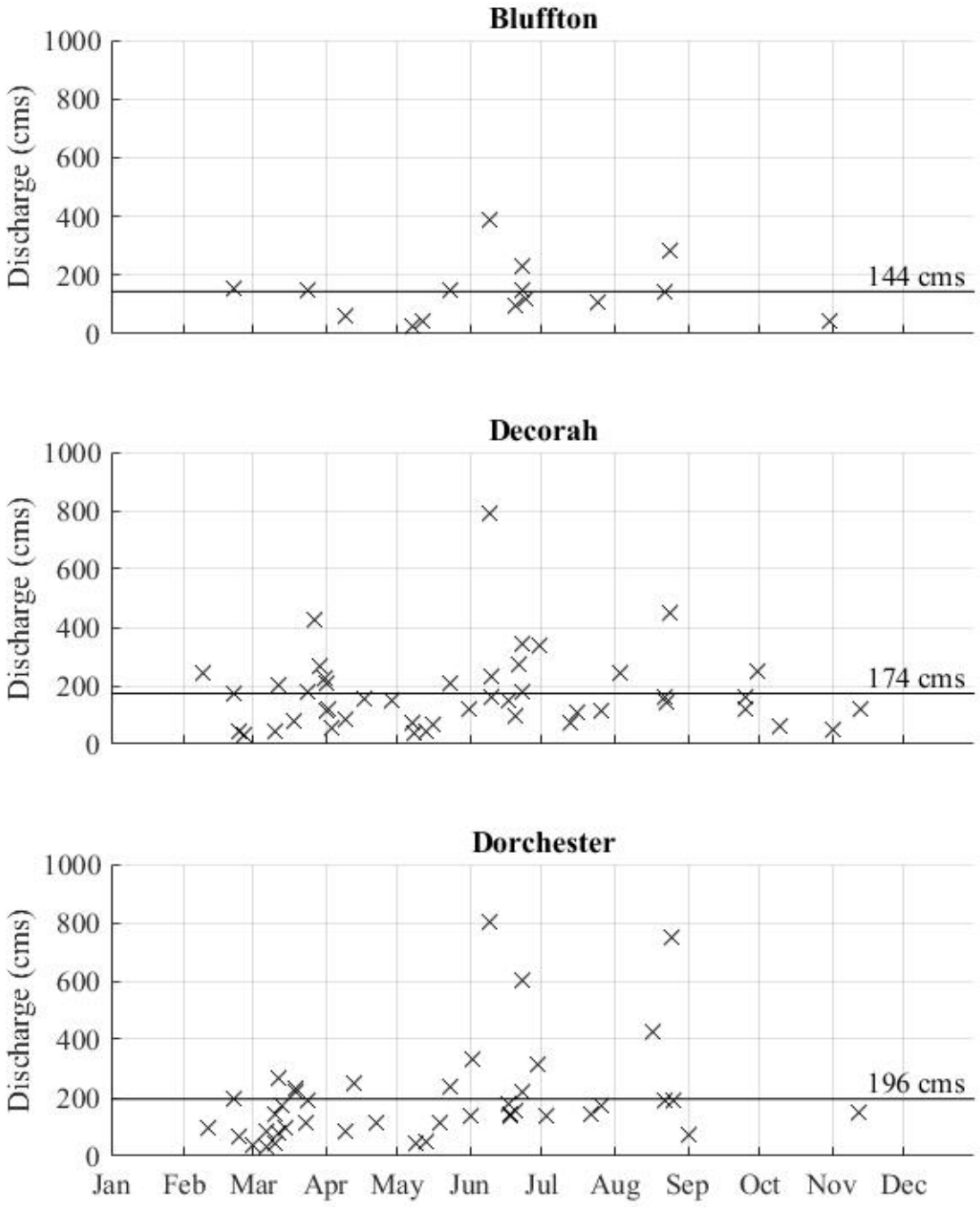

Figure 3.16. Annual maximum flood discharge occurrence in the day of the year for the Upper Iowa watershed at Bluffton, Decorah, and Dorchester and the average annual maximum discharge plotted as a line.

With the assumption that annual maximum discharges above the mean annual maximum discharge causes flooding, the probability of flooding throughout the year by month is calculated by determining the amount of annual maximums within each month (Figure 3.17). From this analysis the highest risk of flooding is through early spring to early summer with the highest risk in March and June. Similar to the monthly discharges, the highest flood risks are in March due to snow melt and June due to large convective storms occurring before evapotranspiration is strongest in late summer (Figure 3.17).

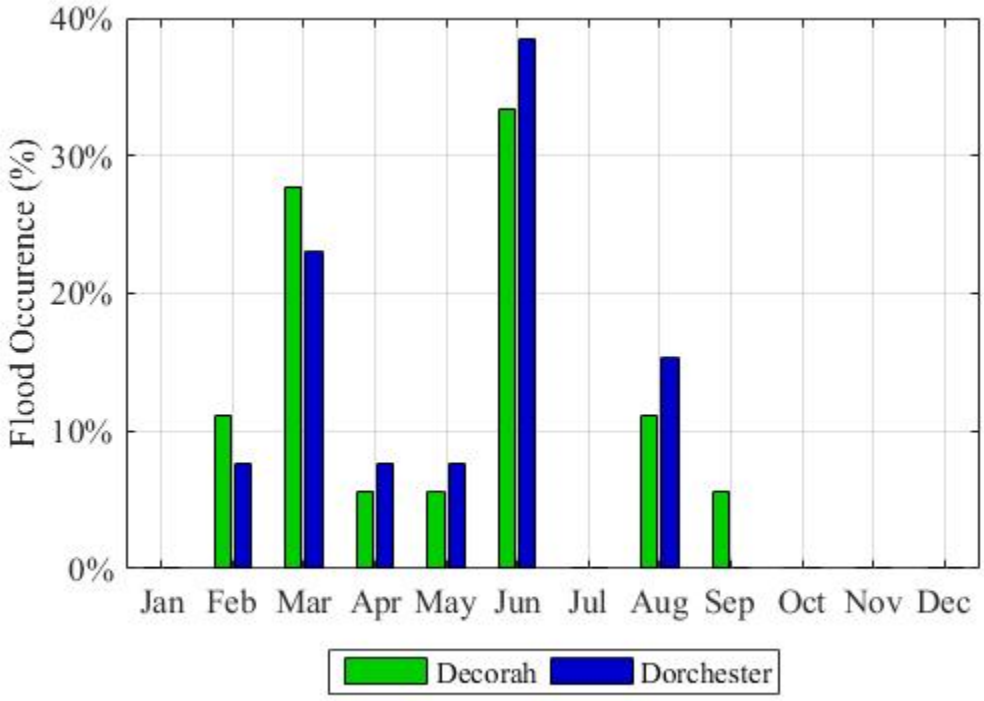

Figure 3.17. The percent of peak annual discharges that exceed the mean annual flood for the Upper Iowa River at Decorah and near Dorchester.

3.2.4 Floods of Records

For the Upper Iowa watershed there were five large flood events (discharge greater than 600 cms near Dorchester). The floods were recorded at the USGS Upper Iowa River stream gage near Dorchester, IA. Four of these events have occurred since 1993: August 24, 2016 with 1076 cms, June 9, 2008 with 883 cms, June 23, 2013 with 722 cms, and August 17, 1993 with 623 cms,

the first, second, fourth and fifth respectively (Table 3.2). These events also were large flood events upstream recorded at the USGS Upper Iowa River gaging station at Decorah and at Bluffton. In addition to the four large flood events, there have been two historic flood events. The first, the third largest recorded near Dorchester in May 31, 1941 with 861 cms and the second, the third largest recorded at Decorah with 572 cms (Table 3.2). Ultimately, the discharge that is observed near Dorchester continues downstream to the Mississippi River.

Table 3.2. Discharge from the Five Largest Flooding Events at USGS Gaging Stations in the Upper Iowa watershed including the Upper Iowa River at Bluffton, Upper Iowa River at Decorah and the Upper Iowa River near Dorchester

Upper Iowa River at Bluffton USGS 05387440 (2003-Present)	6/9/2008 470 cms	8/24/2016 391 cms	6/23/2013 340 cms	8/22/2007 239 cms	7/25/2005 221 cms
Upper Iowa River at Decorah USGS 05387500 (1952-Present)	6/9/2008 966 cms	8/17/1993 580 cms	3/27/1961 572 cms	8/24/2016 561 cms	6/23/2013 481 cms
Upper Iowa River near Dorchester USGS 05388250 (1939-1941, 1976-Present)	8/24/2016 1,076 cms	6/9/2008 883 cms	5/31/1941 861 cms	6/23/2013 722 cms	8/17/1993 623 cms

3.3 Existing Conservation Practices

As discussed in Section 2.1 conservation practices create storage and slow runoff, delaying and diminishing peak flows from a watershed. Within the Upper Iowa watershed existing conservation practices have been built. The IBMP project identified existing practices; fields containing contour buffer strips, fields containing strip cropping, grassed waterways, terraces, pond dams, and WASCOBs for the 2007-2010 time period (ISU GIS Facility, 2016). In total within the Upper Iowa watershed the total number of existing conservation practices are 12,905 ha of agricultural fields with contour buffer strips, 7621 ha of agricultural fields with strip cropping, 1610 ha of grassed waterways, 4811 terraces, 1299 pond dams, and 1091 WASCOBs. The distribution of the conservation practices based on HUC 12 watersheds are shown in Figure 3.18. The majority of WASCOBs, strip cropping and pond dams are located near the outlet of the watershed. In contrast, the least amount of grassed waterways are located within the HUC 12

watersheds close to the outlet of the watershed. Instead, the central watersheds contain the highest amount of terraces and contour buffer strips (Figure 3.18).

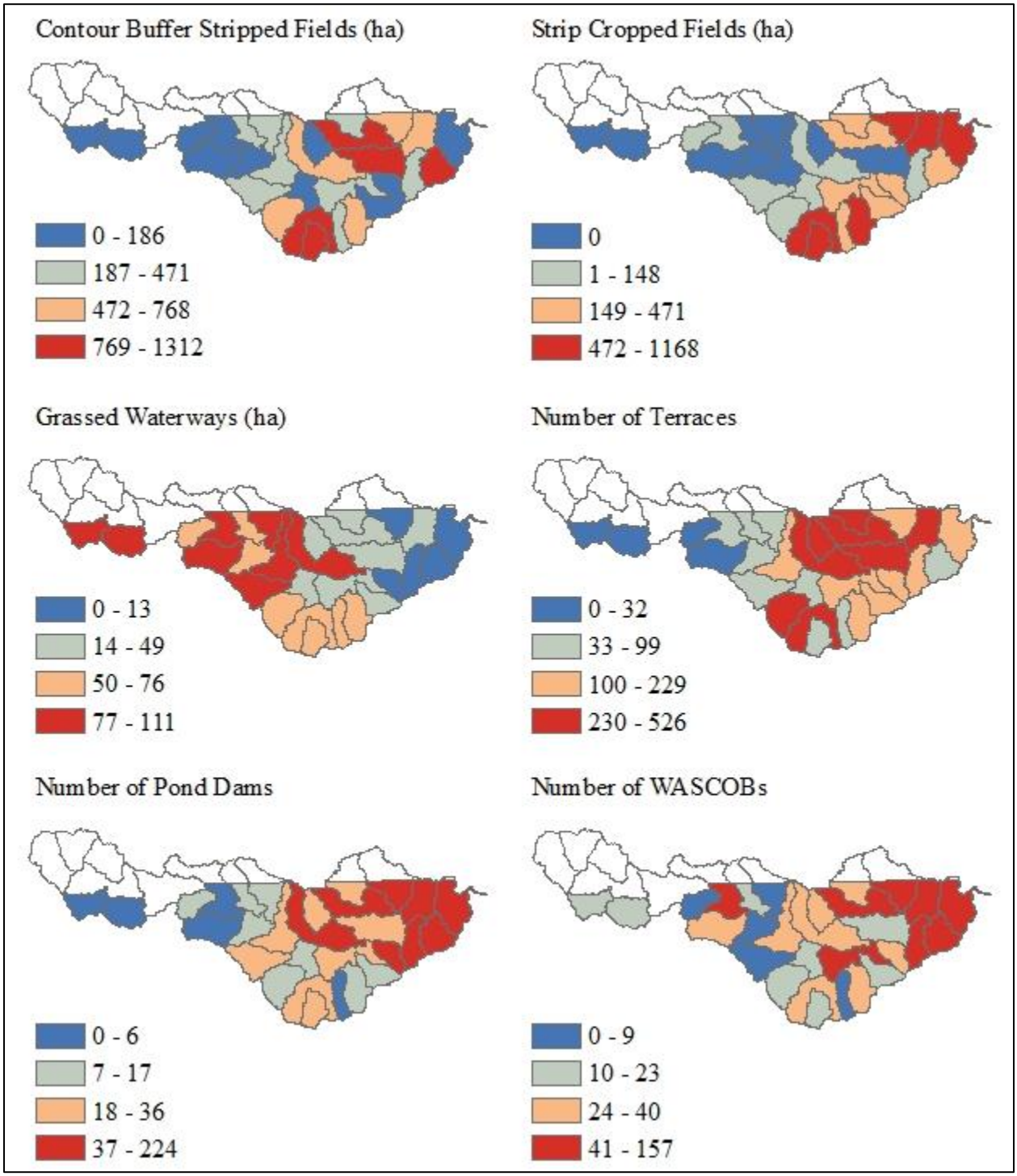

Figure 3.18. Existing conservation practices totaled by HUC 12 watersheds for the Iowa portion of the Upper Iowa watershed (ISU GIS Facility, 2018).

3.4 Summary

The Upper Iowa River watershed drains 2587 km^2 and is located in northeast Iowa and southeast Minnesota. The watershed is mostly agricultural with 45% cultivated crops and 21% pasture and hay. Topographically the watershed alters from west to east as the highest elevation and shallowest slopes in the west transition tothe lowest elevations and steepest slopes in the east. The west-east trend is due to the transition from the Iowan Surface, a glaciated rolling topography, to the Paleozoic Plateau, an unglaciated stepped topography. The soils within the watershed are mostly silt loam (68%) and well drained except within the Iowan Surface with more poorly drained soils. Within the watershed, monitoring networks from NOAA, USGS, and Iowa DNR are recording rainfall, stream discharge, and nutrient concentrations, creating a historical dataset that is used to determine the water balance for the watershed.

Annually, the Upper Iowa River watershed receives 85 cm of precipitation, with 33% leaving the watershed through streamflow and 67% from evapotranspiration. Of the streamflow 73% flows through the subsurface as base flow. The precipitation throughout the year varies with the most precipitation in the summer and least precipitation in the winter. The monthly average discharge is the highest from March to June with snow melt and evapotranspiration factoring into the difference between monthly precipitation and streamflow. Similar to the monthly average streamflow the majority of the annual maximum discharge events occur from March to June. Flooding events classified as discharges above the average annual maximum discharge are most prevalent in March due to snow melt and June and August due to large convective rainfall events.

To reduce the peak flows and nutrient loadings leaving the watershed conservation practices are built within the watershed. The IBMP project has identified 12905 ha of agricultural

fields with contour buffer strips, 7621 acres of agricultural fields with strip cropping, and 1610 ha of grassed waterways, 4811 terraces, 1299 pond dams, and 1091 WASCOBs in the watershed.

Chapter 4. Potential Conservation Practice Siting

Traditionally, when modeling conservation practices within hydrologic models 'typical' conservation practices are used as a default structures and placed throughout the location of the of watershed (Iowa Flood Center 2014; Ayalew et al. 2015). However with the use of geospatial tools, conservation practices closer to potential designed practices incorporating the shape of the landscape can be modeled. One such geospatial tool is the Agricultural Conservation Planning Framework (ACPF) developed by the USDA-ARS National Laboratory for Agriculture & the Environment. The ACPF creates a suite of potential practices that can be implemented within fields, below fields, and within riparian areas (Mark D. Tomer et al. 2013). Used together with different modeling approaches, prioritization of conservation practices selection and location can occur. M. D. Tomer et al. (2015b) used a spreadsheet model with ACPF results to identify scenarios in two HUC-12 watersheds that reduced the total nitrate concentration by 40% while only removing less than 5% of the cropland for production.

4.1 Model Inputs

The ACPF uses five datasets to identify potential conservation practices within a HUC-12 watershed. Four of the datasets can be downloaded as a file geodatabase, including; watershed boundary, gridded NRCS soils information, field boundary information from the USDA Farm Service Agency (FSA), and cropland data layer (CDL) from the USDA National Agricultural Statistics Service (USDA-NASS) (USDA ARS 2016). Using the USDA-NASS CDL information, the field boundaries have been classified by whether they are crops, pasture, or non-agricultural. Thus, ACPF will only identify conservation practices in agricultural fields (crops and/or pasture) within a watershed (M. D. Tomer et al. 2017).

The last dataset required for the ACPF is a LiDAR derived high resolution digital elevation model (DEM). For Iowa, the LiDAR derived DEMs can be obtained from the Iowa State

University GIS Facility at a 2 m resolution (James and Gelder 2016). These DEMs, must be further hydro-enforced. Hydro-enforcing is the manual process of identifying and removing artificial sinks created by roads and other man-made structures. Removing the artificial sinks, creates a DEM with a more realistic flow path.

The first toolset of the ACPF, the Stream Network Development toolset, has tools to aid in hydro-enforcing (Porter et al. 2017). First, from the DEM, the tool generates flow direction raster, the direction of flow for each grid; flow accumulation raster, the accumulation of cells for each cell; filled DEM with all sinks filled; and hillshade raster, the shaded relief of the DEM. Then a flow network can be derived depicting the locations of maximum flow accumulation and a depth grid can be derived from comparing the original DEM and the filled DEM. With the flow network and depth grid, artificial impoundments are identified and cut lines are drawn to correct the elevations as in Figure 4.1. With the hydro-enforced DEM complete, the final step of the Stream Network Development toolset is executed creating a stream network along locations where the user identifies perennial flow and the watershed boundary is estimated.

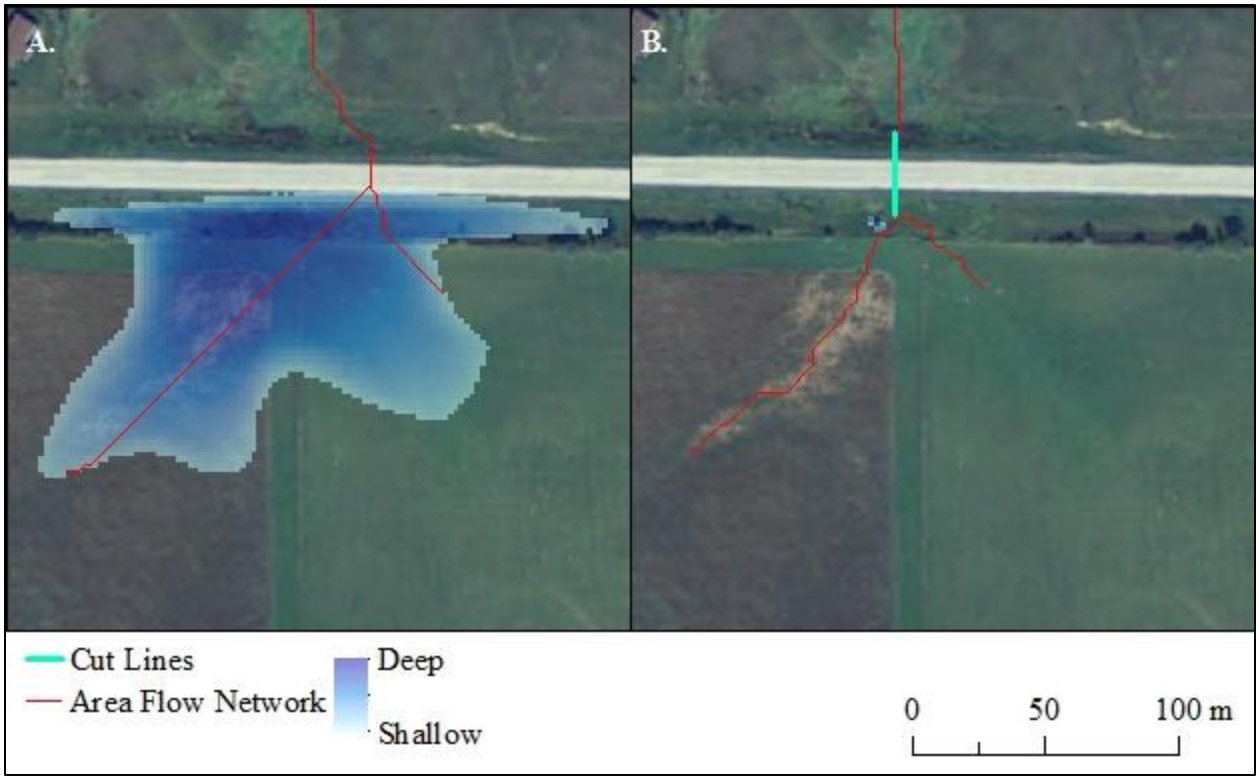

Figure 4.1. Example of the hydro-enforcing aid tools located within the Stream Development Toolset of the ACPF. A. contains pre-hydro-enforced depth grid and area flow network. B. contains post hydro-enforced flow depth grid, area flow network, and cut line.

4.2 ACPF Model Output

With the DEM hydro-enforced, the prioritization of farm fields and the identification of potential conservation practices can be executed. The ACPF has several different characterization schemes that can be used to prioritize farm fields including by slope, sediment delivery ratio (SDR), and run off risk. The slope ranking is based on the 75th percentile slope located within each field boundary. The SDR estimates the sediment delivery based on the distance from the stream (Ouyang and Bartholic 1997). These two parameters are classified as high risk, being the top 20%, medium risk, the next 40%, and low risk, the bottom 40% (Porter et al. 2017). Together, slope and SDR are combined via a two sided matrix to form the runoff risk assessment for each field, where the highest risk is associated with steep farm fields located next to the perennial stream (M. D. Tomer et al. 2015a). Examples of the field prioritization schemes are presented within the Ten

Mile Creek watershed, a HUC 12 watershed within the south central portion of the Upper Iowa watershed (Figure 4.2, Figure 4.3, and Figure 4.4).

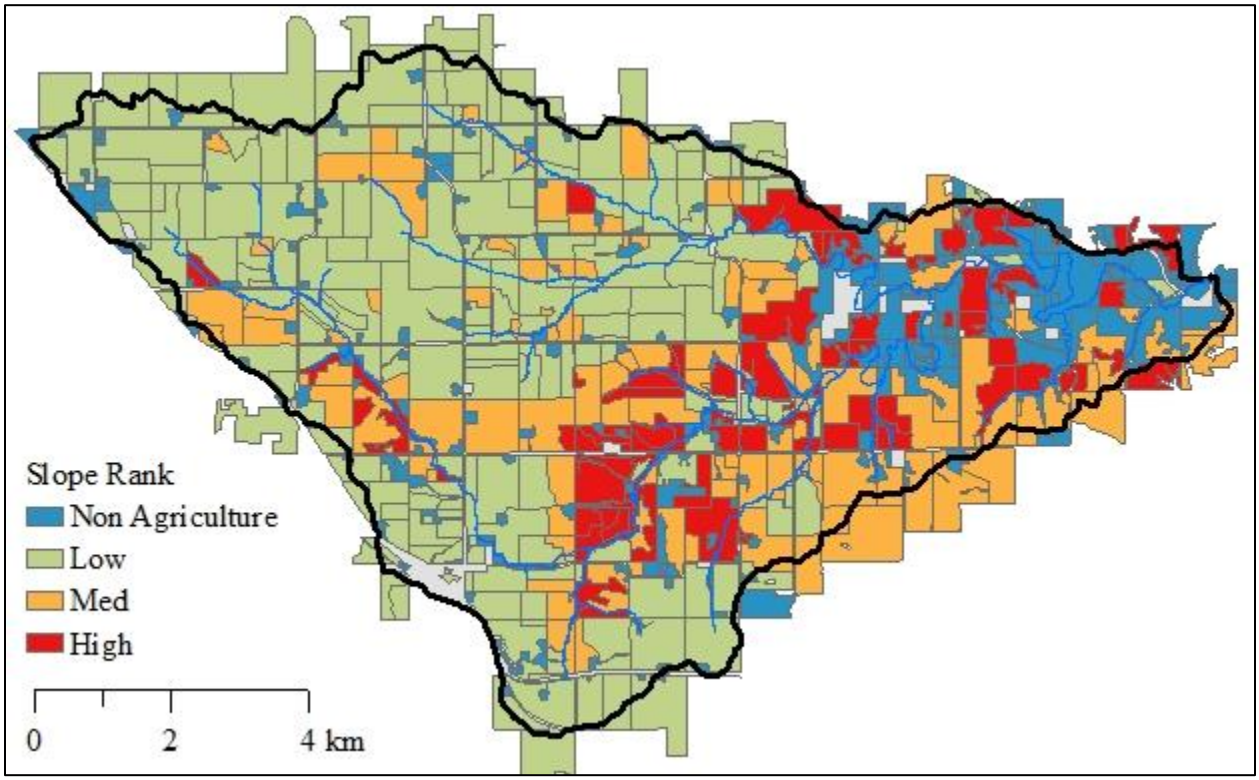

Figure 4.2. Example of the slope rank for Ten Mile Creek watershed.

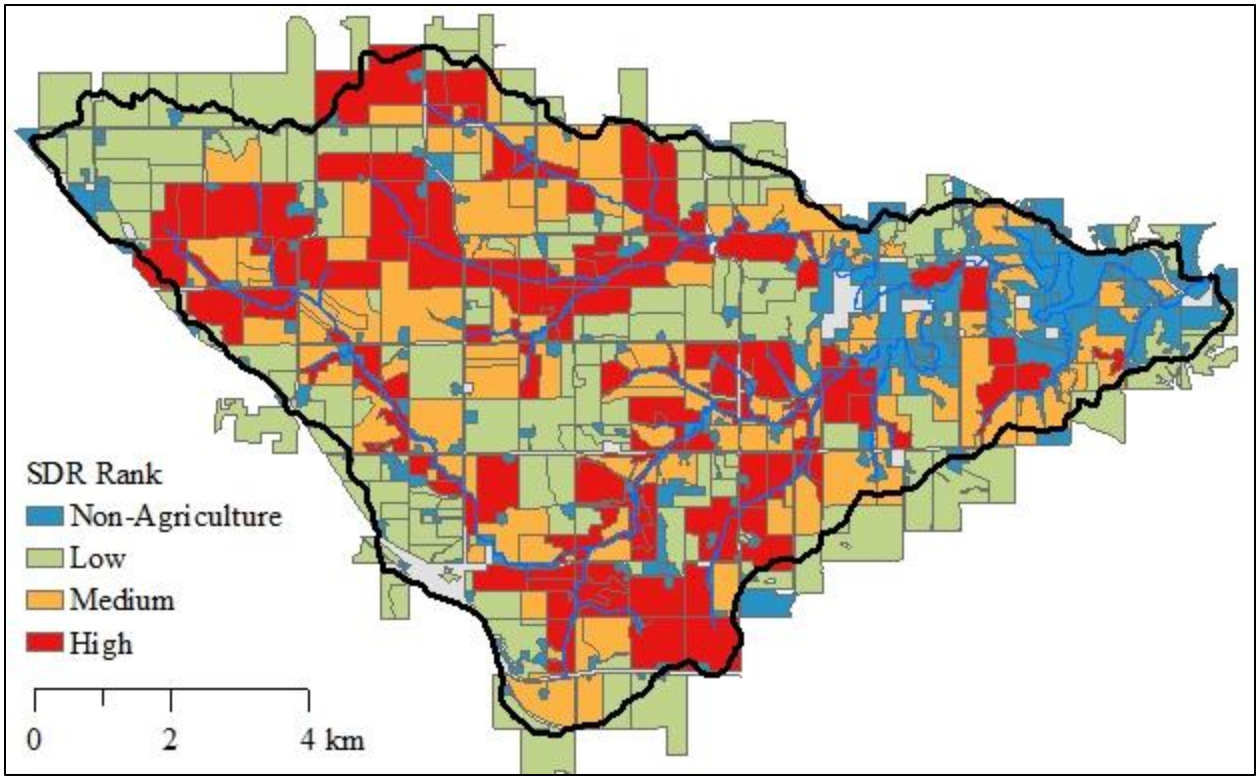

Figure 4.3. Example of the Sediment Delivery Ratio (SDR) rank for Ten Mile Creek watershed.

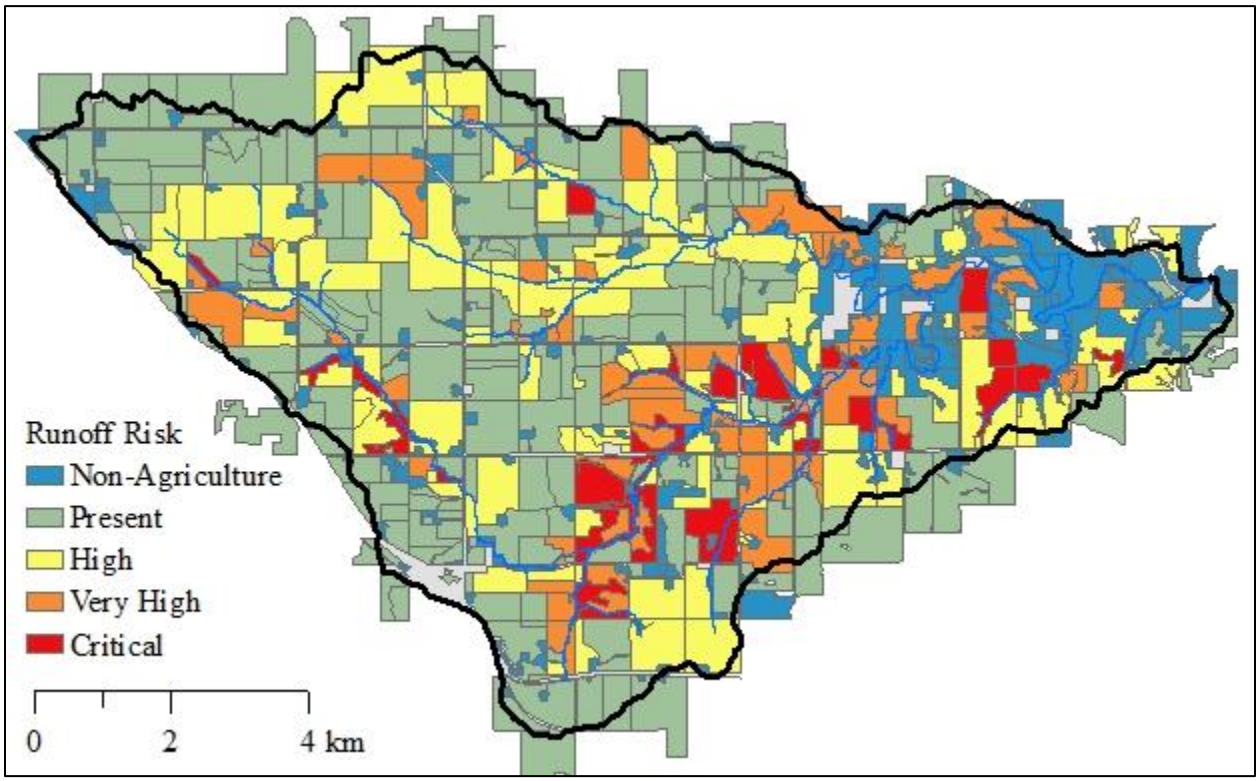

Figure 4.4. Example of the runoff risk for the Ten Mile Creek watershed.

In addition to field prioritization, the ACPF provides a tool to identify likely drain tiled fields. Drain tiled fields have significantly high nitrate concentrations and therefore are important to identify and mitigate there effects. The ACPF identifies them based on two criteria; slope and soil information. The fields are classified as tile drained if greater than 90% of the field has less than 5% slope and/or the soils are either greater than or equal to 10% hydric soils on average or greater than or equal to 40% of the field has dual classification for the hydrologic soil group (Porter et al. 2017). An example of the tile drained fields results are shown in Figure 4.5.

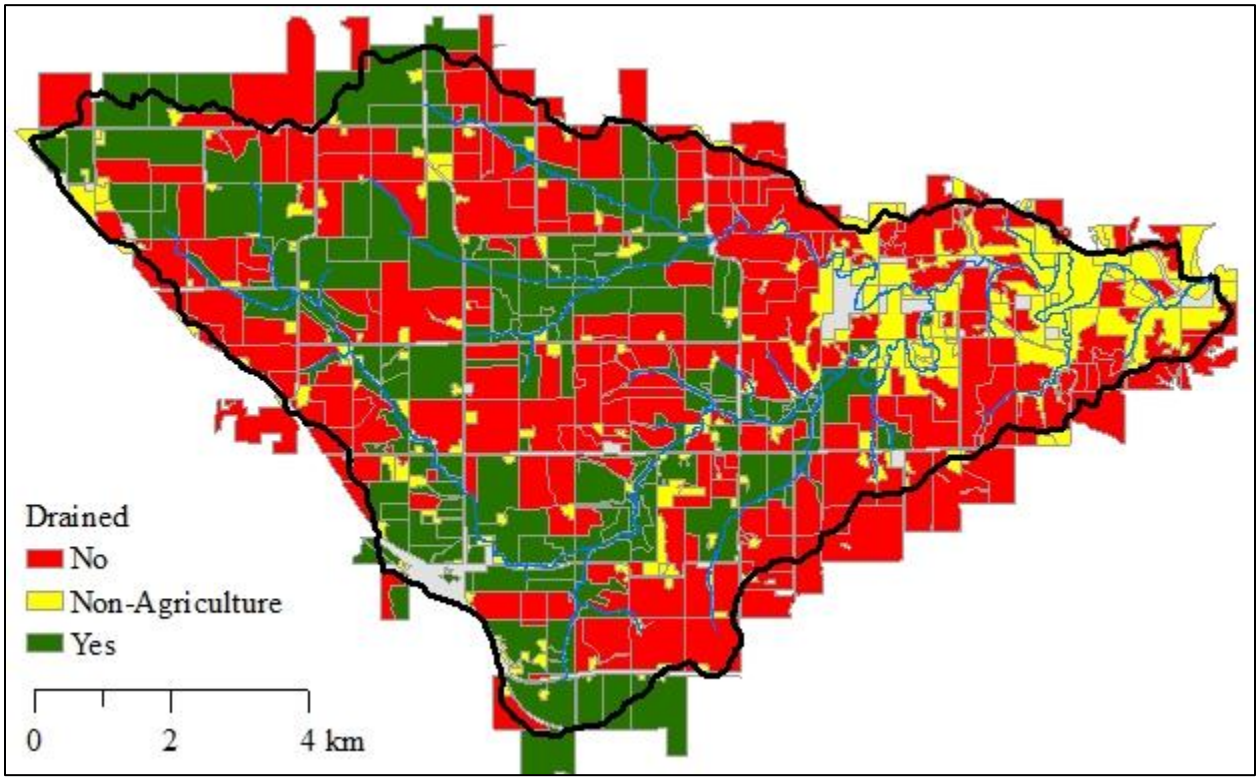

Figure 4.5. Example of ACPF tile drained fields for Ten Mile Creek.

The next set of tools start identifying potential conservation practices within the field and include practices reducing impacts of drain tile flow depression identification, fields applicable to drainage water management, and edge-of-field bioreactors; and practices reducing the impacts of surface flow, grassed waterways and contour buffer strips.

Depression identification, is used to identify potential locations where water drains to a closed depression for example, prairie pot holes within the Des Moines Lobe landform region of Iowa. These areas usually have a drain tile inlets and a common conservation practice is to maintain vegetation filter strips around the inlets to capture nutrients and sediment before entering the drain tile system. Depressions are located by identifying locations similarly to the Identify Impeded Flow tool but, with additional restraints including size criteria, surface area and depth; soil requirements mean percent hydric soils; and location within an agricultural field (Porter et al. 2017).

Drainage water management is a conservation practice used to control the water table within agricultural fields and is specified by NRCS code 554 Drainage Water Management. Controlling the water table gives farmers more control in the water availability for their crop through the year and in turn reduces the drain tile volume out of the fields potentially allowing time for denitrification to occur. The potential for drainage water management locations are identified by calculating the elevation difference within a drain tiled field and breaking the field into different zones based on a user specified contour interval. If any of these zones are larger than the area threshold specified by the user, the area is tagged as having the potential for drainage

water management (Porter et al. 2017). An example of results for one Ten Mile Creek is shown in Figure 4.6.

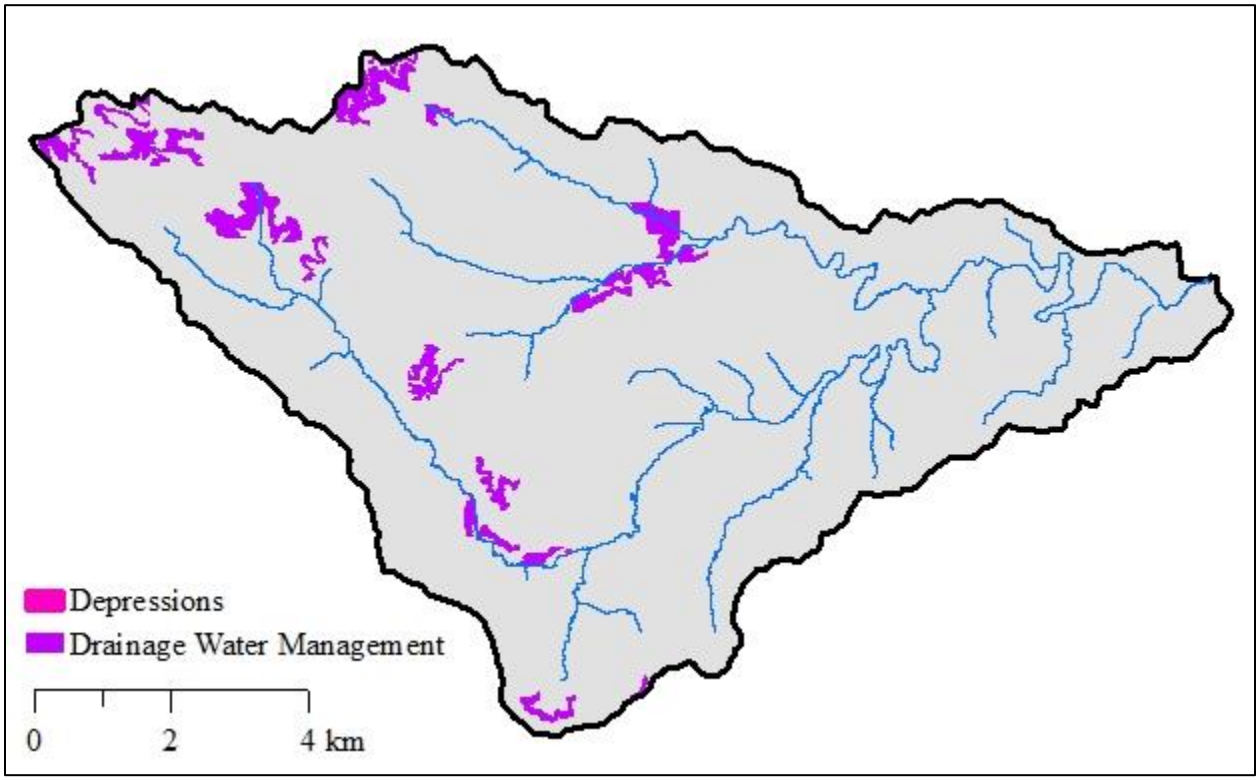

Figure 4.6. Example of the ACPF results for drainage water management located within Ten Mile Creek.

The last within the field drain tile practice identified within the ACPF is the edge-of-field bioreactor (from now on referred to as bioreactors) that are designed to NRCS code 605 Denitrifying Bioreactors. Bioreactors are buried wood chip filled compartments placed to intercept drain tile flow to remove nitrate through denitrification by bacteria. Potential locations for bioreactors are identified by analyzing the flow accumulation around the edges of field boundaries that lie downstream of the field and within a drainage area of 8 ha to 40 ha. With these points, a 100 meter buffer area within the field is applied and the area within 1 m above the elevation of the point is evaluated for the area required to treat the drainage area (greater than or equal to 0.5% of the upstream drainage area) and the soils are less than 90% hydric to avoid placing bioreactors in

poorly drained areas (Porter et al. 2017). An example of the results for bioreactors in Ten Mile Creek are shown in Figure 4.7.

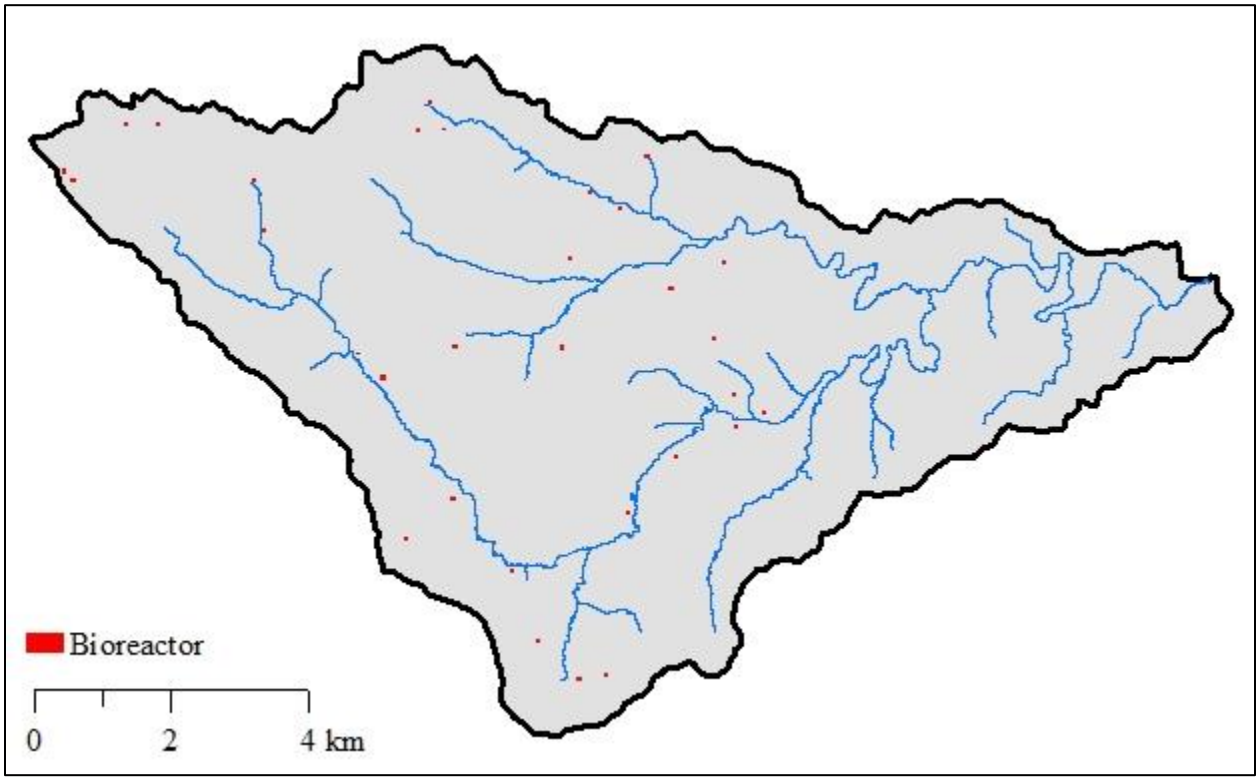

Figure 4.7. Example of the ACPF results for bioreactors located within Ten Mile Creek.

Grassed waterways, specified by NRCS practice code 412, are a conservation practice used to prevent gully formation in concentrated flow paths by planting grass. The grass holds down the soil with a root system, reduce the energy of the flow along the concentrated flow path, and with water flow can lie on the ground and act as a shield for the soil. Potential grassed waterways are identified using a threshold value for the stream power index (SPI). SPI is an estimate of erosive power across the landscape. Assuming the flow is proportional to the specific catchment area or the drainage area per unit length of contour, the SPI predicts erosion in areas of profile convexity and deposition in profile concavity (Porter et al. 2017). An example of the results for the Ten Mile Creek watershed is shown in Figure 4.8.

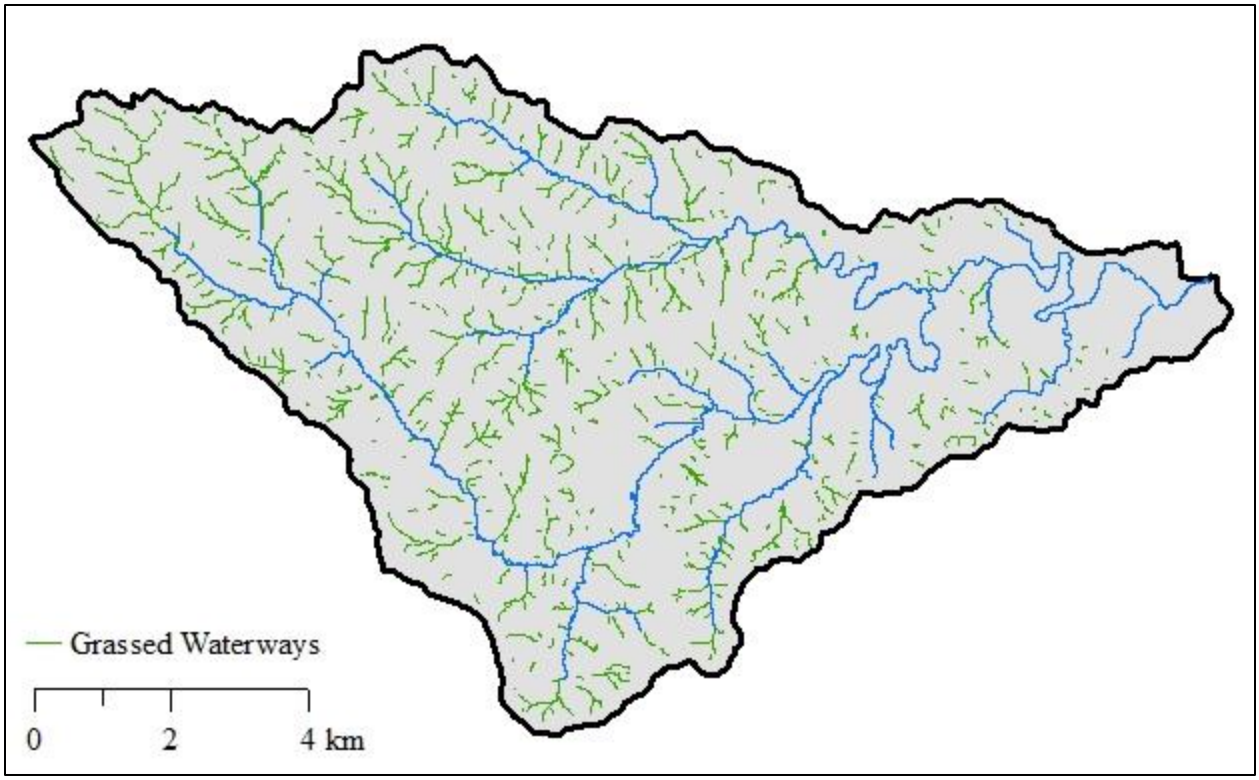

Figure 4.8. Example of the ACPF results for grassed waterways in Ten Mile Creek.

Complimenting grassed waterways are contour buffer strips. Contour buffer strips, specified by the NRCS practice code 332, are strips of perennial vegetation that are planted along the contour to reduce the slope length of the runoff and therefore reducing the energy of the runoff and preventing sheet and rill erosion. Using the 3rd quantile slope, calculated within each field boundary as a guide, the contour buffer strip spacing is created. Features with a length greater than 30.5 m are specified as a contour buffer strip location. An example of the contour buffer strip results are shown in Figure 4.9.

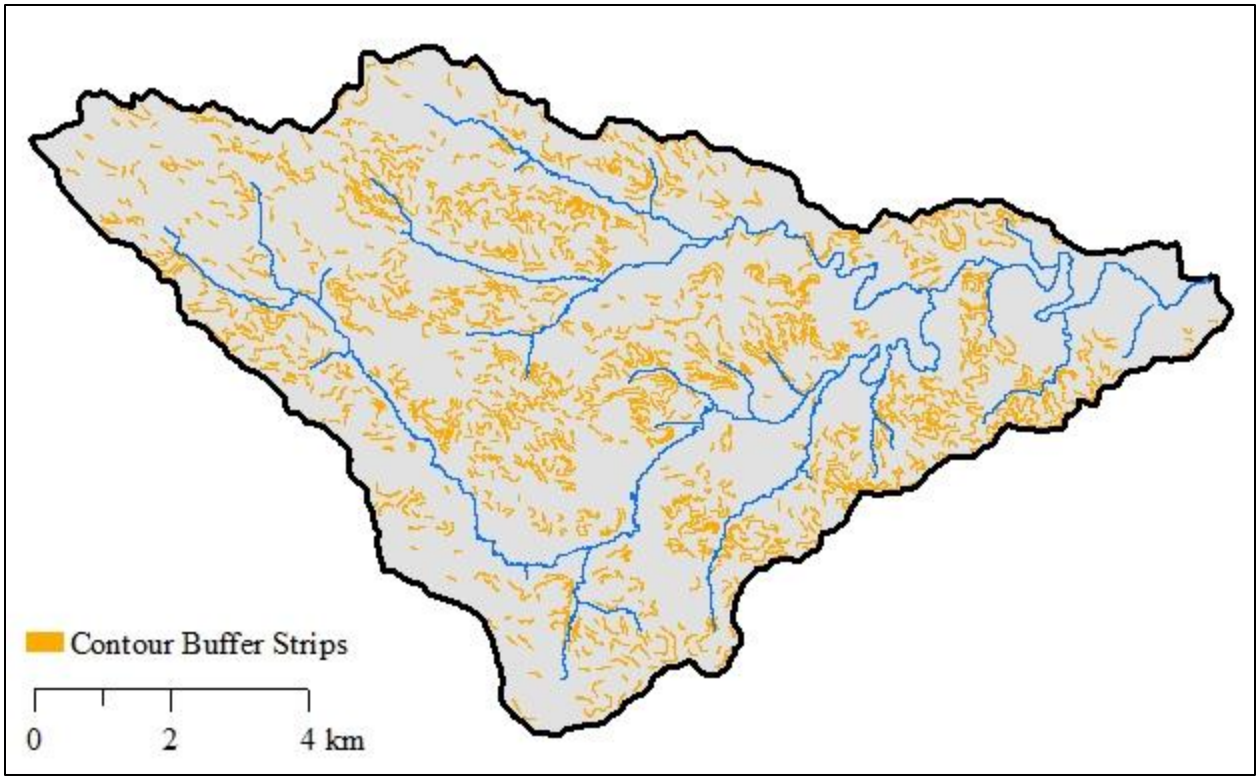

Figure 4.9. Example of the ACPF results for contour buffer strips in Ten Mile Creek.

The next two practices identified by the ACPF are below the field practices WASCOBs and nutrient removal wetlands specified by NRCS code 638 for WASCOBs and both NRCS code 656 Constructed Wetland and NRCS code 658 Wetland Creation for nutrient removal wetlands. Both practices slow runoff from agricultural fields by providing additional storage on the landscape. However, the wetlands have the added benefit of having the potential to remove nitrate from denitrification within a permanent pool. Similar point sampling technique along concentrated flow path networks are used to identify both practices. For WASOCBs transect lines at a user defined height are used to determine if the elevation at the transect line is between the user defined height and twice the defined height. While wetlands are identified using two user defined heights to define a pool area and buffer area from the DEM elevations that will be used to determine if the wetland meets Iowa's Conservation Reserve Enhancement Program (CREP). The CREP program requires the pooled area to drainage area ratio must be between 0.5-2.0% and the buffer area to

pooled area must be greater than 4.0% (Porter et al. 2017). A further difference is the WASCOB tool analyzes the flow path network between 0.8 ha to 20 ha within agricultural fields while the wetland tool analyzes drainage areas greater than 60 ha. Examples of WASCOBs and nutrient removal wetlands for Ten Mile Creek are shown in Figure 4.10 and Figure 4.11 respectively.

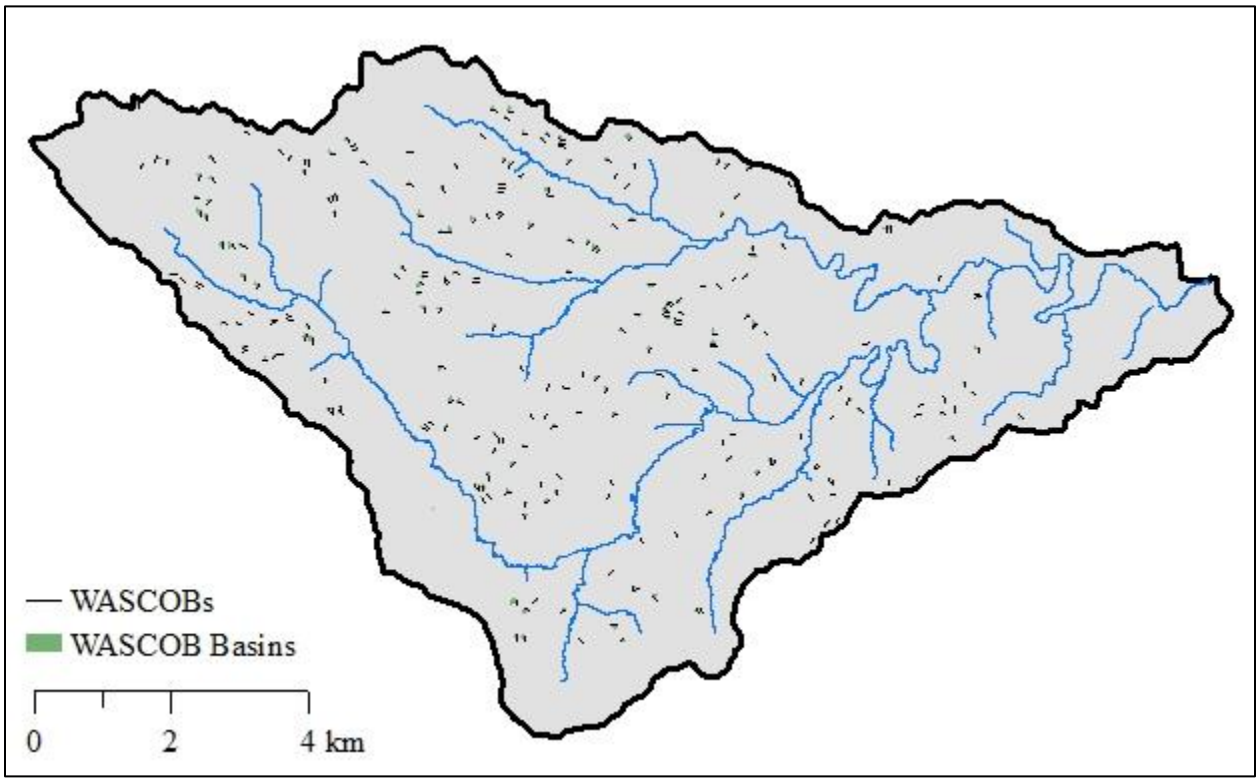

Figure 4.10. Example of the ACPF results for WASCOBs in Ten Mile Creek.

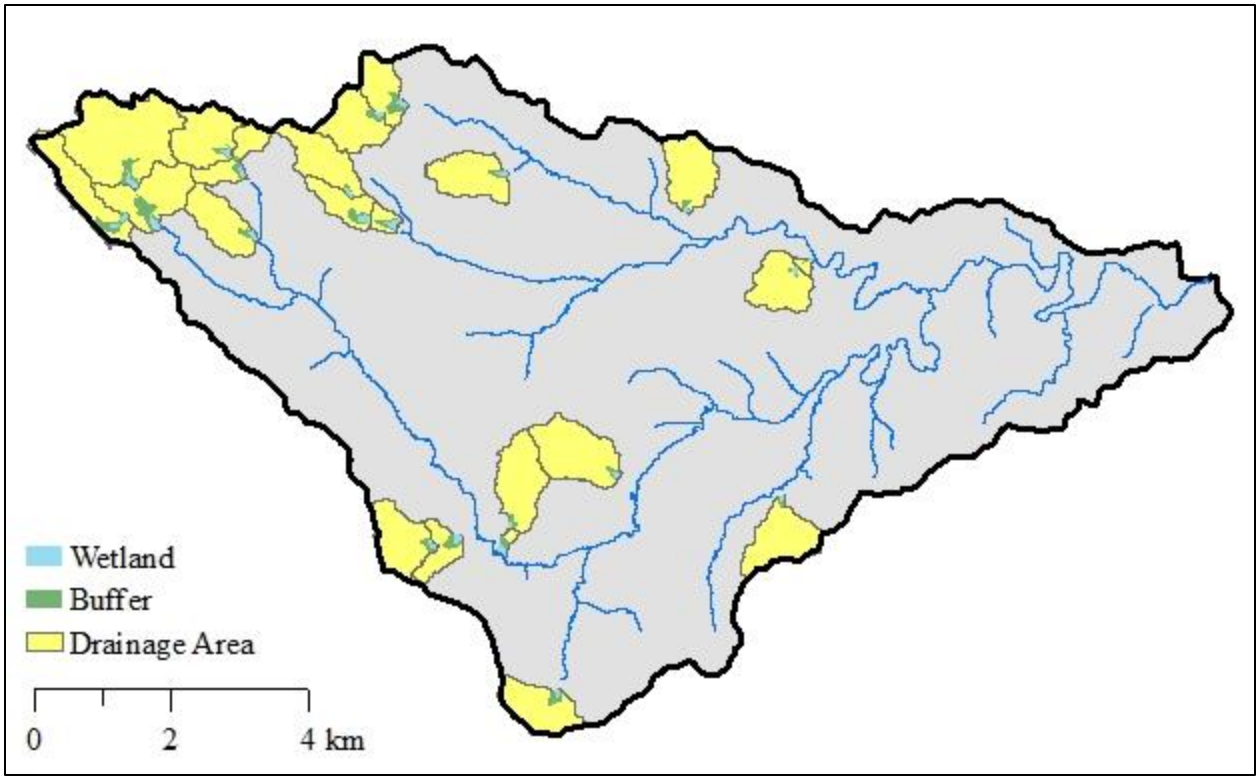

Figure 4.11. Example of ACPF results for nutrient removal wetlands in Ten Mile Creek.

The last set of ACPF tools analyze the riparian zone of a watershed in 250 m by 180 m zones for different types of riparian buffers and saturated buffers. Riparian buffers can be designed to trap runoff, nutrients, and sediment, specified by NRCS practice 391-Riparian Forest Buffer, and; stabilize stream banks, specified by 580-Streambank Protection. The applicability, width, type, and prioritization of practices for riparian buffer and saturated buffers are estimated based on the height above the channel, soils information, and slope. An example for the saturated buffer strips are shown in Figure 4.12.

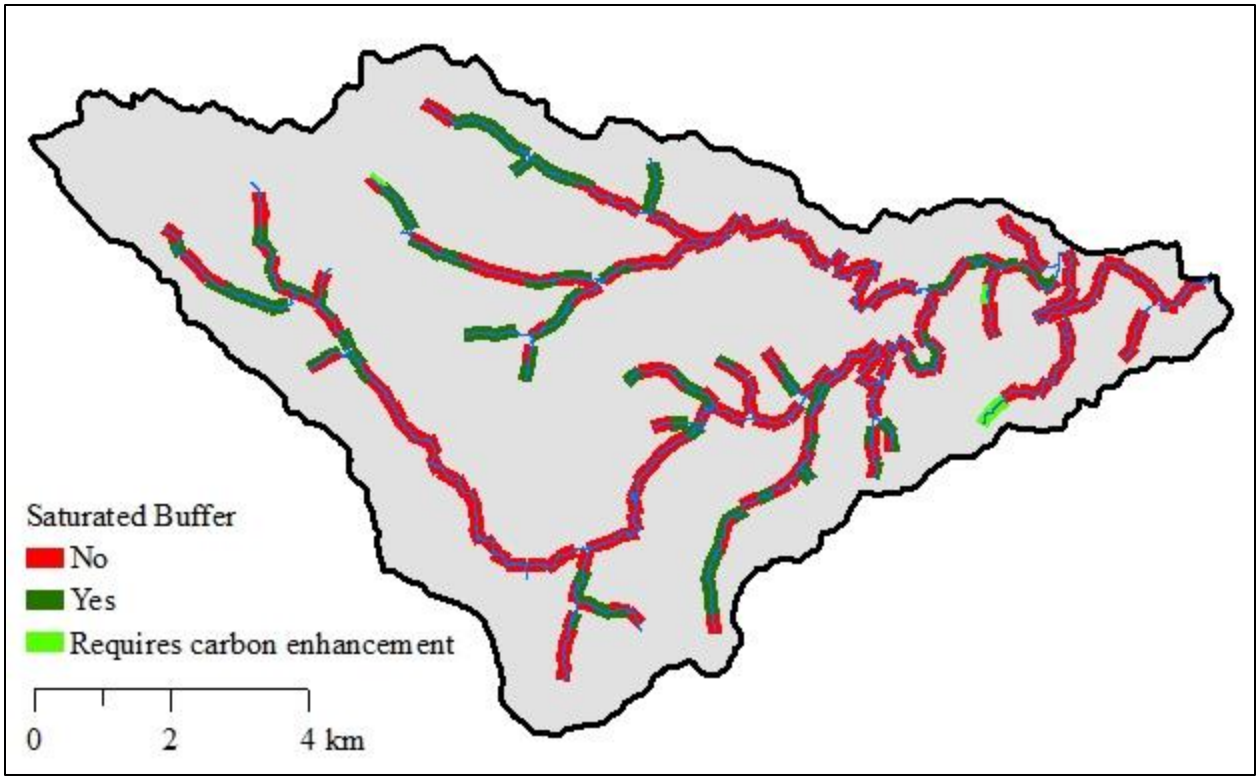

Figure 4.12. Example of the ACPF results for saturated buffer strips in Ten Mile Creek.

4.3 Upper Iowa ACPF Results

The ACPF was executed for the 34 HUC 12 watersheds within the Upper Iowa watershed. The execution involved the summarization of watershed characteristics including slope, Moore terrain derivatives, and land use percentages classified to the field-scale (Figure 4.13), tile drained conservation practice and riparian conservation practice totals (Figure 4.14) and conservation practice totals for surface flow practices (Figure 4.15). The total amount of potential conservation practices identified were 65 depressions, 6303 ha treated by drainage water management, 638 bioreactors, 4694 km of grassed waterways, 3224 ha of contour buffer strips, 5611 WASCOBs, 818 nutrient removal wetlands, and 7356 ha of riparian buffer and 647 km of stream with the potential for saturated buffers were identified. Besides the percentage of land that is pasture, being highest in the central portion of the Upper Iowa watershed, the majority of watershed characteristics follow an east-west trend where the highest values are either in the western portion of the watershed; mean TWI and percentage of agricultural fields or eastern portion of the

watershed; mean SPI, mean slope and non-agricultural land (Figure 4.13). The east-west trend within the Upper Iowa watershed is attributed to the change in geology from the gentler sloped Iowan Surface in the west to the more jagged topography of the Paleozoic Plateau in the east (Figure 3.6).

The tile drained conservation practices continue the east-west trend with the top quantile of tile drained fields, determined as having greater than 10% hydric soils or greater than 90% of the field having less than 5% slope, and top quantile of potential tile drained conservation practices located in the west with values decreasing eastward (Figure 4.14). The close relationship between TWI and tile drained flow has been identified before by Babbar-Sebens et al. (2013) who used TWI to identify potential wetland restoration projects within a watershed. The one exception to east-west trend for drain tile practices is at the outlet of the watershed. The outlet of the watershed has a higher percentage of alluvial plains. Alluvial plains are characterized by relatively flat poorly drained areas (Prior 1976). Thus, tile drainage is prevalent within the HUC 12 outlet watershed (Figure 4.14). In addition to tile drained conservation practices being prevalent in the east, riparian conservation practices are also more prevalent in the eastern half of the watershed, however, with a skew towards the length of perennial streams within the watershed (Figure 4.14).

Unlike the rest of the conservation practices, the ACPF surface flow conservation practices did not follow an east-west trend. Instead, surface flow conservation practices were most present within the central headwater watersheds including: Daisy Valley-Upper Iowa River, Cold Water Creek, and Pine Creek Northwest of Decorah and North Bear Creek and Waterloo Creek Northeast of Decorah Figure 4.15. For WASCOBs and contour buffer strips the least amount of practices were identified in the eastern portion of the watershed and near the outlet of the watershed because either there wasn't enough slope (in the east) for the practice to be needed or there wasn't a high

percentage of agricultural land (in the west). Lastly, a noticeable trend in the wetland implementation was lacking however, the topography relating to the storage created by the land may be the largest contributing factor.

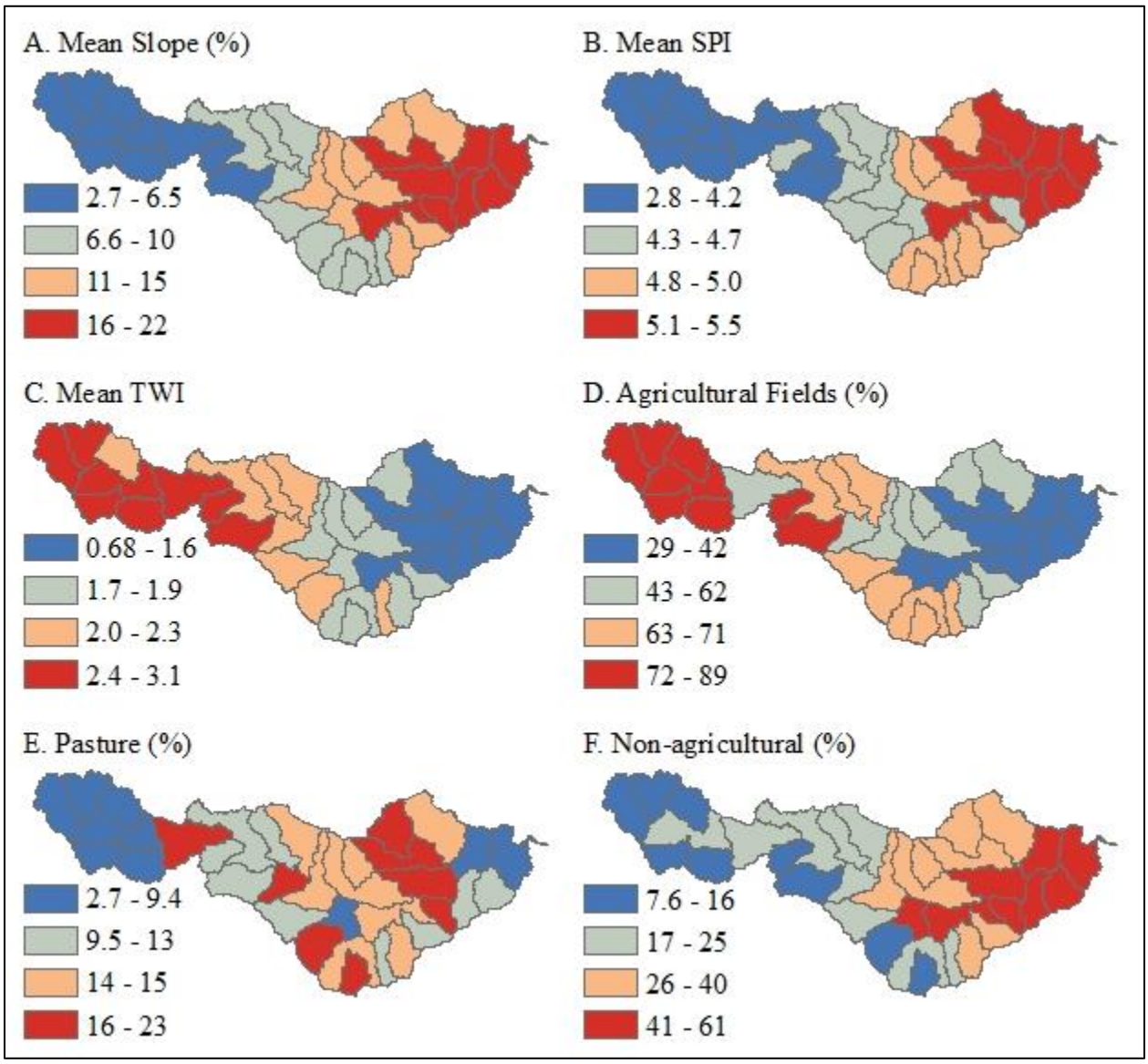

Figure 4.13. ACPF HUC 12 watershed characteristics for the Upper Iowa River watershed including; mean slope (A), mean SPI (B), mean TWI (C), percentage of agricultural fields (D), percentage of pasture (E), and percentage of non-agricultural land (F), divided into four quantiles. Part of the GIS work was performed as part of the IWA project.

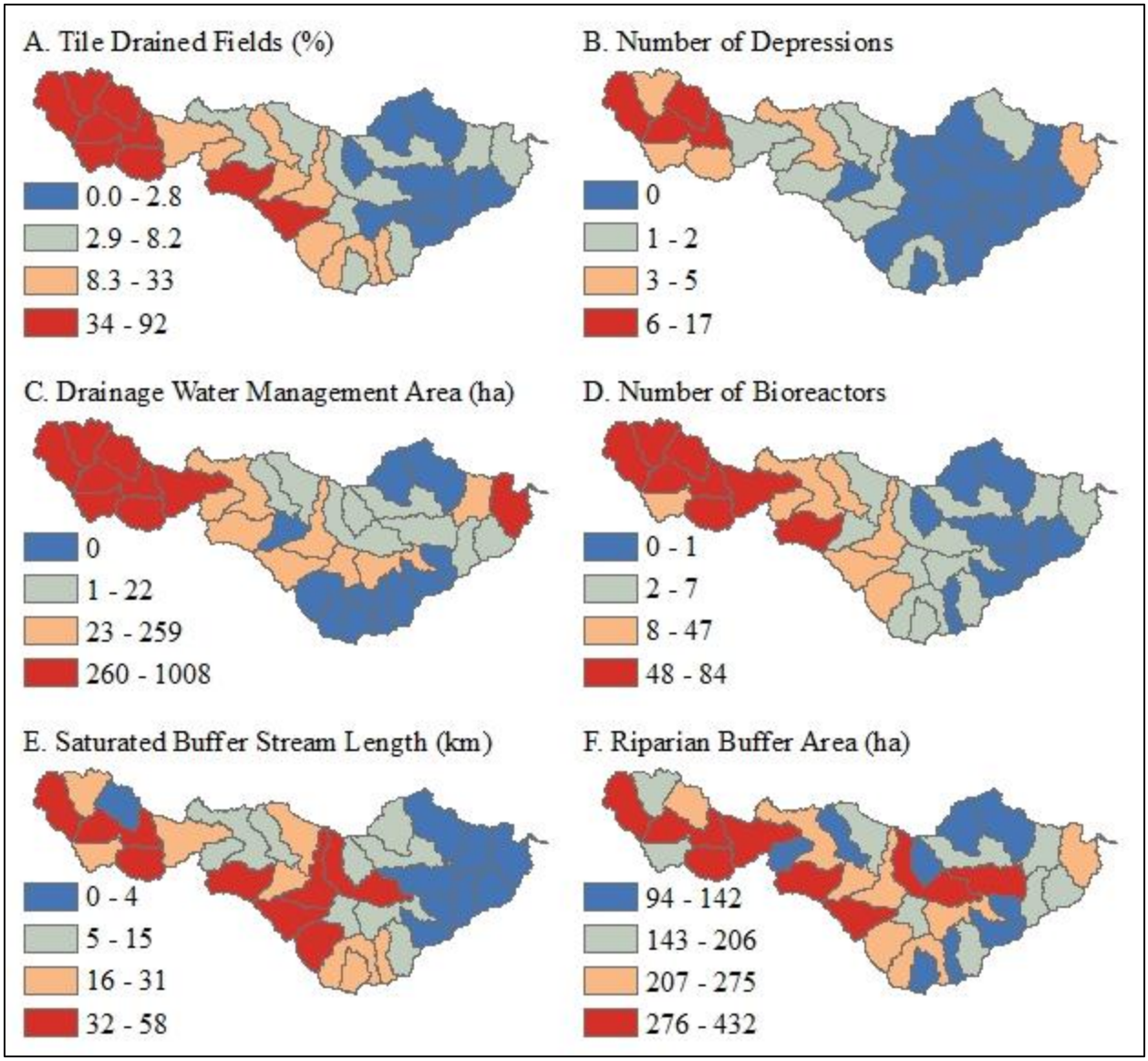

Figure 4.14. ACPF HUC 12 watershed summary for the Upper Iowa River watershed tile drained and riparian conservation practices including; percentage of tile drained fields (A), number of depressions (B), drainage water management area in ha (C), number of bioreactors (D), saturated buffer stream length in km (E), and riparian buffer area in ha, where values are divided into four quantiles. Part of the GIS work was performed as part of the IWA project.

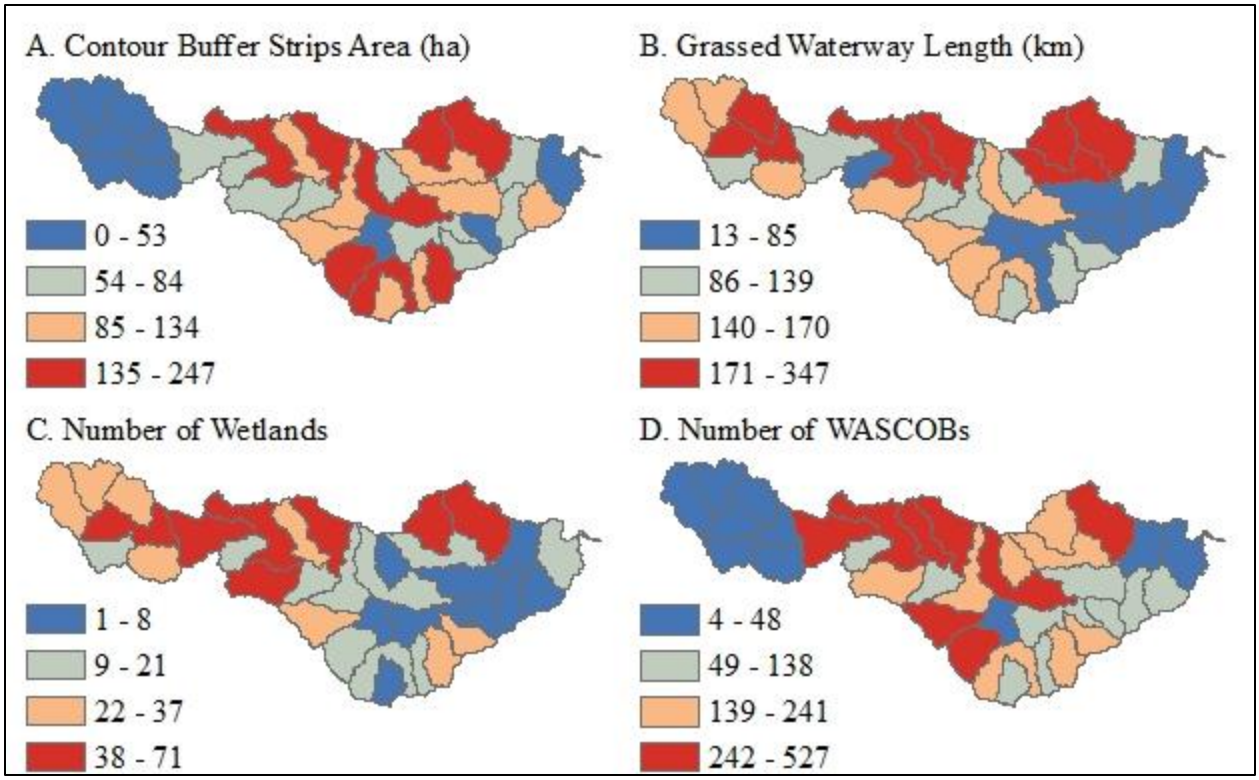

Figure 4.15. ACPF HUC 12 watershed summary for the Upper Iowa watershed surface flow conservation practices including; contour buffer strips area in ha (A), grassed waterway length in km (B), number of wetlands (C), and number of WASCOBs (D) where values are divided into four quantiles. Part of the GIS work was performed as part of the IWA project.

4.4 Summary

The ACPF is a GIS based precision conservation tool developed by the USDA-ARS National Laboratory for Agriculture & the Environment. The tool identifies a suite of potential practices on the field scale for a HUC 12 watershed using high resolution LiDAR elevation, crop data layer land use, NRCS soils, and FSA farm boundary information. The results of the ACPF include field prioritization, field tile drainage estimation, drain tile depression inlets, drainage water management, bioreactors, grassed waterways, contour buffer strips, WASCOBs, nutrient removal wetlands, saturated buffers, and riparian buffer zones. For the 34 HUC 12 watersheds in the Upper Iowa watershed, 65 depressions, 6303 ha treated by drainage water management, 638 bioreactors, 4694 km of grassed waterways, 3224 ha of contour buffer strips, 5611 WASCOBs,

818 nutrient removal wetlands, and 7356 ha of riparian buffer and 647 km of stream with the potential for saturated buffers were identified.

Chapter 5. Comparison of Potential and Existing Conservation Practices

Comparing the potential conservation practices identified by the ACPF to existing conservation practices provides several insights. First, similarities between the datasets can validate the ACPF algorithms. Second, targeting of specific areas lacking conservation but, with high potential can be performed. Lastly, watershed management plans become more realistic as the existing conservation dataset provides a benchmark and the potential conservation dataset provides how much more potential resources could be allocated. The below section was written for a research article (currently under revisions) and portions of the text were taken from it.

Rundhaug, T. J., Geimer, G. R., Drake, C. W., Arenas Amado, A., Bradley, A. A., Wolter, C. F., Weber L. J. (2018). Agricultural Conservation Practices in Iowa Watersheds; Comparing Actual Implementation with Practice Potential. *Environmental Monitoring and Assessment*, in revision.

5.1 Methods

For the comparison, three common conservation practices: grassed waterways, ponds and wetlands, and WASCOBs, were compared. The existing conservation practices were identified by the IBMP discussed in Section 3.3 while the potential conservation practices were identified with the ACPF. Analysis was performed in three different HUC 12 watersheds across three different landform regions in Iowa: Ten Mile Creek (070600020207) of the Upper Iowa River, Hinkle Creek (070802051102) of the Middle Cedar River, and The Headwaters of the North English River (070802090401) of the English River. The characteristics of the study areas are summarized in Table 5.1 and locations depicted in Figure 5.1.

Table 5.1. Basin Characteristics for the three HUC 12 Study Areas

	Ten Mile Creek	Hinkle Creek	Headwaters North English
Landform Region	Paleozoic Plateau/Iowan Surface	Iowan Surface	Southern Iowa Drift Plain
Drainage Area (km^2)	83	79	146
Average Basin Slope (%)	7.9	5.4	7.0
Agricultural Land Use (%)[1]	54	70	75
Agricultural Land Use (%)[2]	64	78	81
Perennial Stream Length (km)	55	67	211
Drainage Density (km^{-1})	0.67	0.84	1.45
Dominant Hydrologic Soil Group	C (57%)	B (85%)	B (74%)

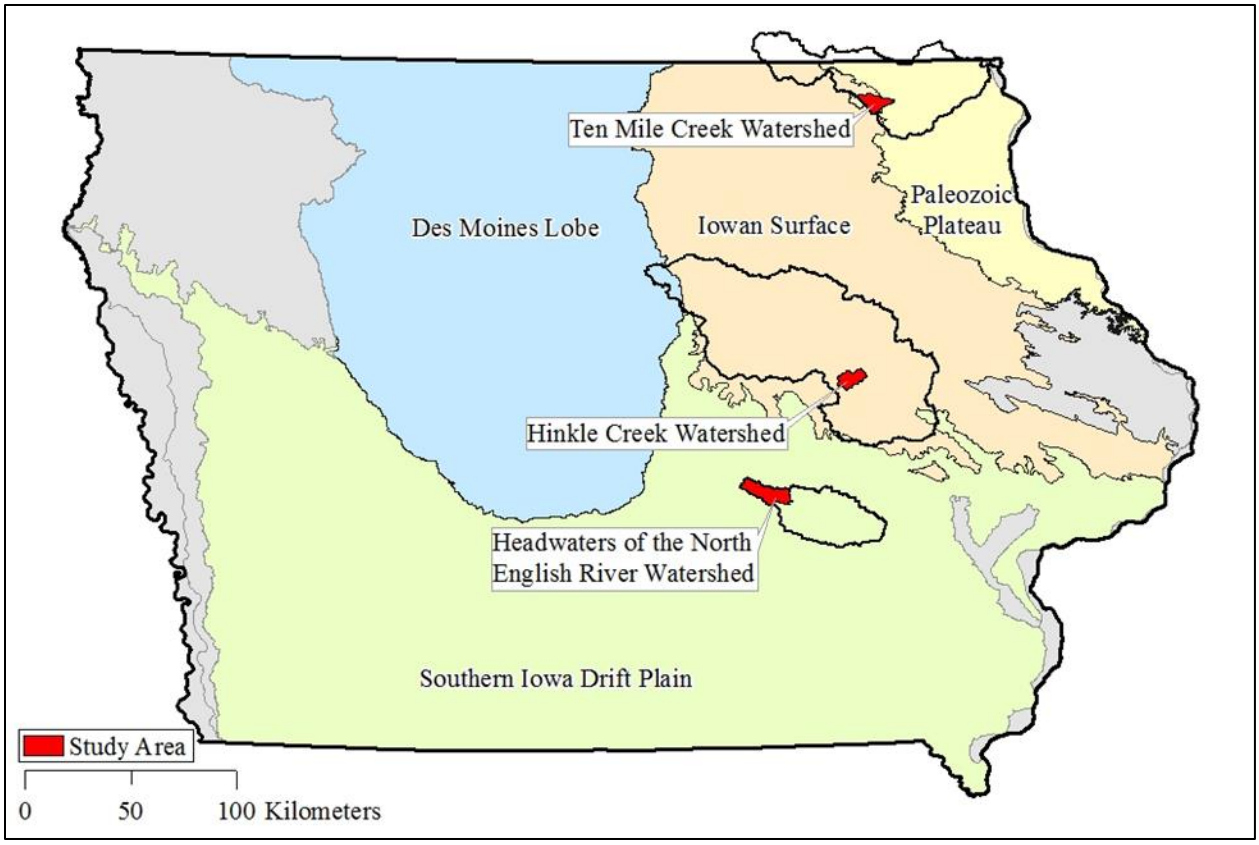

Figure 5.1. Study area map showing the three watershed areas in red (Ten Mile Creek in the Upper Iowa watershed, Hinkle Creek in the English River watershed, Headwaters North English in the Middle Cedar watershed) and the Iowa landform regions.

Ten Mile Creek is located in the south central portion of the Upper Iowa watershed with a drainage area of 83 km^2. The watershed is located on the western edge of the Paleozoic Plateau and the Iowan Surface (Figure 5.1). The Paleozoic Plateau extends across northeast Iowa and was untouched by the Pleistocene glaciers. Therefore, the landscape is very rugged with shallow bedrock, high cliffs, and karst topography (Prior 1976). The average slope for Ten Mile Creek is the highest of the three watersheds at 7.9%. The soils have a moderately high runoff potential (57% hydrologic soil group C) (NRCS 2016) and the land use is comprised of 54% corn and soybeans, 23% grassland and pasture, 10% deciduous forest, and 5% developed areas (USDA-NASS 2015).

Hinkle Creek is located in the southern portion of the Middle Cedar River watershed with a drainage area of 79 km^2. The watershed is located in the Iowan Surface (Figure 5.1). The Iowan

Surface extends across north central Iowa and was last glaciated during the Pre-Illinoisan. The landscape is characterized by low relief, glacial drifts, overlying limestone, and extensive tile drainage (Prior 1976). The average slope of the watershed is the lowest of the three study areas at 5.4%. The soils have a moderately low runoff potential (85% hydrologic soil group B) (NRCS 2016) and the land use is comprised of 70% corn and soybeans, 14% grass and pasture, 4% deciduous forest and 10% developed areas (USDA-NASS 2015).

The Headwaters of the North English River (hereafter referred to as Headwaters North English) is located in the far west portion of the English River with a drainage area of 146 km^2. The watershed is located in the Southern Iowa Drift Plain (Figure 5.1). The Southern Iowa Drift Plain extends across the southern half of Iowa and was last glaciated during the Kansan stage of glaciation. The landscape is characterized by steeply rolling hills interspersed with areas of level uplands and alluvial plains (Prior 1976). The average slope of the watershed is 7.0%. The soils have a moderately low runoff potential (74% hydrologic soil group B) (NRCS 2016) and the land use is comprised of 75% corn and soybeans, 15% grass and pasture, 1% deciduous forest and 7% developed areas (USDA-NASS 2015).

Prior to comparing the two datasets, a method to facilitate a more one-to-one comparison was created for the three conservation practices. The methodology for the IBMP ponds and ACPF wetlands, and WASCOBs comparison is straightforward with the extraction of the drainage area from the flow accumulation raster. On the other hand to compare the grassed waterways, the results were intersected on to a 5 acre flow path network. However, neither the existing grassed waterways due to the manual identification process, nor the potential grassed waterways, due to SPI being a function of flow accumulation and slope directly aligned onto the flow path network. As a result, a five meter buffer was applied to the existing grassed waterways while a design estimation process

was created to estimate the top width and therefore a realistic buffer width for each grassed waterway.

The ACPF grassed waterways buffer was estimated by the top width of the grassed waterway cross section. The estimation process was based on USDA-NRCS Code 412 Grassed Waterways (USDA-NRCS 2015) design standards. The capacity of the grassed waterway was sized to meet the peak flow of the 10-year 24-hour storm estimated from National Oceanic and Atmospheric Administration Atlas 14 precipitation for the Midwest (NOAA 2013), assuming an NRCS unit hydrograph method coupled with the NRCS watershed lag method for estimating time of concentration. The 2011 National Land Cover Database (USGS 2011) and the NRCS gridded soil data (NRCS 2016) were used to calculate the runoff curve number using the NLCD Runoff Table specified by (Mead and Diaz 2013). The sized trapezoidal grass channel have a 6:1 side slope and a Manning's roughness of 0.035. Criteria for the channel were that the bottom width must be between 3.048 m (10 ft) and 30.48 m (100 ft), and the flow velocity must be greater than 0.4572 m/s (1.5 ft/s). The channel bottom width for the design flow was first calculated assuming a water depth of 0.3048 m (1 ft). If the computed width fell outside the limits, the width was set to the appropriate limit (10 or 100 ft) and the design water depth was calculated. If the computed velocity was below the limit, the water depth was increased iteratively until the flow velocity met the minimum criteria for the computed bottom width. From the final channel dimensions, the top width was calculated for the flow depth plus a freeboard of 0.1524 m (0.5 ft). This top width was used as the buffer distance for the ACPF grassed waterways. Using this approach, 98.7%, 99.8%, and 99.4% of the ACPF grassed waterway features overlap with the 2 hectare flow path network for Ten Mile Creek, Hinkle Creek, and the Headwaters of the North English, respectively.

For the IBMP grassed waterways it was determined that a buffer distance of five meters was large enough to capture the discrepancies between the manually drawn polygons and the LiDAR derived 2 hectare flow path network. Using this approach, 92%, 92%, and 85% of the existing grassed waterway features overlap with the 2 hectare flow path network for Ten Mile Creek, Hinkle Creek, and the Headwaters of the North English, respectively. As expected, the overlap of existing grassed waterways with the flow path network is less than for ACPF because ACPF identifies its grassed waterways with the same digital elevation model used to create the network.

5.2 Grassed Waterway Comparison

By intersecting buffered polygon features with the flow path network, we were able to directly compare ACPF and IBMP grassed waterways using stream lengths and areas.

Table 5.2 depicts the total lengths and areas. In terms of area, the ratio between IBMP existing and ACPF potential grassed waterway ranges from 0.78 (Hinkle Creek) to 1.20 (Headwater North English). In terms of flow network length, the ratio ranges from 0.87 (Hinkle Creek) to 1.55 (Ten Mile Creek). These outcomes suggest that existing grassed waterways in these watersheds are of a size and extent comparable to the predicted potential.

Table 5.2. Comparison of Existing (IBMP) and Potential (ACPF) Grassed Waterways for the three HUC 12 Study Areas

	Ten Mile Creek	Hinkle Creek	Headwaters North English
Length (km)			
ACPF (raw outputs)	96	142	159
Area (ha)			
Existing	111	178	230
ACPF	125	227	191
Ratio	0.89	0.78	1.20
2 hectare Flow Network Length (km)			
Existing	96	131	180
ACPF	62	150	165
Ratio	1.55	0.87	1.11

Figure 5.2 depicts the percentage of flow path network length with existing and potential grassed waterways; the percentage overlap of the network by both existing and potential grassed waterways are also depicted. For all three watersheds, the variations in IBMP existing and ACPF potential grassed waterways by flow path order are remarkably similar. Comparing the different watersheds, Hinkle Creek has the most potential and existing grassed waterways. The potential and existing grassed waterways also have the most agreement with the highest percentage of overlap. Hinkle Creek grassed waterway implementation level is followed by Headwaters North English and then by Ten Mile Creek with the least percentage of existing and potential (Figure 5.2).

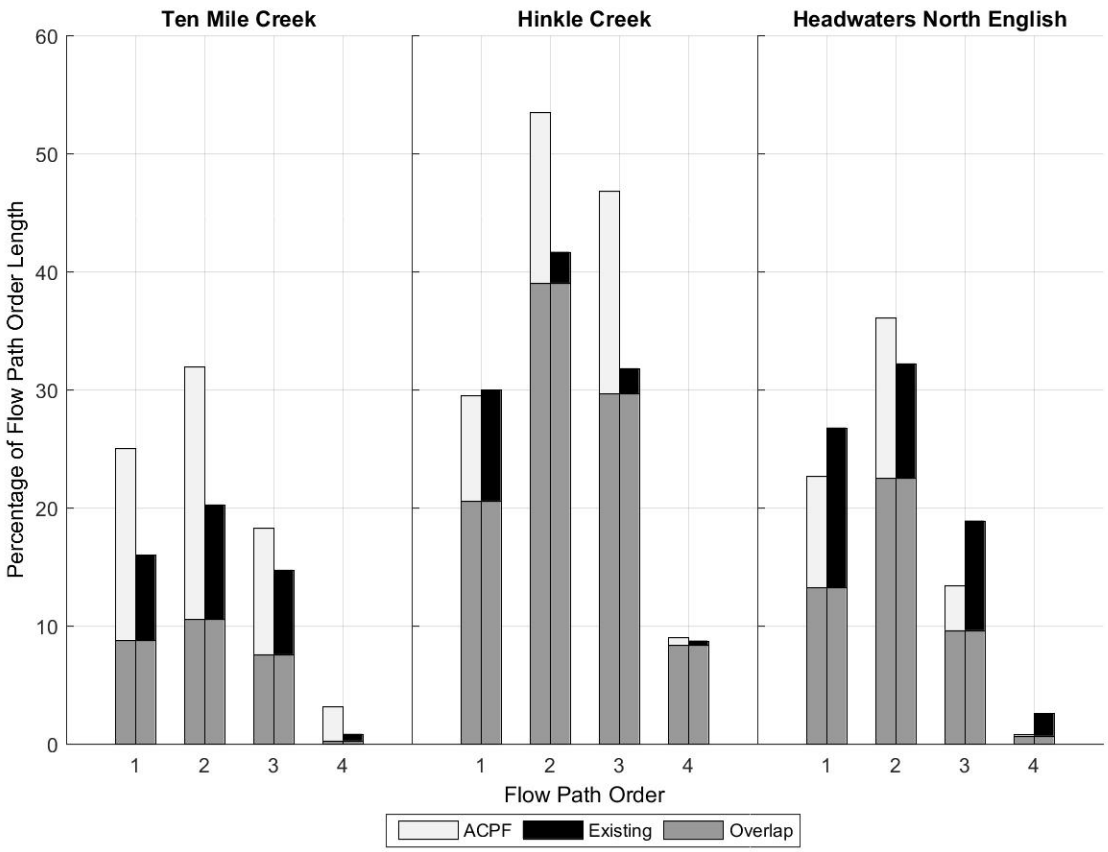

Figure 5.2. Existing, potential, and overlapping grassed waterway length as percentage of flow path order length for Ten Mile Creek, Hinkle Creek, and Headwaters North English.

The similarity between the potential and existing grassed waterways results provides some validation of the ACPF method for siting. For example, the difference between Hinkle Creek and Headwaters North English is due to differences in the topography of the respective watersheds. Hinkle Creek had 6.84% of raster cells above the SPI threshold while Headwaters North English has 3.78% of raster cells above the SPI threshold (Table 5.3). The larger positive tail in the SPI distribution of Hinkle Creek results in more grassed waterway potential. However, the difference between Hinkle Creek and Headwaters North English with Ten Mile Creek is not due to differences in the SPI distribution as there are 5.28% of cells above the SPI threshold (Table 5.3). Instead, the difference is in the land use of the respective watersheds. Where the Headwaters North

English and Hinkle Creek have 72% and 70% agricultural land use, Ten Mile Creek has 56% agricultural land use (Table 5.1).

Table 5.3. Stream Power Index Results for the three Study Areas

	Ten Mile Creek	Hinkle Creek	Headwaters North English
Mean SPI	4.38	4.00	0.07
Standard Deviation	1.78	2.01	1.98
ACPF SPI Threshold	9.72	10.0	6.01
Raster Cells above Threshold (%)	5.28%	6.84%	3.78%

5.3 Pond and Wetland Comparison

The ACPF wetland algorithm is designed to site one type of impoundment, NRCS code 656 Constructed Wetlands, and code 658 Wetland Creation (Porter et al. 2017). The IBMP process, however, identifies wetlands and other types of impoundments, ranging from smaller stock ponds and grade stabilization structures to larger recreational or flood control facilities. This accounts for some of the differences between the two datasets depicted in the map of Ten Mile Creek (Figure 5.3), the distribution of pond and wetland drainage areas (Figure 5.4) and in the summary table (Table 5.4).

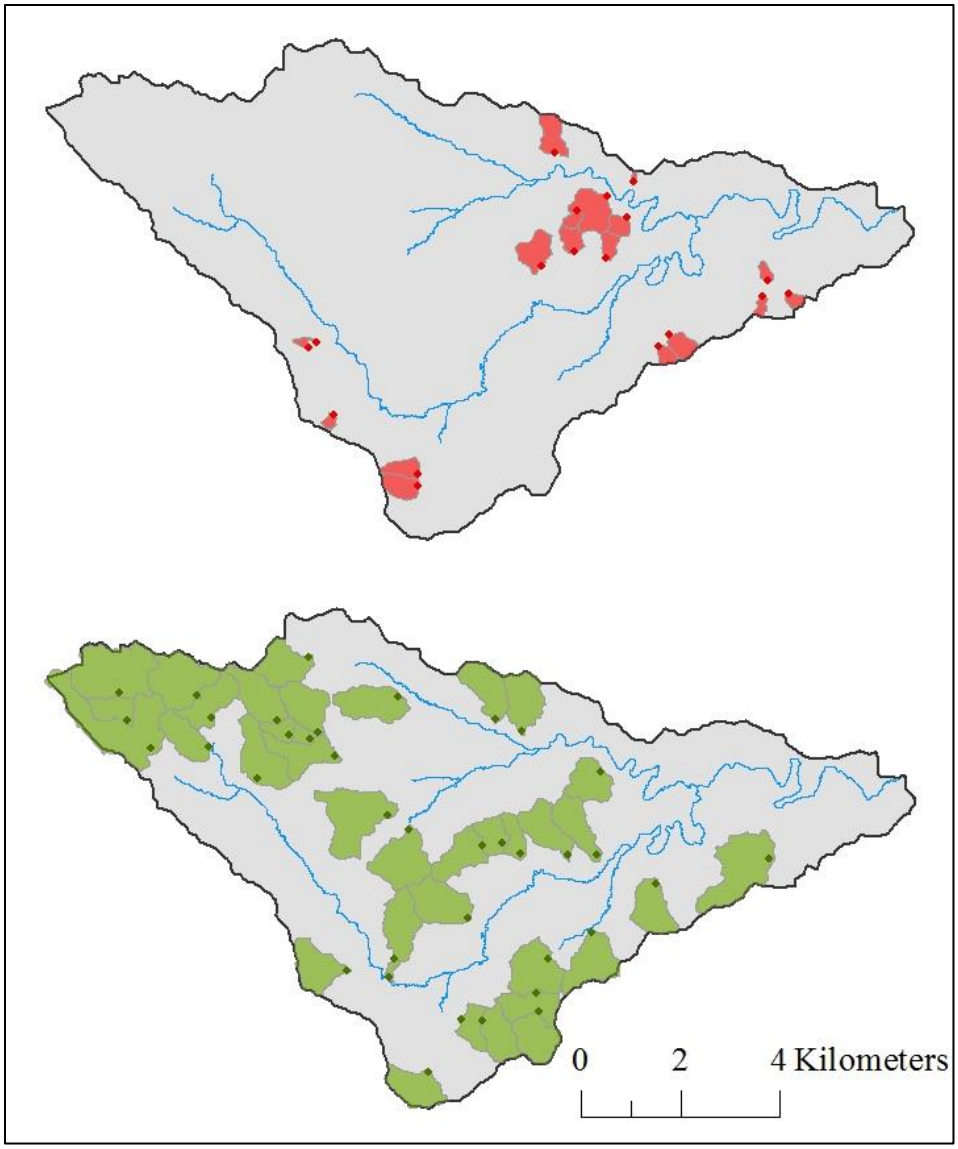

Figure 5.3. Top, drainage areas of existing ponds in Ten Mile Creek shown in red with dam locations as red points. Bottom, drainage areas of Agricultural Conservation Planning Framework (ACPF) nutrient removal wetlands shown in green with impoundment locations as green points.

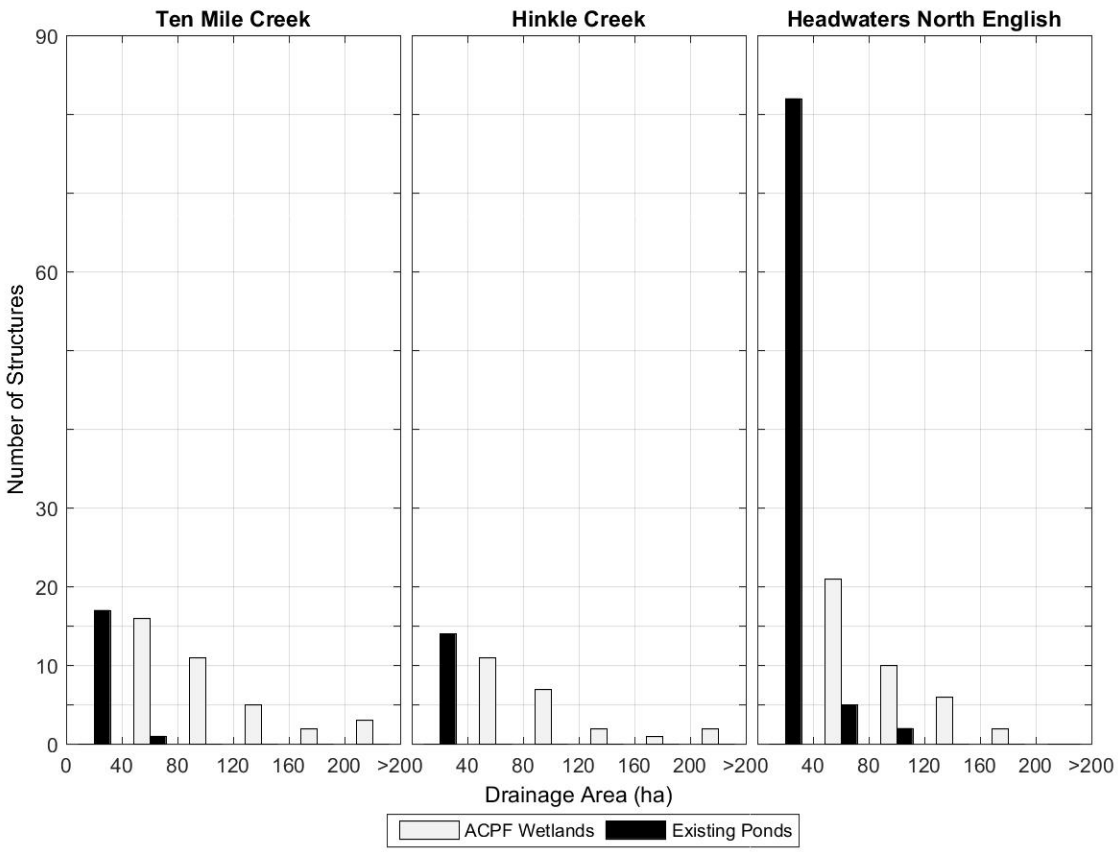

Figure 5.4. Number of Agricultural Conservation Planning Framework (ACPF) nutrient removal wetlands and existing ponds binned into 40 ha increment drainage areas from 0 to greater than 200 ha.

Table 5.4. Comparison of Existing (IBMP) Ponds and Agricultural Conservation Planning Framework (ACPF) Nutrient Removal Wetlands for the three HUC 12 Study Areas

	Ten Mile Creek	Hinkle Creek	Headwaters North English
Existing Ponds			
Number	18	14	89
Average Drainage Area (ha)	17.8	6.9	13.7
Flow Regulation (%)	3.8	1.1	7.3
ACPF Wetland			
Number	37	23	39
Average Drainage Area (ha)	108.9	106.8	89.3
Flow Regulation (%)	32.8	21.7	20.8

In Headwaters North English, 39 potential ACPF wetlands are identified (Table 5.4). The average drainage area for ACPF wetlands is 89 ha. From the IBMP, 90 ponds have been built in

the watershed (Table 5.4). However, most (72 of 90, or 80%) are smaller ponds with drainage areas of 20 ha or less. The average drainage area for existing ponds is 7 ha. Of the 90 existing ponds, the four largest ponds are the size of the ACPF wetlands. These four ponds are all located close to potential ACPF wetlands (Table 5.4). Another 15 ponds are located on tributaries to potential wetland sites. But most of the remaining 71 small ponds are on tributaries not identified as potential nutrient wetland sites.

While the Headwaters North English has the largest utilization of ponds with 90 existing ponds, Hinkle Creek and Ten Mile Creek have much fewer with 17 and 23 existing ponds respectively (Table 5.4). Besides the difference in numbers, the average drainage areas in Hinkle Creek and Ten Mile Creek follow similar values to the Headwaters North English. The average drainage areas for the existing ponds in Hinkle Creek and Ten Mile Creek are both less than 20 ha at 7 ha and 18 ha respectively (Table 5.4). While for the ACPF wetlands, the average drainage areas are close to 10 times the existing drainage areas at 107 ha and 109 ha respectively (Table 5.4). In addition to the difference in average drainage area, the distribution of drainage areas for existing ponds and ACPF wetlands also depict a break between the two datasets. The ACPF algorithm only identifies wetlands with drainage areas greater than 60 ha while the majority of existing ponds are below that threshold (Figure 5.4). The difference in drainage area size between the two datasets is an indicator that past pond and wetland implementation has focused on the smaller field-scale issues while the ACPF wetlands are trying to shift the focus to more watershed and community efforts to reduce runoff and improve water quality on a larger scale.

Among the watersheds, Hinkle Creek has the smallest fraction of flow currently regulated at 1.1%, Ten Mile Creek is next at 4%, and the Headwaters North English River has the most at 7.3%. The most potential for flow regulation, 33%, is in Ten Mile Creek and can be attributed to

its location in the Paleozoic Plateau (Table 5.4). The area has larger topographic relief compared with the other sub-watersheds located in the Southern Iowa Drift Plain (Headwaters North English) and the Iowan Surface (Hinkle Creek). Hinkle Creek and Headwaters North English show similar potential for additional flow regulation at 22% and 21%.

5.4 Water and Sediment Control Basins (WASCOBS) Comparison

The BMP mapping analysis indicates WASCOBs are heavily used in the Headwaters North English and are near the potential predicted by ACPF, whereas few WASCOBs exist in Hinkle Creek and Ten Mile Creek but large potential exists (Table 5.5). The BMP mapping analysis identified 648 WASCOBs in Headwaters North English compared to fewer than 10 in both Hinkle Creek and Ten Mile Creek (Table 5.5). In total, WASCOBs regulate flow from 12.2% of the area in Headwaters North English compared to less than 1% in the other two basins. WASCOB potential is high in all three basins, as ACPF recommended several hundred in each watershed, ranging from 273 in Ten Mile Creek to 826 in Headwaters North English. Potential WASCOB implementation would regulate a similar fraction of the flow in each basin, ranging from 14.1-16.5% of the drainage area. In general, the average drainage area per existing or ACPF WASCOB is similar in all three basins (~4-5 ha).

Table 5.5. Comparison of Existing (IBMP) and Agricultural Conservation Planning Framework (ACPF) Water and Sediment Control Basins (WASCOBs) for the three HUC 12 Study Areas

	Ten Mile Creek	Hinkle Creek	Headwaters North English
Existing WASCOBs			
Number	9	8	648
Average Drainage Area (ha)	4.9	7.7	3.7
Flow Regulation (%)	1.0	0.8	12.2
ACPF WASCOBs			
Number	273	396	826
Average Drainage Area (ha)	4.0	4.5	3.8
Flow Regulation (%)	14.1	15.0	16.5

Figure 5.5 shows the spatial distribution of existing and ACPF WASCOBs and Figure 5.6 shows the drainage area distribution for the Headwaters North English. Results are not shown for Hinkle Creek or Ten Mile Creek because so few WASCOBs exist the ACPF distribution was similar to Headwaters North English. Similar to the pond and wetland comparison, it is clear from Figure 5.6 that existing WASCOBs tend to have much smaller drainage areas than ACPF WASCOBs. Of the 648 existing WASCOBs in Headwaters North English, 90% have a drainage area less than 2 ha and 96% have a drainage area less than 4 ha; of the 826 ACPF WASCOBs, 45% have a drainage area less than 2 ha and 71% have a drainage area less than 4 ha. Nearly a third (29%) of the ACPF WASCOBs have a drainage area greater than 4 ha (but less than or equal to 20 ha). The majority (~90%) of both existing and ACPF WASCOBs in Headwaters North English are located on zero order (58% and 45%, respectively) and first order (32% and 44%, respectively) flow paths.

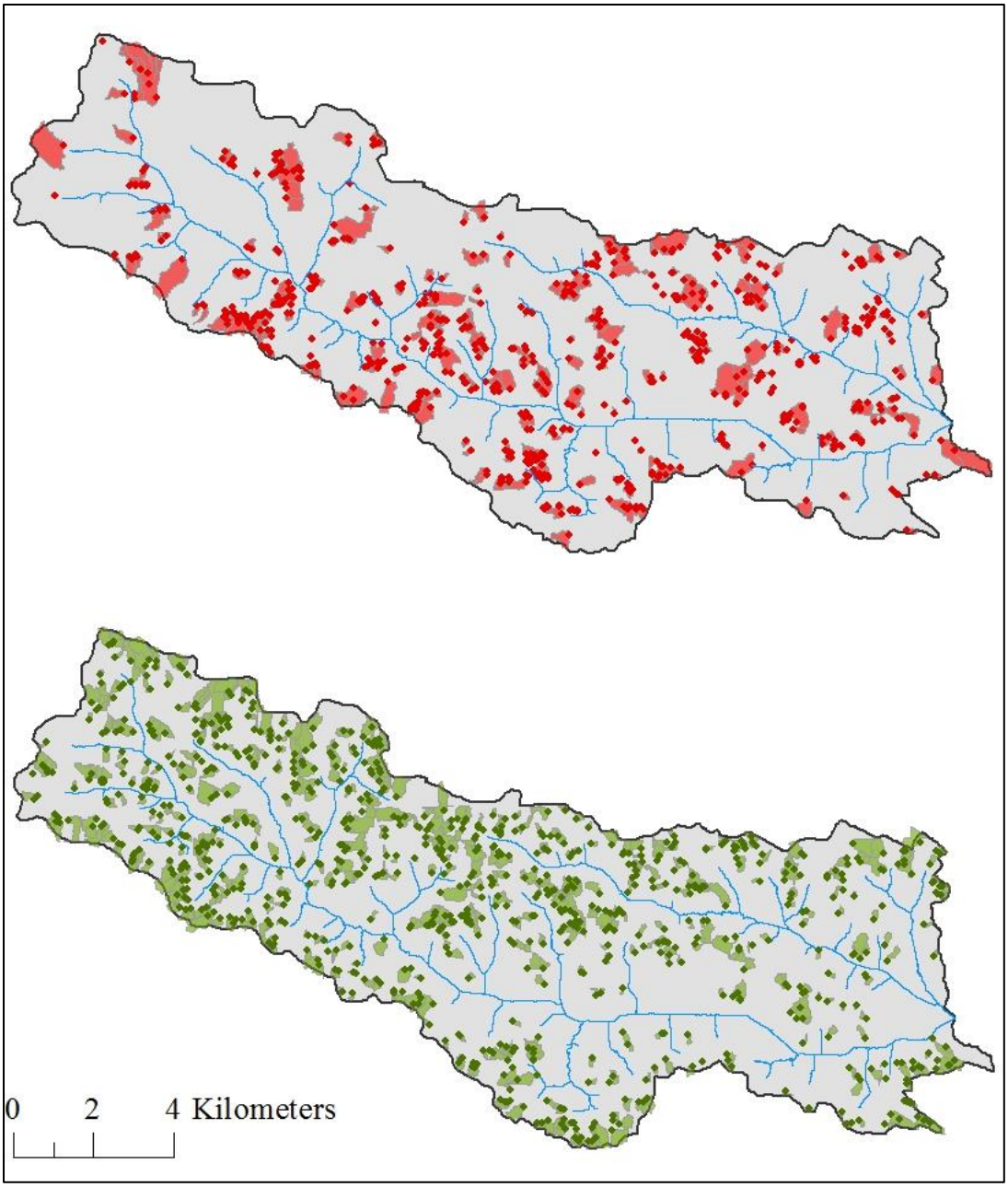

Figure 5.5. Top, drainage areas of existing water and sediment control basins (WASCOBs) shown in red and locations as red points for Headwaters North English. Bottom, drainage areas of Agricultural Conservation Planning Framework (ACPF shown in green and locations as green points.

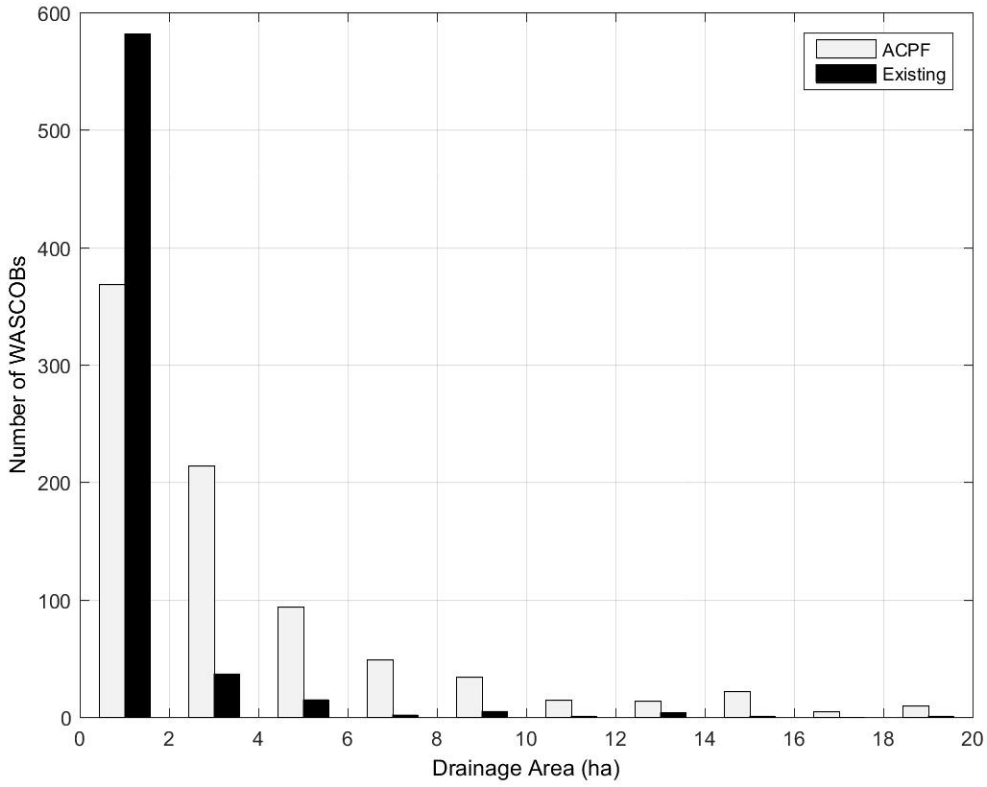

Figure 5.6. Number of water and sediment control basins (WASCOBs) for the Headwaters North English binned by 2 ha increment drainage areas from 0 to 20 ha for existing and potential WASCOBs.

Existing WASCOB implementation differs among HUC-12 basins in part because of practice suitability and conservation funding. While the IBMP project suggests WASCOB use in Hinkle Creek and Ten Mile Creek is minimal, terraces are more commonly used and serve a similar function to reduce surface erosion. While the ACPF does not directly identify potential terraces, the IBMP inventoried a total of 44, 140, and 251 terraces in Ten Mile Creek, Headwaters North English, and Hinkle Creek, respectively. The degree of terrace implementation in each basin is indicative of landform region, as the gently rolling, agriculturally intensive terrain of the Iowan Surface and, to a lesser extent, the Southern Iowa Drift Plain make Hinkle Creek and Headwaters North English more suitable for conventional terrace systems than Ten Mile Creek located in the steeper, more undulating Paleozoic Plateau (Mielke 1985). This claim is further supported by a

review of conservation funding in the county of each HUC-12 basin. From 1998-2015, the Environmental Quality Incentives Program (EQIP), a USDA conservation program, awarded total payments (contracts) of $2.2 M (346), $1.7 M (442), and $8.4 M (731) to Benton County (Hinkle Creek), Poweshiek County (Headwaters North English), and Winneshiek County (Ten Mile Creek), respectively (Environmental Working Group 2017). WASCOBs and terraces accounted for 21% of the total funding in Poweshiek County compared to 9% in Winneshiek County and 4% in Benton County. WASCOBs and terraces accounted for 30% of the total contracts awarded in Poweshiek County compared to 11% in Winneshiek County and 2% in Benton County. While not all encompassing, these statistics suggest targeted funding for WASCOBs (and terraces) is a main reason why current implementation is much higher in Headwaters North English than the other two basins.

Differences in potential WASCOB implementation among HUC 12 basins are more difficult to discern from the ACPF algorithm but appear related to the agricultural intensity and network characteristics in each basin. As described previously, the primary criteria governing WASCOB placement by ACPF are land use (agriculture, including pasture), drainage area (0.8-20.2 ha), and topography (to ensure adequate slope convergence and prevent incision). WASCOB intensity (average number of WASCOBs per agricultural area) increased with agricultural land use percent, from 4.1 WASCOBs/km^2 in Ten Mile Creek (80% agricultural) to 6.3 WASCOBs/km^2 in Headwaters North English (90% agricultural). While the WASCOB intensities in Hinkle Creek (5.8 WASCOBs/km^2; 86% agricultural) and Headwaters North English were proportional to the agricultural land use percent, the WASCOB intensity in Ten Mile Creek was disproportionately lower than its agricultural land use would suggest. Because ACPF also has a drainage area restriction, the drainage network sampled for WASCOB suitability by ACPF was also analyzed.

In this case, the drainage network length was proportional to the agricultural area (km^2) in each basin; stated another way, the network drainage density (total WASCOB network length divided by total agricultural area in the watershed) was similar in all three basins (4.4-4.6/km). As one might expect, the WASCOB network length was directly proportional to the number of sites tested for topographic suitability by ACPF. The final number of WASCOBs identified by ACPF in each basin (Table 5.5) represent 4.6%, 5.9%, and 6.5% of all the sites tested in Ten Mile Creek, Hinkle Creek, and Headwaters North English, respectively. Results of this analysis suggest WASCOB potential predicted by ACPF is proportional to both the agricultural land use (both total area and as a percent) and the flow network associated with potential WASCOB placement, but additional testing in other basins is needed to verify these findings.

5.5 Summary

In this study, existing conservation practices identified by the IBMP project and potential practices placements identified by the ACPF tool were compared for three HUC-12 watersheds in Iowa. Since the same practices are represented differently in the two GIS data sets, procedures for making a consistent comparison were developed. For grassed watersheds, a design estimation method was created for ACPF to map their area and extent, and both ACPF and IBMP grassed waterways were mapped onto a flow path network. From this process, it was determined that grassed waterways are widely implemented within the three watersheds. Furthermore, the SPI process used by the ACPF was validated as the siting of potential practices matched with the existing grassed waterway based on flow path order. For ponds and wetlands, it was determined that the majority of the existing structures are small ponds, being built for field scale remediation issues, while the ACPF tool identified larger wetlands. Although few existing nutrient reduction wetlands were identified in the IBMP analysis, ACPF suggests the potential for greater use of this practice in the Iowa landscape. For the WASCOB comparison the Headwaters North English was

the only watershed to have substantial existing WASCOBs. The difference between Headwaters North English and the other two watersheds was due to differences in conservation spending and preferences. The potential for WASCOBs in a watershed was shown to be proportional to the agricultural land use the percentage of the flow path network located within the area tested by the ACPF.

For all of the conservation practices used in the study topography and land use differences were important in distinguishing the three watersheds in terms of existing and potential conservation. The distribution of SPI along with the agricultural land use percentage were the key parameters in estimating the amount of grassed waterways. The larger topographic relief attributed to the Paleozoic Plateau increased the potential implementation of wetlands as compared to the more gentle landscapes of the Iowan Surface and Southern Iowa Drift Plain.

The development of the two projects, the IBMP and the ACPF, are important resources in handling water quality and quantity issues being addressed by such plans as the INRS. Coupling the IBMP existing practices with the ACPF potential practice placements advances the amount of planning stakeholders of watersheds can implement prior to funding projects. Moreover, it allows water resource professionals to more adequately target areas of improvement as approximate locations for conservation practices are known and more accurate optimization scenarios can be carried through. These tools enhance the watershed planning process allowing for more informed decision making and development of more precise watershed strategies to mitigate flooding and water quality degradation.

Chapter 6. Upper Iowa Model Development & Calibration

This chapter summarizes the development of the Upper Iowa hydrologic model. The model for the Upper Iowa watershed was created using GHOST, a code developed by IIHR Hydroscience & Engineering based on the Multi-Modular Penn State Integrated Hydrologic Model (MM PIHM) (Qu and Duffy 2007; Yu et al. 2013). The spatial information from Chapter 3 for the model was prepared using ESRI ArcGIS and processed in PIHMgis (Kumar et al. 2009).

GHOST is a distributed, physically-based, integrated hydrologic model that is fully described by Politano (2018). Integrated surface/subsurface models solve the surface and subsurface components simultaneously (Condon and Maxwell 2013). Physically-based models use equations that can be derived from the conservation equations of mass, momentum, and energy. Distributed models, discretize the study area into small subunits, usually squares or as in GHOST triangles that allow for more spatial variability in the model and can obtain results throughout the watershed instead of being limited to the outlet. GHOST was chosen for this study because distributed physically-based models provide enough detail to accurately portray potential conservation practices. Furthermore, GHOST is open source and therefore the methods used in the code can be verified and additional functions can be added.

6.1 Mathematical Model Description

GHOST simulates the surface and subsurface interactions in a watershed to predict overland flow and groundwater recharge to a stream during different hydrologic events. The model is organized into three distinct zones: surface zone, unsaturated zone, and saturated zone. In addition with climatological data as an input, interception, evapotranspiration, and snow accumulation and melting processes are simulated.

6.1.1 Climatological forcing

Meteorological forcing data for estimating precipitation and evapotranspiration are required to run simulations with GHOST. The precipitation time series was created from hourly 4 km x 4 km radar rainfall Nexrad Stage IV data (Lin 2011). Precipitation was defined as snow based on temperature where the transition from rain to snow occurs when the temperature drops from 1 °C to -3 °C. The snow melting rate is based on the degree-day method where melting occurs at temperatures greater than 0 °C at a rate defined by a snow melt coefficient (Politano 2018). The data used to calculate evapotranspiration were surface temperature, relative humidity, surface wind speed, short wave radiation, long wave radiation, and pressure. These data were obtained from 11 km x 13 km National Land Data Assimilation Systems Phase 2 dataset (NLDAS-2) (Mitchell et al. 2009). The Nexrad Stage IV precipitation and NLDAS-2 data sets were paired based on the relative closeness of the cell centers of each cell. As a result 184 time series were created across the watershed area, where approximately four Nexrad Stage IV cells were grouped with one NLDAS-2 cell.

6.1.2 Evapotranspiration

Evapotranspiration is calculate in four different components; canopy evaporation, surface water evaporation, soil evaporation, and transpiration. The potential evapotranspiration for each time step is computed from the Penman-Montieth equation following FAO56 (Allen et al. 1998; Allen et al. 2006). Priority first goes to the canopy evaporation where precipitation is intercepted using a bucket model derived by Kristensen and Jensen (1975) and Panday and Huyakorn (2004) where an interception factor and leaf area index (LAI) control the size of the "bucket." Any precipitation greater than the "bucket" will go to the surface. Then assuming there is potential evapotranspiration available, evaporation from the surface is computed as the minimum between the surface water depth and the remaining potential evaporation (Politano 2018).

The last two components of evapotranspiration, soil evaporation and transpiration, are calculated following Panday and Huyakorn (2004). Transpiration is calculated to a depth proportional to the root depth and is a function of the canopy absorption of incident radiation ($f_1(LAI)$) and the soil moisture ($f_2(\theta)$), Equation 1:

$$T_i = \max\left(f_1(LAI_i)\, f_2(\theta_i)\, f_R\left(ET_i^a - E_i^{can} - E_i^{surf}\right), 0\right) \quad (1)$$

where ET_i^a is actual evaporation equal to the product of the reference evaporation, assuming a dense actively growing alfalfa that is 20 inches tall under well-watered conditions, and an empirical crop coefficient that depends on the plant and growth stage. The fraction of canopy absorption is modeled after the Beer Lambert Law, Equation 2:

$$f_1(LAI_i) = \left(1 - \exp\left(-k_i^{ext}\, LAI_i\right)\right) \quad (2)$$

where $k_i^{ext}$is the canopy extinction coefficient (Politano 2018). The dependence of transpiration on soil moisture is modeled by Equation 3:

$$f_2(\theta_i)\begin{cases} 0 & \text{if } 0 < \theta_i \le \theta_i^{WP} \\ 1 - \left(\dfrac{\theta_i^{FC} - \theta_i}{\theta_i^{FC} - \theta_i^{WP}}\right)^{C_3/ET_a} & \text{if } \theta_i^{WP} < \theta_i \le \theta_i^{FC} \\ 1 & \text{if } \theta_i^{FC} < \theta_i \le \theta_i^{O} \\ \left(\dfrac{\theta_i^{AN} - \theta_i}{\theta_i^{AN} - \theta_i^{O}}\right)^{C_3/ET_a} & \text{if } \theta_i^{O} < \theta_i \le \theta_{AN} \\ 0 & \text{if } \theta_i^{AN} < \theta_i \end{cases} \quad (3)$$

where θ_i^{WP}, θ_i^{FC}, θ_i^{O} and θ_i^{AN} are the water contents at, wilting point, field capacity, oxic limit, and anoxic limit respectively and $C_3$is a dimensionless fitting parameter. Soil evaporation is similarly dependent on the fraction of canopy absorption and soil moisture, Equation 4:

$$E_i = \max\left(\left(1 - f_1\left(LAI_i\right)\right) f_3\left(\theta_i\right) f_E\left(ET_i^a - E_i^{can} - E_i^{surf}\right), 0\right) \quad (4)$$

where the remaining incident radiation is used to calculate soil evaporation. The soil moisture is defined by an upper and lower energy limits, Equation 6:

$$f_3\left(\theta_i\right)\begin{cases} 0 & \text{if } \theta_i < \theta_i^{e2} \\ \left(\dfrac{\theta_i - \theta_i^{e2}}{\theta_i^{e1} - \theta_i^{e2}}\right) & \text{if } \theta_i^{e2} < \theta_i \le \theta_i^{e1} \\ 1 & \text{if } \theta_i^{e1} < \theta_i \end{cases} \quad (6)$$

where θ_{e1} and θ_{e2} are the upper and lower energy limiting soil moistures respectively.

6.1.3 Surface Zone

Water depth within the surface zone is calculated by the 2-D diffusive wave-approximation of the St. Venant equation. The full mass conservation equation for the surface zone is given by Politano (2018) in Equation 7:

$$\frac{\partial y^{surf}}{\partial t} + \nabla.\left(\vec{u}^{surf}\, y^{surf}\right) = S^{surf} - q^{surf-uns} + q^{GW-surf} \quad (7)$$

where y^{surf} is the water depth at the surface, $\vec{u}^{surf}$ is the water velocity, calculated using the momentum equation of the diffusive wave and Manning equation, $q^{surf\text{-uns}}$ is the mass flux to the unsaturated zone, $q^{GW\text{-}surf}$ is exfiltration, and S^{surf} is the point source term containing precipitation, drainage from the canopy, snow melt, surface evaporation and a user defined point source.

Overland flow is controlled by the surface water depth, surface elevation and average roughness of surrounding elements and is given by Politano (2018) in Equation 8:

$$q_{ij}^{surf} = \frac{\left(y_{ups}^{surf} + z_{ups}^{ground}\right)^{2/3}}{n_{ij}} sign\left(\left|G_{ij}^{surf}\right|\right)\left(G_{ij}^{surf}\right)^{1/2}\left(y_f^{surf} + z_{ups}^{ground}\right)L_{ij} \quad (8)$$

where q_{ij}^{surf} is the surface mass flux, y_{ups}^{surf} is the water depth upstream, z_{ups}^{ground} is the upstream surface elevation, n_{ij} is the average roughness estimated by manning's n, y_f^{surf} is the average surface water depth of surrounding elements, L_{ij} is the edge length, and G_{ij} is the gradient of the total head. To couple the 2-D domain to the 1-D stream network, a broad crested weir is used where a weir coefficient and weir height are used to control the flux between the two domains (Panday and Huyakorn 2004). Within the 1-D stream network, 1-D St. Venant equation with the same approximations as overland flow is applied (Politano 2018).

Vertical movement to and from the surface and unsaturated zones are coupled based on a first-order exchange coefficient where a coupling length (l_i^{exch}) and a hydraulic conductivity k_i^v term are used to define the connectivity between the two zones (Ebel et al. 2009). The maximum flux is given by Politano (2018), in Equation 9:

$$\Gamma_i^{surf} = \frac{k_i^v}{l_i^{exch}}\left\{\left[y_i^{surf} - \max\left(y_i^{soil} - D^{soil}, 0\right)\right] - \psi_i\right\} \quad (9)$$

where Γ_i^{surf} is the maximum surface to unsaturated flux, y_i^{soil} is the saturated water depth, D^{soil} is the depth of the soil and ψ_i is the capillary head defined by van Genuchten (1980). To avoid numerical errors, a sigmoid function is used to reduce infiltration when the surface water depth approaches the depression storage (Politano 2018). If the subsurface is saturated, exfiltration from the unsaturated zone is preferred and is proportional to the ratio of unsaturated water depth and total soil water. Exfiltration close to the stream network is the only way for subsurface flow to reach the stream.

6.1.4 Subsurface Zone

The subsurface contains an unsaturated zone and a saturated zone that are divided by a fluctuating water table. Within the unsaturated zone the movement of water is controlled through

gravity dominated flow while in the saturated zone water moves laterally based on Darcy Law and Richards equation. Water movement between the two zones is controlled via recharge and is proportional to infiltration and a sigmoid function specified in Politano (2018). The total head between the two zones are calculated together to avoid discontinuities by Politano (2018) in Equation 10:

$$\phi_i \frac{dy_i^{soil}}{dt} = \sum_{j=1}^{3} q_{ij}^{GW} - q^{GW-surf} + q^{surf-uns} - E_i^{uns} - T_i^{uns} - E_i^{GW} - T_i^{GW} \quad (10)$$

where ϕ is porosity, q_{ij}^{GW} is the groundwater flux, and the E and T terms are losses due to evaporation and transpiration within the subsurface. Recharge to the saturated zone is assumed to be directly proportional to infiltration and a sigmoid function that varies recharge with soil moisture (Politano 2018). Lateral groundwater movement is controlled by the average saturated hydraulic conductivity and the gradient of the total head of the ground water.

6.1.5 Limitations

While most hydrologic process are modeled within GHOST models, the code is still in development and improvements can be added. Therefore, the model has some limitations. Two limitations, both within the subsurface are the lack of lateral flow from the subsurface to the stream network and the lack of preferential flow models incorporated in the subsurface. Within the current formulation of GHOST the only way water can leave the subsurface is through exfiltration. As a result, the adjacent elements have limited lateral groundwater flow as water cannot leave through one side of the element. Thus, there is not adequate connectivity between the subsurface and the stream and the subsurface storage becomes limited. Furthermore, the adjacent elements must serve a dual purpose of both supplying base flow to the stream and at the same time having soil storage to limit the impact of rain events. The limitation of no lateral groundwater flow to streams has a large influence within subsurface results. Shen et al. (2016) determined that the influence of the

subsurface stream connectivity spans 25%-50% of the watershed for certain variables including water table depth, recharge, and inundation times. The second limitation in the subsurface model of GHOST is Darcy and Richard's equations flow coupled with a sigmoid function to adjust recharge are the only equations within the model. These equations are derived from ideal experimental conditions and do not account for preferential flow common throughout the Upper Iowa watershed including macro pores, drain tile, and karst flow, that increase subsurface flow (Beven and Germann 2013; Lee and Krothe 2001).

6.2 Model Construction

To model the topography and stream network of the Upper Iowa watershed a mesh is generated. The mesh for GHOST is constructed from an unstructured, triangular, 2-D mesh and a 1-D stream network with stream segments identified as edges of specific elements. Unstructured meshes represent the terrain while decreasing the number of computational elements and represent line features more accurately as compared to structured meshes. For the Upper Iowa hydrologic model the watershed boundary, stream network, and USGS stream gage locations were identified to simulate the terrain of the watershed with the overall goal to simulate ponds throughout the basin. The watershed boundary is the lateral edge of the model and is identified by the topographic high of the watershed. The stream network was delineated based on a 60 ha area threshold. The threshold was chosen based on the minimum area for identifying ACPF wetlands (Porter et al. 2017). As a result, the model would have the potential to simulate the majority of ACPF wetland locations.

With the features created from the DEM the number of computational elements was too high to receive results in a reasonable timeframe. Therefore, a simplification process was used to simplify the features and reduce the number of computational elements. First, first order streams that did not contain an ACPF wetland were removed. Then both the watershed boundary and

stream network were simplified by 500 m and 200 m respectively. Furthermore, the locations of the USGS gages were added to the river segments to reduce interpolation differences caused by comparing slightly different locations in the stream network. Next Delaunay triangulation described by Qu and Duffy (2007) was iteratively applied to the split and merged line network to create triangular elements with a maximum area of 89.8 ha and minimum angle of 20°. Each iteration elements with areas less than 2.83 ha were identified and the line network was adjusted either by adjusting the angle between segments, adjusting a node location to increase the distance between nodes, or removing a node. As a result of the simplification process, the final mesh contained 6491 elements and 2199 river segments (Figure 6.1). Element and river segment statistics are described in Table 6.1.

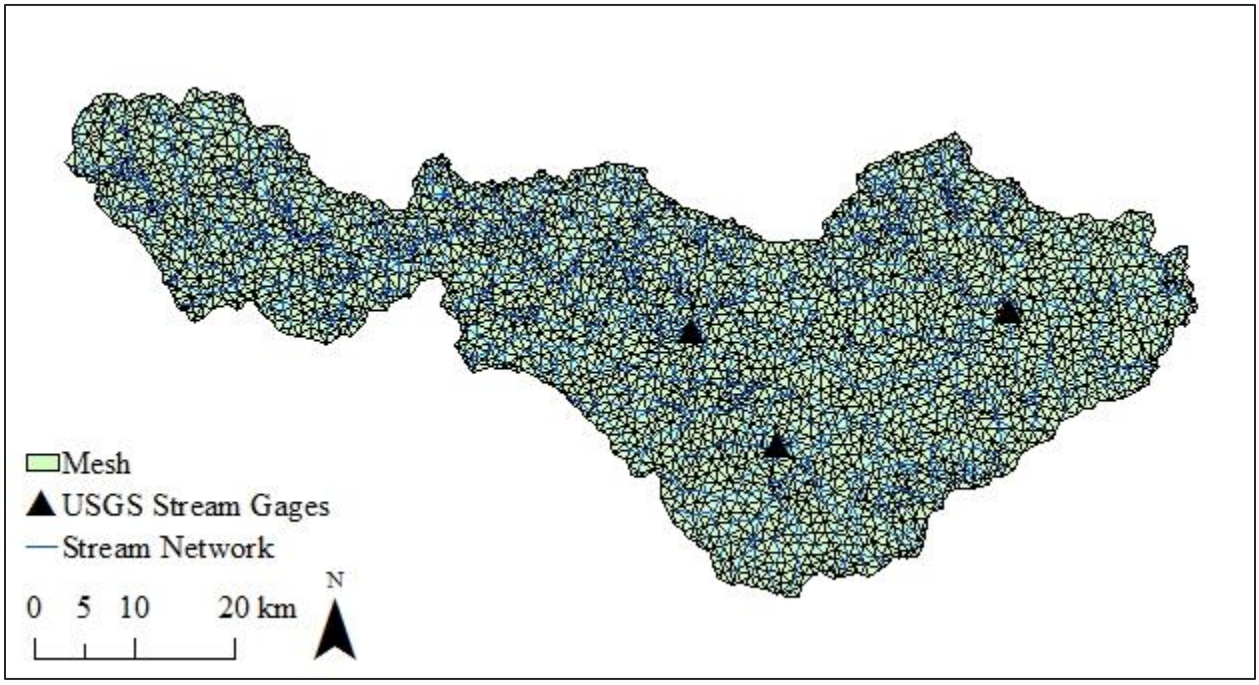

Figure 6.1. Upper Iowa hydrologic model mesh and stream network.

Table 6.1. Upper Iowa GHOST Mesh Element and River Segment Statistics

Statistic	Element Area (ha)	River Segment Length (m)
Mean	40	820
Standard Deviation	20	349
Minimum	2.1	182
Maximum	89.8	2171

With the mesh generated the characteristics of the watershed were incorporated into the mesh. First the elevations of the watershed were extracted to the nodes of the mesh elements from a 30 m aggregated filled DEM derived from 3 m LiDAR. The elevations of the nodes along the river were then adjusted by applying a robust version of loess smoothing to remove locations with adverse slopes. Furthermore, the stream ordering was adjusted to coincide with stream widths identified from 2015 National Agriculture Imagery Program (NAIP) aerial photography (FSA 2017). In total there were six different widths ranging from 3 m to 45 m used within the model with the majority (70%) of the stream segments classified as 3 m wide (Table 6.2). Lastly, for the boundary condition at the stream network outlet critical-depth was used.

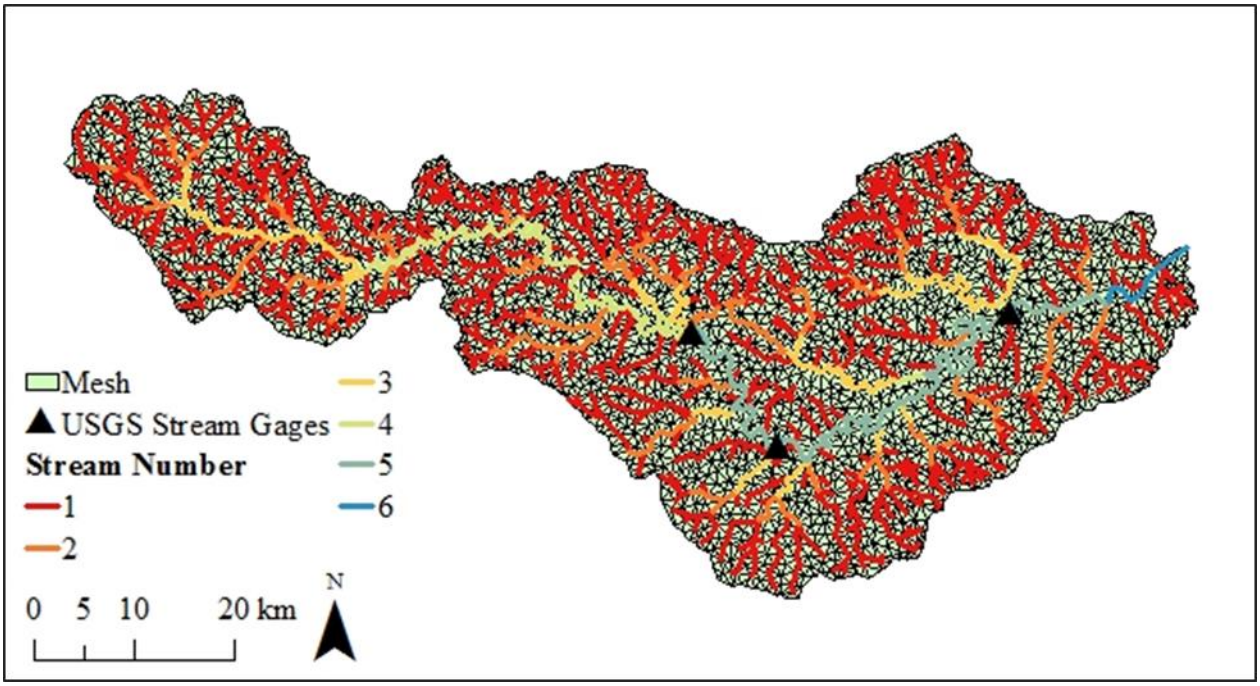

Figure 6.2. Upper Iowa hydrologic model stream numbering based on width.

Table 6.2. Upper Iowa Model Stream Segment Classification by Width

Stream Number	Stream Width (m)	Percent of Total Length (%)
1	3	70%
2	6	13%
3	12	7%
4	25	4%
5	35	5%
6	45	1%

The land cover type of each element was then attributed based on the majority land use within each element. The land cover was determined by a reclassified NLCD 2011 raster (USGS 2011). The NLCD 2011 raster was reclassified by removing all land uses except for developed land covers, grassland, pasture, cropped, and deciduous forest. The developed areas were grouped together and grassland and pasture were grouped together to form four distinct groups. The locations of the different land uses are depicted in Figure 6.3.

The time series characterizing the changes in vegetation for each land use throughout the year that are used to calculate evapotranspiration, LAI, crop coefficient, and root depth, were derived from literature values. The LAI time series were derived from Zhou et al. (2013) for crops and pasture, Fang et al. (2008) for forest and a constant value of 1 was used for developed areas (Figure 6.4). The crop coefficient time series were derived from Allen et al. (1998) for crops and pasture and Corbari et al. (2017) for forest and developed areas, as trees were assumed to be the dominant plant type within developed areas (Figure 6.5). The root depth time series were derived from Zhou et al. (2013) for corn and pasture, Breuer et al. (2003) for forest, and a relatively small constant value of 0.25 was used for developed area because of the amount of impervious area. (Figure 6.6).

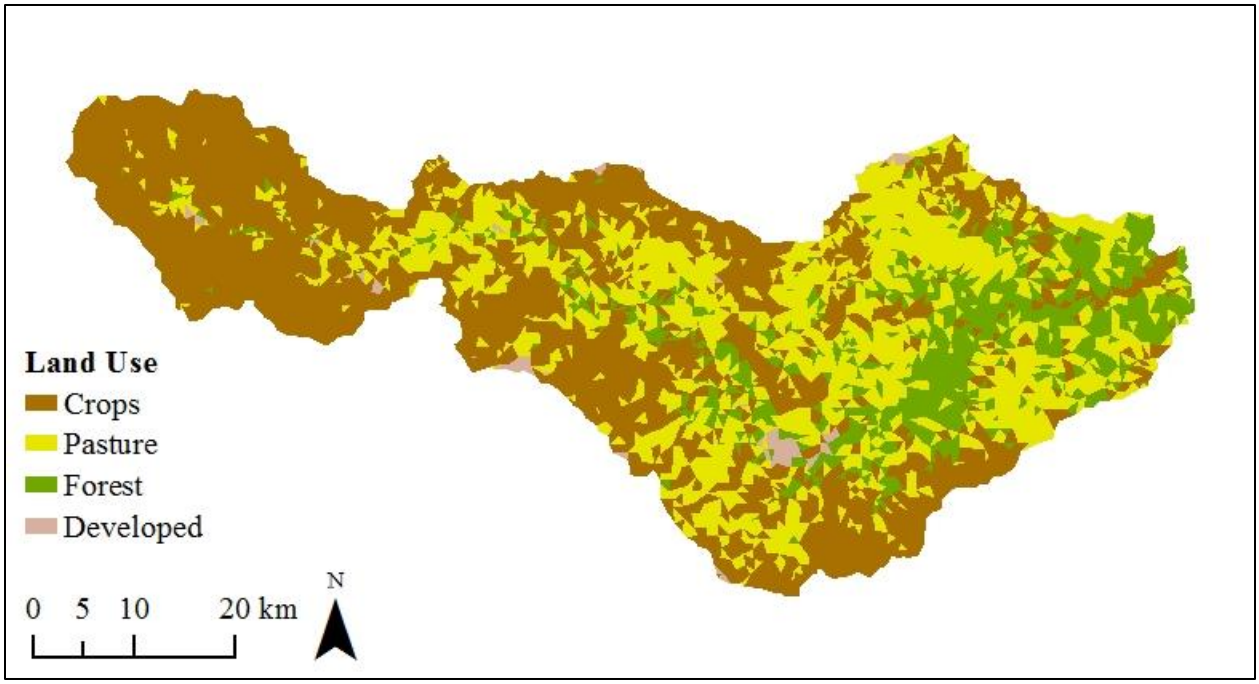

Figure 6.3. Upper Iowa hydrologic model land use.

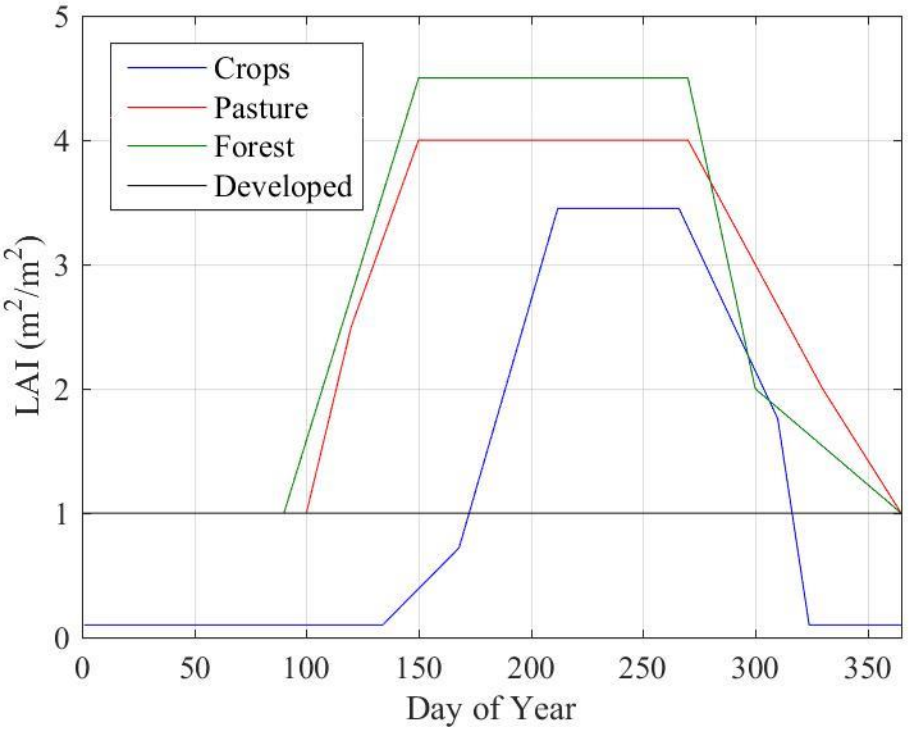

Figure 6.4. Upper Iowa hydrologic model LAI time series for the four different land uses.

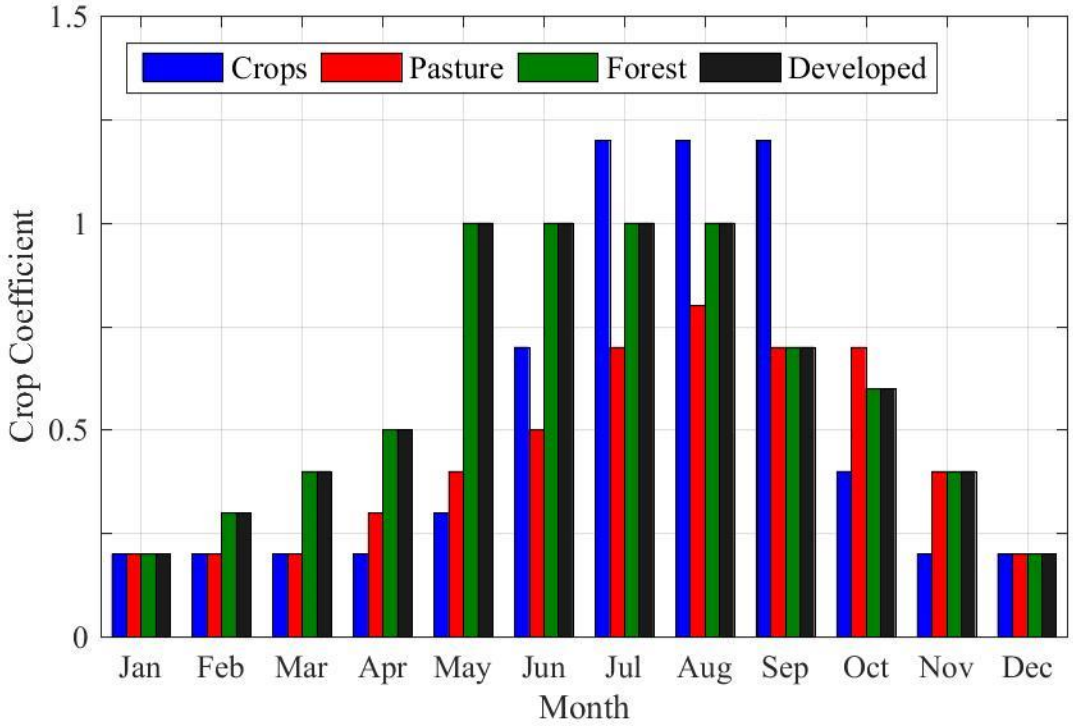

Figure 6.5. Upper Iowa hydrologic model crop coefficient time series for the four different land uses.

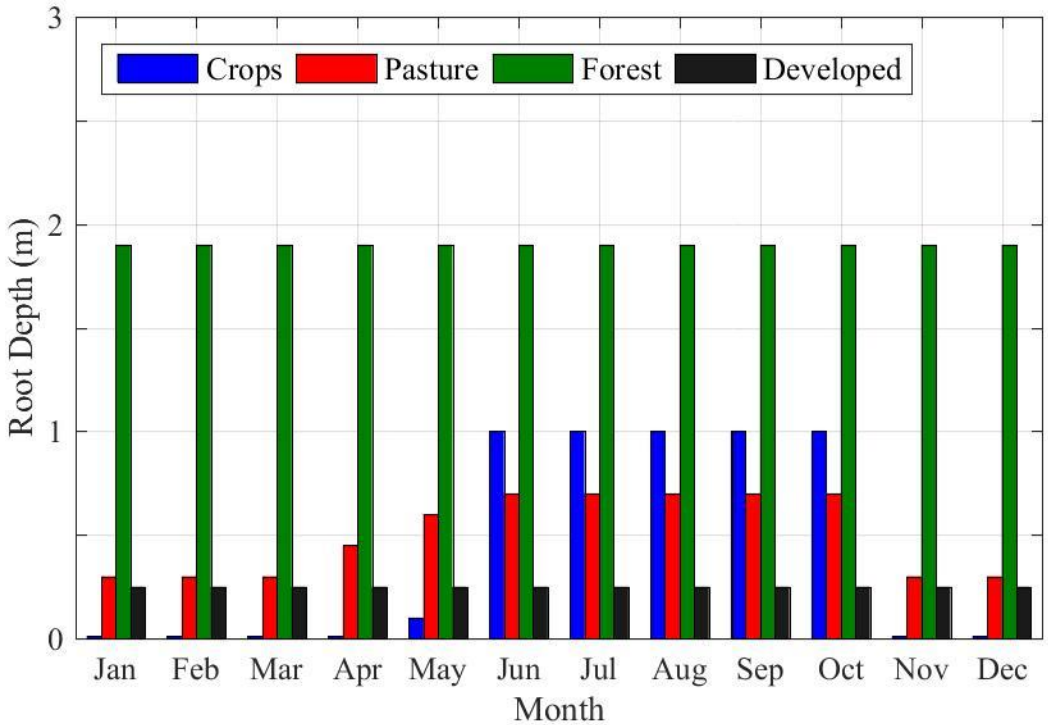

Figure 6.6. Upper Iowa hydrologic model root depth time series for the four different land uses.

Lastly, for simplification purposes the soil criteria was classified based on land cover where crops consisted of loam and everything else was classified as silt loam based on the gSSURGO soil classification (NRCS 2016). The starting van Genuchten parameterization is shown in Table 6.3 and based on the average values of the ROSETTA model (Schaap et al. 2001). For simplification and model stability the subsurface thickness was specified as 20 m below the ground surface. The bottom boundary layer for the model was impermeable.

Table 6.3. ROSETTA average Van Genuchten parameter values for the two Dominant Soil Classes within the Upper Iowa Hydrologic Model

Van Genuchten Parameters	Loam	Silt Loam
Saturated Hydraulic Conductivity (K_{SATH}), m/s	1.39×10^{-6}	2.11×10^{-6}
Porosity (θ_s), m^3/m^3	0.399	0.439
Residual Porosity (θ_r), m^3/m^3	0.061	0.065
α (m^{-1})	1.11	0.51
B	1.47	1.66

6.3 Summary

GHOST is a distributed, physically-based, integrated hydrologic model. The model is forced by Nexrad Stage IV Radar rainfall and NLDAS-2 climatological data. Evapotranspiration is calculated in four components, canopy evaporation, surface water evaporation, soil evaporation, and transpiration using the Penman-Montieth method and methodology described by Panday and Huyakorn (2004). The transport of water within the model is split into three zones the surface zone, governed by 2-D St. Venant equation and 1-D St. Venant Equation for overland flow and stream flow respectively, vertically dominated flow in the unsaturated zone, and Richards Equation in the saturated zone. The watershed is simulated using an irregular triangular mesh that is defined by a simplified watershed boundary and stream network. For the Upper Iowa watershed model the watershed was discretized by 6491 elements and 2199 river segments. The elements were grouped by land cover into four types; cropped, pasture/grassland, forest, and urban. The soil information was matched with the land cover. The river segments were grouped into six different types based

on widths estimated through aerial photography. The number of elements and river segments was adequate for calibrating the model and performing scenarios.

Chapter 7. Model Calibration

Uncertainty is a major limitation in hydrologic modeling. In general, uncertainty can be grouped into four categories: input uncertainty due to measurement error in the forcing data, output uncertainty due to measurement error in the observations used to compare the results of the model, structural uncertainty due to errors caused by mathematical simplifications of the hydrologic processes, and, lastly, parametric uncertainty due to lack of information and variability in model parameter values (Renard et al. 2010). For this project, two common approaches were applied to reduce the uncertainty in model results. The first, model initialization, is a process of determining realistic initial conditions for the state variables within a watershed for a time period of interest, as the amount of data required to determine the initial state of a watershed is unrealistically large to measure. The second, model calibration, is a process of adjusting model parameters within acceptable ranges to improve agreement between model results and observations. In this chapter the approaches used for initialization and calibration of the Upper Iowa River watershed are discussed.

7.1 Model Initialization

Initial conditions greatly affect the results of an integrated hydrologic model (Seck et al. 2015; Hoori Ajami et al. 2015). To reduce the dependence of model results on initial conditions different approaches have been used. Two common approaches both start from constant arbitrary initial conditions, however; one recursively simulates the same year until equilibrium is reached and the other simulates hydrologic forcing data until simulated results match observed data (Hoori. Ajami et al. 2014). For the Upper Iowa watershed model an approach similar to the second method was used. Starting from a constant surface water depth of 1×10^{-3} m, soil moisture of 50% and ground water depth of 4 m below ground surface the model was simulated with forcing data from the time period of Jan. 1, 2004 to Jan. 1, 2012 when the subsurface became pseudo steady-state

with a reasonable initial subsurface moisture conditions (Figure 7.1, Figure 7.2). The initial subsurface moisture is an indicator of the limitations of the model with a dense stream network, where the adjacent elements to the stream network are saturated due to the lack of connectivity between the two systems while the up slope elements have excessive storage (Figure 7.1, Figure 7.2).

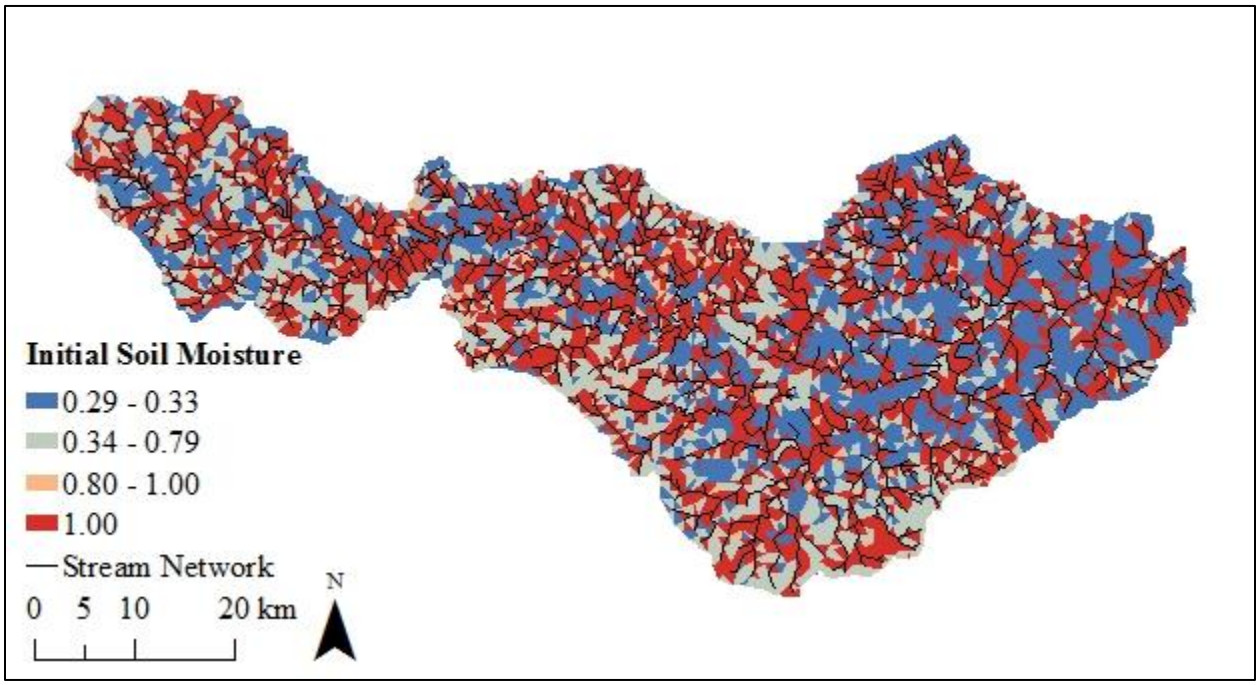

Figure 7.1. Upper Iowa hydrologic model initial soil moisture conditions divided into four quantiles.

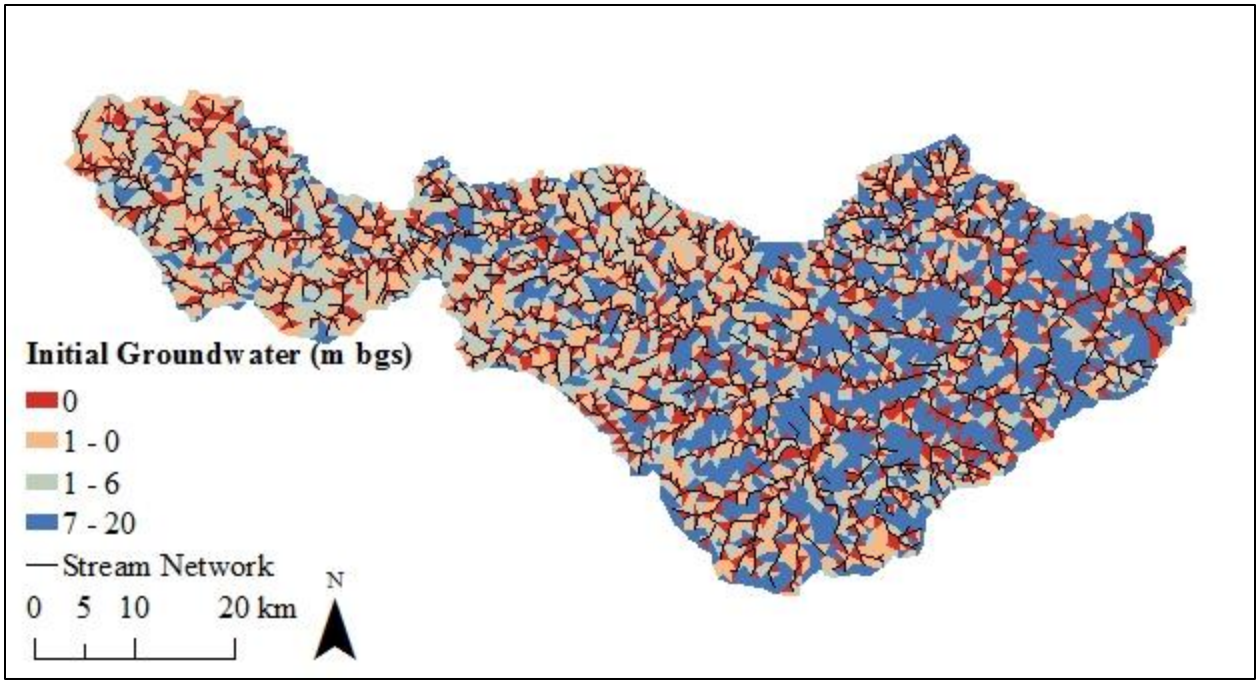

Figure 7.2. Upper Iowa hydrologic model initial groundwater conditions m below the ground surface (bgs) divided into four quantiles.

7.2 Calibration Targets

To evaluate the success of a model calibration process, a set of targets needs to be established. These targets change based on the goals of the overall project. With the focus on stream flow, the targets were based on annual water balance ratios calculated from available measured data along with available global averages observed within the literature. In addition, statistical performance criteria comparing the modeled hydrograph to the measured hydrograph are used.

The annual water balance ratios used as calibration targets included the ratios Q/P, Q_B/Q, ET/P discussed in Section 3.2.1. Furthermore, global continental estimates from literature for transpiration to evapotranspiration (T/ET), canopy evaporation to evapotranspiration (E_C/ET), soil evaporation to evapotranspiration (E_s/ET), and surface water evapotranspiration (E_{sw}/ET) are used as a reference for calibrating the evapotranspiration. Using observed data, Q/P was estimated for the time period of 2002 to 2016 and ranged from 0.15 in dry years to 0.56 in wet years. The Q_B/Q

annual target values were calculated using base flow separation technique developed by Jae Lim et al. (2005) with values ranging from 65% in wet years and 75% in dry years. The annual ET/P target values were calculated based on a simple mass balance for the watershed assuming the change in storage for the year was zero and the influence of subsurface flow crossing watershed boundaries was negligible. Using the water balance approach, ET/P ranged from 0.44 in wet years and 0.85 in dry years. For northeast Iowa, typical ET/P ratios range between 0.5 and 0.7 (Sanford and Selnick 2013). Unfortunately, there are no instruments within the watershed estimating the partitioning of evapotranspiration into the four components. Therefore, values representing global continental averages, estimated by Good et al. (2015) for transpiration to evapotranspiration (T/ET), canopy evaporation to evapotranspiration (E_C/ET), soil evaporation to evapotranspiration (E_s/ET), and surface water evapotranspiration (E_{sw}/ET) and; Schlesinger & Jasechko (2014) for T/ET were used as references during calibration (Table 7.1). Slight deviations from the evapotranspiration targets were expected as evapotranspiration varies as the scaling changes from the global continental scale.

Table 7.1. Ratios of Annual Water Balance Components used in the Calibration Process from Good et al. (2015) and Schlesinger and Jasechko (2014)

Ratio	Reference Calibration Targets
T/ET	0.64, 0.5-0.6*
E_C/ET	0.27
E_s/ET	0.06
E_{sw}/ET	0.03

*(Schlesinger and Jasechko 2014)

The three USGS stream gages located within the watershed allowed for the possibility of performing statistical analyses comparing the simulation hydrograph to measured hydrographs. Two measures were used for calibration. The first was the Nash-Sutcliffe efficiency (NSE) calculated using daily average discharge measurements for each year and 15 minute discharge data for events of interest. NSE defines the skill of the model compared to the mean of the observed values (Nash and Sutcliffe 1970). Values range from negative infinity to 1 with values greater than 0.5 considered reasonable for streamflow (Moriasi et al. 2007). The second statistic used was percent bias (PBIAS). PBIAS is an estimate of the tendency of the simulated data to underestimate or overestimate the observed data (Gupta et al. 1999). PBIAS equaling zero is the optimal value with positive values indicating underestimation and negative values indicating overestimation (Gupta et al. 1999). For streamflow values between ±25% are considered reasonable (Moriasi et al. 2007).

7.3 Calibration of Parameters

Using an initialized model with stable subsurface conditions model parameters were adjusted to meet the calibration targets and to compensate for the limitations of the model discussed in Section 6.1.5. The model calibration involved running the model from the initial conditions from 2007 through 2016. The results of the simulations were then compared to the hydrologic ratio targets, statistical performance scores, and visual comparison between the simulation and measured hydrographs. Based on the comparison, model parameters were iteratively adjusted and improvements from these adjustments were incorporated into the model.

7.3.1 Evapotranspiration Parameters

The evapotranspiration parameters within the Upper Iowa hydrologic model were adjusted to meet the calibration targets for water balance ratios and to decrease the soil moisture that limits transpiration, the largest component of the water balance (Schlesinger and Jasechko 2014). First

to adjust the evapotranspiration ratios along with the ET/P ratio the calibration factors; canopy evaporation factor (E_{CAN}), transpiration factor (E_{TT}), soil evaporation factor (E_{DIR}), and surface water evaporation factor (E_{SURF}) were adjusted. The factors limit the maximum rate of evaporation for each component. For each new simulation the calibration factors were adjusted based on Equation 5:

$$\frac{E_o}{V_o} = \frac{E_n}{V_e} \tag{11}$$

where E_o is the calibration factor used in the simulation, V_o is the simulated evaporation volume, E_n is the new calibration factor and V_e is the estimated evaporation volume based on the water balance equation and ideal calibration target ratios. The final calibration factors are shown in Table 7.2. The largest factor is for transpiration at 1.73. The large factor was needed to compensate for the saturated soils near the stream network as transpiration is reduced as soil moisture increases due to the oxic and anoxic limits (Panday and Huyakorn 2004). However, to further increase the amount of transpiration in the model the oxic and anoxic limits were increased to 0.76 and 0.9 respectively in the pasture, forest, and developed areas, and 0.9 and 0.95 for the cropped area (Table 7.2). The cropped area required higher limits due to the numerous streams surrounding the cropped elements on the western side of the watershed (Figure 6.1). Lastly, to obtain adequate transpiration volumes the root depth within the cropped and pasture areas were doubled throughout the year and the forested areas was increased to 2.5 m (Figure 7.3).

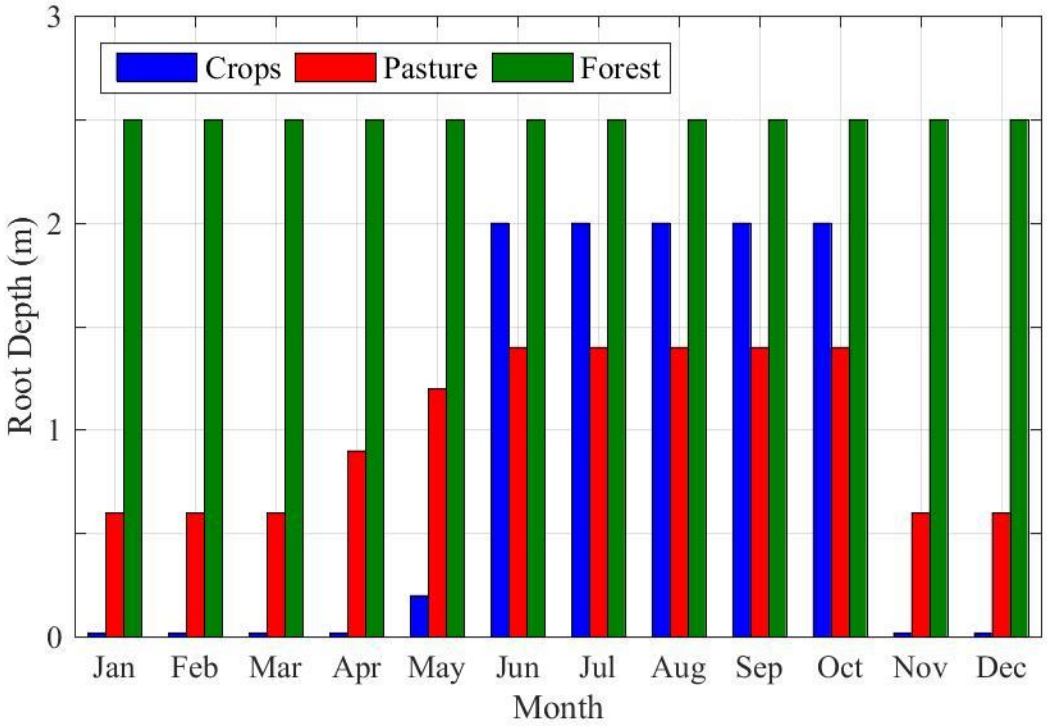

Figure 7.3. Modified root depth time series used with in the Upper Iowa hydrologic model.

The rest of the parameters were set at similar values used in other models. The wilting point, field capacity, and soil evaporation moisture and energy limits were set at 0.2 and 0.32 respectively for evapotranspiration to occur across a wide range of soil moistures (Table 7.2). The interception storage constant was set at 0.001 to meet the canopy evaporation ratio target and also to reduce the peak discharges (Table 7.2). Lastly, the fitting parameter C_3, controlling the shape of the curve between the wilting point and field capacity and oxic limit and anoxic limit, and the evaporation extinction depth, controlling the ration of evaporation in the unsaturated soil and saturated soil were set at standard values of 3×10^{-6} and 0.2 (Table 7.2).

Table 7.2. Evapotranspiration Parameters used in the Upper Iowa Hydrologic Model compared to Literature Values

Parameter	Model Value	Literature Value	Source
E_{CAN}	0.55	NA	-
E_{TT}	1.73	NA	-
E_{DIR}	0.20	NA	-
E_{SURF}	0.04	NA	-
Wilting Point (θ_{wp})	0.2	0.2 0.05-0.2	(Panday and Huyakorn 2004) (Li et al. 2008)
Field Capacity (θ_{fc})	0.32	0.32 0.2-0.32	(Panday and Huyakorn 2004) (Li et al. 2008)
Oxic Limit (θ_o)	0.9* 0.76	0.6 0.76	(Therrien et al. 2010) (Panday and Huyakorn 2004; Li et al. 2008)
Anoxic Limit (θ_{an})	0.95* 0.9	0.8 0.9	(Therrien et al. 2010) (Panday and Huyakorn 2004; Li et al. 2008)
Evaporation Limiting Stage (θ_{e2})	0.2	0.2 0.3	(Panday and Huyakorn 2004; Li et al. 2008) (Thomas 2015)
Energy Limiting Stage (θ_{e1})	0.32	0.32 0.4	(Panday and Huyakorn 2004; Li et al. 2008) (Thomas 2015)
C_3	3×10^{-6}	2.31×10^{-7} 5.8×10^{-8}-3×10^{-6}	(Thomas 2015) (Li et al. 2008)
Evaporation Extinction Depth (B_{soil}) (m)	0.2	0.2 0.4-5	(Therrien et al. 2010) (Li et al. 2008)
Interception Storage Constant (c_{int}) (m)	0.0001	0.00005 0.00005-0.0001 0.04	(Thomas 2015) (Li et al. 2008) (Therrien et al. 2010)

7.3.2 Surface Zone Parameters

The surface zone parameters adjusted in the Upper Iowa hydrologic model included land surface manning's n; stream characteristics manning's n, weir coefficient, height of the weir and river depth; and the snow melting coefficients for the first four months of the year. The manning's n on the land surface impacts the velocity of water movement across the element and thus the timing and shape of high flows within the hydrograph. Typical values for manning's n range from 0.01 to 0.2 (Brunner 2016). A higher manning's n simulates a rougher surface, delaying the flow from the element downstream and creating a longer receding limb. For the Upper Iowa hydrologic model the lowest manning's n was for developed areas (0.05), simulating the impervious surfaces,

while the highest manning's n was for forest (0.15), simulating the trees, litter, and underbrush in forested areas (Table 7.3).

Table 7.3. Manning's Roughness Coefficient for the Upper Iowa Hydrologic Model Compared to Literature Values.

Land Cover Type	Model Value	Literature Values	Source
Cultivated Areas	0.13	0.07-0.2	(Engman 1986)
Pasture	0.13	0.05-0.15	(Engman 1986)
Forest	0.15	0.03-0.2	(Brunner 2016)
Developed	0.05	0.01-0.15	(Brunner 2016)

Similar to the land surface manning's n the river manning's n was adjusted to improve timing of the peaks in the hydrograph. Typical manning's n in the stream is lower than land surface manning's with typical values ranging from 0.025 to 0.15 (Brunner 2016). For the Upper Iowa hydrologic model the manning's n was 0.04 in the smallest stream segment as these areas simulated more grassy areas while 0.03 was used for larger streams as these segments modeled perennial streams (Table 7.4). The last three stream network characteristics control the flow from the 2-D overland mesh to the 1-D stream network by estimating the characteristics of the weir and river. The weir coefficient describes the ease at which water can flow between the two zones. A higher coefficient allows more flow between the two zones while a lower coefficient restricts and delays flow between the two zones. This parameter was used to adjust the magnitudes of the peaks in the hydrograph and also delay flow to increase low flow conditions during dry periods. For the Upper Iowa hydrologic model the weir coefficient ranged from 0.003 for stream number 1 streams to 0.001 for the higher number streams, assuming that water could enter the flow paths and smallest streams easier than the higher order streams that have trees and other obstructions close to the bank (Table 7.4). One drawback from using the weir coefficient to restrict flow is that surface water will pool around the stream network contributing to saturated conditions. To limit the pooling of water near the stream network the height of the weir was set to zero for all of the stream segments (Table 7.4). Therefore, no additional surface water storage was created. Lastly, the river depth was

decreased to 0.1 for all of the stream segments (Table 7.4). The adjustment allowed more transfer of water from the artificially buried river segments, caused from the river smoothing process, to the adjacent elements similar to the storage of water within the riparian areas during flood events.

Table 7.4 Stream Network characteristics for the Upper Iowa Hydrologic Model.

Stream Number	Manning's n	Weir Coefficient	Height of Weir (m)	River Depth (m)
1	0.04	0.0030	0	0.1
2	0.03	0.0012	0	0.1
3	0.03	0.0010	0	0.1
4	0.03	0.0010	0	0.1
5	0.03	0.0010	0	0.1
6	0.03	0.0010	0	0.1

The last change to the hydrologic model required to improve the surface flow was increasing the snow melt coefficients to more closely match the early spring stream flow. The snow melt coefficients for January through April were increased to increase snow melt earlier in the year. January was increased to the average snow melting coefficient while February through March were increased to the maximum melting coefficient of 6.0 specified by Mockus et al. (2004) (Table 7.5).

Table 7.5. Monthly Snow Melting Coefficients for the Upper Iowa Hydrologic Model

Month	Jan	Feb	Mar	Apr
C_{snow} (mm/C)	2.74	6.0	6.0	6.0

7.3.3 Subsurface Parameters

The subsurface parameters adjusted in the Upper Iowa hydrologic model included; the infiltration hydraulic conductivity, coupling length, horizontal saturated hydraulic conductivity, van Genuchten parameters (α, β), and the recharge sigmoid function variables (m, s_n^*). These parameters were adjusted to reduce the soil moisture in the model especially near the stream network, as the model tends to display peaks when there is none. In addition, the modified

parameters were used to increase base flow during low flow conditions when water within the stream network is limited.

To improve performance, the infiltration hydraulic conductivity was increased and coupling length was decreased resulting in increased infiltration, thus reduce the soil saturation, and at the same time; increase base flow to the stream through exfiltration. Another adjustment used to reduce the inundation time within the model was to change the van Genuchten soil retention curve to lessen the soil water retention by decreasing α and increasing β. The last adjustment made to the subsurface was to increase the saturated hydraulic conductivity and adjust the recharge sigmoid function variables increasing base flow through higher lateral flow and recharge. The final parameter values used in the Upper Iowa hydrologic model are shown in Table 7.6.

Table 7.6. Subsurface Parameters used in the Upper Iowa Hydrologic Model compared to Literature Values

Parameter	Model Value	Literature Value*	
Infiltration Hydraulic Conductivty (K_{Inf}) (m/s)	1.4×10^{-5}* 1.8×10^{-5} [a] 1.0×10^{-7}	NA	
Coupling Length (D_{inf}) (m)	0.05	10^{-2} $\leq10^{-2}$ 10^{-1}	(Ebel et al. 2009) (Liggett et al. 2012) (Therrien et al. 2010)
Horizontal Hydraulic Conductivity, K_{Hsat} (m/s)	7×10^{-5}* 4.8×10^{-5}	1.39×10^{-6}* 2.11×10^{-6}	(Schaap et al. 2001)
α (m^{-1})	0.50* 0.50	1.11* 0.51	(Schaap et al. 2001)
B	5.0* 5.0	1.47* 1.66	(Schaap et al. 2001)
m	4	NA	
s_n^*	0.55	NA	

* Crop land use soil parameter

[a] Pasture and Forest soil parameter

In addition to increasing baseflow the final calibration parameters created pseudo-steady state conditions within the subsurface with the area averaged soil moisture varying around 0.65

and a slight increase in the groundwater over the entire calibration time period as depicted in Figure 7.4. Furthermore, the groundwater alternated as expected decreasing in dry periods and increasing in wet periods (Figure 7.4). Lastly, the soil moisture throughout the modeling time period indicated one of the limitations in GHOST with the area averaged soil moisture never decreasing below 0.45 (Figure 7.4). During droughts it is expected that soil moisture should approach the residual soil moisture.

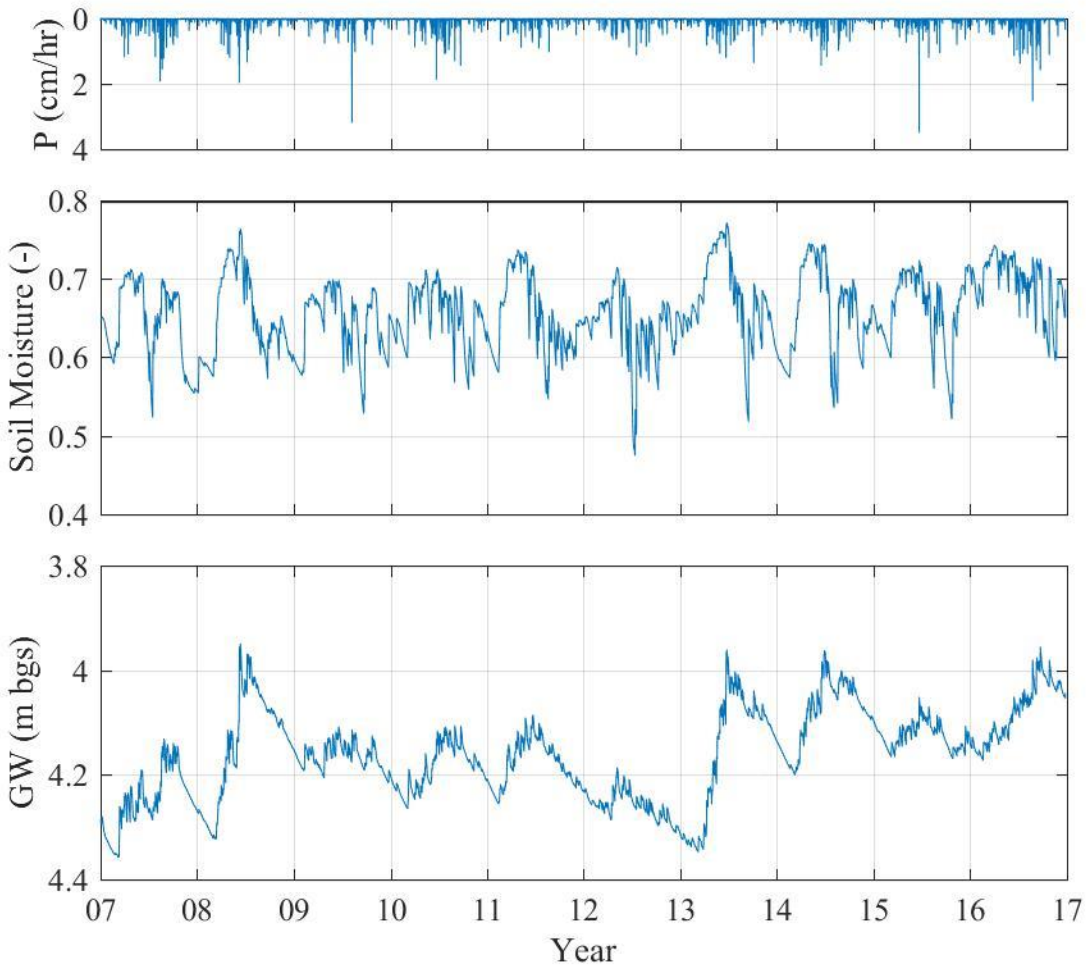

Figure 7.4. Upper Iowa hydrologic model area average soil moisture and ground water table for the time period of 2007 through 2016.

7.4 Calibrated Model Performance

With the final set of parameters, the calibrated model was evaluated. The final set of parameters were chosen because they resulted in higher NSE values, PBIAS values close to zero, and hydrologic ratios closer to the calibration targets. However, during calibration it was determined that due to the extensive stream network within the mesh, created to model pond structures, the limitations of the GHOST model were accentuated. Therefore, the subsurface was overly saturated during the dry years and the dry years of 2009 and 2012 were unable to achieve adequate results. The average years of 2007, 2010-11, and 2014-15 were able to achieve adequate water balance ratios, however, the targets set for NSE and PBIAS were not achieved. The wet years of 2008, 2013, and 2016 were able to achieve adequate calibration results for both the water balance ratios and the NSE and PBIAS performance statistics. In addition, since the eventual use of the model was to estimate discharge reductions from conservation practices, the calibration focused on improving the wet years at the expense of the average years and dry years.

The water balance ratios are depicted in Figure 7.5. The Q/P and ET/P values for average and wet years are reasonable with the average years having slightly higher Q/P and lower ET/P and the wet years having the reverse trend. On the other hand, the dry years of 2009 and 2012 have significantly higher Q/P and lower ET/P ratios (Figure 7.5). The reasoning for the discrepancy in the dry years and the trends between the average and dry years is because of the high near saturated conditions in the river adjacent elements that is required to supply baseflow to the stream network. Thus, the river adjacent elements do not have enough storage for precipitation events that are normally absorbed by the dry soil during droughts increasing the discharge compared to measured data. At the same time, the river adjacent elements do not have enough unsaturated water that is available for transpiration, decreasing the evapotranspiration. The wet years have a high ET/P ratio compared to measured data because the calibration factors are skewed to increase

evapotranspiration in the river adjacent elements and during wet years there is enough precipitation on the up slope elements to overcome the limited evapotranspiration in the river adjacent elements.

During calibration subsurface parameters were adjusted to increase baseflow, the Q_B/Q was still lower than the estimated ratio based on the WHAT base flow separation technique (Jae Lim et al. 2005) (Figure 7.5). The estimated ratios are not measured values but, estimated using a mathematical relationship. Therefore there is uncertainty in both the simulated and estimated ratios. It is still suspected based on the karst topography within the Upper Iowa watershed that baseflow is a major component of the total discharge. Thus an improved subsurface formulation including a preferential flow model would improve the performance of the model with respect to the baseflow of the model.

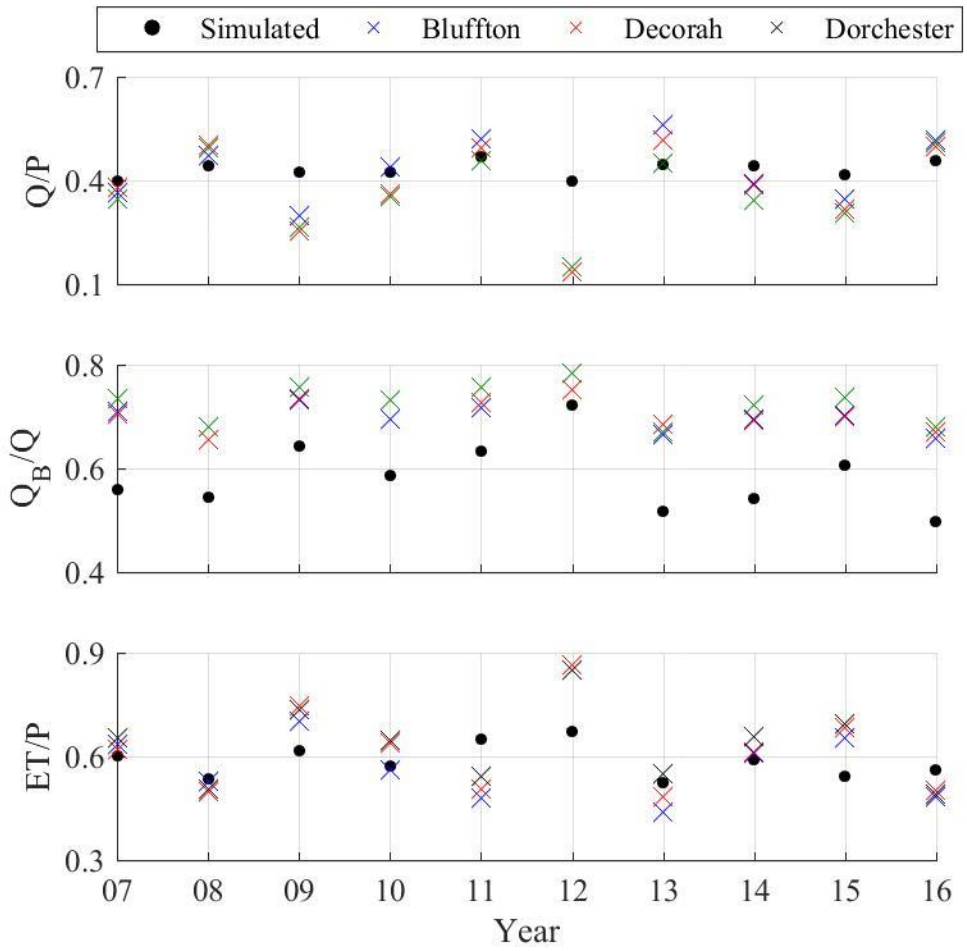

Figure 7.5. Annual water balance ratios; discharge to precipitation (Q/P), baseflow to discharge (Q_B/Q), and evapotranspiration to precipitation (ET/P) for the Upper Iowa hydrologic model for the time period of 2007 through 2016.

The simulated evapotranspiration ratios compared to global continental averages are depicted in Figure 7.6. Overall the T/ET and E_{can}/ET ratios with some scatter were comparable to global averages while the soil evaporation and surface water evaporation were higher as a percentage of the total evapotranspiration. The final calibration parameters had soil evaporation and surface water evaporation above the reference values to increase the available water for transpiration, as transpiration is limited when the soil moisture is close to saturation and the water table is above the root depth. The annual T/ET was also another indicator of the difference in the performance of stream network adjacent elements and upslope elements. During dry years T/ET was low because the up slope elements were dry while the stream network adjacent elements were

still saturated, limiting T/ET (Figure 7.6). Although, in wet years, for example 2016, T/ET was above the reference values because too much transpiration occurred in the up slope elements due to the parameters being skewed to increase evapotranspiration in the stream network adjacent elements (Figure 7.6).

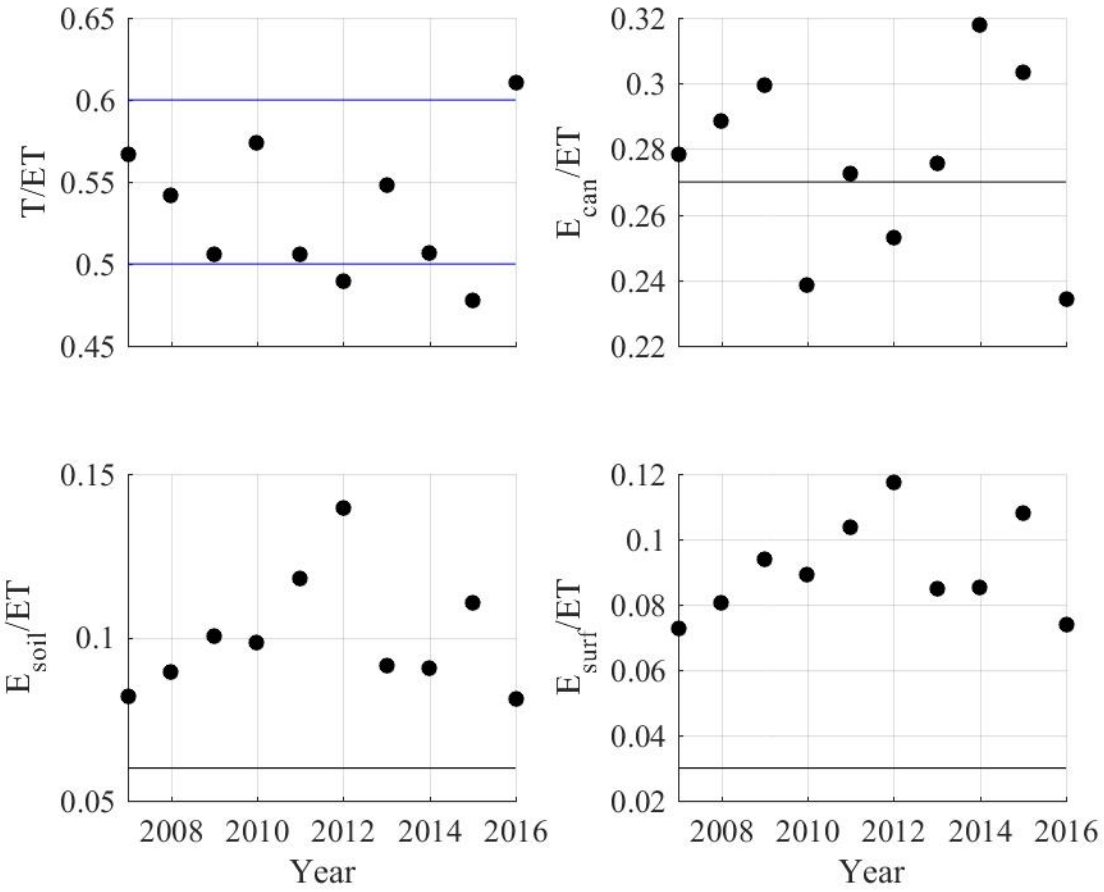

Figure 7.6. Evapotranspiration ratios of the four evapotranspiration components transpiration (T), canopy evaporation (E_{can}), soil evaporation (E_{soil}), and surface water evaporation (E_{sw}) for the time period of 2007 through 2016 at the outlet of the Upper Iowa hydrologic model. Solid black lines indicate the continental evapotranspiration ratios based on Good et al. (2015) while the solid blue lines represent the common T/ET ratio based on Schlesinger and Jasechko (2014).

The hydrologic model performance statistics for the wet years are above the target values, 0.5 for NSE and ±25% for PBIAS, with the lowest annual NSE equal to 0.7 and annual PBIAS equal to 12% for the three USGS stream gage locations (Table 7.7). The average and dry years, on the other hand, indicate poor performance. The worst year occurring in 2012, the driest year, with

NSE of -9.9 and PBIAS of -172% (Table 7.7). In general the performance of the model improves from dry to wet years as depicted in Figure 7.7 where the estimated Q_B/Q is plotted against the NSE for the year. A higher annual Q_B/Q indicates a drier year as more flow is dependent on subsurface flow compared to wet years with a higher percentage of surface runoff. The correlation coefficient of -0.71 indicates an inverse relationship between Q_B/Q and skill (Figure 7.7).

Table 7.7 Upper Iowa Hydrologic Model Performance Statistics, NSE and PBIAS

	NSE			PBIAS (%)		
Year	Bluffton	Decorah	Dorchester	Bluffton	Decorah	Dorchester
2007	-0.38	-0.20	-0.20	-1.3	1.2	-6.5
2008	**0.90**	**0.83**	**0.86**	**4.7**	**11**	**12**
2009	-2.4	-4.0	-3.7	-43	-64	-51
2010	0.14	-0.62	-0.38	-3.3	-20	-14
2011	0.50	0.47	0.41	7.4	5.5	1.6
2012	-7.0	-7.2	-9.9	-150	-172	-135
2013	**0.70**	**0.71**	**0.73**	**8.0**	**5.7**	**0.1**
2014	-0.14	-0.10	-0.29	-37	-33	-41
2015	0.13	0.13	-0.05	-39	-46	-42
2016	**0.78**	**0.81**	**0.77**	**6.0**	**5.2**	**12**
Target	**0.5**			**±25**		

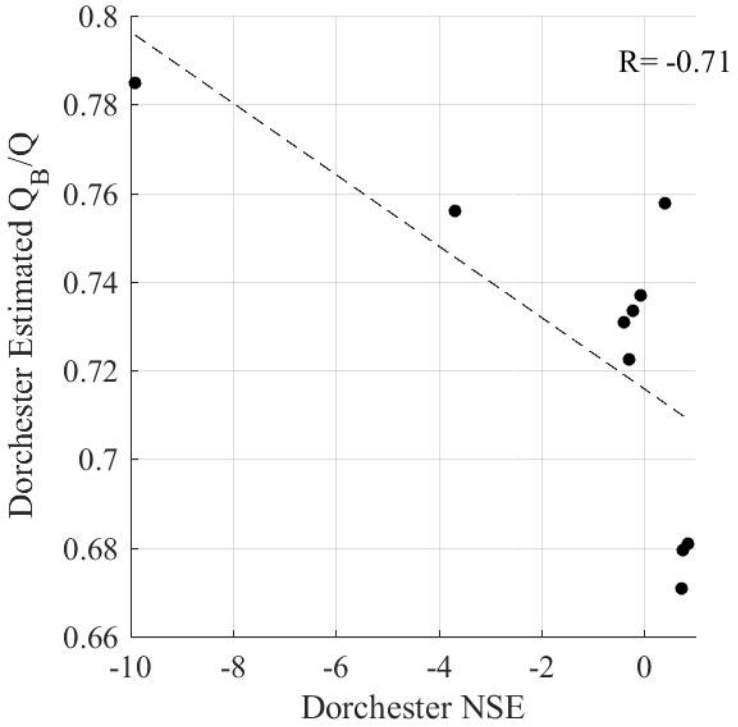

Figure 7.7. WHAT estimated baseflow to discharge ratio (Q_B/Q) at Dorchester plotted against the NSE score for the discharge for each year simulated near Dorchester.

The annual hydrographs were plotted against the USGS stream gage measurements to show the model performance (Figure 7.8, Figure 7.9, Figure 7.10, Figure 7.11). During the dry year of 2012 the model predicts a response with every precipitation event when the measured data does not indicate a response. The reason for the response is once again due to the stream network adjacent elements being unable to drain fast enough with the lack of lateral flow between the stream and the subsurface. The erroneous responses were common during other years and during dry periods within the wet years, October and November 2008 and 2013 (Figure 7.9, Figure 7.10). Further evidence of the limitations in the subsurface, are in the receding limbs of responses where the simulated hydrographs recedes more rapidly than the measured data (Figure 7.9, Figure 7.10, Figure 7.11). Improvement in the receding limb performance would be expected from the inclusion of a secondary preferential flow model that would increase the flow of the water after the peak. For the wet years the model does capture the magnitudes of the annual maximums during the years

of 2008 and 2016 but underestimates the annual maximum of 2013 (Figure 7.9, Figure 7.10, Figure 7.11). Lastly, the changes made to snow melt coefficient improved the model performance by moving snow melt to more closely resemble the typical snow melt in February and early March. As a result, the over prediction of peaks in March and April were limited to a reasonable match for 2013 (Figure 7.9, Figure 7.10, Figure 7.11). Additional hydrographs for the full simulation time at Bluffton, Decorah, and Dorchester are shown in the Appendix.

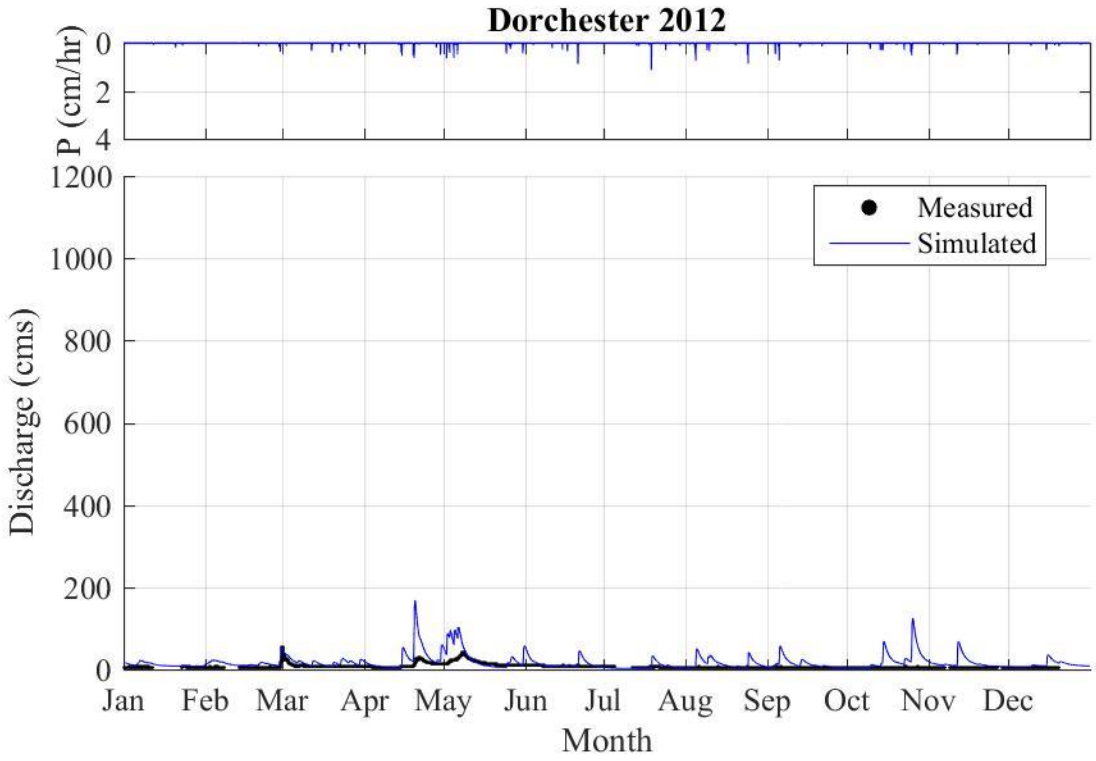

Figure 7.8. Example dry year hydrograph for year 2012 near Dorchester.

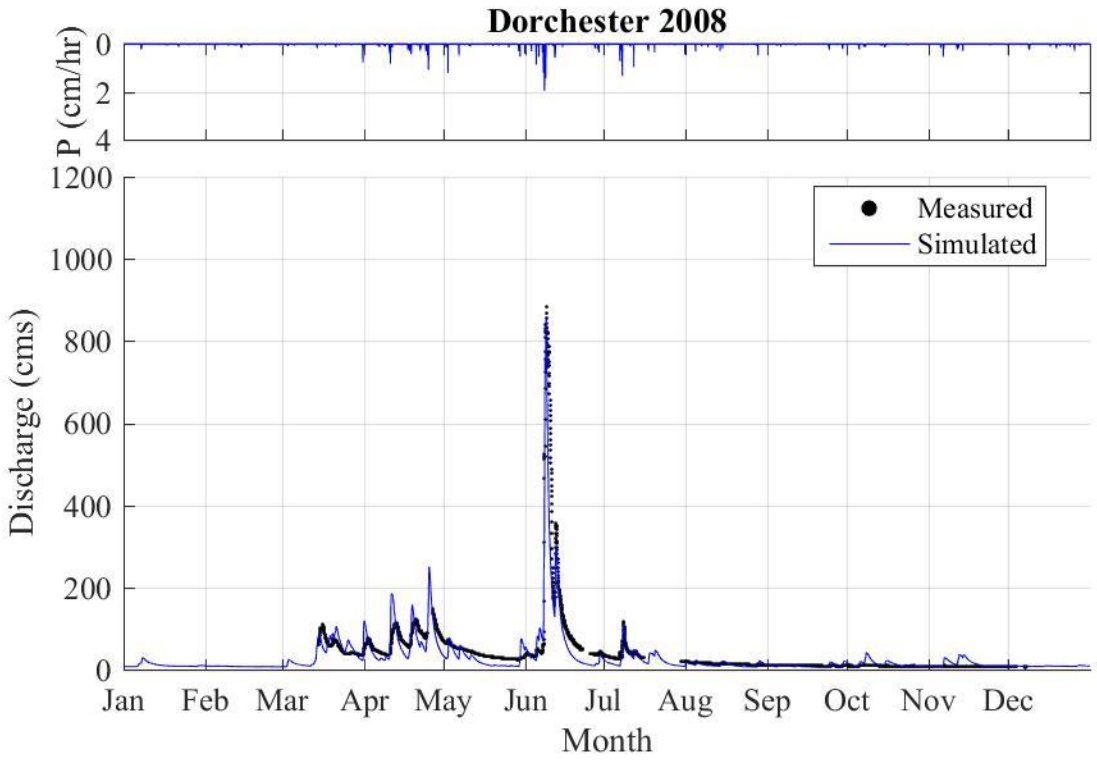

Figure 7.9. Hydrograph for 2008 at the USGS stream gage near Dorchester.

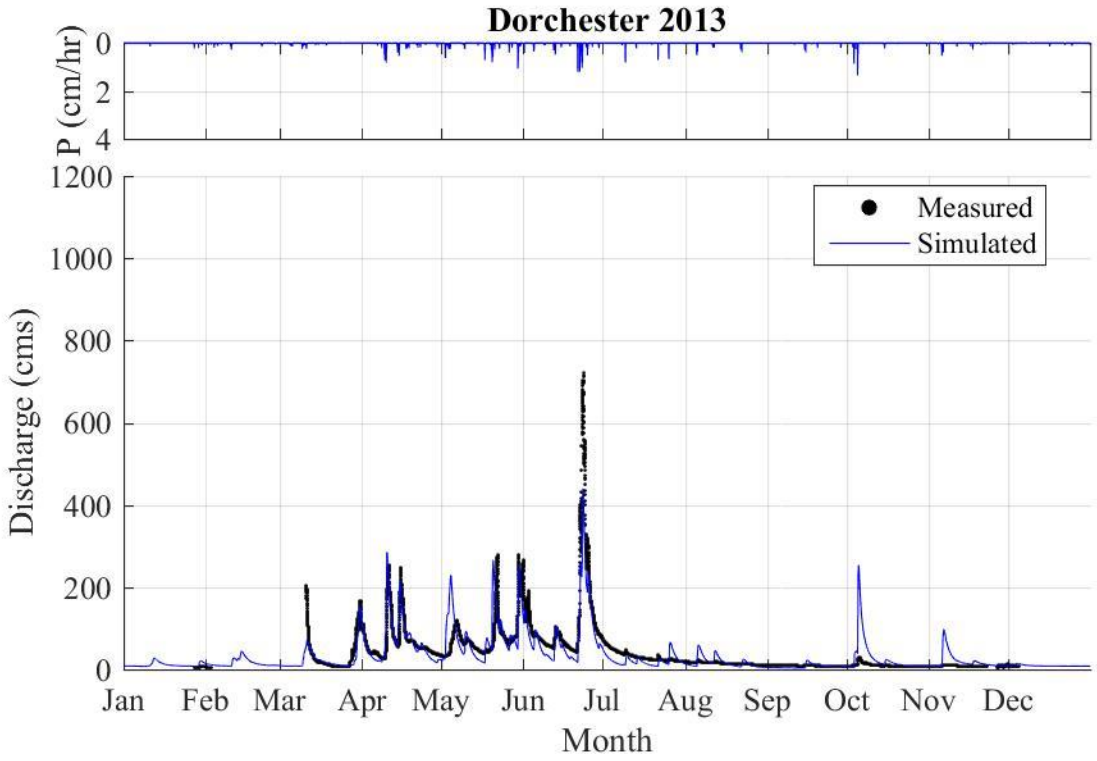

Figure 7.10. Hydrograph for 2013 at the USGS stream gage near Dorchester.

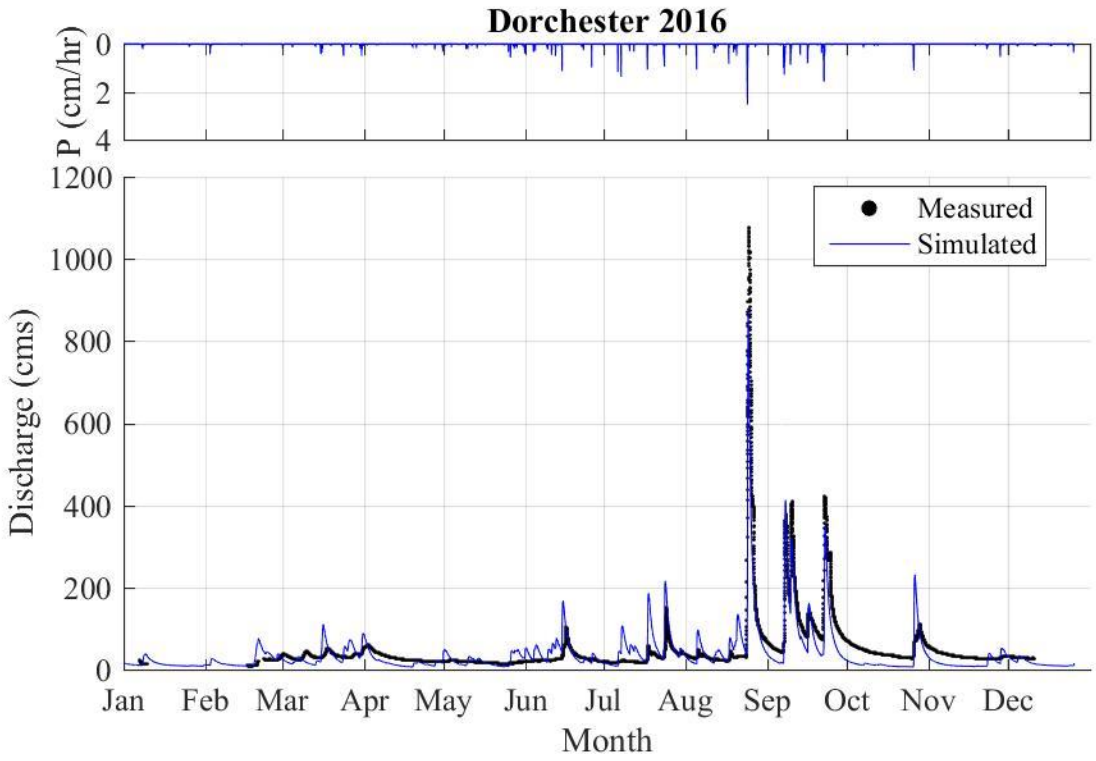

Figure 7.11. Hydrograph for 2016 at the USGS stream gage near Dorchester.

Lastly, because of the emphasis of the IWA on flooding the performance statistics and hydrographs for the two major floods within the study period (2008, 2016) were examined. Both storms had decent skill with NSE above 0.59, and were not biased with one station slightly under estimating the 2016 event near Dorchester with 31% (Table 7.8). For both events the performance decreased moving downstream. For the 2008 event the importance of karst flow was depicted with the duration of high flows in the measured data increasing as the landscape changed from the Iowan Surface landscape upstream of Bluffton to the Paleozoic Plateau landscape with karst flow for Decorah and Dorchester (Figure 7.12). This response was not captured by the simulation.

Table 7.8. Upper Iowa Hydrologic Model Performance Statistics, NSE and PBIAS for the 2008 and 2016 Floods

	NSE			PBIAS (%)		
Event	Bluffton	Decorah	Dorchester	Bluffton	Decorah	Dorchester
2008	0.91	0.74	0.77	8.5	23	21
2016	0.64	0.59	0.63	12	13	31

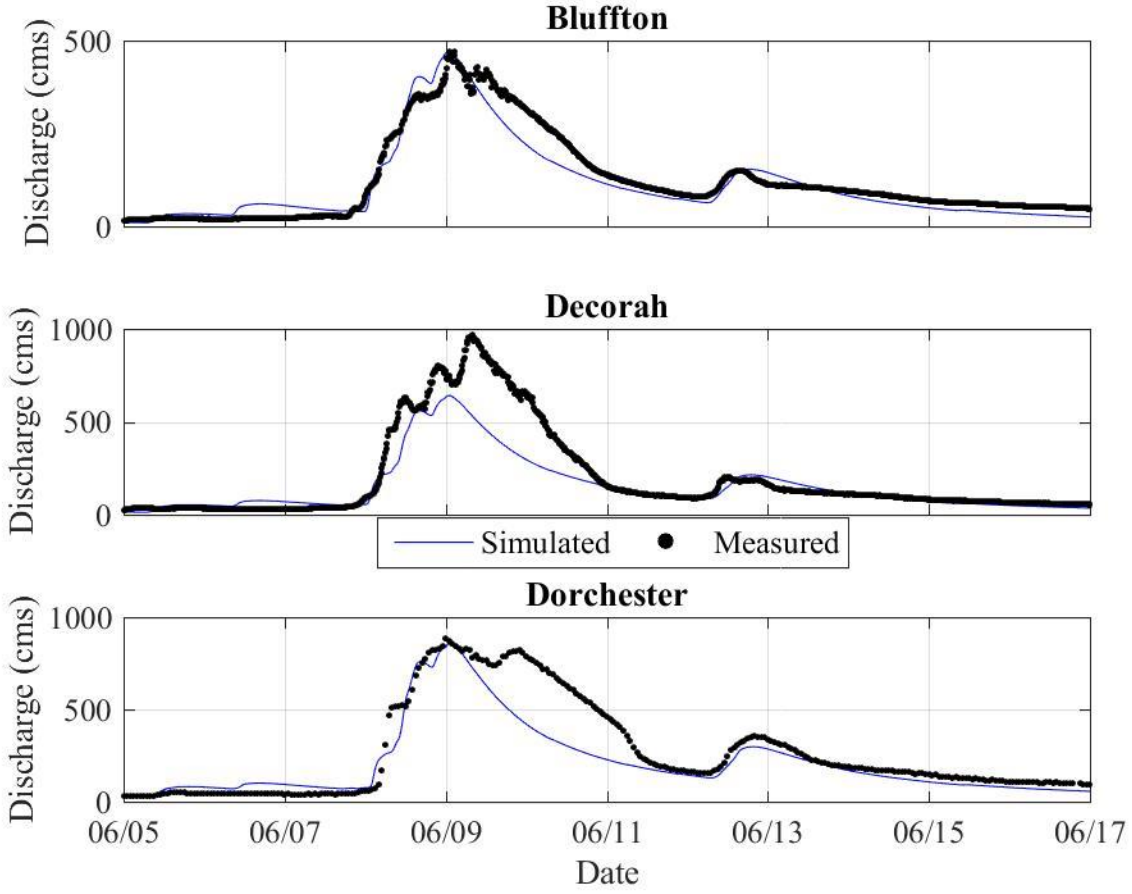

Figure 7.12. Hydrograph of the 2008 flood event at the three USGS stations within the Upper Iowa watershed.

For the 2016 event, the magnitudes of the peaks were close to the measured data except at Dorchester as indicated by the PBIAS of 31% (Figure 7.12, Table 7.8). However, the simulation did not capture a second peak prevalent at Bluffton and the timing of the peak was delayed (Figure 7.12). The difference in timing between the simulated hydrograph and measured hydrograph was caused by the soil moisture not matching the actual soil moisture changing the distribution of

runoff within the model. Another potential reason is within the precipitation input file not matching the variance in the precipitation completely that could have caused the second peak at Bluffton. Lastly, the combination of precipitation and soil moisture representation in the model caused Dorchester to be under predicted as the precipitation was concentrated between Decorah and Dorchester, an area with excessive soil storage in the model. These two events were chosen to show the impact of scenarios on the floods within the Upper Iowa watershed.

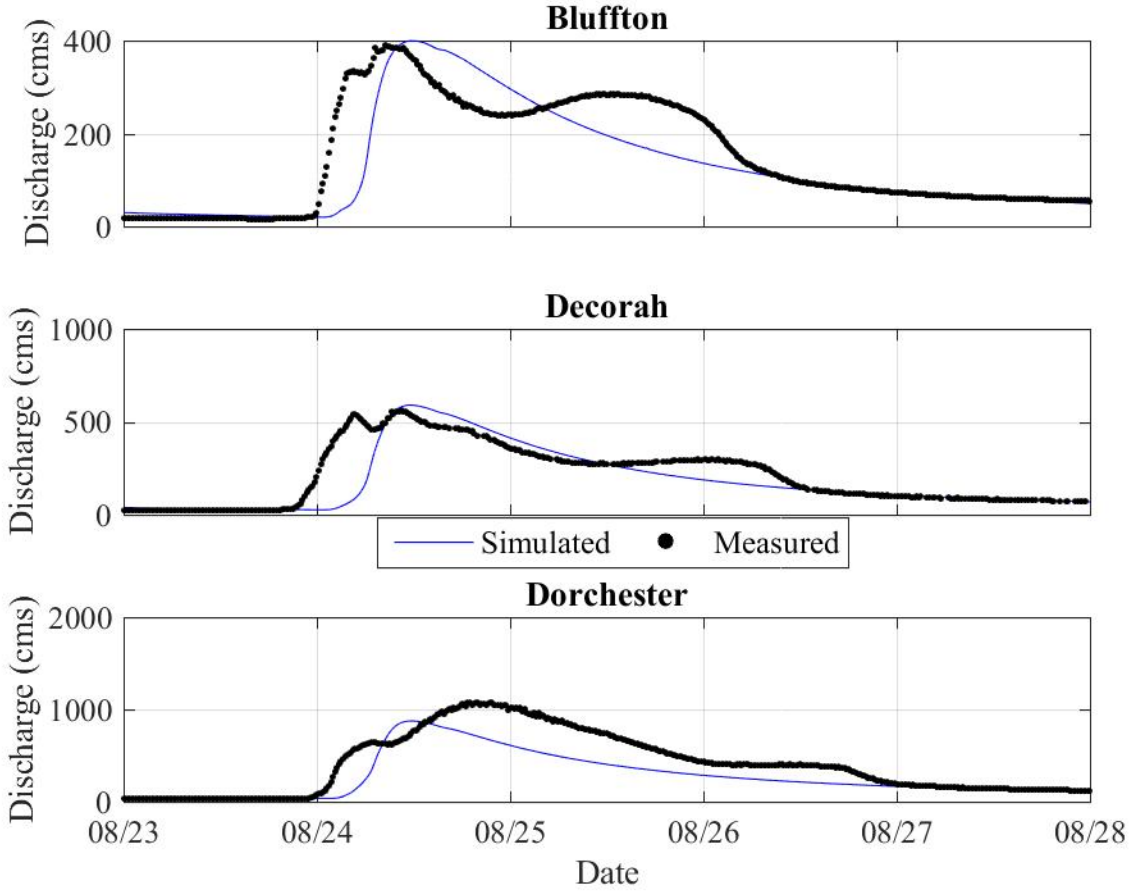

Figure 7.13. Hydrographs for the 2016 flood event at the three USGS stations within the Upper Iowa watershed.

7.5 Summary

Calibration is a necessary part of hydrologic modeling used to reduce the uncertainty in model parameters. For the Upper Iowa hydrologic model initial conditions were created by forcing the hydrologic model with meteorological data for the time period of 2002 to 2012 when the

groundwater achieved reasonable values and pseudo-steady state conditions. Using these initial conditions the model was then calibrated over the time period of 2007 through 2016. For calibration parameter values were changed iteratively and the model results were compared to calibration targets. The calibration targets for the model were to achieve realistic annual water balance ratios compared to measured data and meet NSE scores above 0.5 and PBIAS between ±25%. It was determined that due to the limitations of subsurface formulation in GHOST the dry years (2009 and 2012) were unable to achieve the calibration targets. However, the average years achieved adequate water balance ratios and the wet years (2008, 2013, and 2016), the main focus of this study, achieved adequate performance achieving reasonable water balance ratios, NSE scores above 0.7 and PBIAS between ±12%. The Upper Iowa hydrologic model also had good performance for the 2008 and 2016 flood events where the 2008 event had excellent performance besides a secondary volume of water caused by preferential flow within the watershed and the 2016 event matched the peak with inaccuracy in the timing and shape due to a secondary peak in the measured data. Due to the good performance of the flood events, they were chosen to access the scenarios.

Chapter 8. Simulated Conservation Practice Scenarios

After calibrating and evaluating the performance of the Upper Iowa hydrologic model, the model was used to estimate the potential benefits of continuous cover crops. The scenarios involved first varying the amount of implementation within the watershed to characterize a trend as cover crops became more popular. Then continuous cover crops benefits were simulated under potential future precipitation trends.

8.1 Cover Crops Scenario

The first scenario investigated the increased use of continuous cover crops within the Upper Iowa watershed over the ten year simulation time period. Cover crops are crops planted after the harvest of corn or soybeans that grow when the ground would usually be fallow. Cover crops increase the use of solar energy to increase evapotranspiration from the soil while simultaneously reducing sediment transport and improving soil water quality (Dabney et al. 2007). Within the Upper Iowa there is the potential to implement the practice on 116,150 ha of cultivated crops (Table 8.1). The potential cost for the government to subsidize the first year of implementation would be $11.5 million based on the $99.16/ha 2016 Iowa EQIP Basic payment rate for chemical or mechanical kill species (Tyndall and Bowman 2016).

To simulate the impact of cover crops on the Upper Iowa watershed the evapotranspiration time series modeling the growth of vegetation were modified by incorporating winter wheat time series based on Breuer et al. (2003) and Fang et al. (2008) for LAI and root depth and Allen et al. (1998) for the crop coefficient within the evapotranspiration time series for crops. The different evapotranspiration time series; LAI, crop coefficient, and root depth, for the three different implementation are shown in Figure 8.1, Figure 8.2, and Figure 8.3 respectively. With the new time series the scenario was simulated for the entire calibration time period. In addition to full implementation, 50% and 25% implementation were simulated to characterize the trend in benefits

as the use of continuous cover crops is increased. The approximate cover cropped areas simulated for each scenarios are shown in (Table 8.1). To simulate the different implementation scenarios, the average between the crop time series and the full cover crop implementation was calculated. In this way, uniform implementation was achieved throughout the watershed eliminating the impact of the variable precipitation within the forcing data on the simulation results.

Table 8.1 Cover Crop Area Potential within the Upper Iowa Watershed and the Area simulated within the Upper Iowa Hydrologic Model Scenarios

	Area (ha)
NLCD 2011 Cultivated Crops	116,150
100% Cover Crops	131,977
50% Cover Crops	65,989
25% Cover Crops	32,994

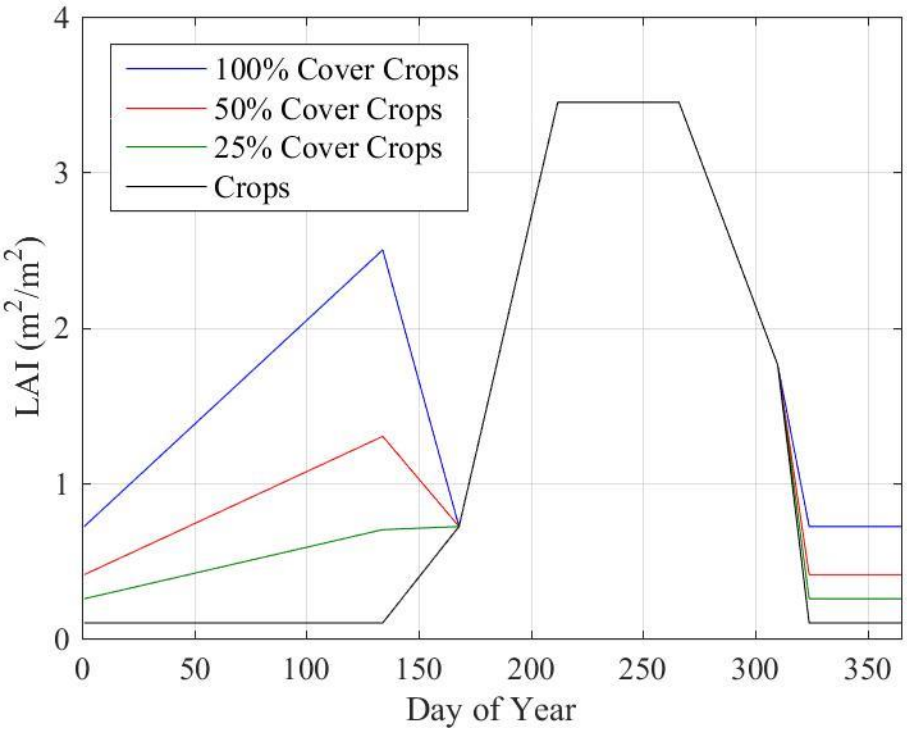

Figure 8.1. LAI time series for different cover crop implementation schemes ranging from 25% to 100%.

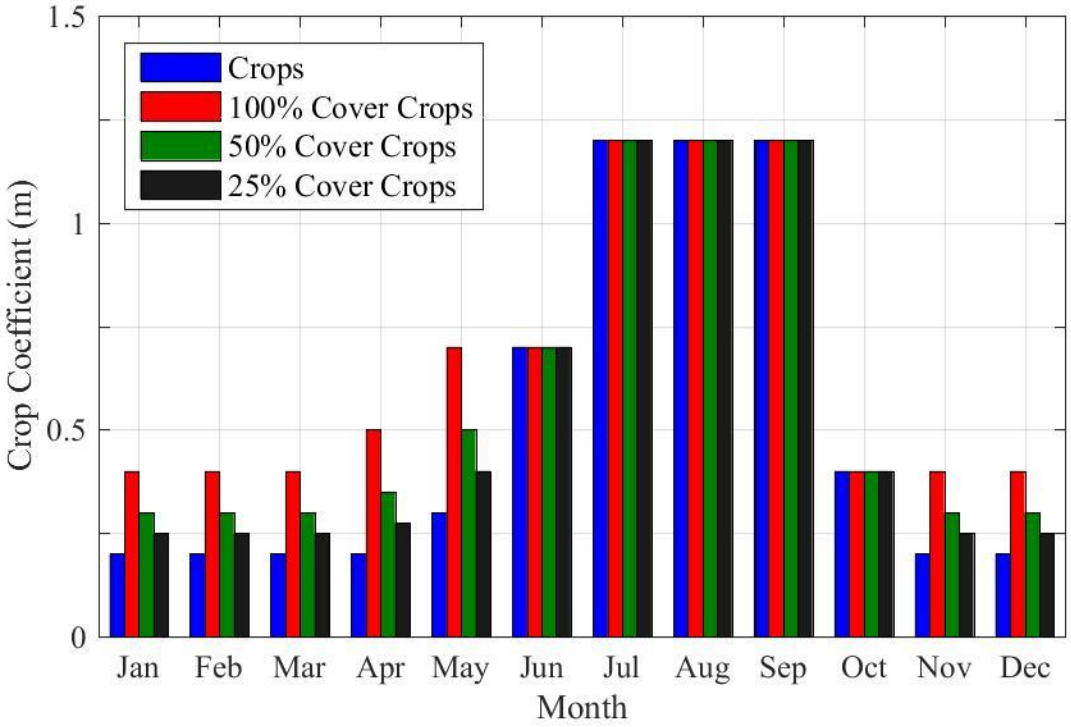

Figure 8.2. Crop coefficient time series for different cover crop implementation schemes ranging from 25% to 100%.

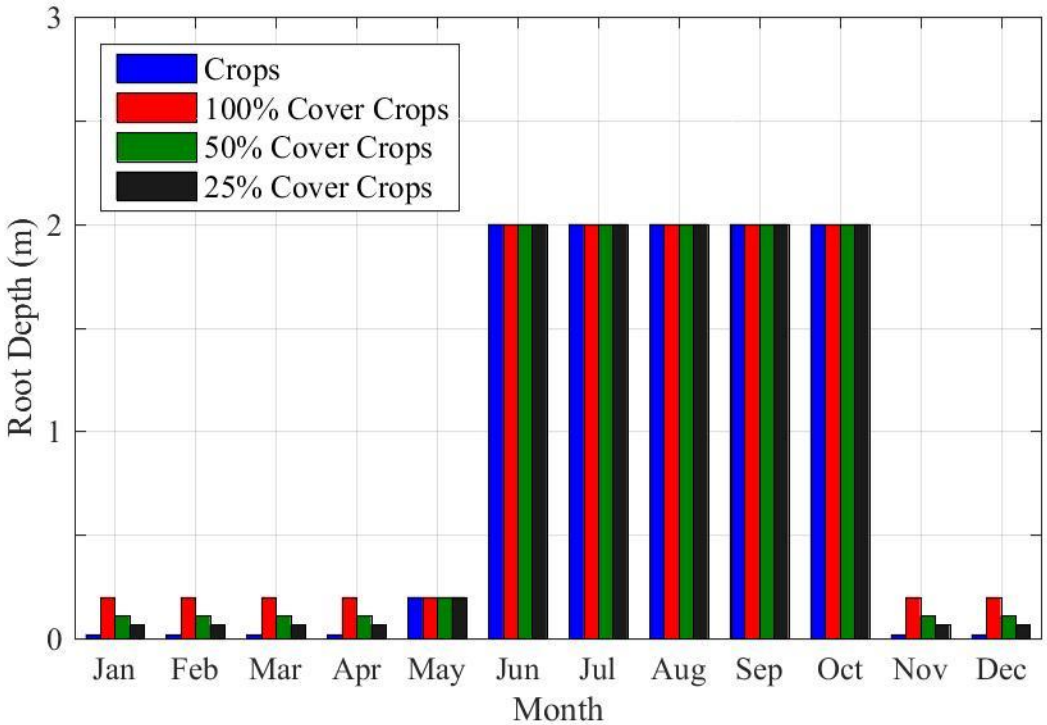

Figure 8.3. Root depth time series for different cover crop implementation schemes ranging from 25% to 100%.

To estimate the hydrologic benefits of the continuous use of cover crops within the Upper Iowa watershed the overall water balance ratios for the entire calibration time period 2007 through 2016 were calculated for each implementation scenario and compared to the baseline. As a result of increased cover crops the Q/P ratio decreased 5% to 40% of the precipitation due to increased evapotranspiration (Figure 8.4). Further analysis of the increased evapotranspiration indicated that the partitioning of the evapotranspiration also changes with increased cover crops. Due to the cover crops both canopy evaporation and transpiration increase while soil and surface water evaporation decrease. Transpiration increased the most and as a percentage of evapotranspiration increasing 7% to as much as 58% of evapotranspiration for full implementation (Figure 8.5). Besides the quantity of evapotranspiration, the timing of evapotranspiration shifted as indicated in Figure 8.6. The cover crops increase evapotranspiration during the first five months of the year with the largest increase occurring during the hydrologically active month of May with 3 cm more evapotranspiration. The side effect of the evapotranspiration caused by the cover crops was that there is less water available later in the year for the corn or soybeans as indicated by the decrease in total evapotranspiration in June and July (Figure 8.6).

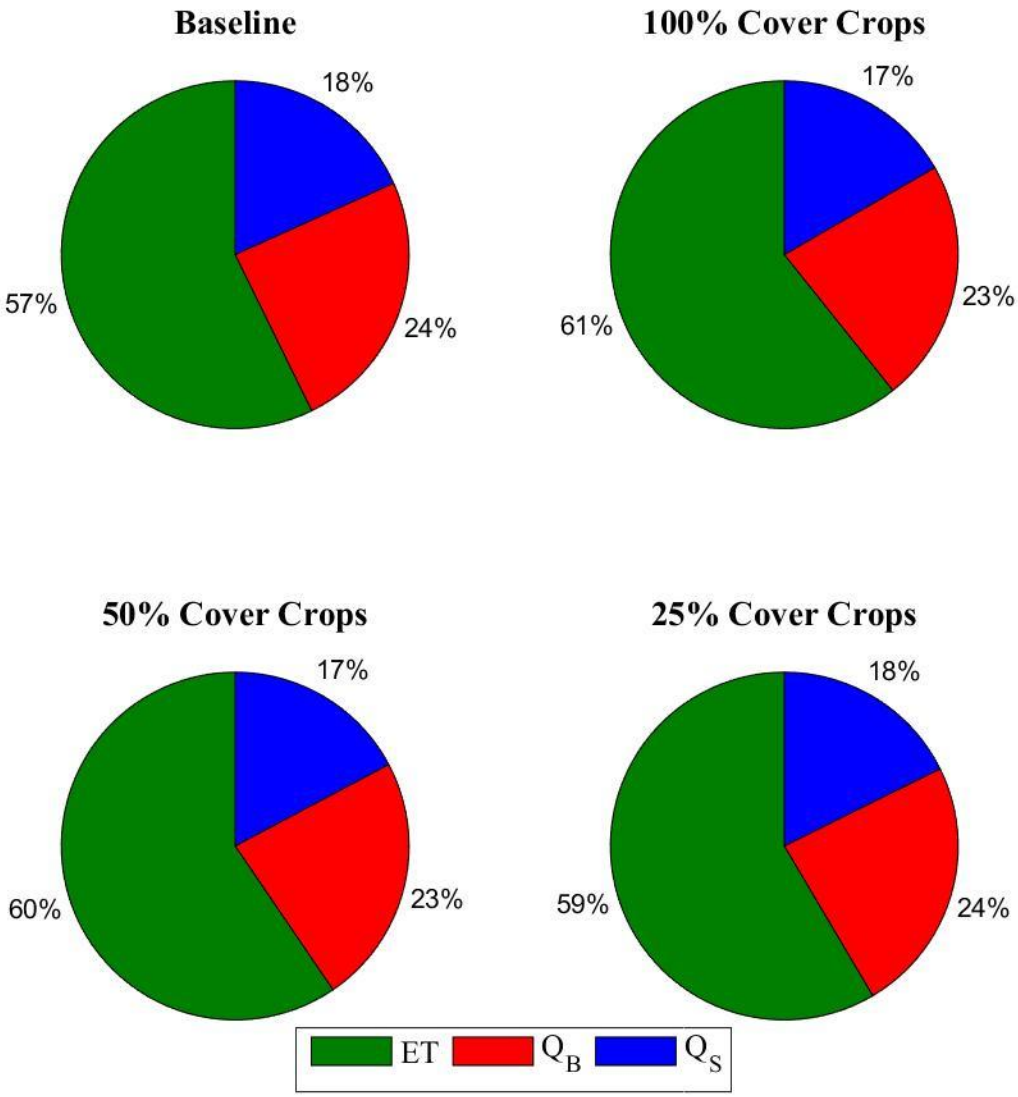

Figure 8.4. Water balance ratios, calculated from the simulated time period of 2007-2016, where ET is evapotranspiration, Q_B is base flow and Q_S is surface flow, for different cover crop implementation scenarios. All values are with respect to precipitation.

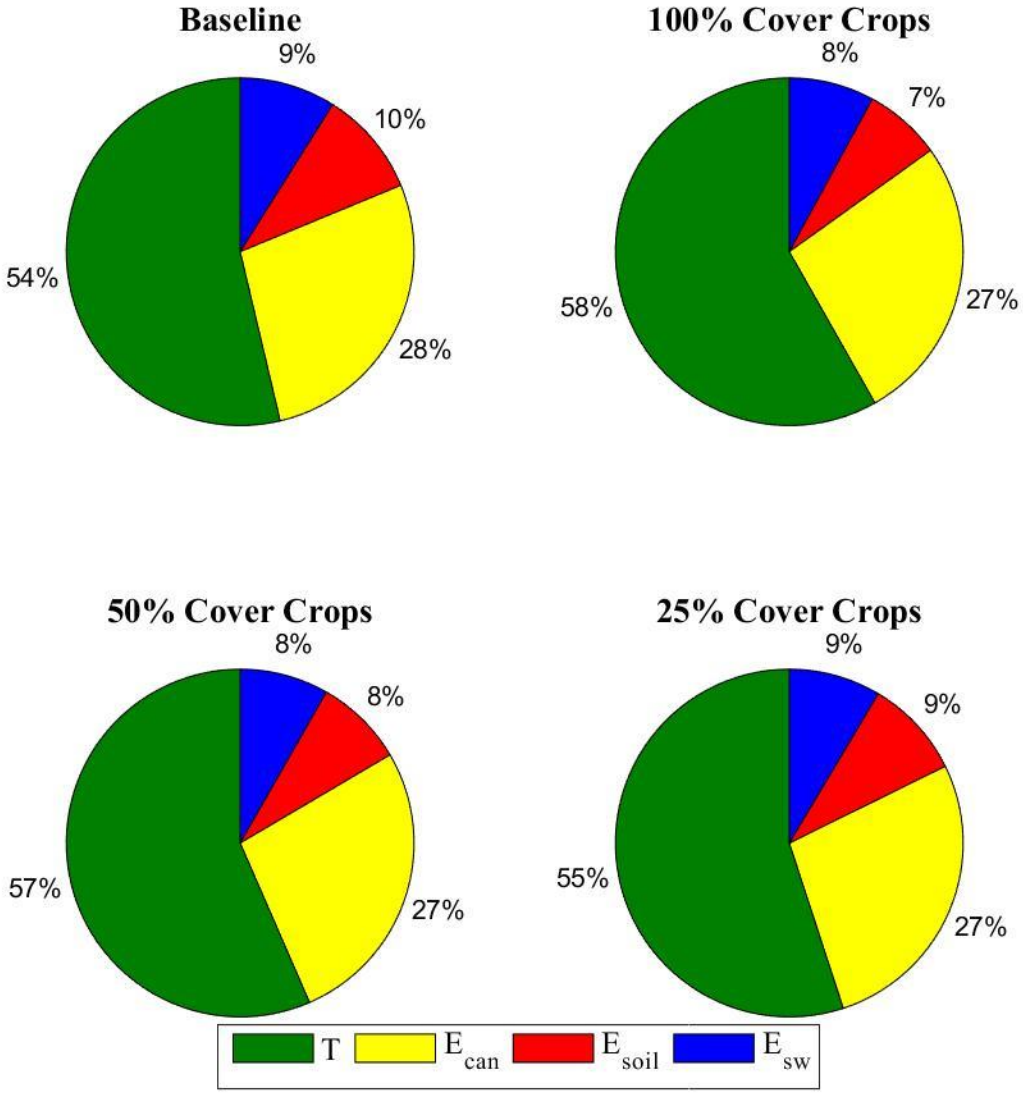

Figure 8.5. Evapotranspiration ratios, calculated for the simulated time period of 2007-2016, where T is transpiration, E_{can} is evaporation from the canopy, E_{soil} is evaporation from the soil, and E_{sw} is evaporation from surface water for the different cover crop implementation scenarios compared to the baseline. All values are with respect to the total evapotranspiration.

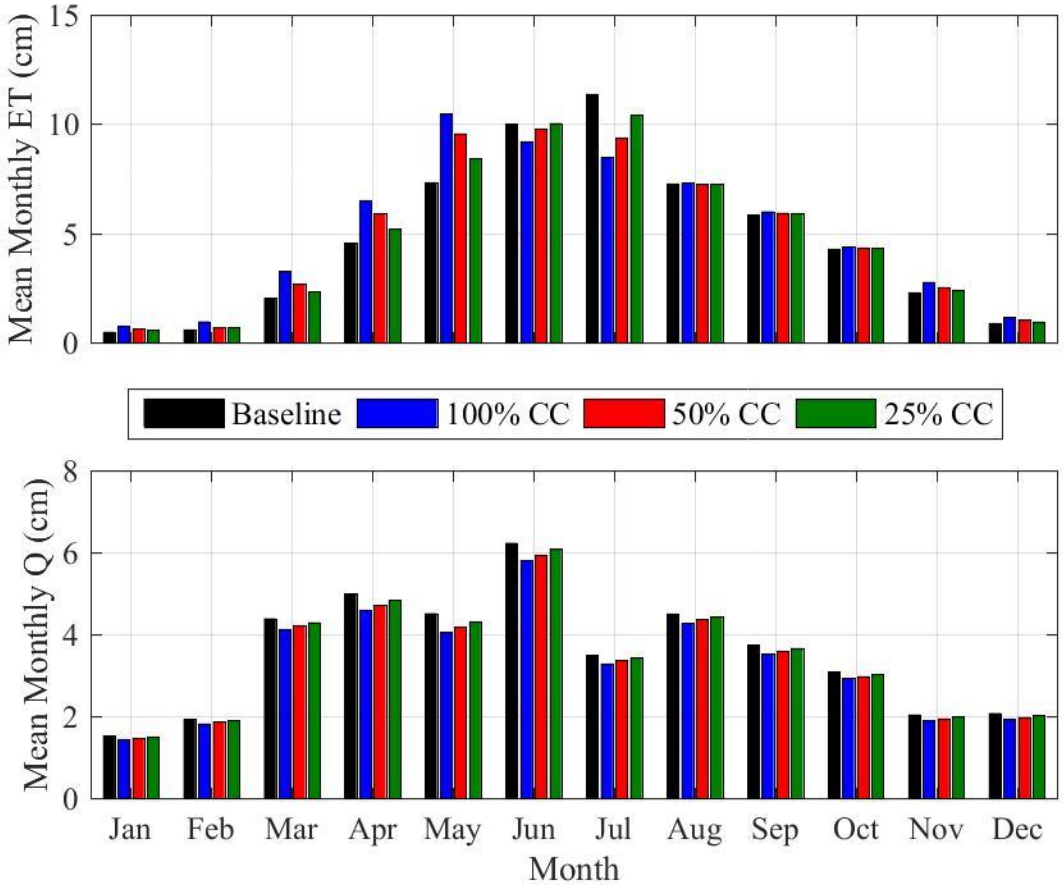

Figure 8.6. Mean monthly evapotranspiration (ET) and discharge (Q) depths (cm) for the different cover crop implementation scenarios.

To investigate the impact of continuous cover crops on the subsurface conditions in the Upper Iowa watershed a histogram of the area averaged soil moisture conditions throughout the simulation and the area averaged groundwater table elevations were plotted (Figure 8.7, Figure 8.8). As expected with increased evapotranspiration the median soil moisture decreased as much as 8% in the full implementation scheme to 60.5% moisture with decreases diminishing with less implementation (Figure 8.7). Continuous cover crops also decreased the area averaged ground water table as the cover crops take up more water than fallow ground with total changes equaling a decrease of 0.4 m, 0.2 m, and 0.1 m for 100%, 50% and 25% implementation respectively (Figure 8.8).

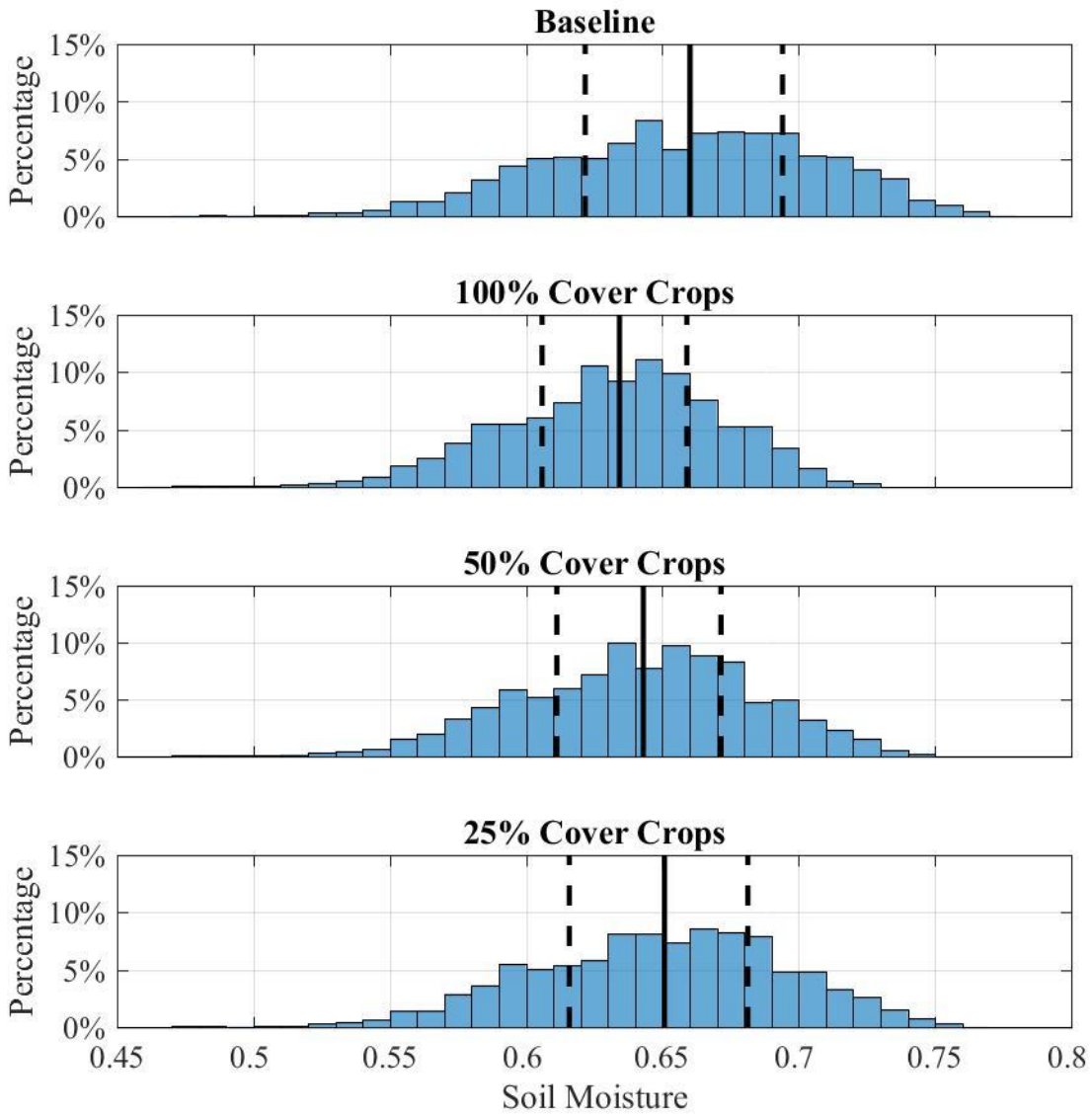

Figure 8.7. Histogram of the area averaged soil moisture over the simulated time period of 2007-2016 for different cover crop implementation scenarios.

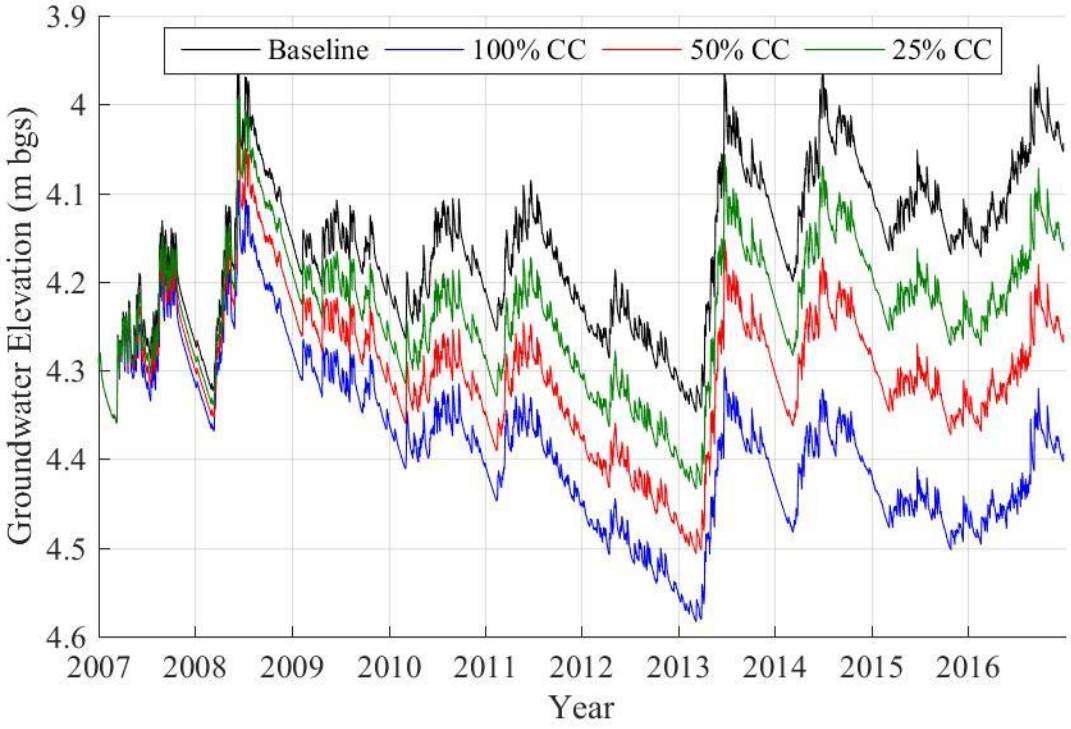

Figure 8.8. Area averaged ground water elevation (m below ground surface) for the simulated time period of 2007-2016 for different cover crop (CC) implementation scenarios.

Lastly, the impact of the continuous cover crops on flood events, 2008, indicating the potential after 1 full year of implementation and 2016, indicating the potential benefit after 10 years of cover crops, was calculated in terms of peak flow and volume reductions. Both event hydrographs show discharge reductions with the impact of full implementation for the two events depicted in Figure 8.9 and Figure 8.10. The peak discharges, peak discharge reductions, stage calculated from USGS rating curves, stage reductions and volume reductions for the two flood events at three USGS stream gage locations are shown in Table 8.2, Table 8.3, Table 8.4, Table 8.5, and Table 8.6 respectively. The maximum flood reduction occurred with the highest percentage of cover cropped area at Bluffton with a 7% peak flow reduction for the 2008 event and 16% peak flow reduction for the 2016 flood event. The benefit in peak flow reduction decreased downstream (Table 8.3). In addition, the simulations showed that benefits of continuous cover crops increase with each consecutive year of implementation as evident by the peak flow

reductions doubling between the 2008 flood event and 2016 flood event (Table 8.3). These peak flow reductions translated into stage reductions ranging from 0.05 m to 0.3 m with increasing stage reductions closer to the cover crop area and the longer the cover crops are implemented (Table 8.5). Similar trends were seen in the volume reductions in the hydrograph as well (Table 8.6).

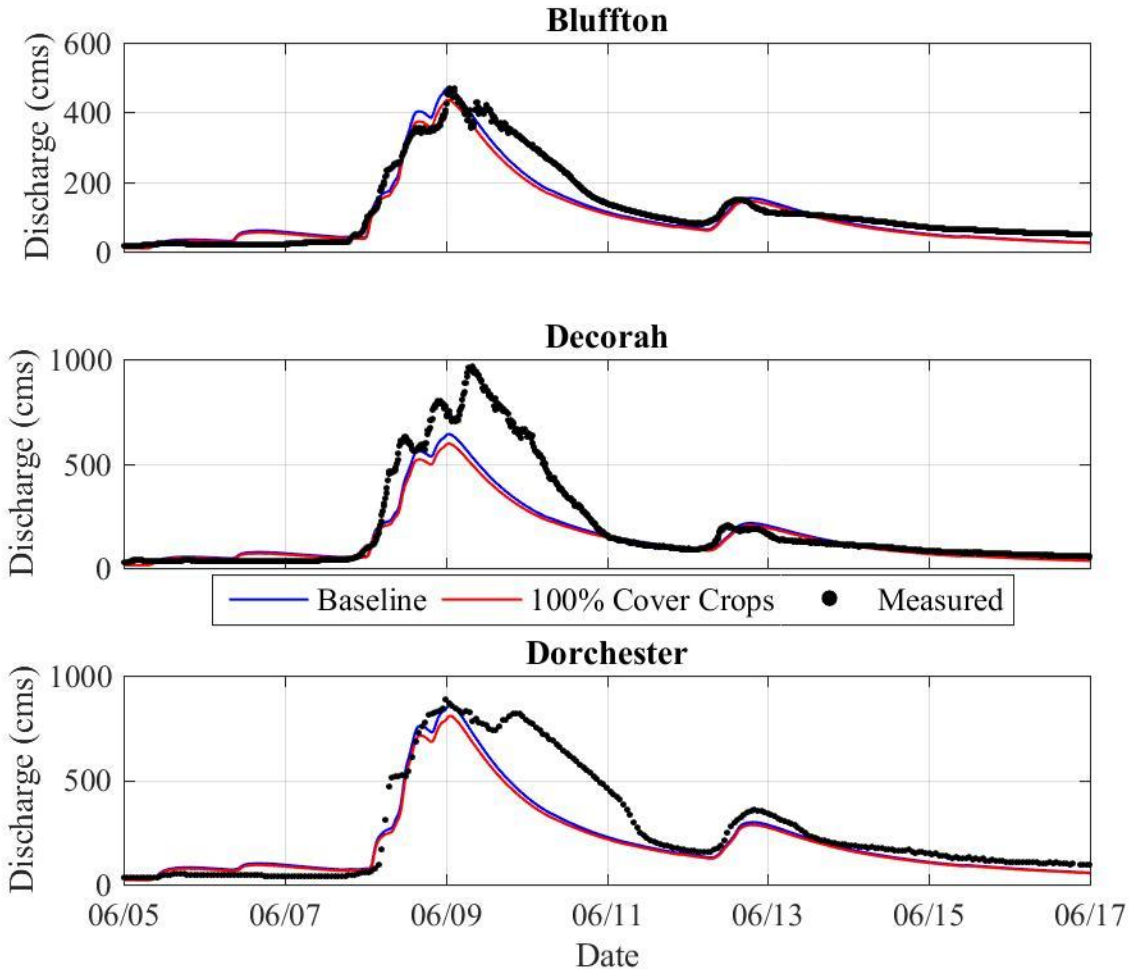

Figure 8.9. June 2008 flood event hydrograph where the baseline is in blue, the reduction in discharge from full cover crop implementation is in red and USGS measured data is in black.

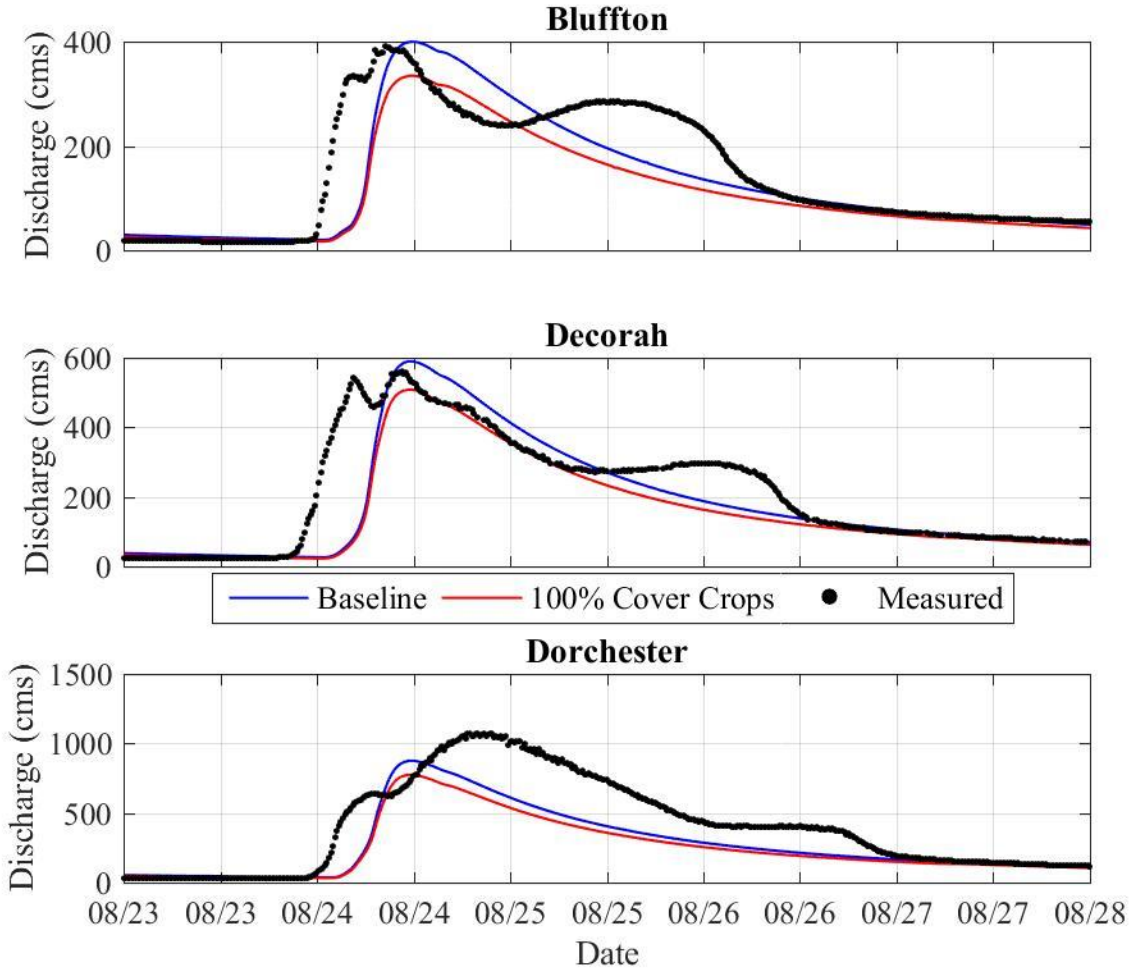

Figure 8.10. August 2016 Flood Event hydrograph where the baseline is in blue, the reduction in discharge from full cover crop implementation is in red and USGS measured data is in black.

Table 8.2. Peak Discharge for the 2008 and 2016 floods under different cover crop implementation schemes

2008 Flood Event				
	Simulated Peak Discharge (cms)	Peak Discharge with 100% CC (cms)	Peak Discharge with 50% CC (cms)	Peak Discharge with 25% CC (cms)
Bluffton	469	436	447	457
Decorah	642	597	614	627
Dorchester	860	808	826	842
2016 Flood Event				
Bluffton	400	335	362	380
Decorah	590	508	540	561
Dorchester	876	774	811	837

Table 8.3. Peak Discharge Reductions (%) for the 2008 and 2016 floods under different cover crop implementation schemes

2008 Flood Event			
	Peak Flow Reduction from 100% CC (%)	Peak Flow Reduction from 50% CC (%)	Peak Flow Reduction from 25% CC (%)
Bluffton	7	5	3
Decorah	7	4	2
Dorchester	6	4	2
2016 Flood Event			
Bluffton	16	10	5
Decorah	14	8	5
Dorchester	12	7	5

Table 8.4. Peak Stage (m) for the 2008 and 2016 floods based on the USGS rating curves for Bluffton, Decorah and Dorchester (USGS 2018) under different cover crop implementation schemes

2008 Flood Event				
	Peak Stage (m)	Peak Stage with 100% CC (m)	Peak Stage with 50% CC (m)	Peak Stage with 25% CC (m)
Bluffton	4.8	4.6	4.7	4.7
Decorah	4.2	4.0	4.1	4.1
Dorchester	6.8	6.6	6.7	6.7
2016 Flood Event				
Bluffton	4.4	4.1	4.2	4.3
Decorah	4.0	3.7	3.8	3.9
Dorchester	6.8	6.5	6.6	6.7

Table 8.5. Stage Reduction (m) for the 2008 and 2016 floods under different cover crop implementation schemes.

2008 Flood Event			
	Stage Reduction from 100% CC (m)	Stage Reduction from 50% CC (m)	Stage Reduction from 25% CC (m)
Bluffton	0.2	0.1	0.06
Decorah	0.2	0.1	0.05
Dorchester	0.2	0.1	0.05
2016 Flood Event			
Bluffton	0.3	0.2	0.09
Decorah	0.3	0.2	0.1
Dorchester	0.3	0.2	0.1

Table 8.6 Volume Reduction (%) for the 2008 and 2016 floods under different cover crop implementation schemes.

2008 Flood Event			
	Volume Reduction from 100% CC (%)	Volume Reduction from 50% CC (%)	Volume Reduction from 25% CC (%)
Bluffton	7	6	5
Decorah	4	4	4
Dorchester	2	2	2
2016 Flood Event			
Bluffton	15	13	11
Decorah	9	8	7
Dorchester	5	5	4

8.2 Extreme Precipitation Scenario

The next scenario simulated the benefits of continuous cover crops under future precipitation patterns. First, however, a simulation with increased extreme precipitation was simulated to establish a new baseline. According to the Climate Science Special Report, extreme precipitation events tend to increase in intensity by about 6% to 7% per degree Celsius of temperature increase and using the past 20 years as a record it is projected that the 99% percentile precipitation events will increase in intensity by 10% (Easterling et al. 2017). To simulate this change in the Upper Iowa watershed, the average daily precipitation was calculated for each time series and the 99% percentile average daily precipitation days had the precipitation intensity increased by 10% to match expected increases over the first half of this century (Easterling et al. 2017). The resulting impact on precipitation is depicted for 2008 where the small precipitation events were unchanged while the extreme precipitation events have increased precipitation intensity (Figure 8.11). After establishing a new baseline for increased precipitation intensities, the increased precipitation scenario was combined with the 100% continuous cover crops scenario to determine if the cover crops could offset the increased stream flow of precipitation during extreme events.

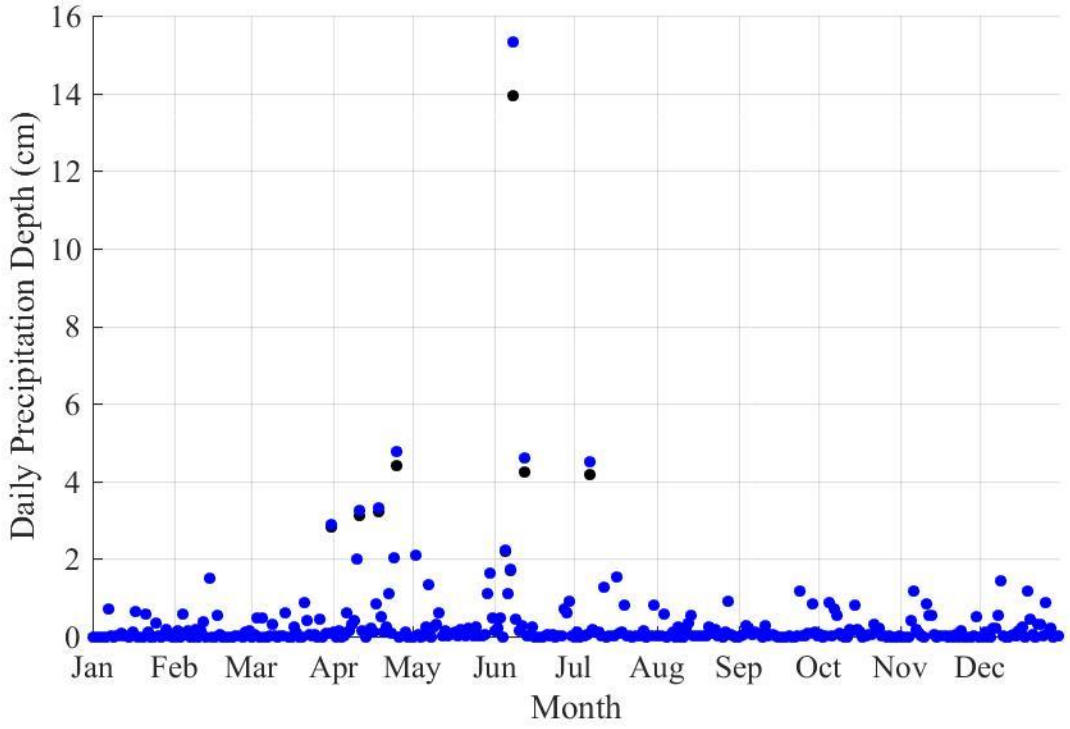

Figure 8.11. Daily precipitation depth (cm) for the year 2008 comparing the increased precipitation scenario to the baseline precipitation.

The result of the increased extreme precipitation changed the water balance minimally with slight increase in evapotranspiration, discharge and subsurface storage (Figure 8.12). Differences in the two simulations were only evident in days above the 0.01 exceedance probability (Figure 8.13). Above the 0.01 exceedance probability the increased extreme precipitation scenario increased the number of days above the original threshold by 8 days with the average intensity increasing 7% as well (Figure 8.13).

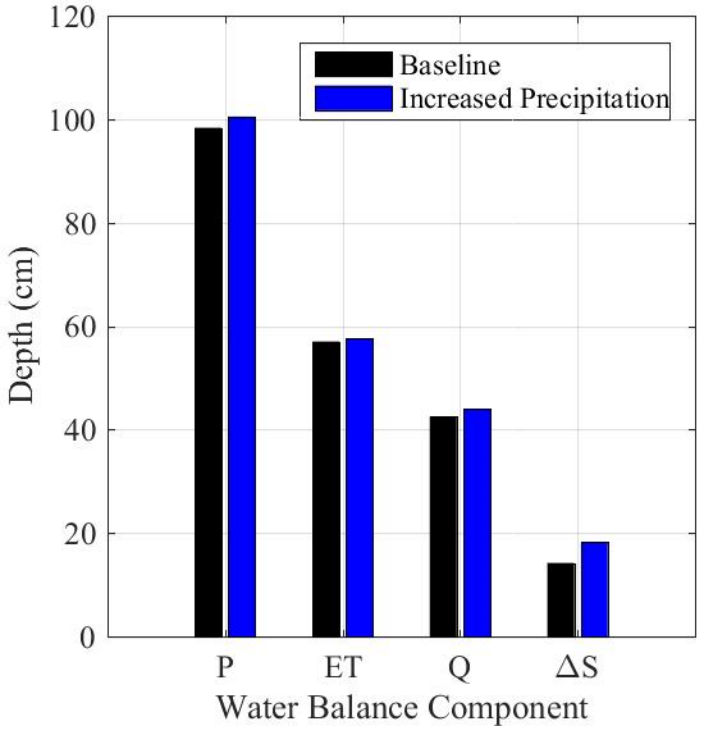

Figure 8.12. Precipitation (P), evapotranspiration (ET), discharge (Q) and change in subsurface storage (ΔS) depths for baseline and increased precipitation simulations for the time period 2007 through 2016.

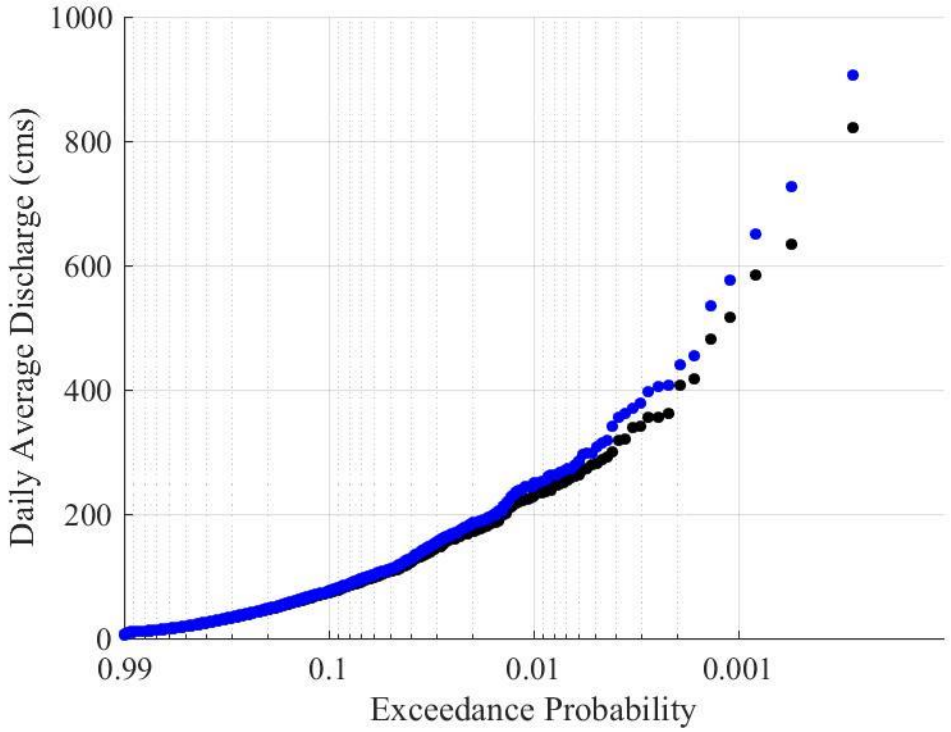

Figure 8.13 Daily average discharge exceedance probability for the baseline (black) and increased extreme precipitation (blue).

Translating to the annual peak discharges for each year, the peak discharges increased between 10% and 15% except for 2011 and 2012 (Figure 8.14). The annual maximum discharges of 2011 and 2012 were not impacted as much with increases close to 2%, indicating the severity of the drought where only a portion of the precipitation files were impacted by the change in extreme precipitation. The extreme precipitation increased the 2008 peak discharge by 12% from 860 cms to 963 cms for the Dorchester stream gage (Table 8.7). Using the USGS rating curve for the station, the stage increased 0.3 m (Table 8.8). For the 2016 flood event the peak discharge increased 17% from 876 cms to 1024 cms (Table 8.9). The result in terms of stage was an increase of 0.4 m (Table 8.10).

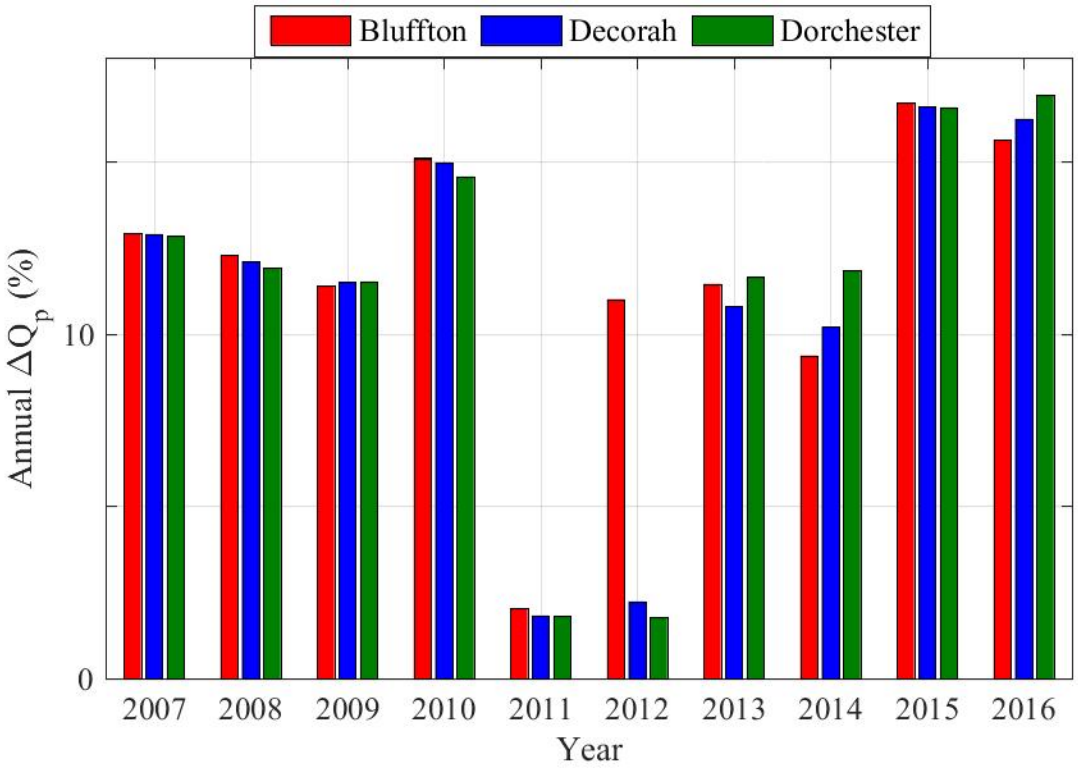

Figure 8.14. Annual peak discharge increase (%) between increased extreme precipitation and baseline conditions.

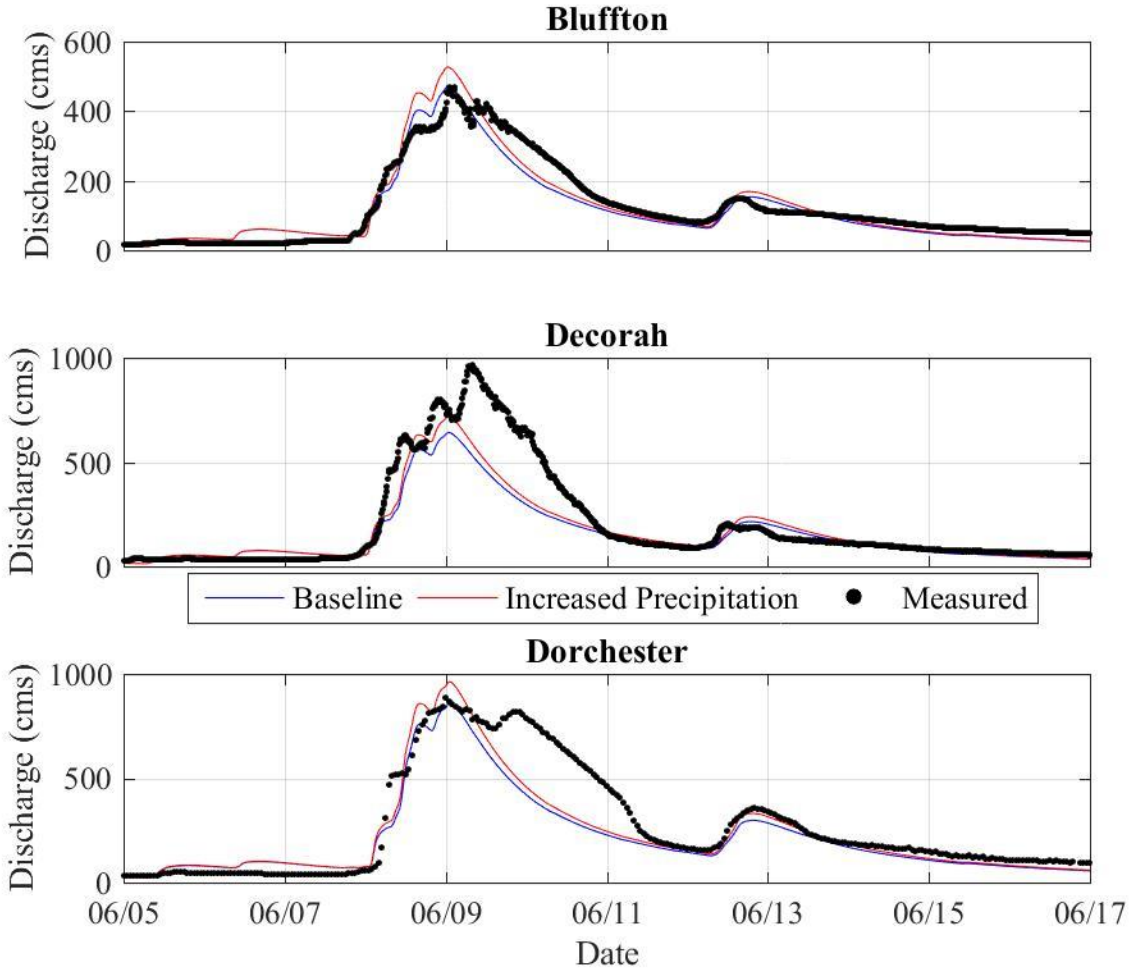

Figure 8.15. Hydrograph for the 2008 flood event at the three USGS stations in the Upper Iowa watershed where the baseline is in blue, the increased precipitation is in red and measured data is in black.

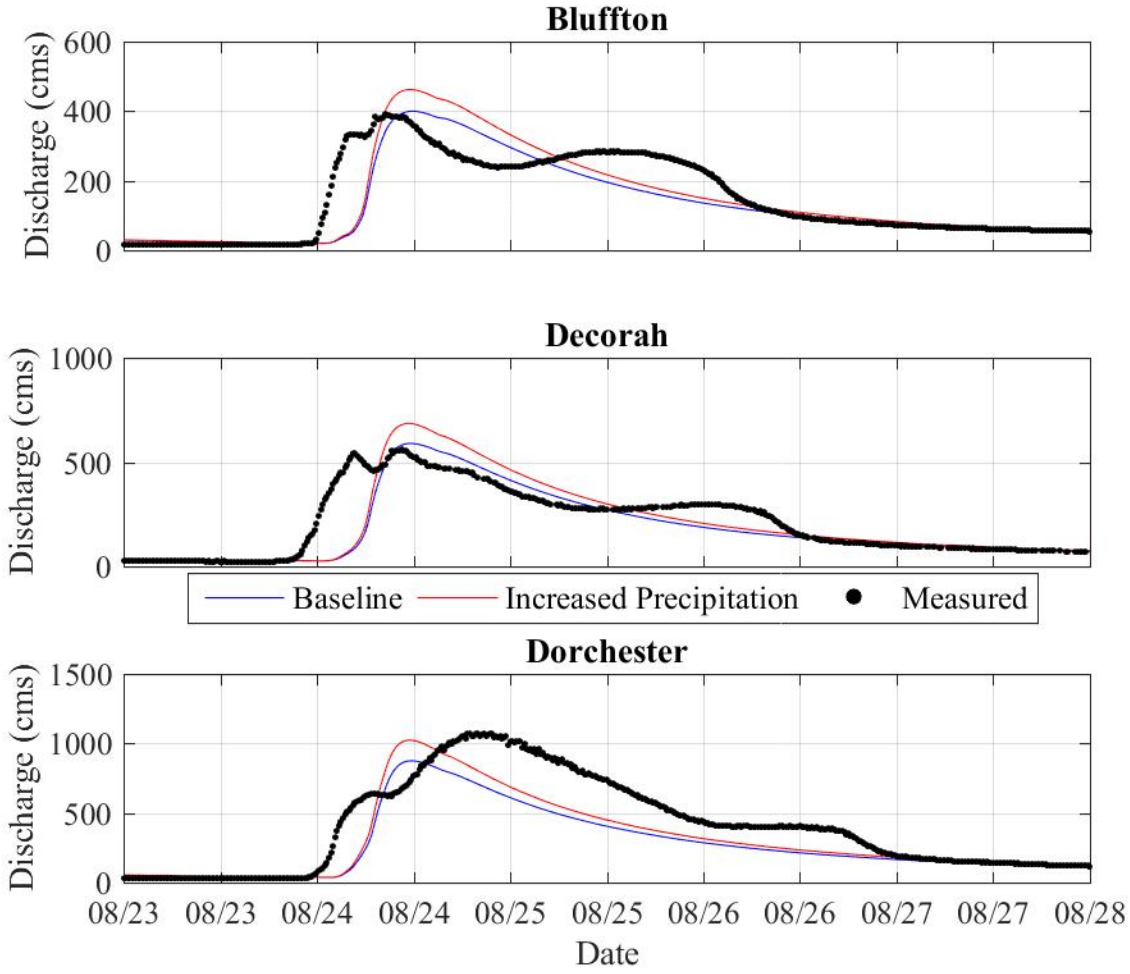

Figure 8.16. Hydrograph for the 2016 flood event at the three USGS stations in the Upper Iowa watershed where the baseline is in blue, the increased precipitation is in red and measured data is in black.

Table 8.7 Peak Discharge Increase for the 2008 Flood Event at the three USGS stream gages in the Upper Iowa Watershed.

USGS Station	Simulated Peak Discharge (cms)	Peak Discharge with Increased Precipitation (cms)	Peak Discharge Increase (%)
Bluffton	469	527	12
Decorah	642	719	12
Dorchester	860	963	12

Table 8.8 Stage Increases for the 2008 Flood Event calculated using USGS Rating Curves (USGS 2018) at the three USGS stations in the Upper Iowa Watershed

USGS Station	Simulated Peak Stage (m)	Peak Stage with Increased Precipitation (m)	Peak Stage Increase (m)
Bluffton	4.8	5.0	0.2
Decorah	4.2	4.5	0.3
Dorchester	6.8	7.1	0.3

Table 8.9 Peak Discharge Increase for the 2016 flood event at the three USGS stations in the Upper Iowa watershed.

USGS Station	Simulated Peak Discharge (cms)	Peak Discharge with Increased Precipitation (cms)	Peak Discharge Increase (%)
Bluffton	400	462	16
Decorah	590	686	16
Dorchester	876	1024	17

Table 8.10 Stage Increases for the 2016 Flood Event calculated using USGS Rating Curves (USGS 2018) at the three USGS stations in the Upper Iowa Watershed

USGS Station	Simulated Peak Stage (m)	Peak Stage with Increased Precipitation (m)	Peak Stage Increase (m)
Bluffton	4.4	4.7	0.3
Decorah	4.0	4.4	0.3
Dorchester	6.8	7.3	0.4

The combined extreme precipitation with continuous cover crops scenario was investigated to determine whether continuous cover crops could offset the increased peak discharges caused by the potential future increases in extreme precipitation intensity. To simulate this scenario the full implementation LAI, crop coefficient, and root depth time series were simulated with the increased precipitation forcing data. The focus of this scenario was on the flood events in 2008 and 2016. After one year of cover crops in 2008, the implementation of cover crops reduced the flooding,

however, the peak discharge still increased 5% where the combined scenario was in between the increased precipitation and baseline hydrographs (Table 8.11, Figure 8.17). Interestingly, after 10 years of continuous cover crops the increase in peak discharges were offset with a 0% increase in peak discharge and the combined scenario hydrograph followed the original baseline (Table 8.11, Figure 8.18).

Table 8.11 Changes in Peak Discharge with and without cover crops for the increased precipitation scenario at the three USGS stations in the Upper Iowa watershed

2008 Flood Event				
USGS Station	Simulated Peak Discharge (cms)	Peak Discharge with Increased Precipitation (cms)	Peak Discharge with Increased Precipitation and Cover Crops (cms)	Peak Discharge Increase (%)
Bluffton	469	527	489	4
Decorah	642	719	671	5
Dorchester	860	963	907	5
2016 Flood Event				
Bluffton	400	462	390	-2
Decorah	590	686	592	0
Dorchester	876	1024	903	0

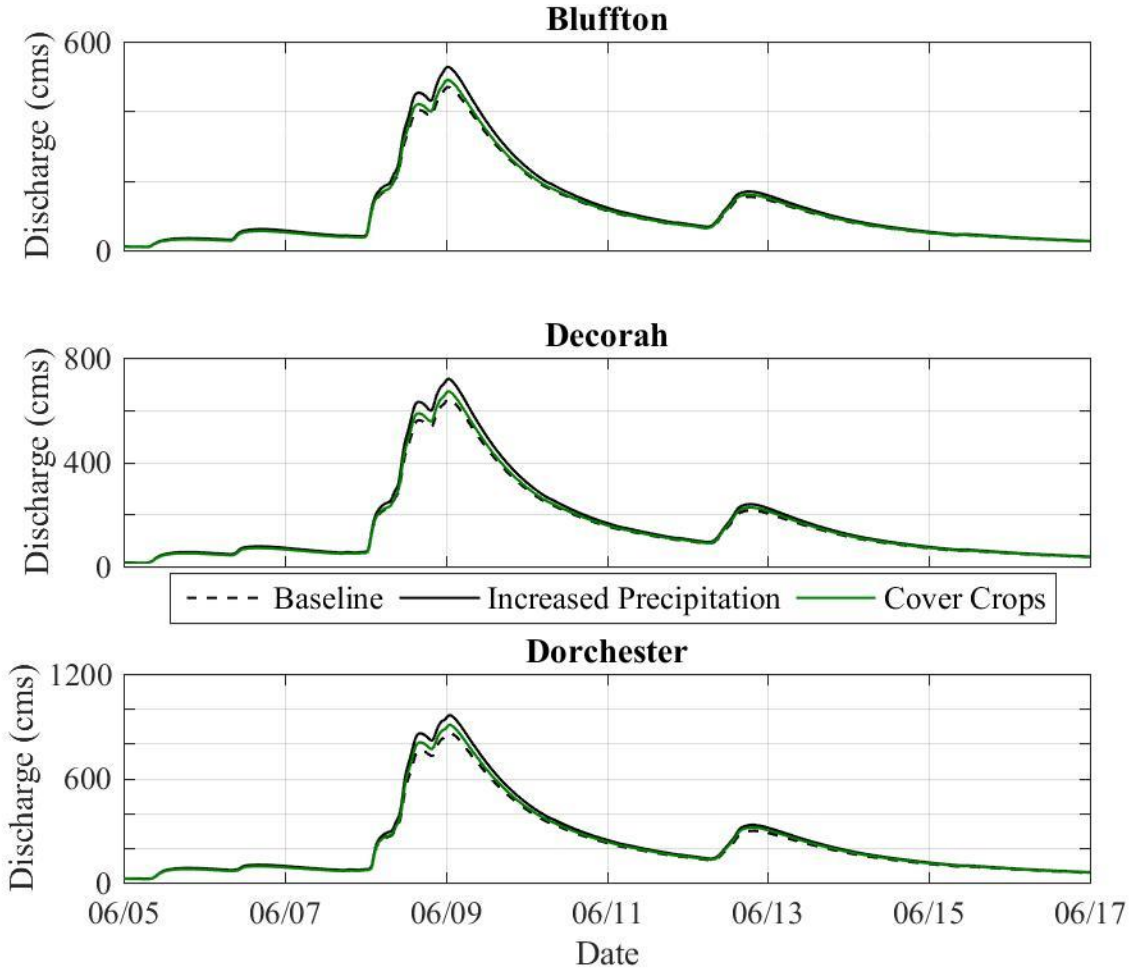

Figure 8.17 The 2008 flood event hydrograph for 100% cover crop implementation with increased precipitation compared to the baseline and increased precipitation hydrographs.

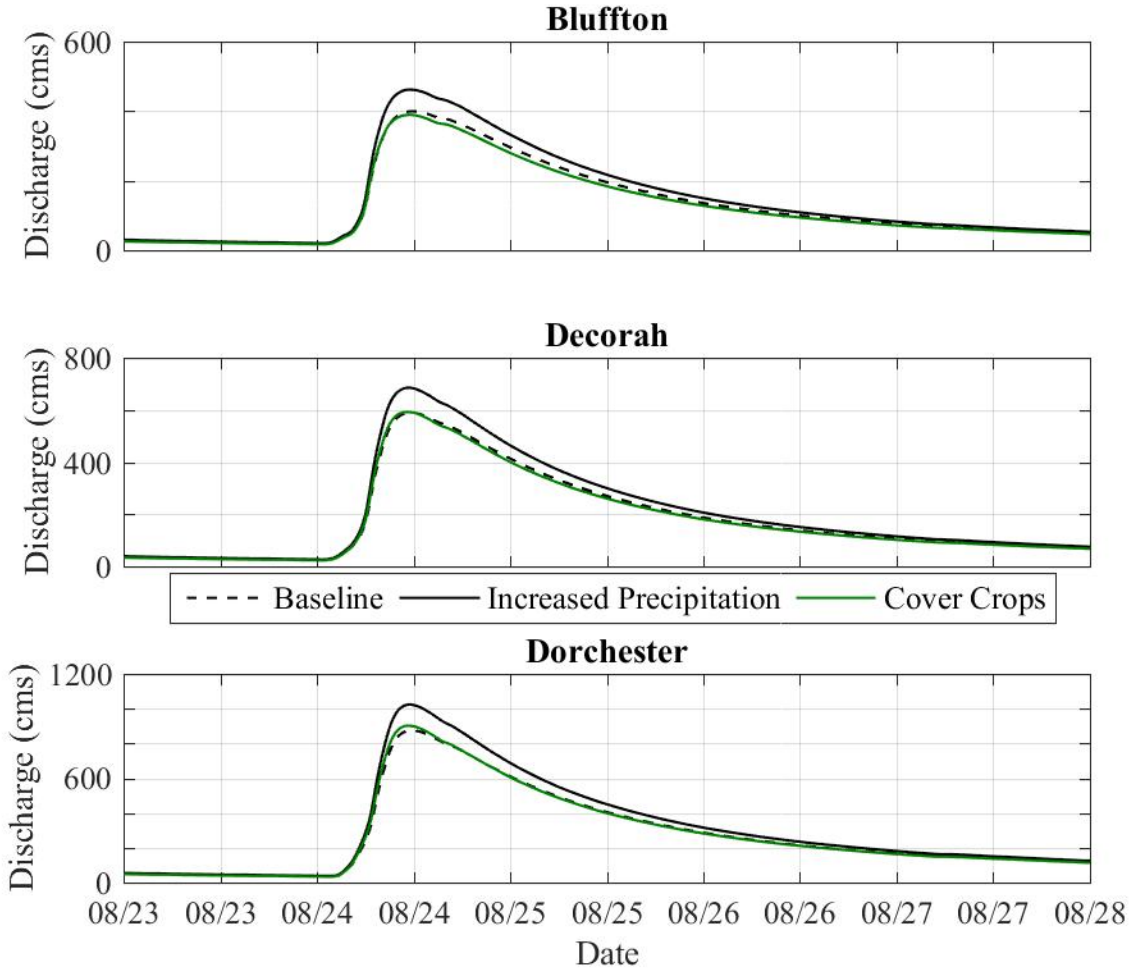

Figure 8.18 The 2008 flood event hydrograph for 100% cover crop implementation with increased precipitation compared to the baseline and increased precipitation hydrographs.

8.3 Summary

With the calibrated Upper Iowa hydrologic model two scenarios were investigated with a focus on cover crops. The first investigated the benefits from different implementation of continuous cover crops within the watershed. The second investigated the impact of extreme precipitation on the watershed and the potential benefit of implementing continuous cover crops with those conditions. Cover crops were implemented in both scenarios by incorporating winter wheat LAI, crop coefficient, and root depth into the crop time series. As a result of continuous use cover crops, the total water balance of the watershed changed with a decrease in discharge due to

an increase in evapotranspiration. The increase in evapotranspiration occurred during the early part of the year with the largest impact in May due to increases in the transpiration and canopy evaporation components. In addition, the additional evapotranspiration resulted in more storage in the subsurface that in turn reduced event peak discharges and volumes. Overall the benefits of cover crops were shown to be cumulative year to year and increased as the percentage of the cover cropped area within the watershed increased.

The second scenario investigated the impact of the expected increase in extreme precipitation intensity by mid-century due to climate change. To simulate this condition, the daily average precipitation was calculated and the days above the 99% precipitation had the precipitation intensity increased by 10%. The result was minimal on an overall water balance scale and within the subsurface. The extreme events however, increased in both the duration and discharge for the 99% percentile discharge days. The annual peak discharge generally increased from 10% to 15% with 2008 and 2016 floods increasing 12% and 16% respectively. Lastly, the cover crops and extreme precipitation were simulated together to determine if cover crops could reduce the impact of future extreme precipitation. 100% implementation of continuous cover crops on cropped areas wasn't able to eliminate the impacts of extreme precipitation during the first year in 2008 with a 5% increase in peak discharge, however; the cumulative impact of cover crops was able to eliminate the impact of extreme precipitation after 10 years of continuous implementation with a 0% increase in peak discharge.

Chapter 9. Summary and Conclusion

The goal of this Master's thesis was to first identify and validate potential conservation practices and second analyze the benefits of conservation with a calibrated hydrologic model within the Upper Iowa watershed in northeast Iowa. To accomplish these goals, the ACPF tool, a GIS tool that uses hydro-enforced LiDAR DEMs, gSSURGO soils, NASS CDL land use, and FSA field boundaries to identify potential practice placements at a HUC 12 scale, was used throughout the 34 HUC 12 basins of the Upper Iowa watershed. Then the results of the ACPF potential practices including grassed waterways, ponds and wetlands, and WASCOBs, from three HUC 12s in three different landform regions were compared to similar existing projects identified by the IBMP project. During this process, a methodology was created to compare the two potential state wide datasets including a tool that estimates the size of grassed waterways based on NRCS guidelines.

Then using a new hydrologic model called GHOST, a distributed, physically-based, integrated hydrologic model, a model of the Upper Iowa watershed was created. The hydrologic model had an average element size of 40 ha and a dense stream network defined up to an area threshold of 60 ha. Using realistic parameter values, the model was initialized by simulating the watershed with Nexrad Stage IV precipitation and NLDAS-2 meteorological data from 2002 until the subsurface storage was pseudo-steady state in January 2012. With a realistic subsurface the model was calibrated based on water balance ratios and model performance statistics calculated from measured data. To calibrate the model the years 2007 through 2016 were used. It was determined that the dry years were unable to achieve adequate performance because the extensive stream network within the model accentuated the limitations of GHOST where exfiltration is the only connection between the subsurface and the stream network. As a result the stream network adjacent elements were continuously saturated creating erroneous peaks in dry periods and limiting

transpiration. Therefore, the focus of the calibration was on improving the wet years of 2008, 2013, and 2016 as the overall goal of model was in simulating flood events. With the calibrated model, scenarios investigating the benefit of continuous use of cover crops and the potential increase of streamflow from increased extreme precipitation intensities were investigated.

9.1 Evaluation of Potential Conservation Practices

For the 34 HUC 12 watersheds in the Upper Iowa watershed, 65 depressions, 6303 ha treated by drainage water management, 638 bioreactors, 4694 km of grassed waterways, 3224 ha of contour buffer strips, 5611 WASCOBs, 818 nutrient removal wetlands, and 7356 ha of riparian buffer and 647 km of stream with the potential for saturated buffers were identified. As expected, the surface flow conservation practices (grassed waterways, WASCOBs, and contour buffer strips), were influenced by the slope, and land use of the respective HUC 12 basins with the majority occurring in the center of the Upper Iowa watershed where the slope was still steep and agricultural land use still dominated. The majority of drain tile practices (drainage water management and bioreactors) and riparian practices (saturated buffers and riparian buffers) on the other hand were located in the western portion of the watershed as these practices are generally more common in areas with less slope and poorly drained soils common in the Iowan Surface.

The comparison of the ACPF potential conservation practice placement to the IBMP existing conservation practices determined that grassed waterways were widely implemented within the three watersheds (Ten Mile Creek of the Upper Iowa River, Hinkle Creek of the Middle Cedar River, and Headwaters North English of the English River) and the ACPF process for identifying grassed waterways was validated as the siting of potential practices matched with the existing grassed waterway based on flow path order. For ponds and wetlands, it was determined that the majority of the existing structures are small ponds, being built for field scale remediation

issues, while the ACPF tool identified larger wetlands, that were lacking across the landscape. Lastly for WASCOBs, the preferences of stakeholders within the watershed and resulting differences in conservation spending was shown to influence the amount of practices. Only one watershed, the Headwater of the North English, where funding for practices was evident, had significant existing WASCOBs while the ACPF identified potential across the three watersheds.

For all of the conservation practices used in the study topography and land use differences were important in distinguishing the three watersheds in terms of existing and potential conservation. The distribution of SPI along with the agricultural land use percentage were the key parameters in estimating the amount of grassed waterways. The larger topographic relief attributed to the Paleozoic Plateau increased the potential implementation of wetlands as compared to the more gentle landscapes of the Iowan Surface and Southern Iowa Drift Plain. Overall the ACPF and IBMP tools enhance the watershed planning process allowing for more informed decision making and development of more precise watershed strategies to mitigate flooding and water quality degradation.

9.2 Evaluation of the Upper Iowa Hydrologic Model

Through calibration the Upper Iowa hydrologic model achieved Q/P and ET/P close to the measured ratios where the average years had slightly higher Q/P and lower ET/P and the wet years had the reverse trend. One reason for the deviations from the measured ratios was due to the near saturated stream network adjacent elements limiting transpiration and subsurface storage. The simulated Q_B/Q was lower than the WHAT estimated ratio. To improve the baseflow in the model, implementation of a secondary preferential flow model in the subsurface would be needed. For the performance statistics the wet years of 2008, 2013, and 2016 achieved good NSE greater than 0.7 and PBIAS between ±12% while the other years didn't achieve the calibration targets. In general, the model performed best during wet years with performance decreasing in dryer years. The good

performance was also achieved for the two large flood events of 2008 and 2016 as well. The model captured the rising limb and peak discharge of the 2008 event and the peak discharge of the 2016 event. Because of the good performance the two flood events were used to evaluate the continuous cover crop scenarios.

Implementation of continuous cover crops in the model indicated that increased implementation of continuous cover crops could change the water balance within the watershed by increasing evapotranspiration, especially in the spring. As a result of the evapotranspiration, there was more storage in the subsurface for extreme events during the summer. The benefits of continuous cover crops was shown to be cumulative increasing with each consecutive year and increasing with increased usage of cover crops within the watershed. Then to show how cover crops would benefit the watershed under future precipitation estimate the 99% precipitation intensity was increased by 10% within the Upper Iowa hydrologic model. The result changed the overall water balance of the watershed minimally, however, the amount of days above the 0.01 exceedance probability for daily average discharge increased by 8 days and the intensity of those days increased by 7%. For the two largest flood events in 2008 and 2016 the peak discharge increased 12% and 16% respectively. Lastly, the full cover crop implementation under future precipitation trends indicated that the cumulative benefits of 100% continuous cover crops were able to decrease future peak discharge of flood events to current peak discharges within the Upper Iowa watershed.

9.3 Final Remarks

As part of the IWA, the overall focus of this thesis was on the hydrologic assessment of the Upper Iowa watershed. The first portion of this thesis involved the identification of potential conservation practices and then the comparison of this dataset to existing conservation practices. This work not only informed stakeholders of the Upper Iowa watershed on the options available

to them within their watershed but also, provided information that will inform watershed professionals across the Midwest by creating a replicable comparison framework between the two datasets and by showing how the characteristics of the watershed along with stakeholder preferences can impact conservation implementation. Future insight could be drawn, however, by performing this analysis on a larger study area where more significant trends could be developed. Furthermore, comparison of different conservation practices that have similar function within watersheds could show how stakeholder preferences change across the landscape. The second component of this thesis was the development and calibration of the Upper Iowa hydrologic model. This thesis was one of the first HUC 8 sized watersheds to be calibrated using the GHOST model and the model was able to simulate wet years very well. In addition, continuous cover crops were able to be simulated and the benefits of the practice were shown. Future development of the model could improve and broaden the results of this thesis especially, the addition of a lateral subsurface connection to the stream network, the addition of a preferential flow model in the subsurface to simulate karst flow, drain tile, and macro pores, and the addition of ways to simulate smaller scale conservation practices. In general, this work will immediately benefit the watershed planning process in Phase II of the IWA, where conservation practices will be designed and constructed. Furthermore, the results explained within this document will hopefully impact any future conservation work within other similar agricultural watersheds.

References

Ajami, H., Evans, J. P., McCabe, M. F., & Stisen, S. (2014). Technical Note: Reducing the spin-up time of integrated surface water–groundwater models. *Hydrology and Earth System Sciences, 18*(12), 5169-5179, doi:10.5194/hess-18-5169-2014.

Ajami, H., McCabe, M. F., & Evans, J. P. (2015). Impacts of model initialization on an integrated surface water-groundwater model. *Hydrological Processes, 29*(17), 3790-3801, doi:10.1002/hyp.10478.

Allen, R. G., Pereira, L. S., Raes, D., & Smith, M. (1998). Crop evapotranspiration - Guidelines for omputing crop water requirements - FAO Irrigation and drainage paper 56. Rome, Italy: Food and Agriculture Organization of the United Nations.

Allen, R. G., Pruitt, W. O., Wright, J. L., Howell, T. A., Ventura, F., Snyder, R., et al. (2006). A recommendation on standardized surface resistance for hourly calculation of reference ETo by the FAO56 Penman-Monteith method. *Agricultural Water Management, 81*(1-2), 1-22, doi:10.1016/j.agwat.2005.03.007.

Arbuckle, J. G. (2013). Farmer Attitudes toward Proactive Targeting of Agricultural Conservation Programs. *Society & Natural Resources, 26*(6), 625-641, doi:10.1080/08941920.2012.671450.

Arnold, J. G., Srinivasan, R., Muttiah, R. S., & Willimas, J. R. (1998). Large Area Hydrologic Modeling and Assessment Part 1: Model Development. *Journal of the American Water Resources Association, 34*(1), 73-89.

Ayalew, T. B., Krajewski, W. F., & Mantilla, R. (2015). Insights into Expected Changes in Regulated Flood Frequencies due to the Spatial Configuration of Flood Retention Ponds. *Journal of Hydrologic Engineering, 20*(10), 04015010, doi:10.1061/(asce)he.1943-5584.0001173.

Ayalew, T. B., Krajewski, W. F., Mantilla, R., Wright, D. B., & Small, S. J. (2017). Effect of Spatially Distributed Small Dams on Flood Frequency: Insights from the Soap Creek Watershed. *Journal of Hydrologic Engineering, 22*(7), 04017011, doi:10.1061/(asce)he.1943-5584.0001513.

Babbar-Sebens, M., Barr, R. C., Tedesco, L. P., & Anderson, M. (2013). Spatial identification and optimization of upland wetlands in agricultural watersheds. *Ecological Engineering, 52*, 130-142, doi:10.1016/j.ecoleng.2012.12.085.

Beven, K., & Germann, P. (2013). Macropores and water flow in soils revisited. *Water Resources Research, 49*(6), 3071-3092, doi:10.1002/wrcr.20156.

Breuer, L., Eckhardt, K., & Frede, H.-G. (2003). Plant parameter values for models in temperate climates. *Ecological Modelling, 169*(2-3), 237-293, doi:10.1016/s0304-3800(03)00274-6.

Brunner, G. W. (2016). HEC-RAS, River Analysis System Hydraulic Reference Manual Version 5.0. (pp. 3-14 - 13-15). Davis, California, USA: US Army Corps of Engineers Hydrologic Engineering Center (HEC).

Buchmiller, R. C., & Eash, D. A. (2010). Floods of May and June 2008 in Iowa. (Vol. 1096). Reston, Virgina: U.S. Geological Survey.

Burkart, M. R., Oberle, S. L., Hewitt, M. J., & Pickus, J. (1994). A Framework for Regional Agroecosystems Characterization Using the National Resources Inverntory. *J. Environ. Qual., 23*, 866-874.

Cain, Z., & Lovejoy, S. (2004, History and Outlook for Farm Bill Conservation Programs. *Choices*, pp. 37-42.

Condon, L. E., & Maxwell, R. M. (2013). Implementation of a linear optimization water allocation algorithm into a fully integrated physical hydrology model. *Advances in Water Resources, 60*, 135-147, doi:10.1016/j.advwatres.2013.07.012.

Corbari, C., Ravazzani, G., Galvagno, M., Cremonese, E., & Mancini, M. (2017). Assessing Crop Coefficients for Natural Vegetated Areas Using Satellite Data and Eddy Covariance Stations. *Sensors (Basel), 17*(11), doi:10.3390/s17112664.

Dabney, S. M., Delgado, J. A., & Reeves, D. W. (2007). Using Winter Cover Crops to Improve Soil and Water Quality. Communications in Soil Science and Plant Analysis, 32(7-8), 1221-1250, doi:10.1081/css-100104110.

Delgado, J. A., & Berry, J. K. (2008). Advances in Precision Conservation. *Advances in Agronomy, 98*, 1-44, doi:10.1016/S0065-2113(08)00201-0.

Devia, G. K., Ganasri, B. P., & Dwarakish, G. S. (2015). A Review on Hydrological Models. *Aquatic Procedia, 4*, 1001-1007, doi:10.1016/j.aqpro.2015.02.126.

Dosskey, M. G., Neelakantan, S., Mueller, T. G., Kellerman, T., Helmers, M. J., & Rienzi, E. (2015). AgBufferBuilder: A geographic information system (GIS) tool for precision design and performance assessment of filter strips. *Journal of Soil and Water Conservation, 70*(4), 209-217, doi:10.2489/jswc.70.4.209.

Drake, C. W. (2014). *Assessment of flood mitigation strategies for reducing peak discharges in the Upper Cedar River watershed*. University of Iowa, Ioa City, IA.

Easterling, D. R., Kunkel, K. E., Arnold, J. R., Knutson, T., LeGrande, A. N., Leung, L. R., et al. (2017). Precipitation changine the United States. In D. J. Wuebbles, D. W. Fahey, K. A. Hibbard, D. J. Dokken, B. C. Stewart, & M. T.K. (Eds.), *Fourth National Climate Assessment* (Vol. I, pp. 207-230). Washington D.C., USA: U.S. Global Change Research Program.

Ebel, B. A., Mirus, B. B., Heppner, C. S., VanderKwaak, J. E., & Loague, K. (2009). First-order exchange coefficient coupling for simulating surface water-groundwater interactions: parameter sensitivity and consistency with a physics-based approach. *Hydrological Processes, 23*(13), 1949-1959, doi:10.1002/hyp.7279.

Engman, E. T. (1986). Roughness Coefficients for Routing Surface Runoff. *Journal of Irrigation and Drainage Engineering, 112*(1), 39-53.

EPA, U. S. (2011). Water Assessed as Impaired due to Nutrient-Related Causes. https://www.epa.gov/nutrient-policy-data/waters-assessed-impaired-due-nutrient-related-causes. Accessed March 2 2018.

Fang, H., Liang, S., Townshend, J., & Dickinson, R. (2008). Spatially and temporally continuous LAI data sets based on an integrated filtering method: Examples from North America. *Remote Sensing of Environment, 112*(1), 75-93, doi:10.1016/j.rse.2006.07.026.

Fiener, P., & Auerswald, K. (2003). Effectiveness of Grassed Waterways in Reducing Runoff and Sediment Delivery from Agricultural Watershed. *J. Environ. Qual., 32*, 927-936.

2015 NAIP Aerial Photography of Iowa (2017). Iowa State University GIS Facility.

Gallant, A. L., Sadinski, W., Roth, M. F., & Rewa, C. A. (2011). Changes in historical Iowa land cover as context for assessing the environmental benefits of current and future conservation efforts on agricultural lands. *Journal of Soil and Water Conservation, 66*(3), 67A-77A, doi:10.2489/jswc.66.3.67A.

Gao, J., Holden, J., & Kirkby, M. (2017). Modelling impacts of agricultural practice on flood peaks in upland catchments: An application of the distributed TOPMODEL. *Hydrological Processes, 31*(23), 4206-4216, doi:10.1002/hyp.11355.

Good, S. P., Noone, D., & Bowen, G. (2015). Hydrologic connectivity constrains partitioning of global terrestrial water fluxes. *Science, 349*(6244), 175-177.

Goolsby, D. A., Battaglin, W. A., Lawrence, G. B., Artz, R. S., Aulenbach, B. T., Hooper, R. P., et al. (1999). Flux and Sources of Nutrients in the Mississippi-Atchafalaya River Basin: Topic 3 Report for the Integrated Assessment on Hypoxia in the Gulf of Mexico. (Vol. Decision Analysis Series no 17). Silver Spirng (MD): NOAA Coastal Ocean Office.

Gupta, H. V., Sorooshian, S., & OYapo, P. O. (1999). Status of Automatic Calibration for Hydrologic Models: Comparison with Multilevel Expert Calibration. *Journal of Hydrologic Engineering, 4*(2), 135-143.

Hatfield, J. L., McMullen, L. D., & Jones, C. S. (2009). Nitrate-nitrogen patterns in the Raccoon River Basin related to agricultural practices. *Journal of Soil and Water Conservation, 64*(3), 190-199, doi:10.2489/jswc.64.3.190.

Howarth, R. W., Sharpley, A., & Walker, D. (2002). Sources of Nutrient Pollution to Coastal Waters in the United States: Implications for Achieving Coastal Water Quality Goals. *Estuaries, 25*(4b), 656-676.

IIIHR (2015). All Urban & Rural Iowa Watershed Approach Map. Iowa City, IA.

Iowa BMP Mapping Project (2018). https://www.gis.iastate.edu/gisf/projects/conservation-practices. Accessed 10/01 2017.

Islam, Z. (2011). Literature Review on Physically Based Hydrologic Modeling. Alberta Canada: Department of Civil and Environmental Engineering, University of Alberta.

ISU GIS Facility. (2016). Iowa BMP Mapping Project: Download Iowa Conservation Practices by HUC-12. https://athene.gis.iastate.edu/consprac/consprac.html. Accessed Oct. 1 2017

Jae Lim, K., Engel, B. A., Tang, Z., Choi, J., Kim, K.-S., Muthukrishnan, S., et al. (2005). Automated Web GIS based Hydrograph AnalysisTool, WHAT. *Journal of the American Water Resources Association, 41*(6), 1407-1416, doi:41(6):1407-1416.

The Iowa HUC12 S-Library: Elevation Rasters at 2-meter resolution (2016). https://www.gis.iastate.edu/gisf/projects/acpf. Accessed October 1, 2016.

Iowa Flood Center (2014). Hydrologic Assessment of the Turkey River Watershed. *IIHR Technical Report No. 488* (pp. 1-110). Iowa City, IA: IIHR-Hydroscience and Engineering. University of Iowa.

Kalcic, M. M., Frankenberger, J., & Chaubey, I. (2015). Spatial Optimization of Six Conservation Practices Using Swat in Tile-Drained Agricultural Watersheds. *JAWRA Journal of the American Water Resources Association, 51*(4), 956-972, doi:10.1111/1752-1688.12338.

Knight, B. I. (2005). Precision Conservation. *Journal of Soil and Water Conservation, 60*(6), 137A.

Kremen, C., Williams, N. M., Aizen, M. A., Gemmill-Herren, B., LeBuhn, G., Minckley, R., et al. (2007). Pollination and other ecosystem services produced by mobile organisms: a conceptual framework for the effects of land-use change. *Ecol Lett, 10*(4), 299-314, doi:10.1111/j.1461-0248.2007.01018.x.

Kristensen, K. J., & Jensen, S. E. (1975). A Model for estimating Actual Evapotranspiration from Potential Evapotranspiration. *Nordic Hydrology, 6*(3), 170-188.

Kumar, M., Bhatt, G., & Duffy, C. J. (2009). An efficient domain decomposition framework for accurate representation of geodata in distributed hydrologic models. *International Journal of Geographical Information Science, 23*(12), 1569-1596, doi:10.1080/13658810802344143.

Lawler, J. J., Lewis, D. J., Nelson, E., Plantinga, A. J., Polasky, S., Whitney, J. C., et al. (2014). Projected land-use change impacts on ecosystem services in the United States. *PNAS, 111*(20), 7492-7497, doi:10.1073/pnas.1405557111.

Lee, E. S., & Krothe, N. C. (2001). A four-component mixing model for water in a karst terrain in south-central Indiana, USA. Using solute concentration and stable isotopes as tracers. *Chemical Geology, 179*, 129-143.

Li, Q., Unger, A. J. A., Sudicky, E. A., Kassenaar, D., Wexler, E. J., & Shikaze, S. (2008). Simulating the multi-seasonal response of a large-scale watershed with a 3D physically-based hydrologic model. *Journal of Hydrology, 357*(3-4), 317-336, doi:10.1016/j.jhydrol.2008.05.024.

Liggett, J. E., Werner, A. D., & Simmons, C. T. (2012). Influence of the first-order exchange coefficient on simulation of coupled surface–subsurface flow. *Journal of Hydrology, 414-415*, 503-515, doi:10.1016/j.jhydrol.2011.11.028.

Lin, Y. (2011). GCIP/EOP Surface: Precipitation NCEP/EMC 4KM Gridded Data (GRIB) Stage IV Data. Version 1.0. In U. N.-E. O. Laboratory (Ed.).

Lizotte, R. E., Yasarer, L. M., Locke, M. A., Bingner, R. L., & Knight, S. S. (2017). Lake Nutrient Responses to Integrated Conservation Practices in an Agricultural Watershed. *J Environ Qual, 46*(2), 330-338, doi:10.2134/jeq2016.08.0324.

Mallakpour, I., & Villarini, G. (2015). The changing nature of flooding across the central United States. *Nature Climate Change, 5*(3), 250-254, doi:10.1038/nclimate2516.

Maxwell, R. M., Putti, M., Meyerhoff, S., Delfs, J.-O., Ferguson, I. M., Ivanov, V., et al. (2014). Surface-subsurface model intercomparison: A first set of benchmark results to diagnose integrated hydrology and feedbacks. *Water Resources Research, 50*(2), 1531-1549, doi:10.1002/2013wr013725.

Mielke, L. N. (1985). Performance of water and sediment control basins in northeastern Nebraska. *Journal of Soil and Water Conservation, 40*(6), 4.

Miller, G., Sassman, A., & Burras, C. L. (2017). Iowa Corn and Soybean Acres Planted. In -. C. S. A. Planted (Ed.). Ames, IA: USDA-NASS, Upper Midwest Region (Iowa Field Office).

Mitchell, K. E., Lohmann, D., Houser, P. R., Wood, E. F., Schaake, J. C., Robock, A., et al. (2009). NLDAS Forcing Data L4 Hourly 0.125 x 0.125 degree V001 Edited by David Mocko. In NASA/GSFC/HSL (Ed.). Greenbelt, Maryland, USA: Goddard Earth Sciences Data and Information Services Center (GES DISC).

Mockus, V., Van Mullen, J. A., Garen, D., & Woodwar, D. E. (2004). Chapter 11 Snowmelt. *Part 630 Hydrology National Engineering Handbook*. Washington D.C.: USDA NRCS.

Moriasi, D. N., Arnold, J. G., Van Liew, M. W., Bingner, R. L., Harmel, R. D., & Veith, T. L. (2007). Model Evaluation Guidelines for Systematic Quantification of Accuracy in Watershed Simulations. *Transactions of the ASABE, 50*(3), 885-900.

Musgrave, G. W., & Norton, R. A. (1937). Soil and Water Conservation Investigations at the Soil Conservation Experiment Station Missouri Valley Loess Region Clarinda, Iowa In U. S. D. o. Agriculture (Ed.), (pp. 1-182). Washington D.C.

Nash, J. E., & Sutcliffe, J. V. (1970). River Flow Forecasting through Conceptual Models Part I - A Discussion of Principles. *Journal of Hydrology, 10*, 282-290.

Description of gridded soil survey geographic (gSSURGO) database. (2016). USDA Natural Resources Conservation Service. http://www.nrcs.usda.gov/wps/portal/nrcs/detail/soils/survey/geo/?cid=nrcs142p2_053628 1. Accessed October 1, 2016.

Ouyang, D., & Bartholic, J. (1997). Estimating sediment Delivery ratios from three midwestern drainage basins. *World Resources Institute*. Washington D.C.

Panday, S., & Huyakorn, P. S. (2004). A fully coupled physically-based spatially-distributed model for evaluating surface/subsurface flow. *Advances in Water Resources, 27*(4), 361-382, doi:10.1016/j.advwatres.2004.02.016.

Parrett, C., Melcher, N. B., & James Jr., R. W. (1993). Flood Discharges in the Upper Mississppi River Basin 1993. . In U. G. S. Circular (Ed.), *Floods in the Upper Mississippi River Basin* (Vol. 1120-A): U.S. Geological Survey.

Politano, M. (2018). GHOST - Generic Hydrologic Overland-Subsurface Toolkit Theory Guide. (pp. 1-19). Iowa City, IA: The University of Iowa College of Engineering IIHR - Hydroscience & Engineering

Porter, S. A., Tomer, M. D., James, D. E., & Boomer, K. M. B. (2017). Agricultural Conservation Planning Framework ArcGIS Toolbox User's Manual Version 2.2. (pp. 1-82): National Laboratory for Agriculture & the Environment, USDA.

Prior, J. C. (1976). *A Regional Guide to Iowa Landforms* (Educational Series 3). Iowa City, IA: The State of Iowa.

PRISM Climate Group. Oregon State University. http://prism.oregonstate.edu. Accessd September 1, 2016.

Qu, Y., & Duffy, C. J. (2007). A semidiscrete finite volume formulation for multiprocess watershed simulation. *Water Resources Research, 43*(8), doi:10.1029/2006wr005752.

Quad Cities, I. I. W. F. O. (2016). September 2016 Major Flooding Recap. https://www.weather.gov/dvn/summary_092720162018.

Rao, M., Fan, G., Thomas, J., Cherian, G., Chudiwale, V., & Awawdeh, M. (2007). A web-based GIS Decision Support System for managing and planning USDA's Conservation Reserve Program (CRP). *Environmental Modelling & Software, 22*(9), 1270-1280, doi:10.1016/j.envsoft.2006.08.003.

Raymond, P. A., Oh, N.-H., Turner, R. E., & Broussard, W. (2008). Anthropogenically enhanced fluxes of water and carbon from the Mississippi River. *Nature, 451*(7177), 449-452, doi:10.1038/nature06505.

Sanford, W. E., & Selnick, D. L. (2013). Estimation of Evapotranspiration across the counterminous United States using a Regression with Climate and Land-Cover Data. *Journal of the American Water Resources Association, 49*(1), 217-230, doi:10.1111/jawr.12010.

Schaap, M. G., Leij, F. J., & van Genuchten, M. T. (2001). ROSETTA: a computer program for estimating soil hydraulic parameters with hierarchical pedotransfer functions. *Journal of Hydrology, 251*, 163-176.

Schilling, K. E. (2000). Patterns of Discharge and suspended sediment Transport in the Walnut and Squaw Creek Watersheds, Jasper County, Iowa:Water Years 1996-1998. In G. S. Bureau (Ed.), *Technical Information Series 412* (pp. 1-45): Iowa Department of Natural Resources.

Schilling, K. E., & Spooner, J. (2006). Effects of watershed-scale land use change on stream nitrate concentrations. *J Environ Qual, 35*(6), 2132-2145, doi:10.2134/jeq2006.0157.

Schilling, K. E., & Wolter, C. F. (2005). Estimation of Streamflow, Base Flow, and Nitrate-Nitrogen Loads in Iowa using Multiple Linear Regression Models. *Journal of the American Water Resources Association, 41*(6), 1333-1346.

Schlesinger, W. H., & Jasechko, S. (2014). Transpiration in the global water cycle. *Agricultural and Forest Meteorology, 189-190*, 115-117, doi:10.1016/j.agrformet.2014.01.011.

Seck, A., Welty, C., & Maxwell, R. M. (2015). Spin-up behavior and effects of initial conditions for an integrated hydrologic model. *Water Resources Research, 51*, 2188-2210, doi:10.1002/2014WR016371.

Shen, C., Riley, W. J., Smithgall, K. R., Melack, J. M., & Fang, K. (2016). The fan of influence of streams and channel feedbacks to simulated land surface water and carbon dynamics. *Water Resources Research, 52*(2), 880-902, doi:10.1002/2015wr018086.

Singh, V. P., & Woolhiser, D. A. (2002). Mathematical Modeling of Watershed Hydrology. *Journal of Hydrologic Engineering, 7*(4), 270-292, doi:10.1061//ASCE/1084-0699/2002/7:4/270.

Iowa Nutrient Reduction Strategy Science Team. (2017). Iowa Nutrient Reduction Strategy *A science and technology-based framework to assess and reduce nutrients to Iowa waters and the Gulf of Mexico*. Ames, IA: Iowa Department of Agriculture and Land Stewardship, Iowa Department of Natural Resources, Iowa State University College of Agriculture and Life Sciences.

Therrien, R., McLaren, R. G., Sudicky, E. A., & Panday, S. M. (2010). HydroGeoSphere A Three-dimensional Numerical Model Describing Fully-integrated Subsurface and Surface Flow and Solute Transport. Waterloo, Ontario: Groundwater Simulations Group.

Thomas, N. W. (2015). *Simulating the hydrologic impact of distributed flood mitigation practices, tile drainage, and terraces in an agricultural catchment*. University of Iowa, Iowa City, IA.

Tomer, M. D., Boomer, K. M., Porter, S. A., Gelder, B. K., James, D. E., & McLellan, E. (2015a). Agricultural conservation planning framework: 2. Classification of riparian buffer design types with application to assess and map stream corridors. *J Environ Qual, 44*(3), 768-779, doi:10.2134/jeq2014.09.0387.

Tomer, M. D., James, D. E., & Sandoval-Green, C. M. J. (2017). Agricultural Conservation Planning Framework: 3. Land Use and Field Boundary Database Development and Structure. *J Environ Qual, 46*(3), 676-686, doi:10.2134/jeq2016.09.0363.

Tomer, M. D., Moorman, T. B., James, D. E., Hadish, G., & Rossi, C. G. (2008). Assessment of the Iowa River's South Fork watershed: Part 2. Conservation practices. *Journal of Soil and Water Conservation, 63*(6), 371-379, doi:10.2489/jswc.63.6.371.

Tomer, M. D., Porter, S. A., Boomer, K. M., James, D. E., Kostel, J. A., Helmers, M. J., et al. (2015b). Agricultural conservation planning framework: 1. Developing multipractice watershed planning scenarios and assessing nutrient reduction potential. *J Environ Qual, 44*(3), 754-767, doi:10.2134/jeq2014.09.0386.

Tomer, M. D., Porter, S. A., James, D. E., Boomer, K. M. B., Kostel, J. A., & McLellan, E. (2013). Combining precision conservation technologies into a flexible framework to facilitate agricultural watershed planning. *Journal of Soil and Water Conservation, 68*(5), 113A-120A, doi:10.2489/jswc.68.5.113A.

Tomer, M. D., Sadler, E. J., Lizotte, R. E., Bryant, R. B., Potter, T. L., Moore, M. T., et al. (2014). A decade of conservation effects assessment research by the USDA Agricultural Research Service: Progress overview and future outlook. *Journal of Soil and Water Conservation, 69*(5), 365-373, doi:10.2489/jswc.69.5.365.

Trimble, S. W., & Lund, S. W. (1982). Soil Conservation and the Reduction of Erosion and Sedimentation in the Coon Creek Basin, Wiscosnin. In Interior (Ed.), (pp. 40).

ACPF Watershed Database Land Used Viewing and Data Downloading (2016). USDA ARS. https://www.nrrig.mwa.ars.usda.gov/st40_huc/dwnldACPF.html.

National Land Cover Database (2011). https://www.mrlc.gov/nlcd11_data.php.

NWIS Rating Curve (2018). USGS. Accessed 5/25/2018.

Tyndall & Bowman (2016). IA NRCS Cost Tool Overview-Land Use Practices Cover Crops (Cereal Rye Example) Iowa State University, Draft, 1-3

van Genuchten, M. T. (1980). A Closed-form Equation for Predicting the Hydraulic Conductivity of Unsaturated Soils1. *Soil Science Society of America Journal, 44*(5), 892, doi:10.2136/sssaj1980.03615995004400050002x.

Villarini, G., Smith, J. A., & Vecchi, G. A. (2013). Changing Frequency of Heavy Rainfall over the Central United States. *Journal of Climate, 26*(1), 351-357, doi:10.1175/jcli-d-12-00043.1.

Vymazal, J. (2007). Removal of nutrients in various types of constructed wetlands. *Sci Total Environ, 380*(1-3), 48-65, doi:10.1016/j.scitotenv.2006.09.014.

Weber, L. J., Muste, M., Bradley, A. A., Amado, A. A., Demir, I., Drake, C. W., et al. (2017). The Iowa Watersheds Project: Iowa's prototype for engaging communities and professionals in watershed hazard mitigation. *International Journal of River Basin Management*, 1-14, doi:10.1080/15715124.2017.1387127.

Yu, X., Bhatt, G., Duffy, C., & Shi, Y. (2013). Parameterization for distributed watershed modeling using national data and evolutionary algorithm. *Computers & Geosciences, 58*, 80-90, doi:10.1016/j.cageo.2013.04.025.

Zhang, Y.-K., & Schilling, K. E. (2006). Increasing streamflow and baseflow in Mississippi River since the 1940s: Effect of land use change. *Journal of Hydrology, 324*(1-4), 412-422, doi:10.1016/j.jhydrol.2005.09.033.

Zhou, X., Helmers, M., & Qi, Z. (2013). Modeling of Subsurface Tile Drainage using MIKE SHE. *Applied Engineering in Agriculture*, 865-873, doi:10.13031/aea.29.9568.

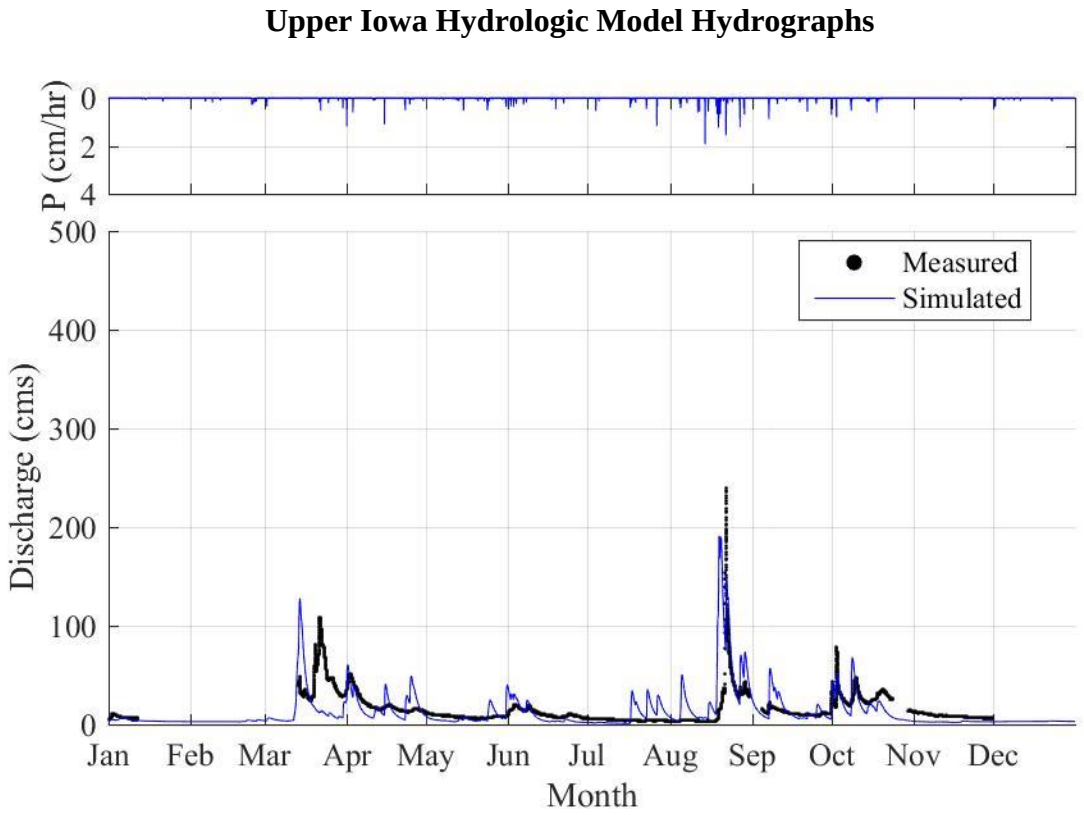

Figure A.1. Hydrograph for 2007 at the USGS stream gage at Bluffton.

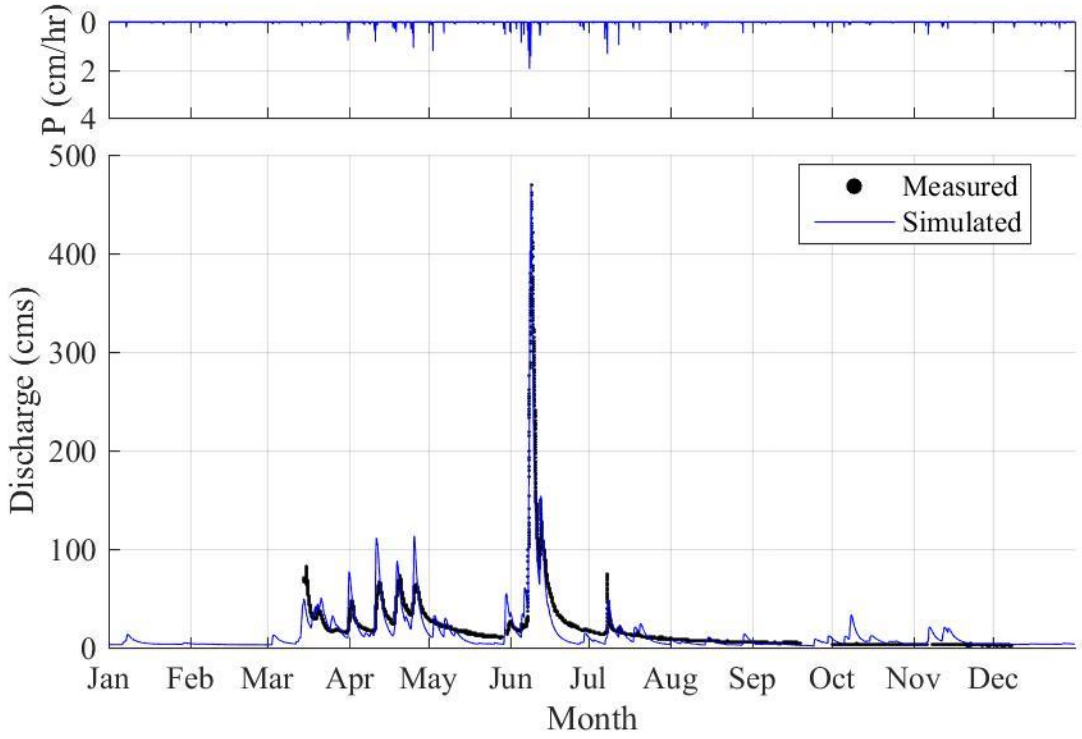

Figure A.2. Hydrograph for 2008 at the USGS stream gage at Bluffton.

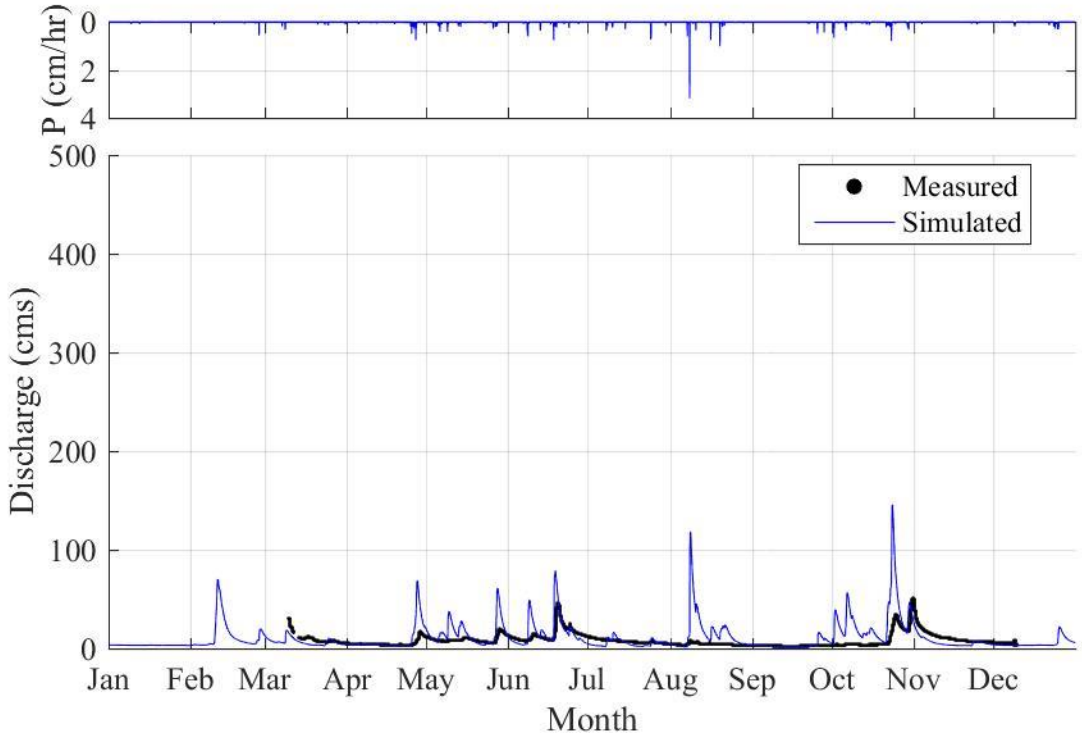

Figure A.3. Hydrograph for 2009 at the USGS stream gage at Bluffton.

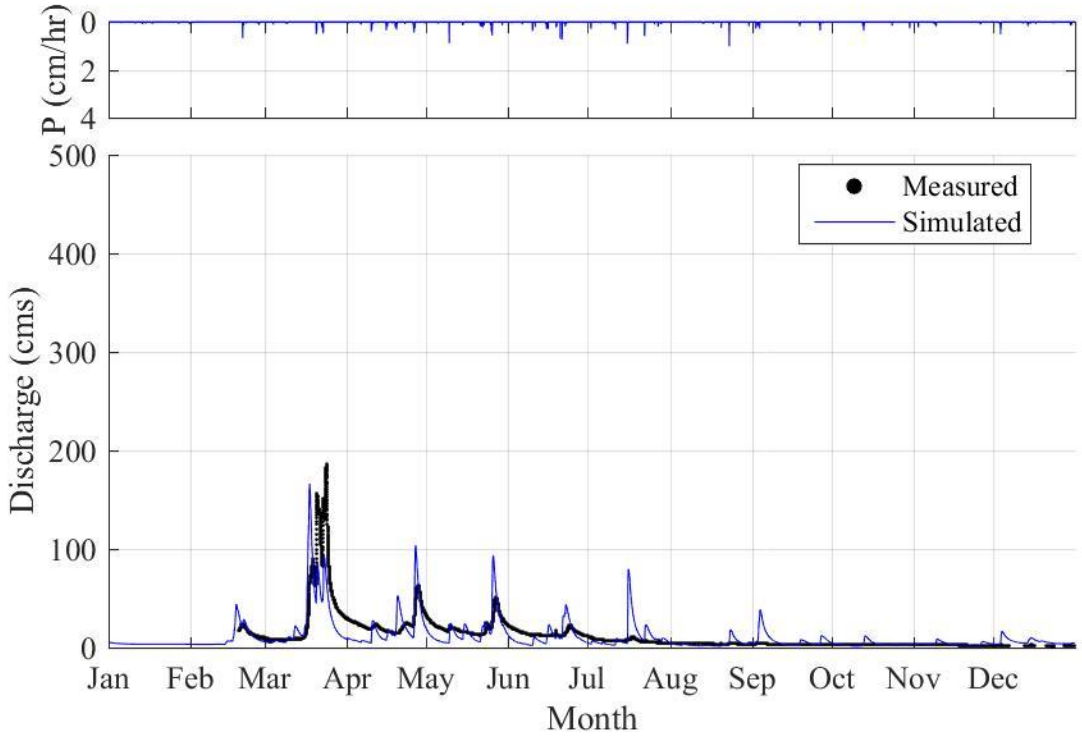

Figure A.4 Hydrograph for 2010 at the USGS stream gage at Bluffton.

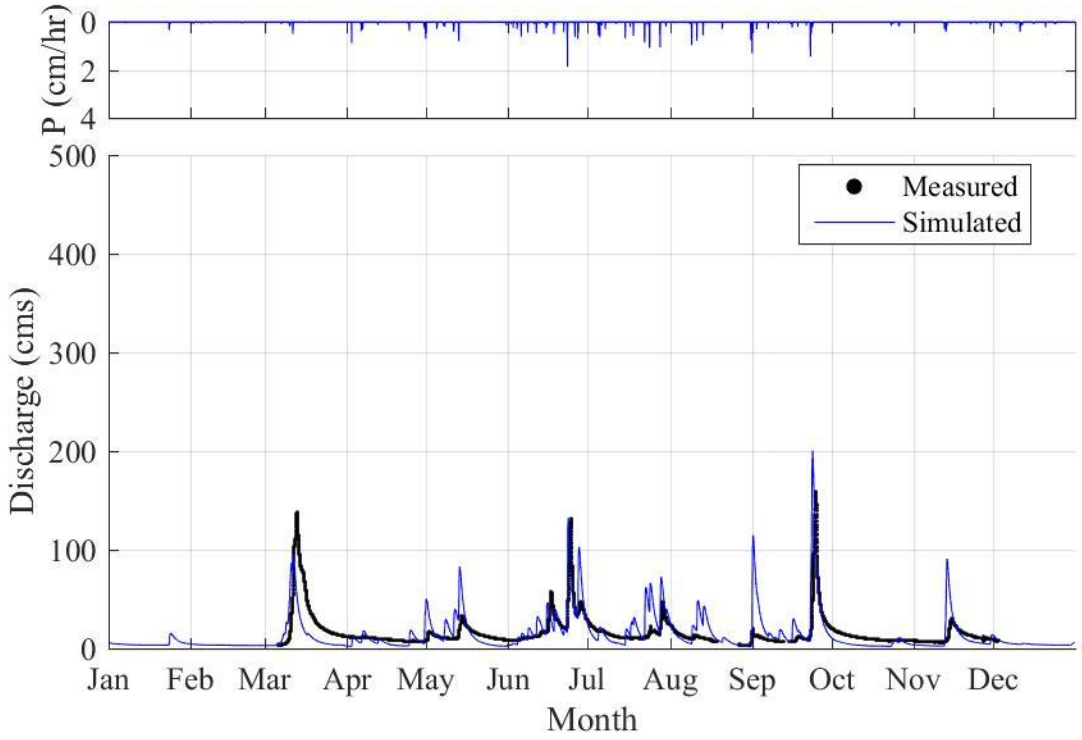

Figure A.5. Hydrograph for 2011 at the USGS stream gage at Bluffton.

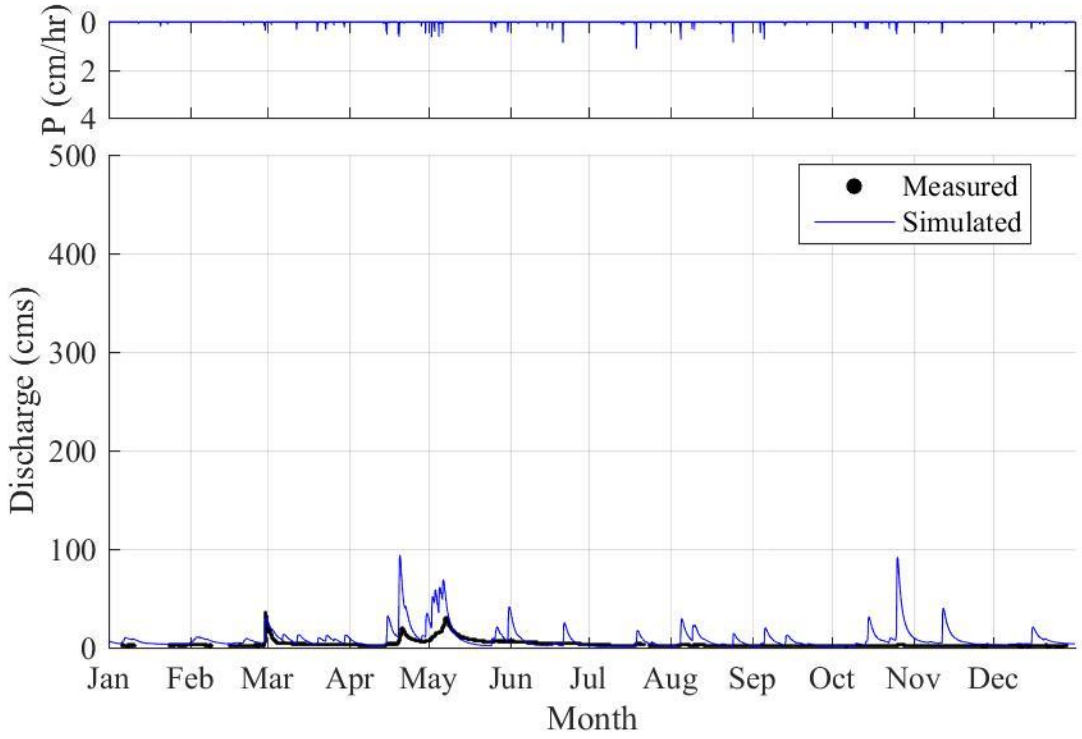

Figure A.6. Hydrograph for 2012 at the USGS stream gage at Bluffton.

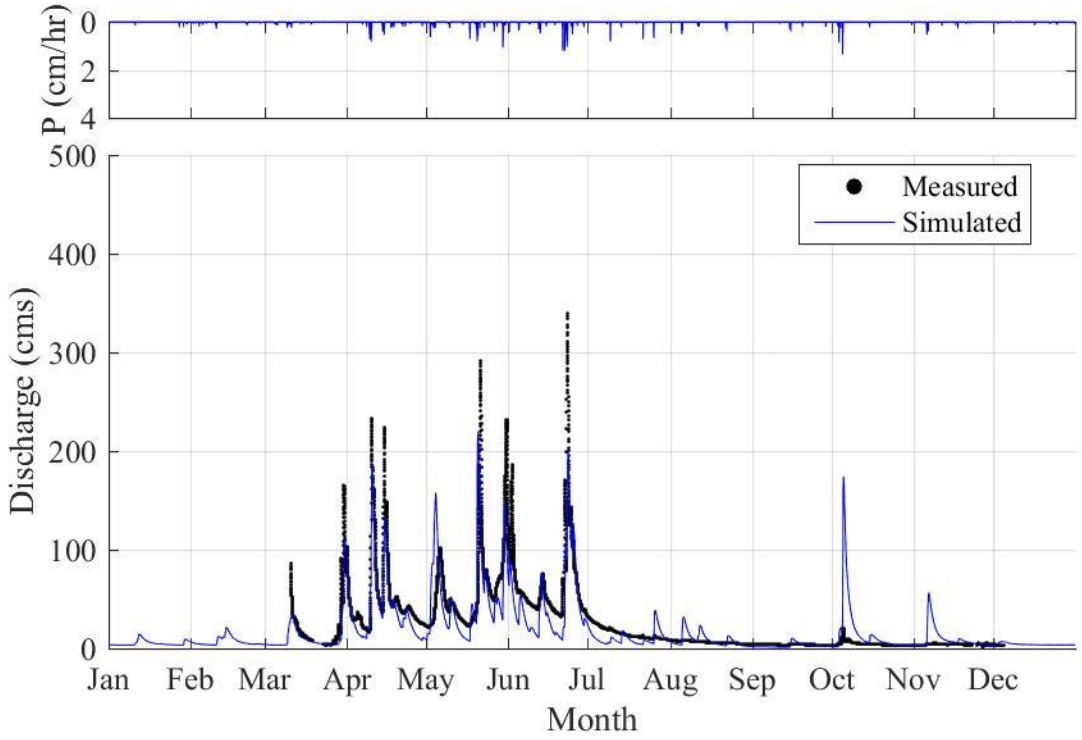

Figure A.7. Hydrograph for 2013 at the USGS stream gage at Bluffton.

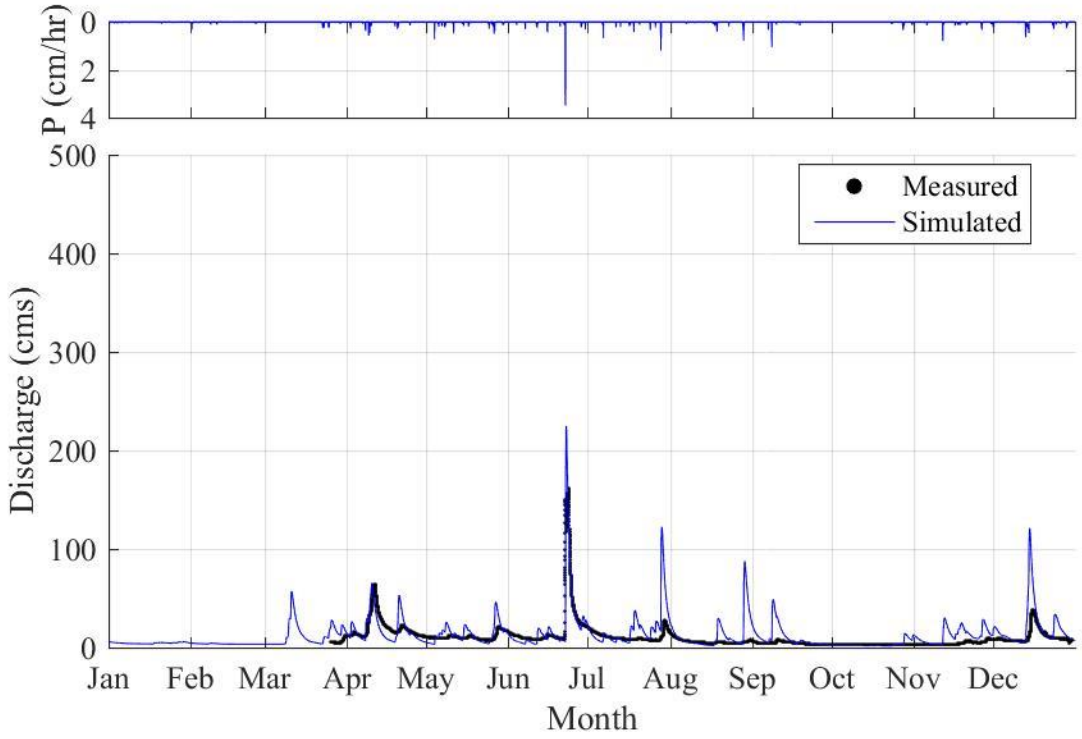

Figure A.8. Hydrograph for 2014 at the USGS stream gage at Bluffton.

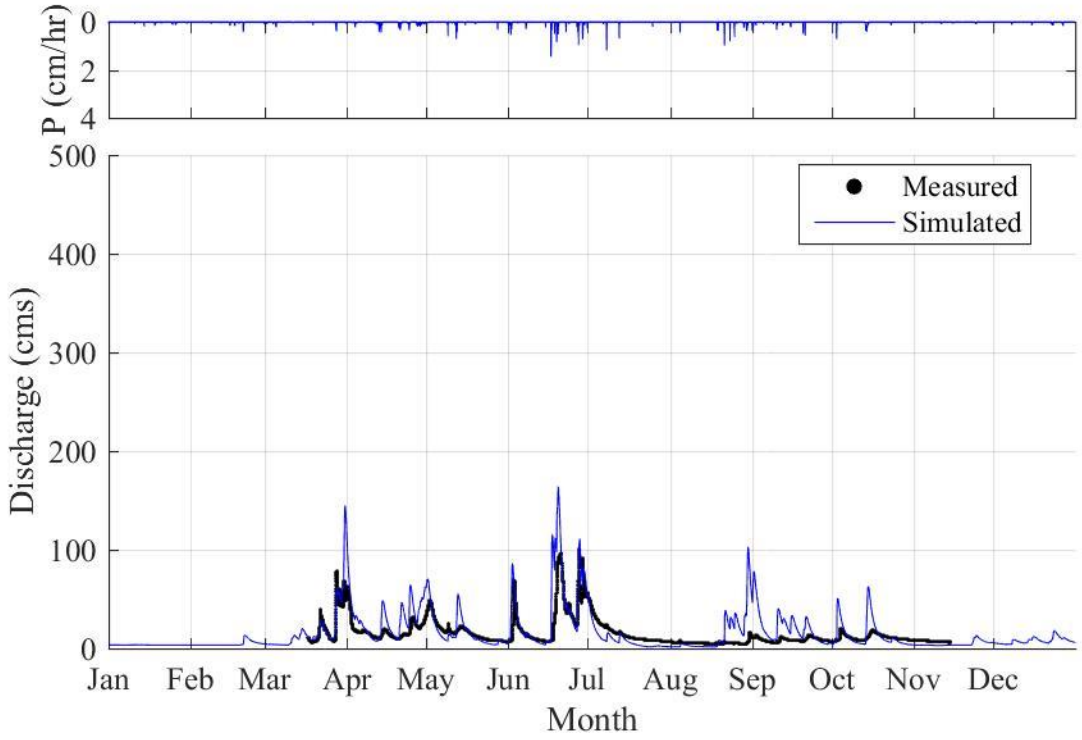

Figure A.9. Hydrograph for 2015 at the USGS stream gage at Bluffton.

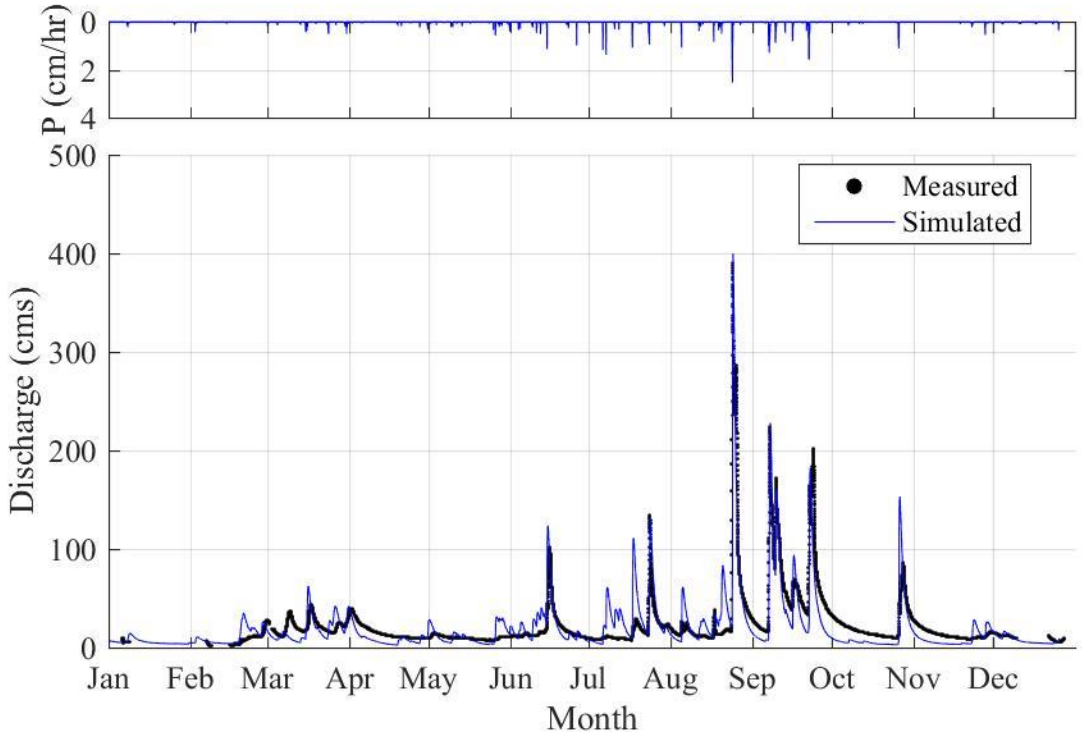

Figure A.10. Hydrograph for 2016 at the USGS stream gage at Bluffton.

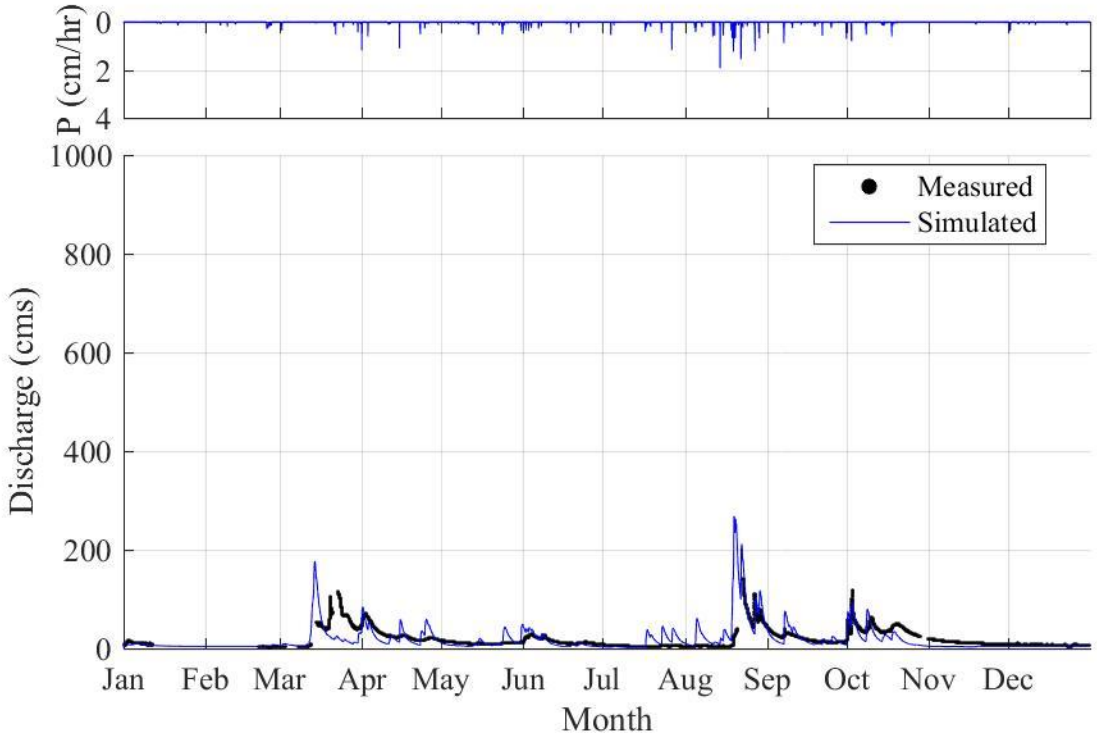

Figure A.11. Hydrograph for 2007 at the USGS stream gage at Decorah.

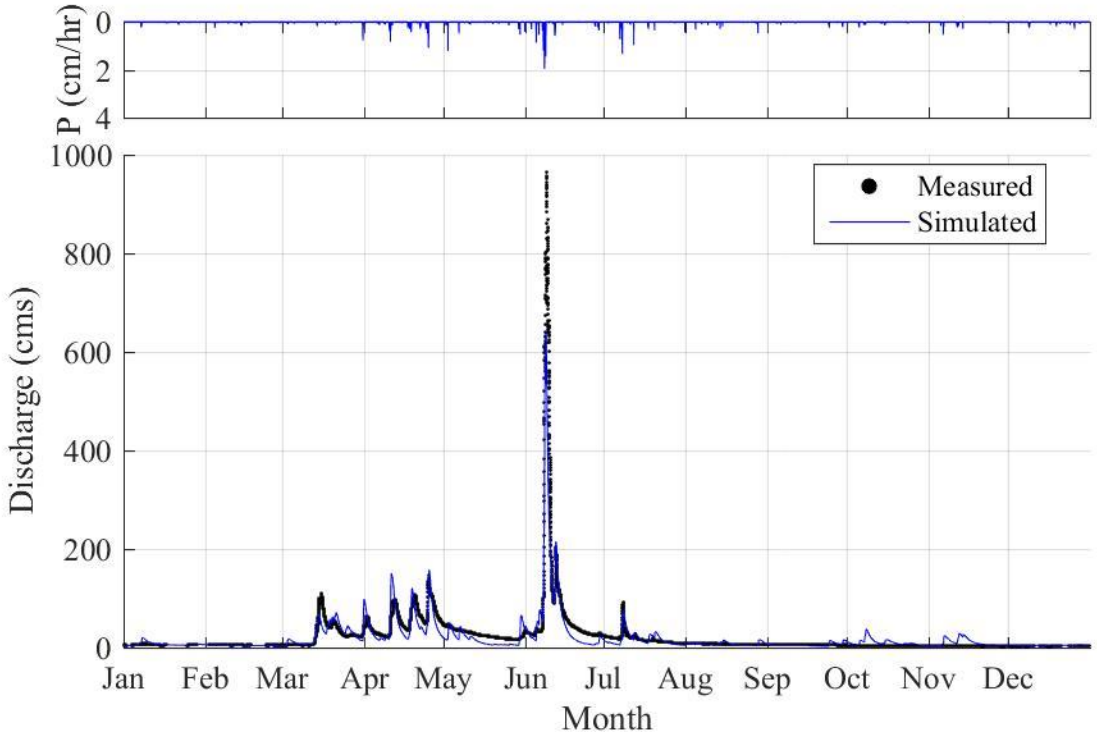

Figure A.12. Hydrograph for 2008 at the USGS stream gage at Decorah.

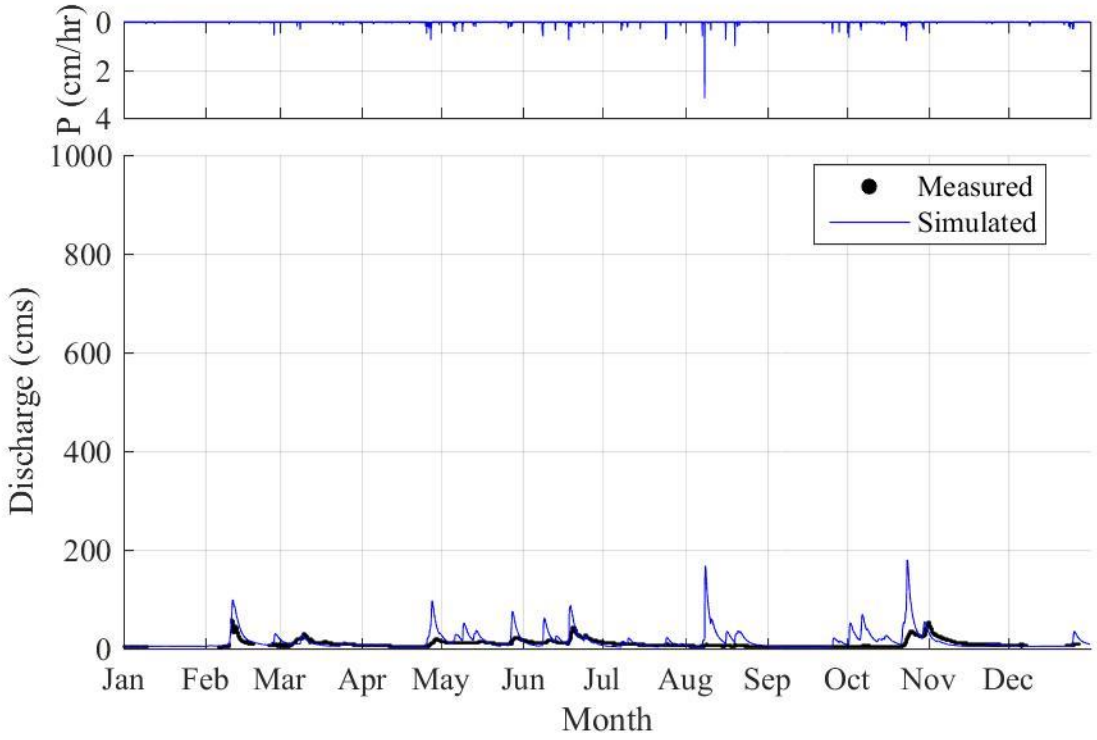

Figure A.13. Hydrograph for 2009 at the USGS stream gage at Decorah.

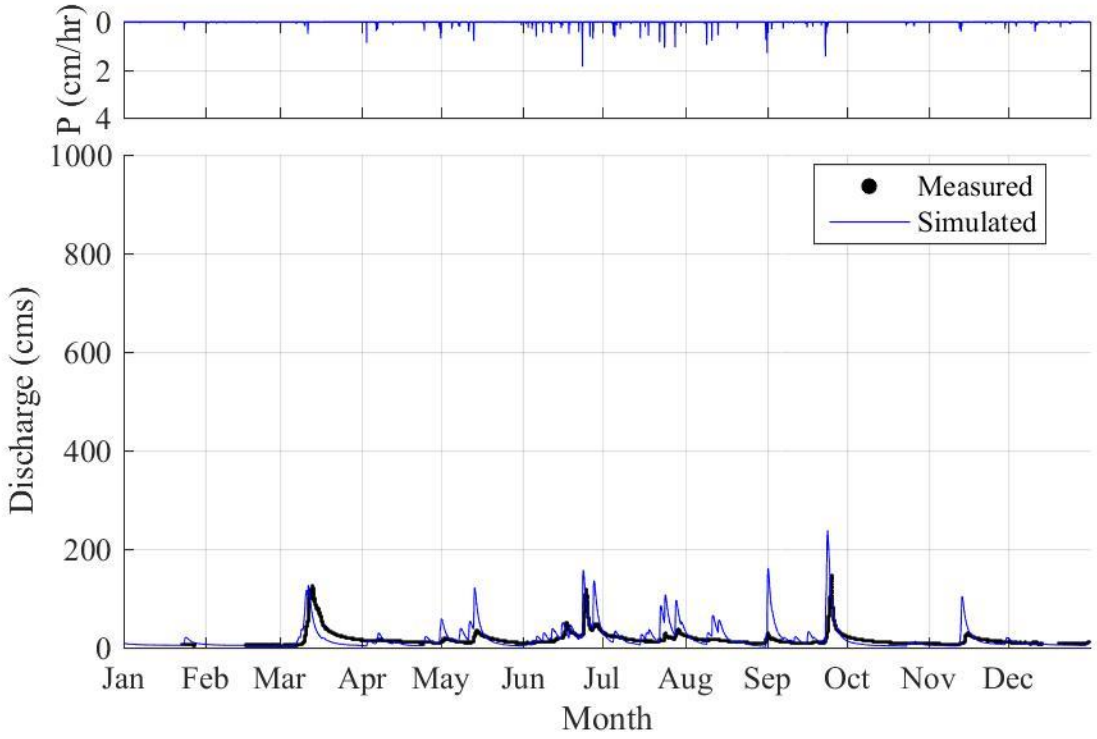

Figure A.14. Hydrograph for 2010 at the USGS stream gage at Decorah.

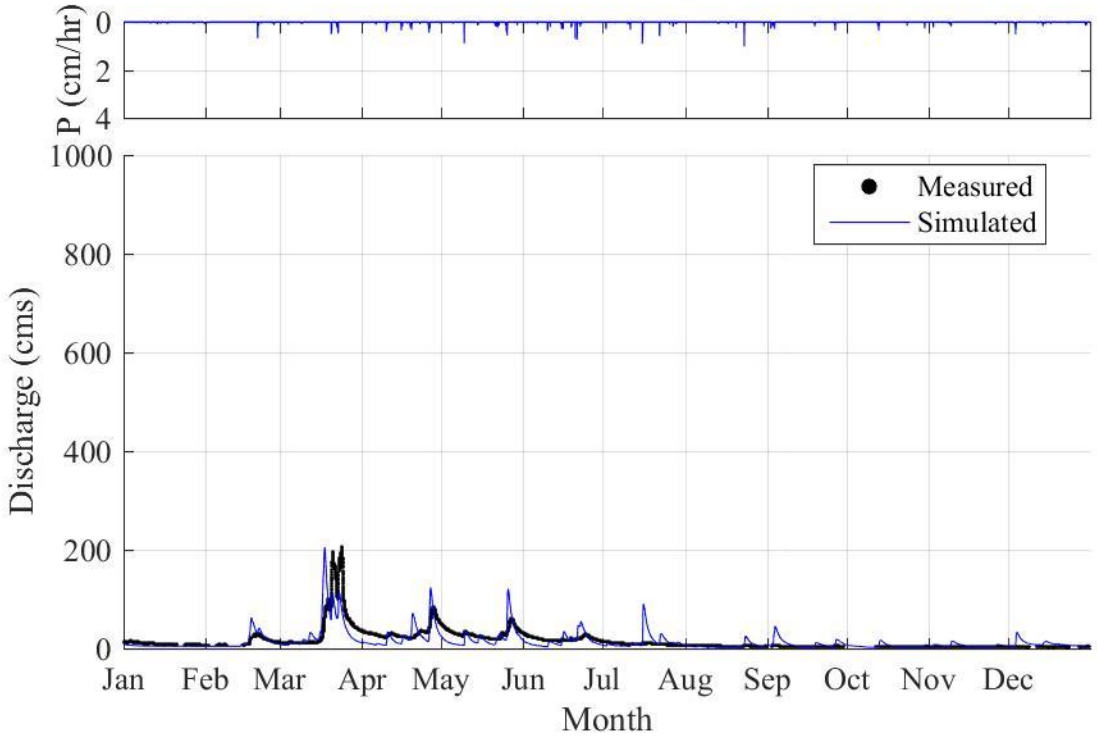

Figure A.15. Hydrograph for 2011 at the USGS stream gage at Decorah.

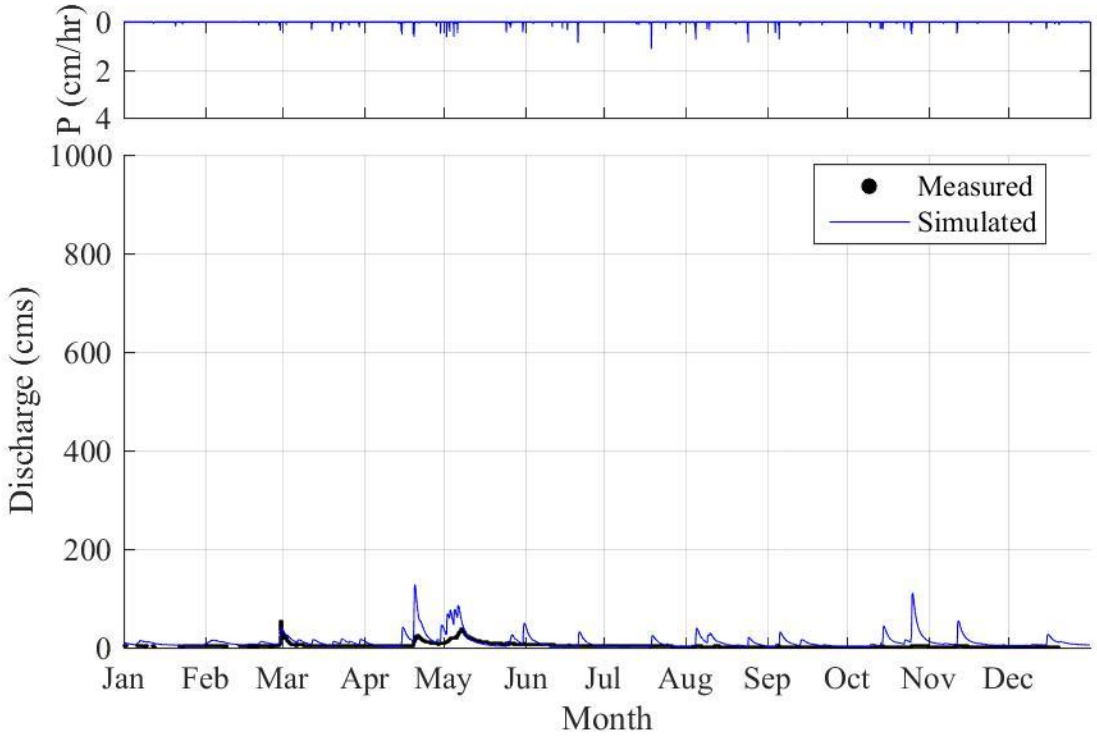

Figure A.16. Hydrograph for 2012 at the USGS stream gage at Decorah.

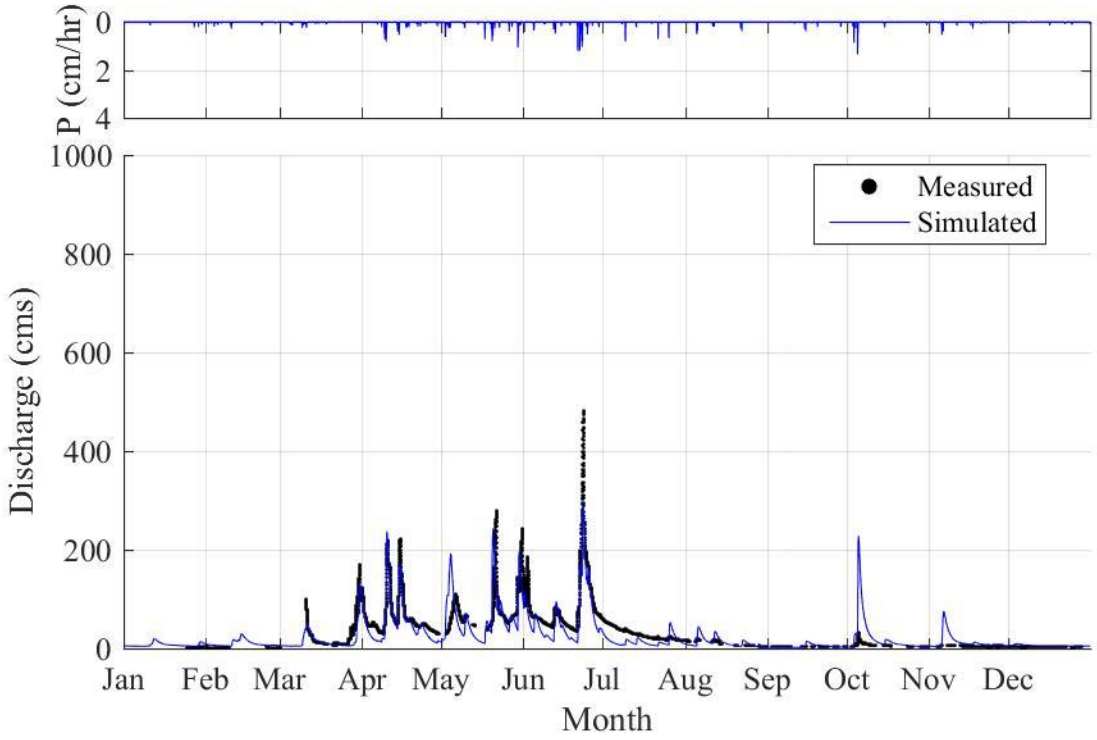

Figure A.17. Hydrograph for 2013 at the USGS stream gage at Decorah.

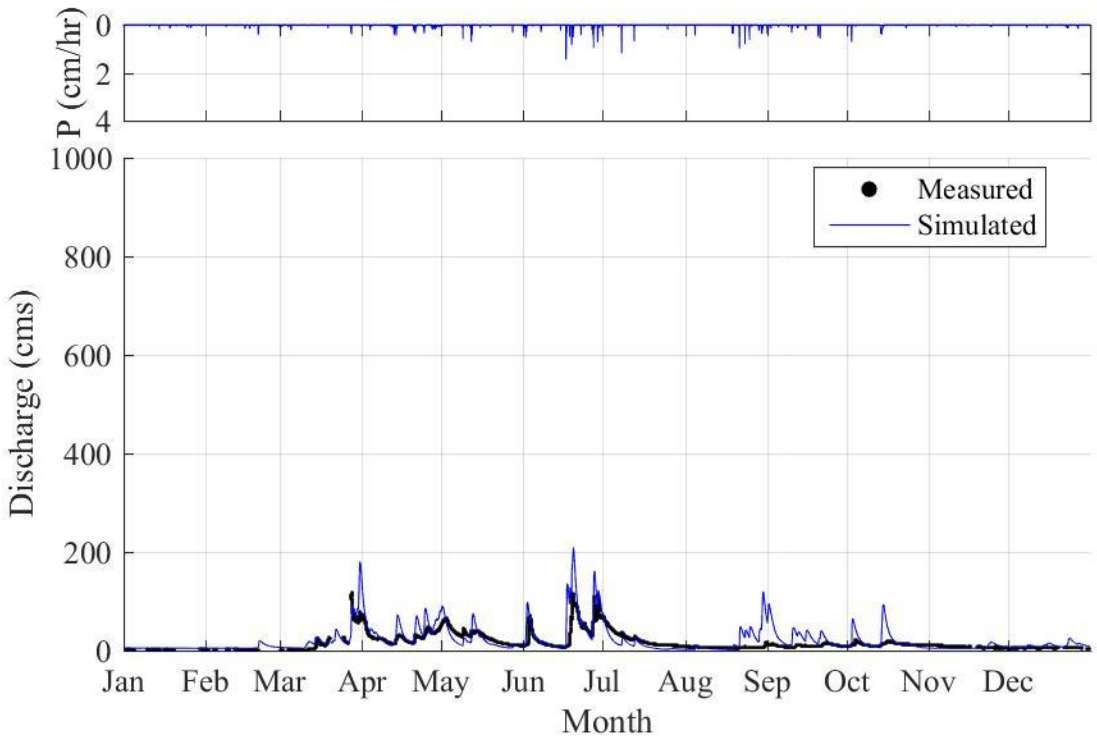

Figure A.18. Hydrograph for 2014 at the USGS stream gage at Decorah.

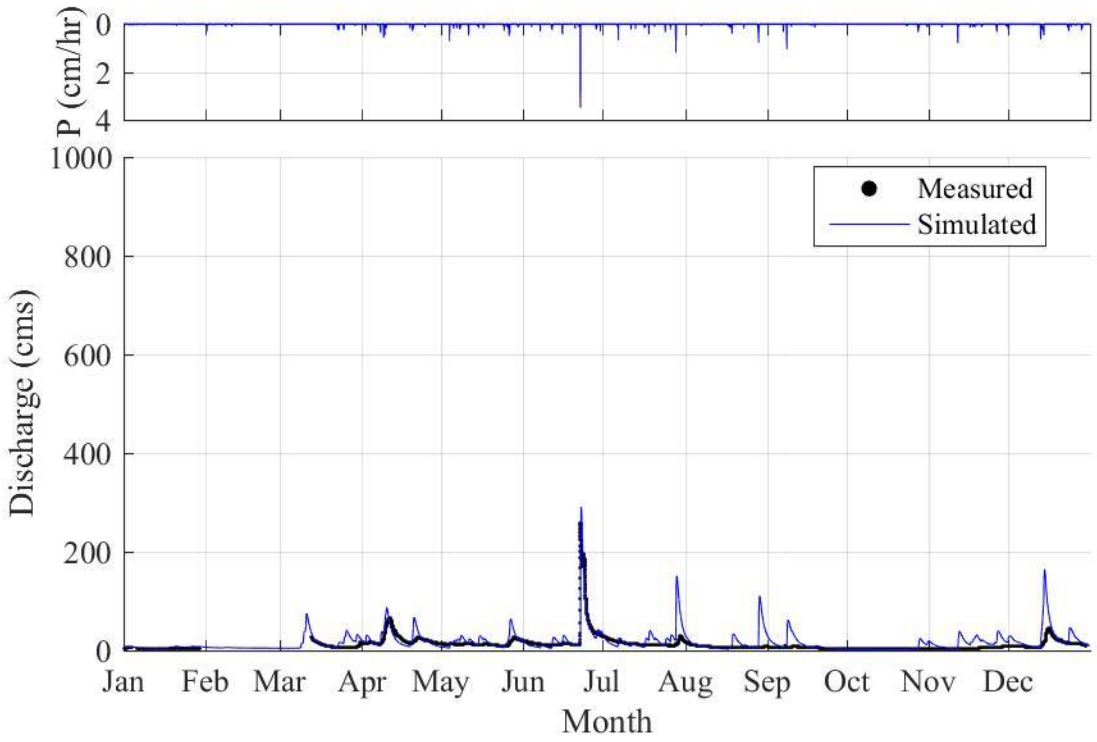

Figure A.19. Hydrograph for 2015 at the USGS stream gage at Decorah.

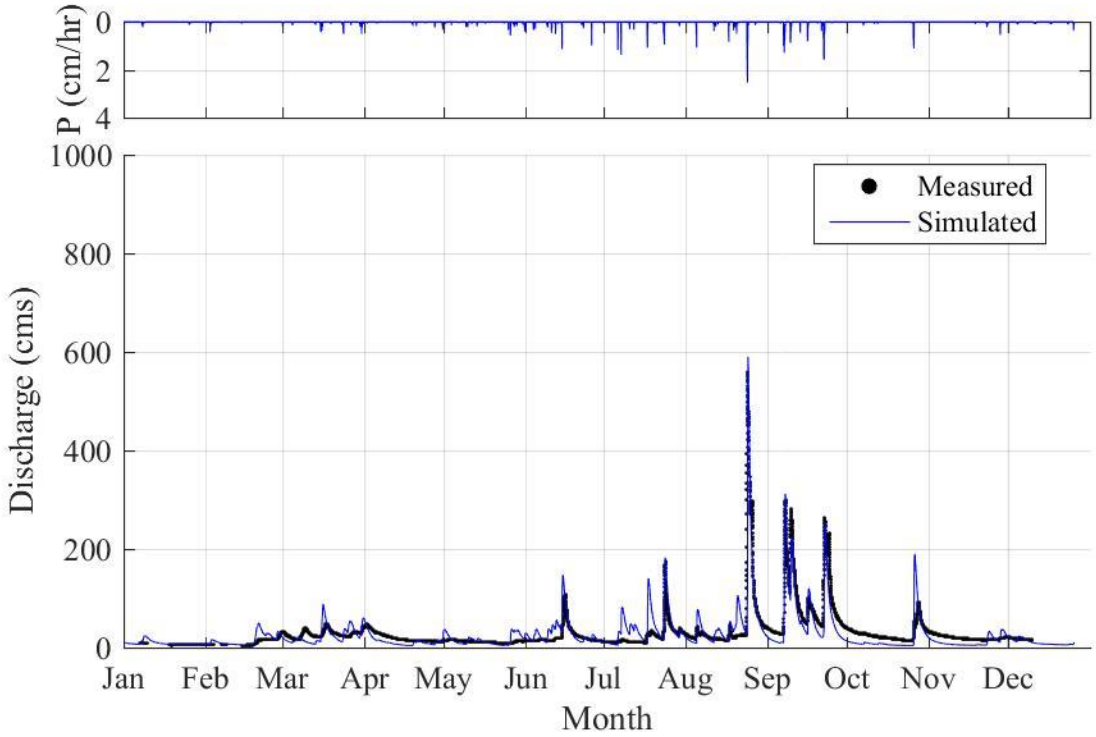

Figure A.20. Hydrograph for 2016 at the USGS stream gage at Decorah.

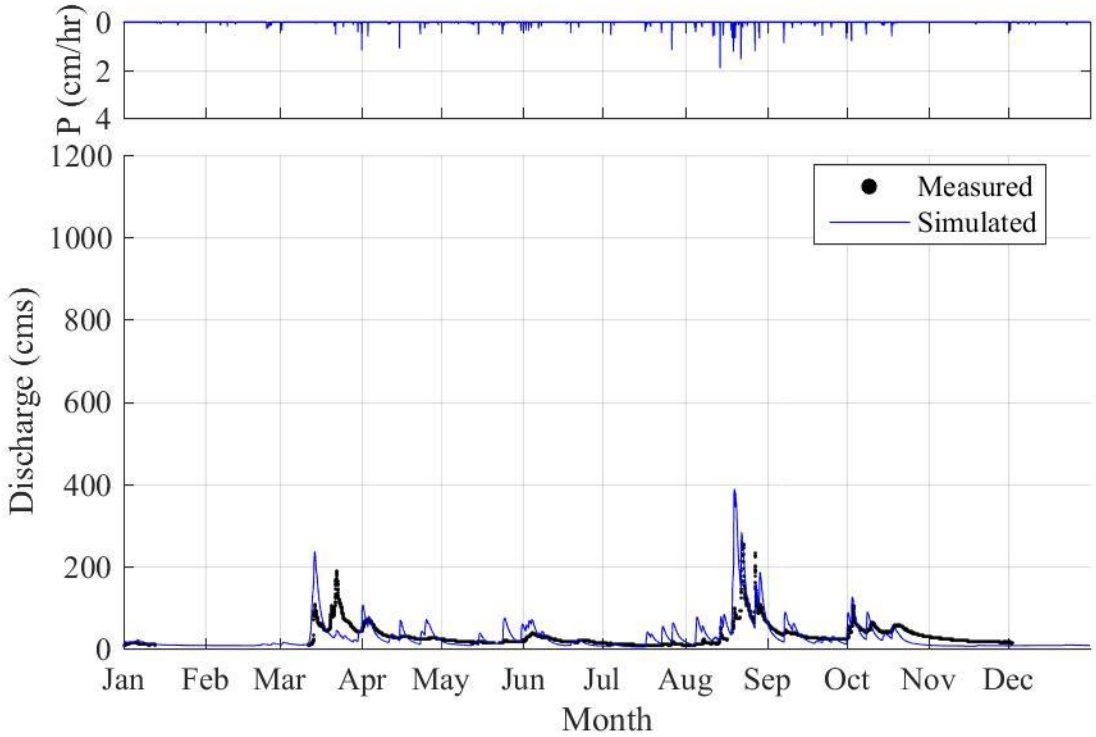

Figure A.21. Hydrograph for 2007 at the USGS stream gage near Dorchester.

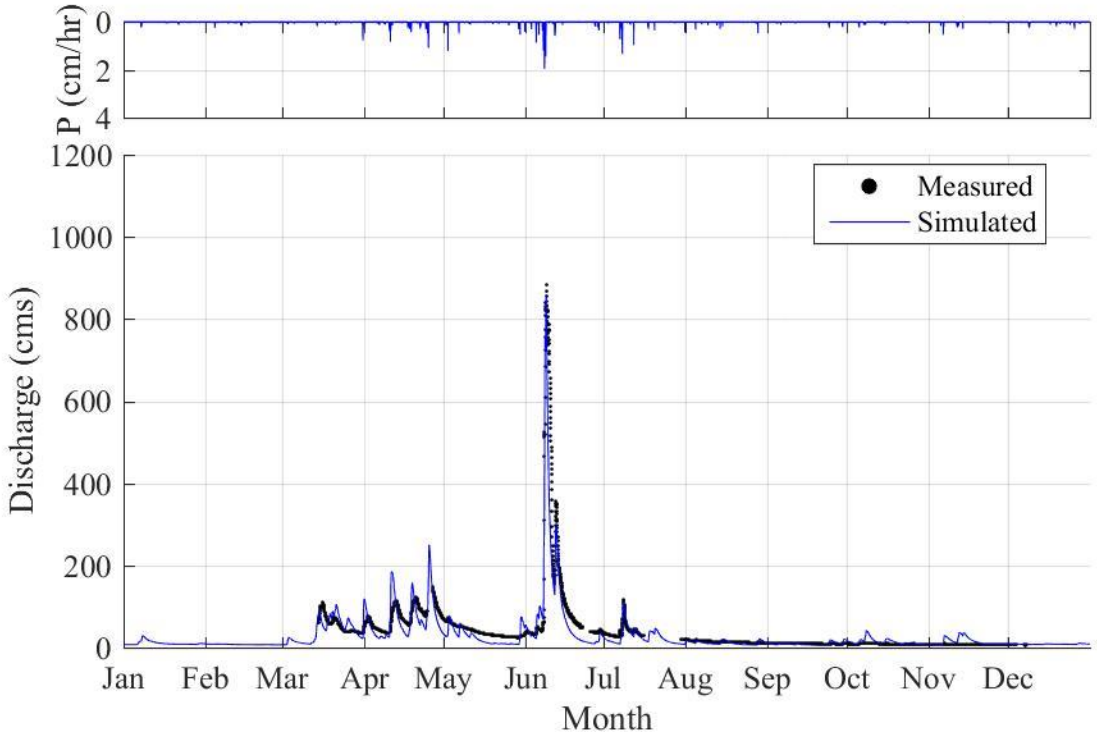

Figure A.22. Hydrograph for 2008 at the USGS stream gage near Dorchester.

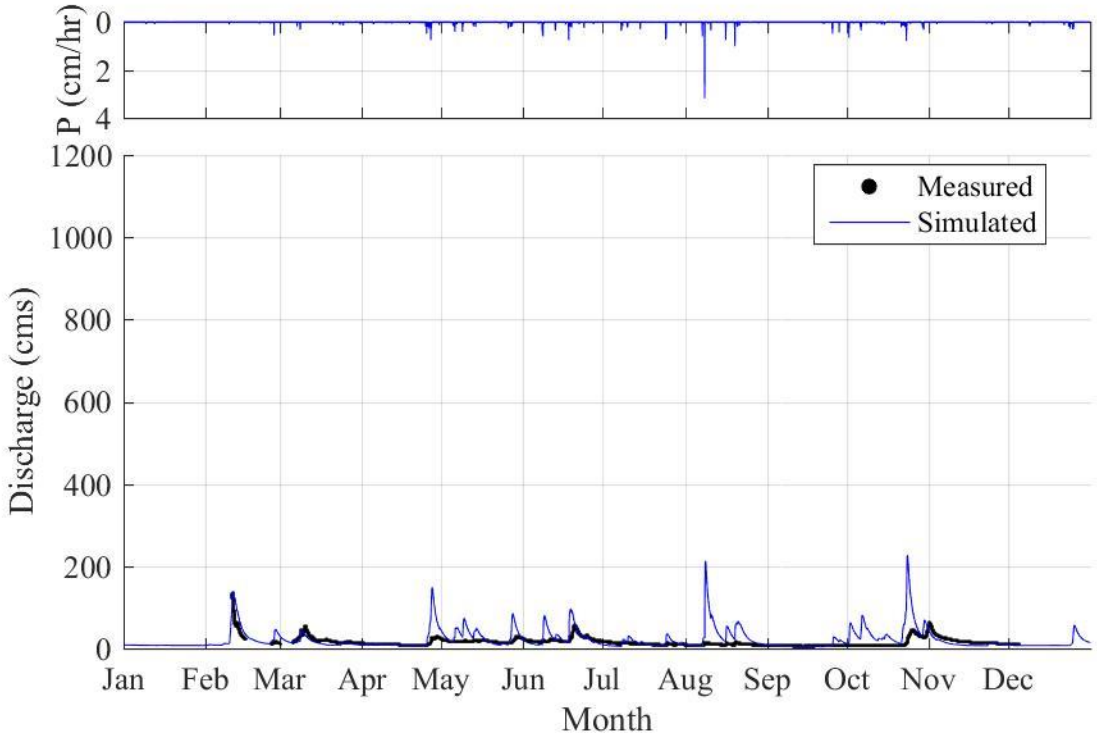

Figure A.23. Hydrograph for 2009 at the USGS stream gage near Dorchester.

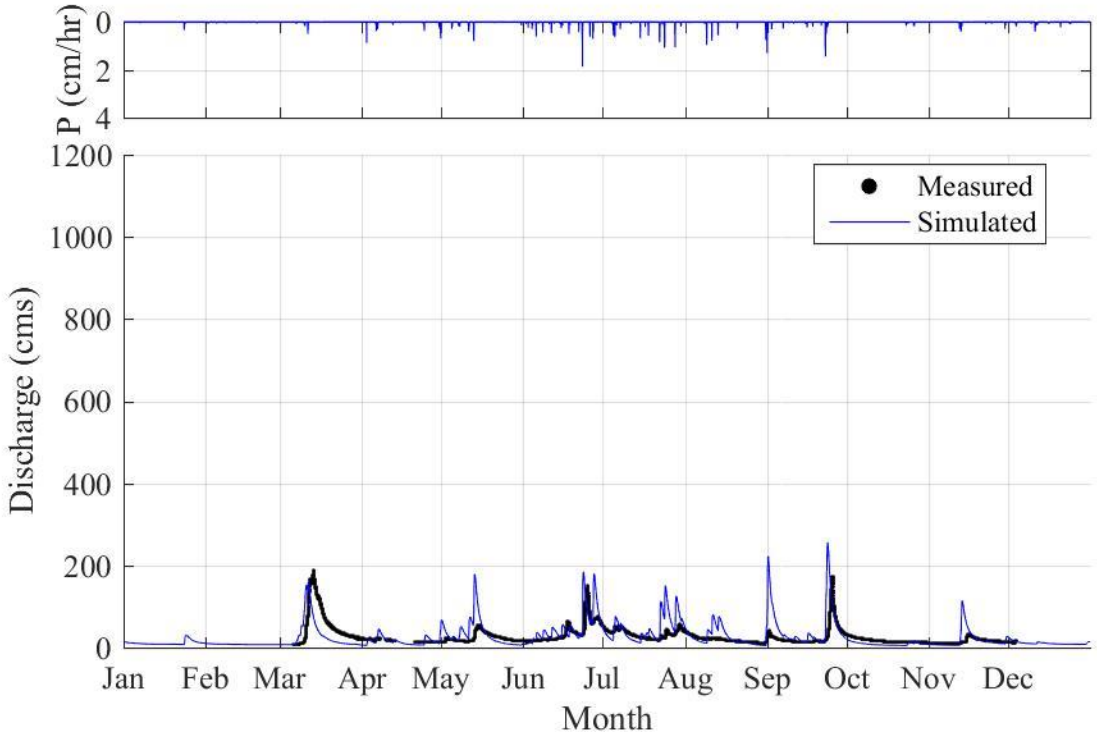

Figure A.24. Hydrograph for 2010 at the USGS stream gage near Dorchester.

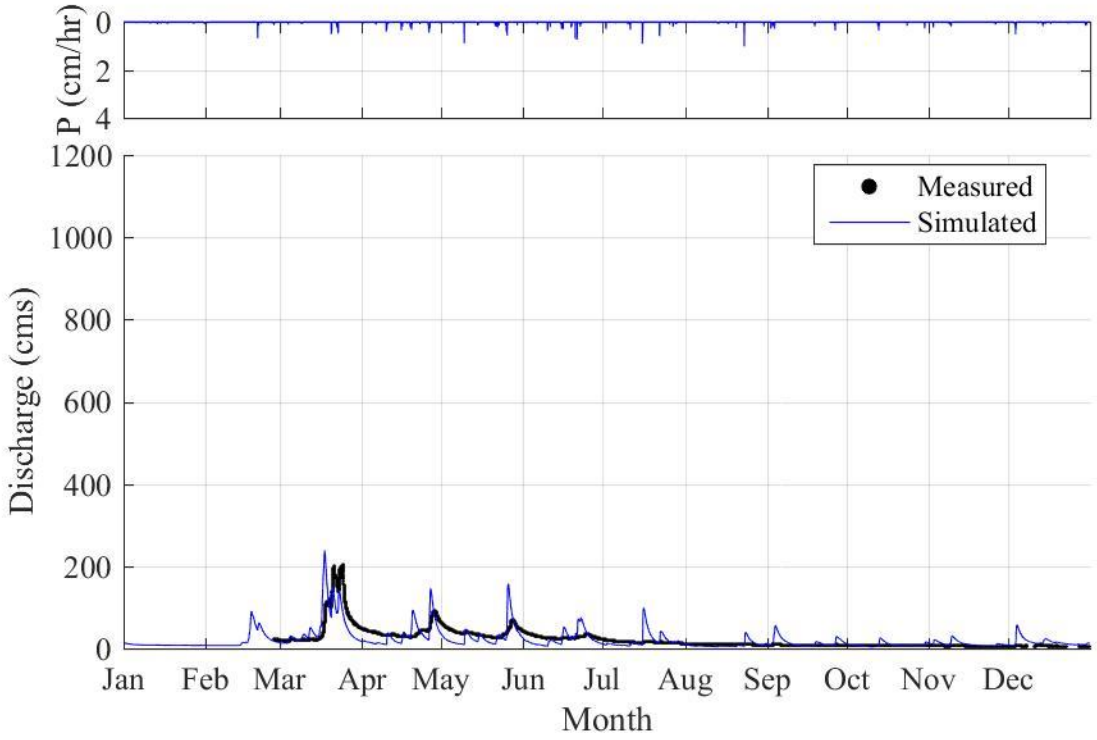

Figure A.25. Hydrograph for 2011 at the USGS stream gage near Dorchester.

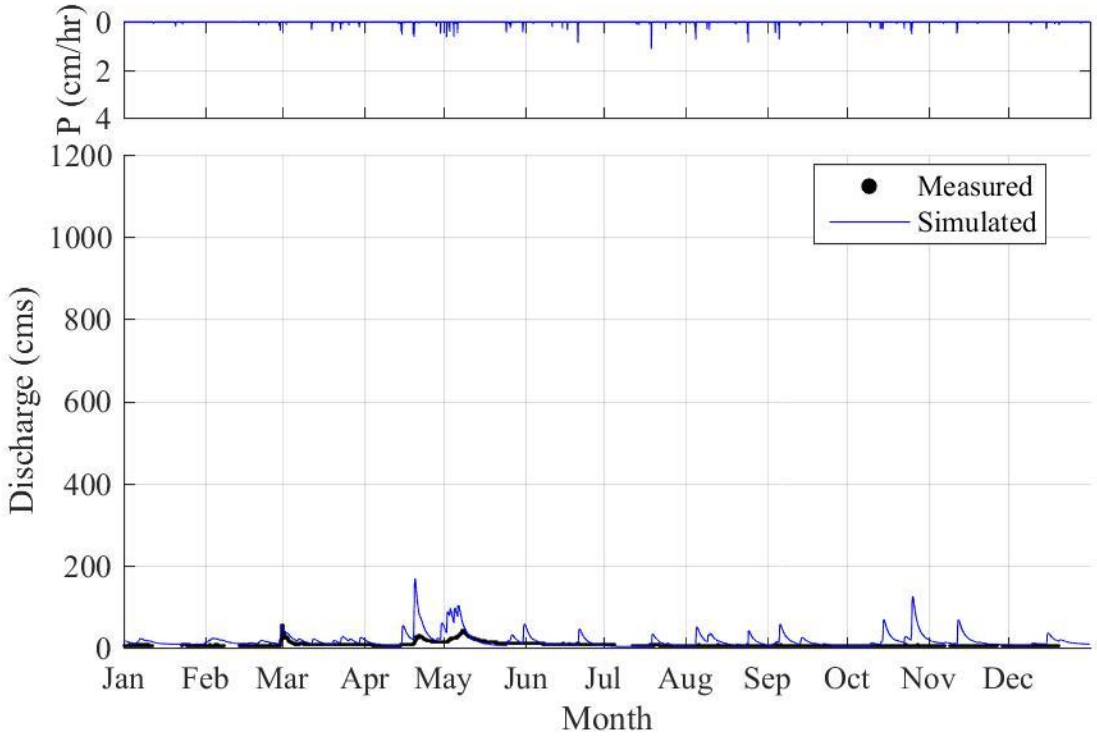

Figure A.26. Hydrograph for 2012 at the USGS stream gage near Dorchester.

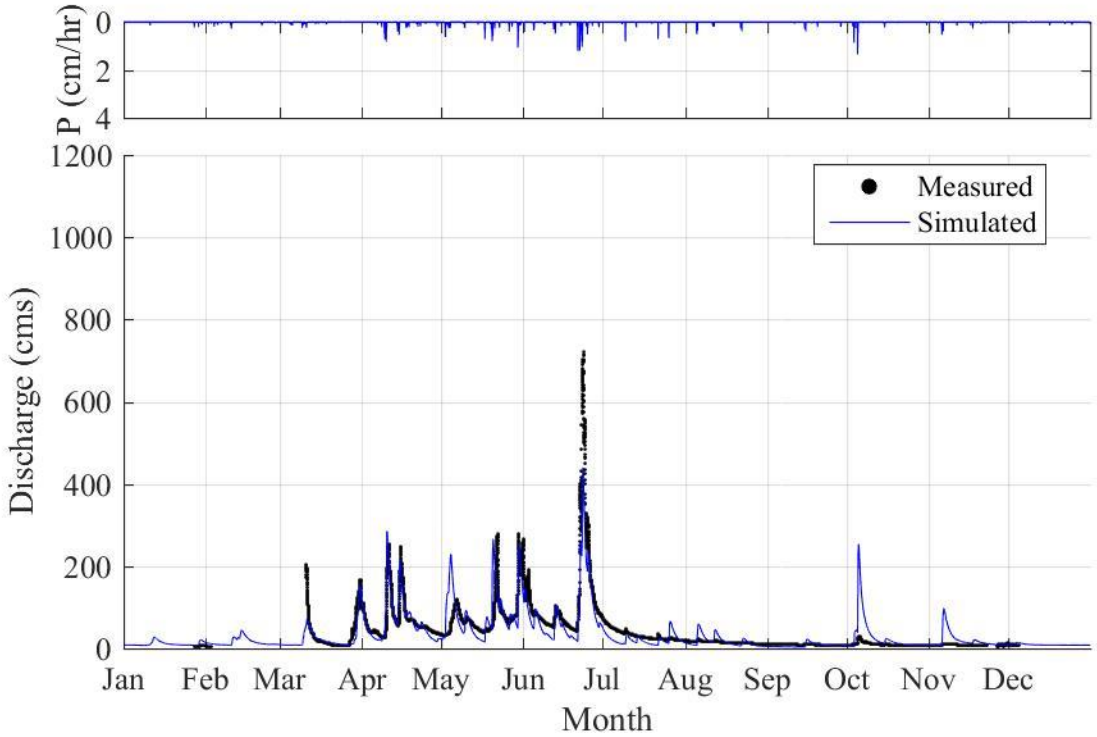

Figure A.27. Hydrograph for 2013 at the USGS stream gage near Dorchester.

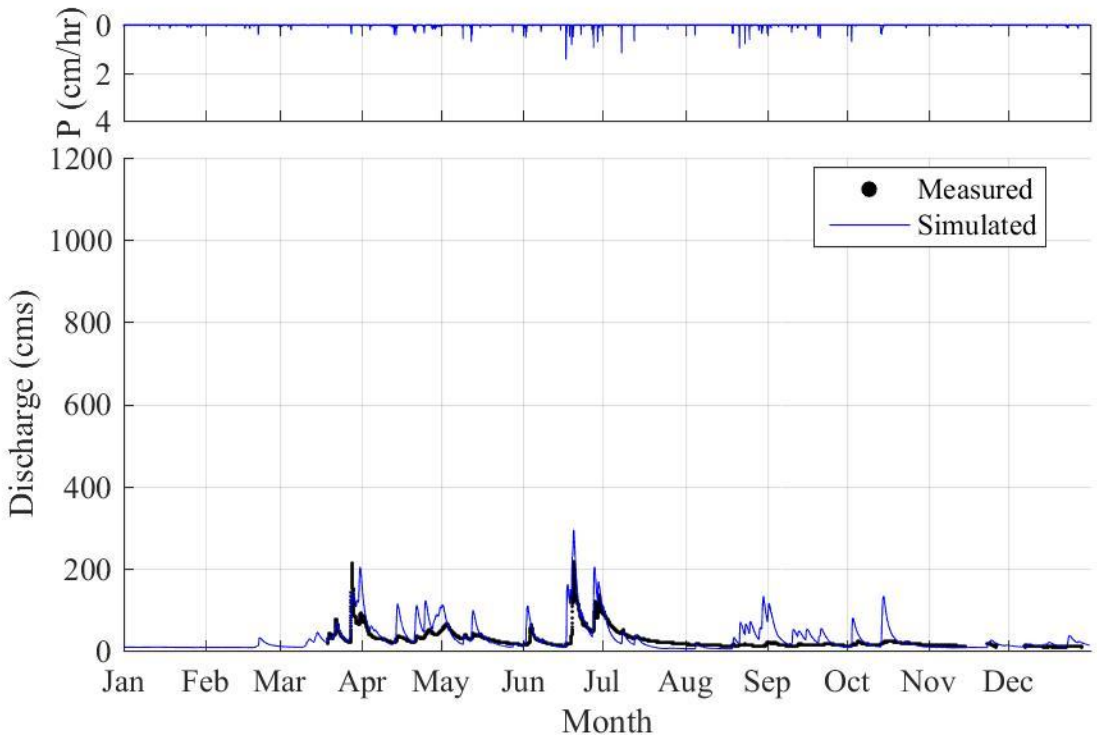

Figure A.28. Hydrograph for 2014 at the USGS stream gage near Dorchester.

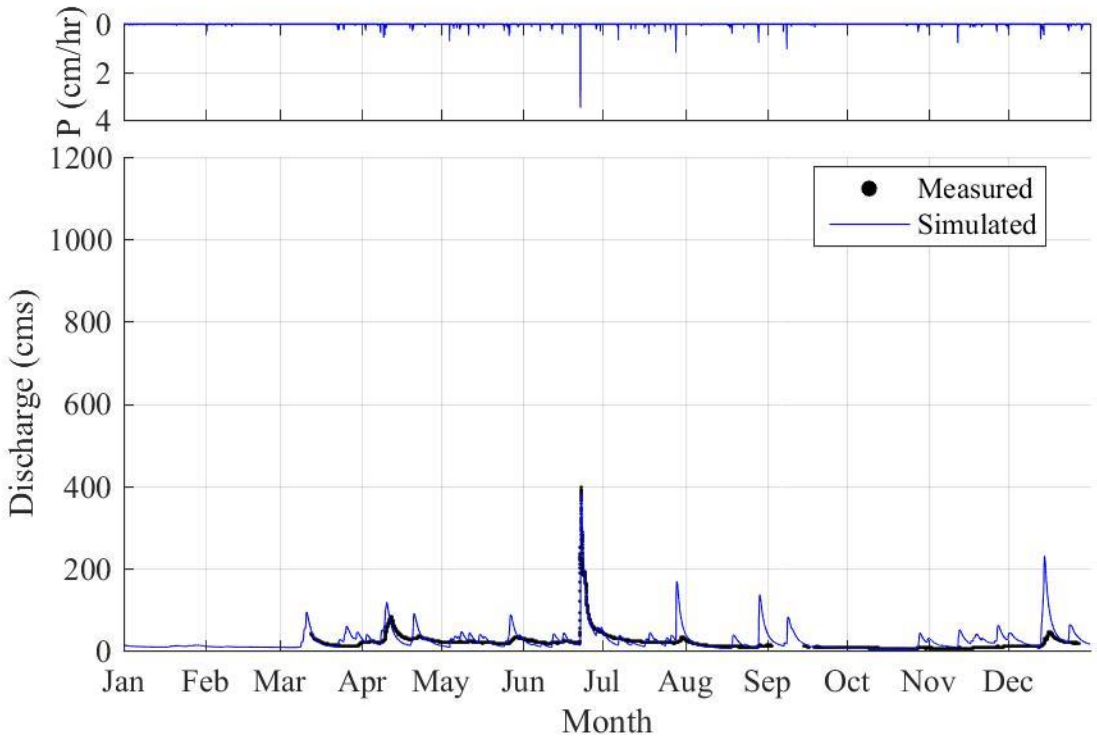

Figure A.29. Hydrograph for 2015 at the USGS stream gage near Dorchester.

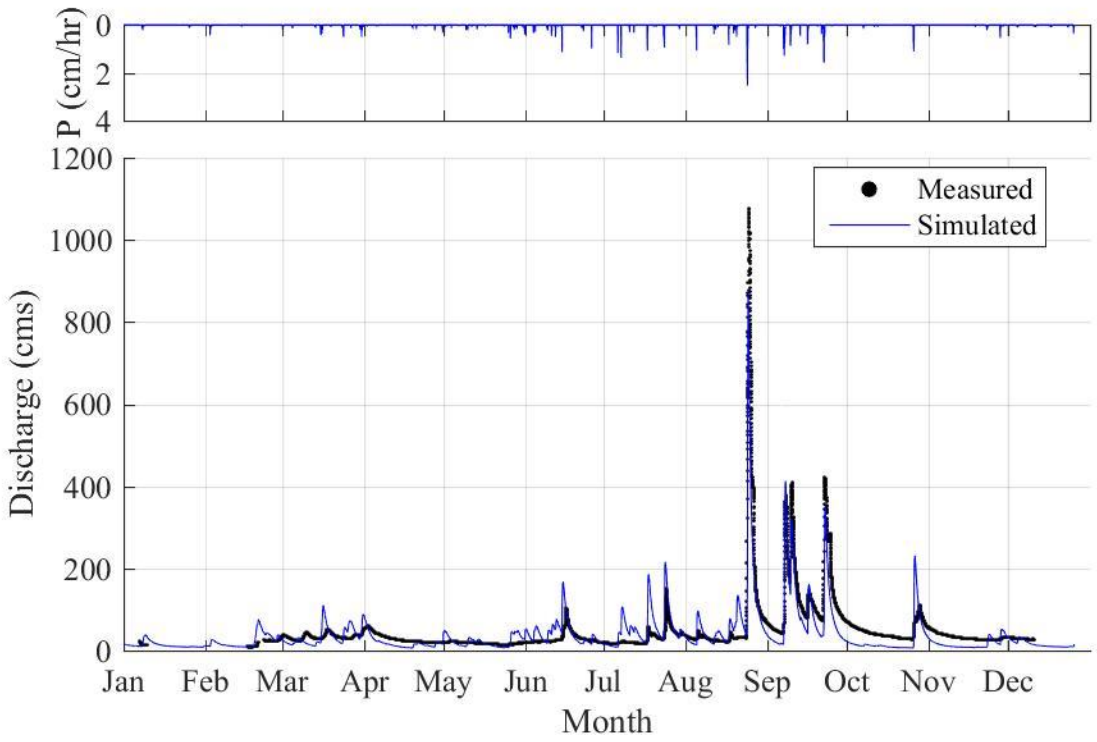

Figure A.30. Hydrograph for 2016 at the USGS stream gage near Dorchester.

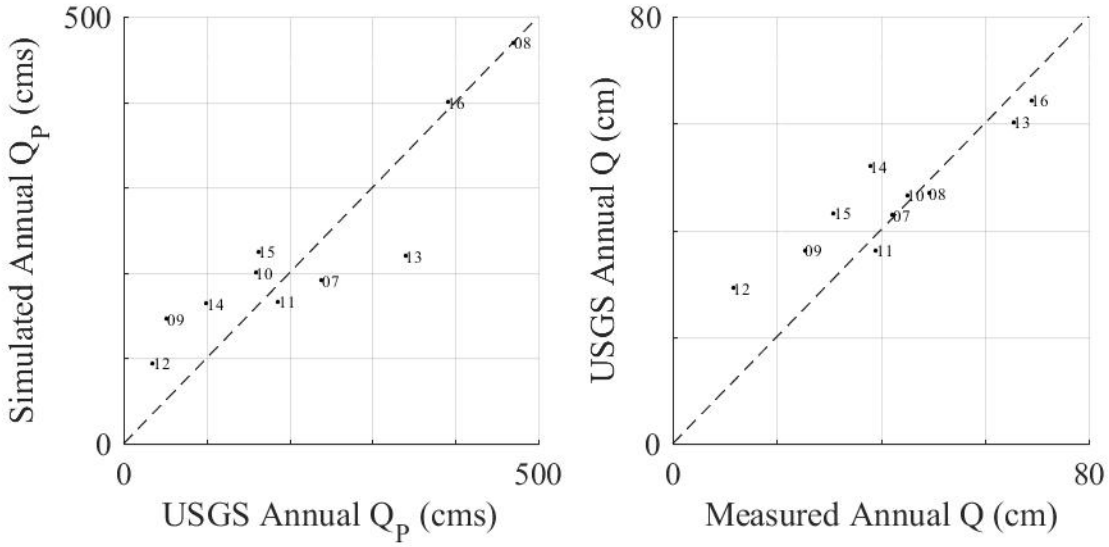

Figure A.31. Discharge characteristics annual peak discharge (Q_P) in cms and annual volume (Q) in cm for the calibration time period 2007-2016 for the Upper Iowa hydrologic model both at Bluffton.

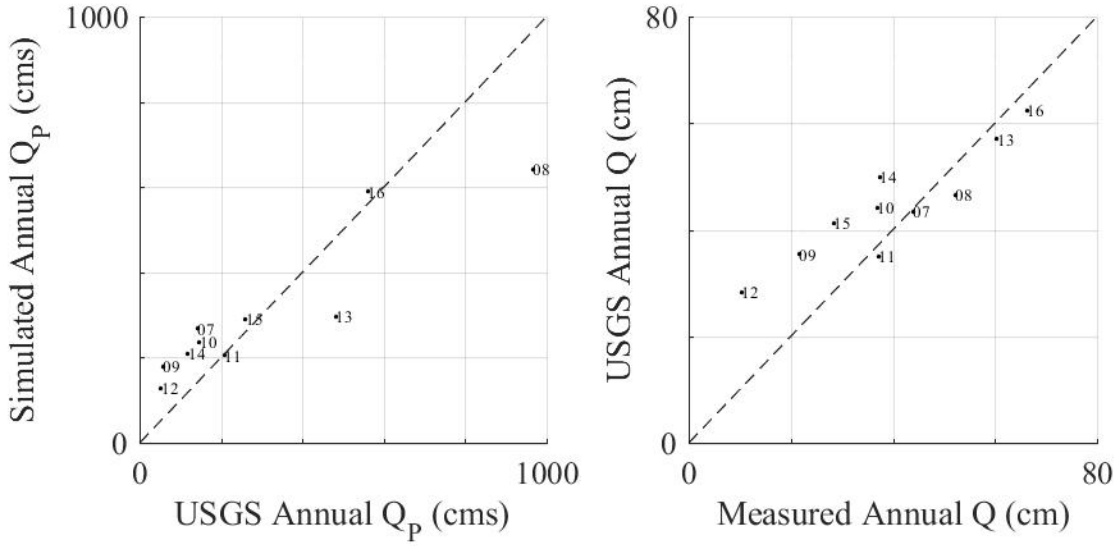

Figure A.32. Discharge characteristics annual peak discharge (Q_P) in cms and annual volume (Q) in cm for the calibration time period 2007-2016 for the Upper Iowa hydrologic model both at Decorah.

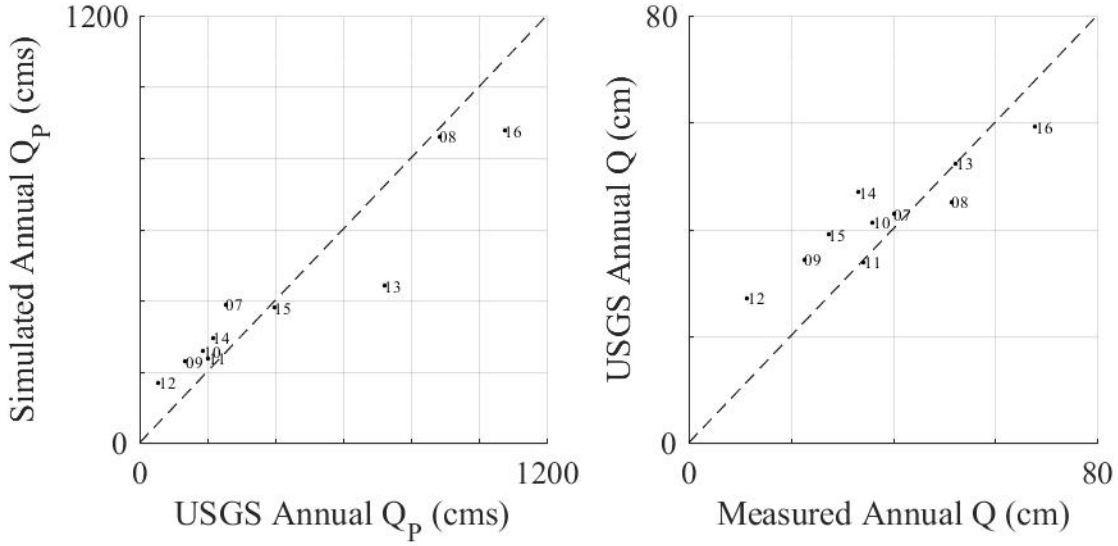

Figure A.33. Discharge characteristics annual peak discharge (Q_P) in cms and annual volume (Q) in cm for the calibration time period 2007-2016 for the Upper Iowa hydrologic model both near Dorchester.